

Machine Learning in Survival Analysis

Getting Started

Main Title

Standard blurb goes here

%%Placeholder for Half title

Series page goes here (if applicable); otherwise blank

Machine Learning in Survival Analysis

Raphael Sonabend, Andreas Bender

Imprint page here; PE will provide text

Table of contents

Getting Started	3
Preface	xiii
Authors	xvii
Acknowledgments	xix
Symbols and Notation	1
Symbols and Notation	1
Matrices and vectors	1
Functions	2
Variables and acronyms	2
1 Introduction	5
1.1 Defining Machine Learning Survival Analysis	6
1.1.1 Survival analysis	6
1.1.2 Machine learning survival analysis	8
1.2 Censoring and Truncation	9
1.3 Start to finish	11
1.4 Reproducibility and online book	13
I Survival Analysis and Machine Learning	15
2 Machine Learning	17
2.1 Basic workflow	17
2.2 Tasks	18
2.2.1 Regression	18
2.2.2 Classification	19
2.3 Training and predicting	19
2.4 Evaluating and benchmarking	20
2.5 Hyperparameter Optimization	22
2.6 Conclusion	24
3 Survival Analysis	25
3.1 Quantifying the Distribution of Event Times	25
3.1.1 Continuous Time	26
3.1.2 Discrete Time	27
3.2 Single-event, right-censored data	28
3.3 Types of Censoring	29
3.3.1 Right-censoring	30

3.3.2	Left- and Interval-censoring	31
3.4	Censoring vs. Truncation	33
3.4.1	Left-truncation	33
3.4.2	Right-truncation	34
3.5	Estimation	35
3.5.1	Parametric estimation	35
3.5.2	Non-parametric estimation	37
3.5.2.1	Kaplan-Meier estimator	37
3.5.2.2	Nelson-Aalen	38
3.5.2.3	Left truncation	39
3.6	Estimation of the censoring distribution	42
3.6.1	The Kaplan-Meier estimator for the censoring distribution	42
3.6.2	Inverse probability of censoring weights (IPCW)	42
3.7	Conclusion	43
4	Event-history Analysis	45
4.1	A process point of view	47
4.2	Competing Risks	47
4.2.1	Notation and Definitions	48
4.2.2	Non-parametric estimators	49
4.2.3	Application to mortality of ICU patients	50
4.2.4	Independent Censoring vs. Competing Risks	50
4.3	Multi-state Models	51
4.3.1	Notation and Definitions	54
4.3.2	Transition probabilities	54
4.3.3	Transition probabilities and hazards	57
4.3.4	Non-parametric estimation of transition probabilities	57
4.3.5	Application to liver cirrhosis patients	58
4.4	Conclusion	58
5	Survival Task	61
5.1	Survival prediction types	61
5.2	Predicting distributions	64
5.3	Predicting relative risks	65
5.3.1	Distributions and risks	66
5.4	Predicting survival times	67
5.4.1	Times and risks	67
5.4.2	Times and distributions	67
5.5	Prognostic index predictions	69
5.5.1	Prognostic index, risks, and times	70
5.5.2	Prognostic index and distributions	71
5.6	Conclusion	71
II	Evaluation	73
6	Discrimination	75
6.1	Time-Independent Measures	75
6.1.1	Concordance Indices	76
6.1.2	Choosing a C-index	78
6.2	Time-Dependent Measures	78

6.2.1	Concordance Indices	79
6.2.2	Area Under the Curve	79
6.3	Extensions	82
6.3.1	Competing risks	82
6.3.2	Other censoring and truncation types	83
6.3.3	Truncation	84
7	Calibration	87
7.1	Point Calibration	87
7.1.1	Calibration by Reduction	88
7.1.2	Houwelingen's α	88
7.2	Probabilistic Calibration	89
7.2.1	Kaplan-Meier Comparison	89
7.2.2	D-Calibration	89
7.3	Extensions	91
7.3.1	Competing risks	91
7.3.2	Other censoring and truncation types	92
8	Scoring Rules	93
8.1	Classification Losses	93
8.2	Survival Losses	94
8.2.1	Squared Losses	95
8.2.2	Logarithmic losses	96
8.2.3	Absolute Losses	97
8.3	Prediction Error Curves	98
8.4	Baselines and ERV	99
8.5	Extensions	99
8.5.1	Competing risks	99
8.5.2	Other censoring and truncation types	100
8.6	Conclusion	100
9	Distance Measures	103
9.1	Conclusion	103
III	Models	105
10	Traditional Survival Models	107
10.1	Non-Parametric Estimators	107
10.1.1	Unconditional estimators	107
10.1.2	Conditional estimators	109
10.2	Proportional Hazards	109
10.2.1	Semi-Parametric PH	110
10.2.2	Parametric PH	112
10.2.3	Competing risks	113
10.3	Accelerated Failure Time	117
10.3.1	Understanding acceleration	117
10.3.2	Parametric AFTs	119
10.4	Proportional Odds	121
10.5	Flexible Parametric Models	122
10.6	Improving traditional models	123

10.6.1 Non-linear effects	124
10.6.2 Dimension reduction and feature selection	124
10.6.3 Ensemble methods	126
10.7 Conclusion	127
11 Random Forests	129
11.1 Random Forests for Regression	129
11.1.1 Decision Trees	129
11.1.2 Random Forests	132
11.2 Random Survival Forests	133
11.2.1 Splitting Rules	133
11.2.2 Terminal Node Prediction	136
11.3 Conclusion	140
12 Support Vector Machines	143
12.1 SVMs for Regression	143
12.2 SVMs for Survival Analysis	147
12.2.1 Survival time SSVMs	147
12.2.2 Ranking SSVMs	148
12.2.3 Hybrid SSVMs	150
12.3 Conclusion	152
13 Boosting Methods	155
13.1 GBMs for Regression	155
13.2 GBMs for Survival Analysis	158
13.2.1 PH and AFT GBMs	158
13.2.2 Discrimination Boosting	159
13.2.3 CoxBoost	160
13.3 Conclusion	161
14 Neural Networks	163
14.0.1 Neural Networks for Regression	163
14.0.2 Neural Networks for Survival Analysis	166
14.0.2.1 Probabilistic Survival Models	167
14.0.2.2 Deterministic Survival Models	174
14.0.3 Conclusions	174
IV Reduction Techniques	177
15 Reduction Techniques for Survival Analysis	179
16 IPC weighted classification	181
16.1 Conclusion	183
17 Pseudo-value regression	185
17.1 Pseudo-values for Survival Probability	186
17.2 Pseudo-values for RMST	189
17.3 Pseudo-values in Event-History Analysis	190
17.3.1 Pseudo-values for Competing Risks	190
17.3.2 Pseudo-values for Multi-State Models	191
17.4 Advantages and Limitations	191

<i>Contents</i>	xi
17.5 Conclusion	192
18 Partition based reductions	195
18.1 Data Transformation	196
18.2 Discrete Time Survival Analysis	197
18.2.1 Example: Logistic Regression	198
18.3 Survival Stacking	200
18.4 Piecewise Constant Hazards	201
18.4.1 Example: Poisson Regression	203
18.5 Choice of Interval Boundaries	203
19 Reductions for Event-History Analysis	205
20 FAQs and Outlook	207
20.1 Common problems in survival analysis	207
20.1.1 Data cleaning	207
20.1.2 Evaluation and prediction	208
20.1.3 Choosing models and measures	208
20.1.4 Competing risks	209
20.1.4.1 How should competing risks be handled?	209
20.2 What's next for machine learning survival analysis?	210
References	211
References	211

Preface

“Everything happens to everybody sooner or later if there is time enough” - George Bernard Shaw

“...but in this world nothing can be said to be certain, except death and taxes.” - Benjamin Franklin

A logical consequence of Bernard Shaw’s quote is that if there is time enough, then everybody will have experienced a given event at some point. This is one of the central assumptions to survival analysis (specifically to single-event analysis, but we’ll get to that later). As nothing can be certain (except death and taxes), machine learning can be used to predict the probability people will experience the event and *when*. This is exactly the problem that this book tackles.

With immortality only being a theoretical concept, there is never ‘time enough’, hence survival analysis assumes that the event of interest is guaranteed to occur within an object’s lifetime. This event could be a patient entering remission after a cancer diagnosis, the lifetime of a lightbulb after manufacturing, the time taken to finish a race, or any other event that is observed over time. Survival analysis differs from other fields of Statistics in that uncertainty is explicit encoded in the survival problem; this uncertainty is known as ‘censoring’. For example, say a model is being built to predict when a marathon runner will finish a race and to learn this information the model is fed data from every marathon over the past five years. Across this period, there will be many runners who never finish their race. Instead, these runners are said to be ‘censored’ and the model uses all information up until the point of censoring (dropping out of the race), and learns that they ran for at least as long as their censoring time (the time they dropped out). Censoring is unique to survival analysis and without the presence of censoring, survival analysis is mathematically equivalent to regression.

This book covers survival analysis in the most common right-censoring setting for independent censoring, as well as discussing competing risk frameworks for dependent censoring - these terms will all be covered in the introduction of the book.

A note from Raphael: I wrote my PhD thesis about machine learning applications to survival analysis as I was interested in understanding why more researchers were not using machine learning models for survival analysis. Since then I’ve had the pleasure to work with, and advise, researchers across different sectors, including pharmaceutical companies, governmental agencies, funding organisations, and research institutions. I hope that this book continues to help researchers discover machine learning survival analysis and to navigate the nuances and complexities it presents.

A note from Andreas: FIXME.

Overview

This textbook is intended to fill a gap in the literature by providing a comprehensive introduction to machine learning in the survival setting. If you are interested in machine learning or survival analysis separately then you might consider James et al. (2013), Hastie, Tibshirani, and Friedman (2001), Bishop (2006) for machine learning and Collett (2014), John D. Kalbfleisch and Prentice (1980) for survival analysis. This book serves as a complement to the above examples and introduces common machine learning terminology from simpler settings such as regression and classification, but without diving into the detail found in other sources, instead focusing on extension to the survival analysis setting.

This book may be useful for Masters or PhD students who are specialising in machine learning in survival analysis, machine learning practitioners looking to work in the survival setting, or statisticians who are familiar with survival analysis but less so with machine learning. The book could be read cover-to-cover, but this is not advised. Instead it may be preferable to dip into sections of the book as required and use the ‘signposts’ that direct the reader to sections of the book that are relevant to each other.

The book is split into five parts:

Part I: Survival Analysis and Machine Learning The book begins by introducing the basics of survival analysis and machine learning and unifying terminology between the two to enable meaningful description of ‘machine learning in survival analysis’ (MLSA). In particular, the survival analysis ‘task’ and survival ‘prediction types’ are defined.

Part II: Evaluation The second part of the book discusses one of the most important parts of the machine learning workflow, model evaluation. In the simplest case, without evaluation there is no way to know if predictions from a trained machine learning model are any good. Whether one uses a Kaplan-Meier estimator, a complex neural network, or anything in between, there is no guarantee any of these methods will actually make useful predictions for a given dataset. This could be because the dataset is inherently difficult for any model to be trained on, perhaps because it is very ‘noisy’, or because a model is simply ill-suited to the task, for example using a Cox Proportional Hazards model when its key assumptions are violated. Evaluation is therefore crucial to trusting any predictions made from a model.

The measures in Part II are presented in different classes that reflect the prediction types identified in Part I. In-sample measures, which evaluate the quality of a model’s ‘fit’ to data, are not included as this book primarily focuses on external validation of predictive machine learning models. Readers who are interested in this are directed to Collett (2014) and Hosmer Jr, Lemeshow, and May (2011) for discussion on residuals; Choodari-Oskooei, Royston, and Parmar (2012a) and Royston and Sauerbrei (2004) for R^2 type measures; and Volinsky and Raftery (2000), Hurvich and Tsai (1989), and Liang and Zou (2008) for information criterion measures.

In each chapter, the measure class is introduced, particular metrics are listed, and commentary is provided on how and when to use the measures. Recommendations for choosing measures are discussed in Chapter 20.

Part III: Models Part III is a deep dive into machine learning models for solving survival analysis problems. This begins with ‘classical’ models that may not be considered ‘machine learning’ and then continues by exploring different classes of machine learning models including random forests, support vector machines, gradient boosting machines, neural networks, and other less common classes. Each model class is introduced in the simpler regression setting and then extensions to survival analysis are discussed. Differences between

model implementations are not discussed, instead the focus is on understanding how these models are built for survival analysis - in this way readers are well-equipped to independently follow individual papers introducing specific implementations.

Part IV: Reduction Techniques The next part of the book introduces reduction techniques in survival analysis, which is the process of solving the survival analysis task by using methods from other fields. In particular, chapters focus on demonstrating how any survival model can be used in the competing risks setting, discrete time modelling, Poisson methods, pseudovalues (reduction to regression), and other advanced modelling methods.

Part V: Extensions and Outlook The final part of the book provides some miscellaneous chapters that may be of use to readers. The first chapter lists common practical problems that occur when running survival analysis experiments and solutions that we have found useful. The next lists open-source software at the time of writing for running machine learning survival analysis experiments. The final chapter is our outlook on survival analysis and where the field may be heading.

Citing this book

Whilst this book remains a work in progress you can cite it as

Sonabend. R, Bender. A. (2025). Machine Learning in Survival Analysis.
<https://www.mlsabook.com>.

```
@book{MLSA2025
  title = {Machine Learning in Survival Analysis},
  editor = {Raphael Sonabend, Andreas Bender},
  url = {https://www.mlsabook.com},
  year = {2025}
}
```

Please see the front page of the book website (<https://www.mlsabook.com>) for full licensing details.

We hope you enjoy reading this book.

Raphael and Andreas

Authors

Raphael Sonabend is the CEO and Co-Founder of OSPO Now, a company providing virtual open-source program offices as a service. They are also a Visiting Researcher at Imperial College London. Raphael holds a PhD in statistics, specializing in machine learning applications for survival analysis. They created the R packages `mlr3proba`, `survivalmodels`, and the Julia package `SurvivalAnalysis.jl`. Raphael co-edited and co-authored *Applied Machine Learning Using mlr3 in R* (Bischl et al. 2024).

Andreas Bender is...

Acknowledgments

We would like to gratefully acknowledge our colleagues that reviewed the content of this book, including: Lukas Burk, Cesaire Fouodo.

Symbols and Notation

The most common symbols and notation used in this book are presented below. We will do our best to stick to these throughout but any deviations will be made clear from context.

Matrices and vectors

A lower-case letter in normal font, x , refers to a single, fixed observation. When in bold font, a lower-case letter, \mathbf{x} , refers to a vector of fixed observations, and an upper-case letter, \mathbf{X} , represents a matrix. Calligraphic letters, \mathcal{X} , are used to denote sets.

A matrix will always be defined with its dimensions using the notation, $\mathbf{X} \in \mathcal{X}^{n \times p}$, or if for example \mathcal{X} is the set of Reals, it may be written as “ \mathbf{X} is a $n \times p$ Real-valued matrix”, analogously for matrices of Integers, Naturals, etc. By default, a ‘vector’ will refer to a column vector, which may be thought of as a matrix with n rows and one column, and may be represented as:

$$\mathbf{x} = \begin{pmatrix} x_1 \\ x_2 \\ \vdots \\ x_n \end{pmatrix}$$

Vectors are usually defined using transpose notation, for example the vector above may instead be written as $\mathbf{x}^\top = (x_1 \ x_2 \cdots x_n)$ or $\mathbf{x} = (x_1 \ x_2 \cdots x_n)^\top$. Vectors may also be defined in a shortened format as $\mathbf{x} \in \mathcal{X}^n$, which implies a column vector of length n with elements as represented above.

Let $\mathbf{X} \in \mathcal{X}^{n \times p}$ be a matrix. A letter in normal font with two subscripts is used to reference a single element of a matrix, for example $x_{i,j} \in \mathcal{X}$ would be the element in the i th row and j th column of \mathbf{X} . A bold-face, lower-case letter with a single subscript refers to a row of a matrix, for example the i th row of \mathbf{X} would be $\mathbf{x}_i = (x_{i,1} \ x_{i,2} \cdots x_{i,p})^\top$. Note that whilst \mathbf{x}_i refers to the row of a matrix, we continue to use the column vector notation to maintain the convention that vectors are column-vectors. A column is referenced with a dot in place of the row index, for example the j th column of \mathbf{X} would be $\mathbf{x}_{\cdot j} = (x_{1,j} \ x_{2,j} \cdots x_{n,j})^\top$. A letter in normal font with one subscript refers to a single element from a vector. For example, given $\mathbf{x} \in \mathcal{X}^n$, the i th element is denoted x_i .

Functions

Typically, a ‘hat’, \hat{x} , will refer to the prediction or estimation of a variable, x , with bold-face used again to represent vectors. A ‘bar’, \bar{x} , refers to the sample mean of a vector \mathbf{x} . Capital letters in normal font, X , refer to scalar or vector random variables, which will be made clear from context. $\mathbb{E}(X)$ is the expectation of the random variable X .

$f : \mathcal{A} \rightarrow \mathcal{B}$ denotes a function f from some domain \mathcal{A} to some codomain \mathcal{B} . Given a random variable, X , then f_X denotes the probability density function, and analogously for other distribution defining functions such as the cumulative distribution function, survival function, etc. In the context of probability distributions, a subscript 0 refers to a baseline function, for example, S_0 is the baseline survival function.

Finally, \exp , refers to the exponential function, $f(x) = e^x$, and \log refers to the natural logarithm $\ln(x) = \log_e(x)$.

Variables and acronyms

Common variables and acronyms used in the book are given in Table 0.1 and Table 0.2 respectively.

Table 0.1: Common variables used throughout the book.

Variable	Definition
$\mathbb{R}, \mathbb{R}_{>0}, \mathbb{R}_{\geq 0}, \bar{\mathbb{R}}$	Set of Reals, positive Reals (excluding zero), non-negative Reals (including zero), and Reals including $\pm\infty$.
$\mathbb{N}_0, \mathbb{N}_{>0}$	Set of Naturals and positive Naturals (excluding zero).
$(\mathbf{X}, \mathbf{t}, \boldsymbol{\delta})$	Survival data where $\mathbf{X} \in \mathbb{R}^{n \times p}$ is a real-valued matrix of n observations (rows) and p features (columns), $\mathbf{t} \in \mathbb{R}^n$ is a vector of observed outcome times, and $\boldsymbol{\delta} \in \mathbb{N}_0^n$ is a vector of observed outcome indicators.
$\boldsymbol{\beta}$	Vector of model coefficients/weights, $\boldsymbol{\beta} \in \mathbb{R}^p$.
$\boldsymbol{\eta}$	Vector of linear predictors, $\boldsymbol{\eta} = (\eta_1 \ \eta_2 \ \dots \ \eta_n)^\top$, where $\boldsymbol{\eta} = \mathbf{X}\boldsymbol{\beta}$ and $\eta_i = \mathbf{x}_i^\top \boldsymbol{\beta}$.
$\mathcal{D}, \mathcal{D}_{train}, \mathcal{D}_{test}$	Dataset, training data, and testing data.

Table 0.2: Common acronyms used throughout the book.

Acronym	Definition
AFT	Accelerated Failure Time
CDF	Cumulative Distribution Function
CPH	Cox Proportional Hazards
GBM	Gradient Boosting Machine
IPC(W)	Inverse Probability of Censoring (Weighted)
ML	Machine Learning
PDF	Probability Density Function

Acronym	Definition
PH	Proportional Hazards
RSF	Random Survival Forest
(S)SVM	(Survival) Support Vector Machine

1

Introduction

This chapter introduces the foundations of machine learning survival analysis and motivates why time-to-event data require methods beyond standard regression and classification. Survival analysis is framed as a general paradigm for modeling the timing of events that may be incompletely observed due to censoring, with applications spanning medicine, engineering, and economics. The chapter begins to clarify key distinctions between survival analysis, event history analysis, and conventional supervised learning (regression and classification). In addition, the chapter starts to outline the prediction tasks that appear throughout the book including predicting survival distributions, time-to-event, and relative risks. Particular attention is given to censoring, truncation, competing risks, and common biases such as delayed entry and immortal time bias. The chapter concludes with a start-to-finish overview of a machine learning survival analysis workflow, providing a conceptual roadmap that sets the stage for the methodological developments in the remainder of the book.



Minor changes expected!

This page is a work in progress and minor changes will be made over time.

In the broadest sense, survival analysis is concerned with predicting the time until an event occurs. This definition will be refined in this chapter and Part I. Survival analysis has important applications to fields that directly impact day-to-day life, including healthcare, finance, and engineering. Machine learning techniques can identify patterns and make predictions on unseen data, even in very large datasets with many covariates and/or large sample sizes. Despite this, the canonical machine learning texts focus almost entirely on regression and classification (Bishop 2006; Hastie, Tibshirani, and Friedman 2001; James et al. 2013). There are also excellent books dedicated to survival analysis, such as Collett (2014) and John D. Kalbfleisch and Prentice (1980), but they do not include modern machine learning algorithms such as random forests, neural networks or gradient boosting machines. To-date, the most comprehensive treatment for the combined fields is a light-touch but comprehensive survey in P. Wang, Li, and Reddy (2019). Using regression or classification models to solve problems based on survival datasets can lead to biased results as they poorly capture ‘censored’ observations – those subjects that do not experience the event of interest within an observation window. This book is intended to bridge the gap between survival analysis and machine learning to formalize and demystify the combined field of ‘machine learning survival analysis’.

This book is focused entirely on survival predictions for observations given some variables (‘supervised learning’), this book does not cover in-sample estimation, predicting ‘remaining lifetime’ for censored observations, nor pattern recognition methods such as clustering.

1.1 Defining Machine Learning Survival Analysis

This chapter highlights the importance of survival analysis and why predictions in a survival setting differ from regression and classification. Some motivating examples are first provided and then important concepts for survival analysis and machine learning are introduced.

1.1.1 Survival analysis

The term survival analysis highlights the field's close relation to medical statistics and in particular predicting survival times (the time until death). However, this is certainly not the only application of the field. In engineering, the field is often referred to as *reliability analysis*, as a common task is predicting the reliability of a component in a machine, for example predicting when an engine in a plane needs to be replaced. In economics, the term *duration analysis* is often found, and in other areas *failure-time analysis* may also be used.

In Chapter 3, 'survival analysis' is introduced to specifically refer to the case when the event of interest can occur exactly once, for example, predicting when a patient may die after diagnosis of Stage IV non-small cell lung cancer. In Chapter 4, 'event history analysis' is defined, which is a generalization of survival analysis to the case when one or more events can occur one or more times, for example, predicting when a patient will have relapses of multiple sclerosis. To align with common practice, the term 'survival analysis' is used throughout the book and context will make clear when the more general event history methods apply.

One of the key aims in this book is to highlight the ubiquitous nature of survival analysis and to encourage more machine learning practitioners to use survival analysis when appropriate. Machine learning practitioners are likely familiar with regression and classification. However, there are many cases when survival analysis should be used instead, for example at your local bus stop...

Waiting for a bus

Every day you are making survival predictions. For example, by guessing how long it will take before a bus arrives at your stop. At first glance, this might appear to be a regression problem, as regression is tasked with making continuous predictions. However, regression analysis assumes the outcome is always observed. In this example, a regression model would assume you are predicting when the bus will arrive based on the knowledge you have about how long it usually takes to arrive. In reality, that is unlikely to be the true dataset you have built in your mind. It is possible that on many occasions after waiting five minutes you decide to walk instead. On that day, these five minutes are your *observation period*, the period for which you are monitoring observations (bus arrivals). In principle, even if your exact bus broke down or was diverted, eventually a bus on your route will arrive at that stop. However, by leaving the bus stop, you no longer know when it will arrive, you just know it took at least five minutes. In this example, five minutes is known as the *censoring time*, it represents the amount of time that was observed without the event taking place.

A defining characteristic of survival analysis is that censored observations are used for model training, not dismissed as missing data. In other words, whilst your bus did not arrive, it is still a learning opportunity to know it took at least five minutes.

Figure 1.1 illustrates these concepts, where the bottom, red bus arrives two minutes after leaving the previous stop. Whereas it took the top, blue bus four minutes between leaving

the previous bus stop and breaking down.

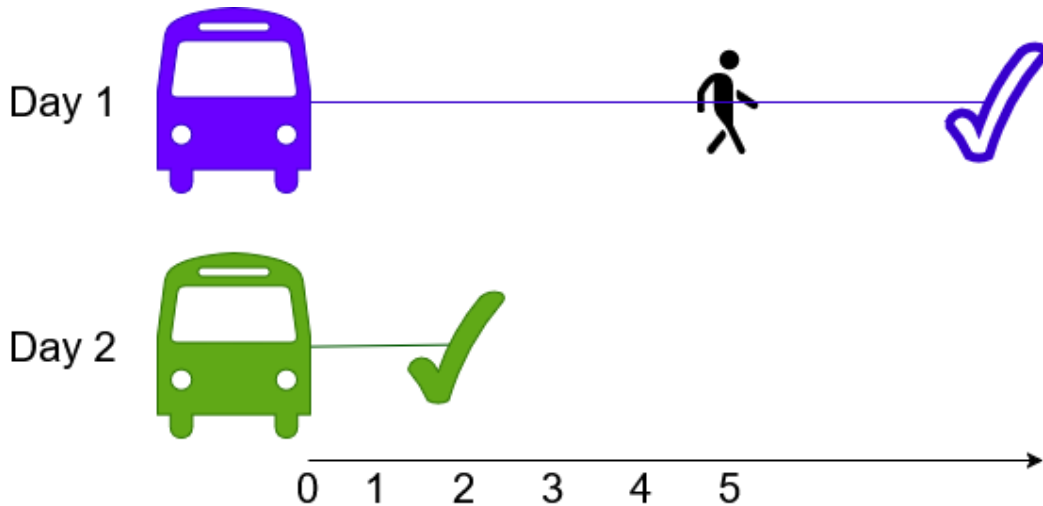


Figure 1.1: Demonstrating censoring across two days of waiting at the bus stop. On the first day, the person stops waiting for their bus at five minutes so the bus is ‘censored’ at this time, the true arrival time is unknown but is greater than five minutes. On the second day, the bus is known to arrive after two minutes.

Hospital prioritization

As well as survival distribution predictions, another common task in survival analysis is to rank observations or separate them into risk groups, for example to allocate resources. Take the example of prioritizing when patients are seen in an emergency department. A patient presents with a set of symptoms and is compared to all other patients arriving at the emergency department. Their symptoms are assessed to understand how urgently they need to receive help and how their level of risk compares to others. This is again a survival prediction where the event of interest is escalation of care, and reasons for censoring might include the patient leaving before being seen. As will be seen in Chapter 5, risk rankings are mathematically tied to survival distributions.

T-year survival probabilities

The bus example highlighted the relationship between survival analysis and regression. This example examines the close connection to classification. Suppose an elderly man is diagnosed with prostate cancer, the oncologist might tell him (in some softer words) “the ten-year survival rate of cancer in 75-year old males is 67.5%”. This initially appears as a probabilistic classification problem as the clinician is implicitly saying “if we look at who did or did not die from prostate cancer (the outcome), given a sample of similar people (the covariates), then approximately 67.5% survived”. But in the real-world, data is rarely this clean and there will be many patients in a dataset for whom it is unknown if they did or not die from their cancer 10 years from diagnosis. Perhaps because they moved abroad, died of another cause, or simply stopped turning up for appointments – each of these is a censoring event. Once again, using techniques from survival analysis would allow more precise modelling of these censored observations. In fact, one can actually use a combination of classification and survival analysis methods through reductions and this will be returned to in Section 18.2.

1.1.2 Machine learning survival analysis

Machine learning is an interdisciplinary field primarily concerned with building models that learn structure from data, for example to predict outputs from inputs or to identify patterns within observed data (Hastie, Tibshirani, and Friedman 2001). Defining if a model should be called ‘machine learning’ is surprisingly difficult; there is no clear boundary separating ‘classical’ statistical estimators from what are now often labelled machine learning methods. This book defines *machine learning* in a pragmatic sense to denote statistical models whose parameters or structure are learned from data by optimizing an explicit objective function and whose success is judged by empirical performance on new data. This definition tightly couples the concept of machine learning with the need for robust evaluation (Part II). This definition allows for a range of models (Part III) to be considered machine learning, such as simple linear regression. In fact, in Chapter 10 we will describe how the performance of these apparently ‘simple’ models can compare very favorably to more modern machine learning algorithms - hence their inclusion in this book.

This book focuses on the supervised learning setting, where the goal is to predict outcomes from labelled training data. Relative to other areas of supervised learning, development in survival analysis has been slow, as will be seen when discussing models in Part III. Despite this, development of models has converged on three primary tasks of interest, or *survival problems*, which are defined by the type of prediction the model makes. The mathematical definition of a machine learning survival analysis task is provided in Chapter 5. Generally, one is encountering a survival problem if training a model on data where censoring is present in order to predict one of:

- i. A *survival distribution*: The probability distribution over event times (the bus example above).
- ii. A *relative risk*: The risk of an event taking place compared to other observations in the same sample (the hospital example above).
- iii. A *survival time*: The time at which the event will take place.

Each prediction type serves a different purpose and you may require training multiple models to optimally estimate each prediction type. However, as will be seen in Chapter 5, there are mathematical methods to transform these tasks between one another. As an example, an engineer is unlikely to care about the exact time at which a plane engine fails, but they might greatly value knowing when the probability of failure increases above 5% – a survival distribution prediction. Returning to the hospital example, a physician cannot process a survival distribution prediction to make urgent decisions, but they could assign limited resources if it is clear that one patient is at substantially greater risk than another – a relative risk prediction.

When it comes to making distribution predictions, survival analysis stands out again. Common *distribution defining functions*, functions that uniquely define a probability distribution, are the probability density function (PDF) and cumulative distribution function (CDF). In survival settings, interpreting the PDF can be counter-intuitive as it is an unconditional quantity that does not account for whether the event has or has not already occurred. The CDF is the probability that the event has ‘already’ taken place at t , which is opposite to the usual survival prediction: whether the event ‘will’ take place. Therefore, survival analysis focuses instead on predicting the *survival function*, which is simply one minus the CDF, and the *hazard function*, which is the conditional rate of the event occurring at t given that the observation has survived up to t .

These functions are formally defined in Chapter 3 and are visualized in Figure 1.2 with a

Gompertz distribution, which is often chosen to model adult lifespans. The figure demonstrates the utility of the survival and hazard functions for survival analysis. The survival function (bottom right) is a decreasing function from one to zero. This is the probability of surviving until a given time, t , or equivalently the probability that the event of interest has not yet occurred. The hazard function (top right), starts at zero and is not upper-bounded at one as it is a conditional probability. Even though the PDF peaks just before 0.5, the hazard function continues to increase as it is conditioned on not having experienced the event, hence the risk of event continues to increase.

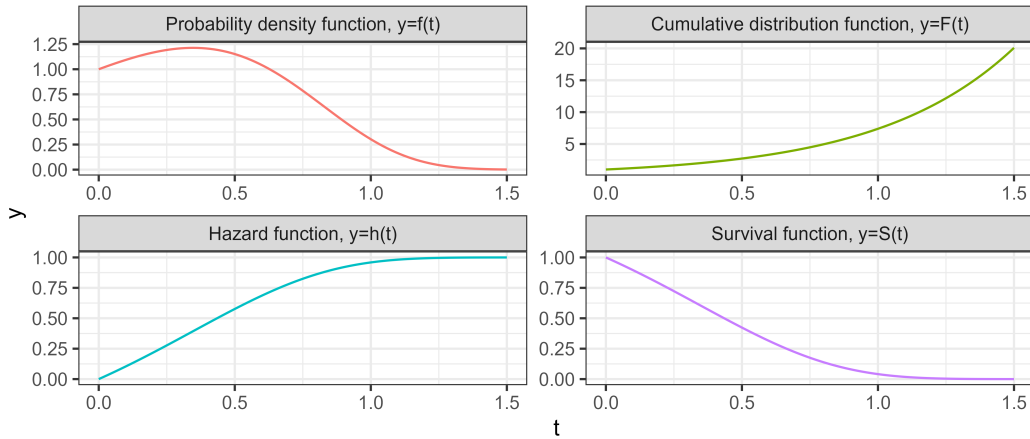


Figure 1.2: Probability density (top left), hazard (top right), cumulative density (bottom left), and survival (bottom right) functions of a Gompertz(1, 2) distribution.

1.2 Censoring and Truncation

As already discussed, censoring is a defining feature of survival analysis. In addition to censoring, survival data can include *truncation*, which means portions of follow-up time are excluded. The precise definitions of different types of censoring and truncation are provided in Chapter 3, non-technical summaries of the most common forms of censoring and truncation are provided below.

The most common form of censoring is right-censoring (Figure 1.3, second row), this occurs when the true survival time is greater than ('to the right of,' if you imagine a number line) the observed censoring time. The examples in Section 1.1 are all forms of right-censoring. Left-censoring is recorded when the event of interest is less than ('to the left of') the observed censoring time. Chapter 3 provides an example of someone telling an interviewer that they started using a phone (the event of interest) before the interview, but they do not remember when. If the time-to-event outcome is "age at first phone use" then a 23-year-old who is using a phone but cannot remember when they started, is left-censored at '23'. Right- and left-censoring can occur completely independently of the outcome of interest, or they may directly affect the outcome of interest, in which case the censoring event is known as a *competing risk* (Chapter 4). For example, if you are waiting for a bus and decide to walk after five minutes, the bus arrival time is censored as you no longer observe when it will arrive, but your decision to walk does not impact the bus in any way, it's eventual arrival

time is unchanged. In contrast, if the bus broke down, then this breakdown would be a competing risk as it directly affects its probability of arriving. Handling competing risks forms a large part of this book.

Left-truncation is the more common form of truncation and involves data before the truncation time being excluded. Left-censoring occurs because the event of interest has already happened but not known when. Left-truncation occurs because a portion of data that occurred before the study start is removed but the event of interest has not yet occurred. Another way to look at it is to note that truncation times affect enrollment into a study whereas censoring affects outcome observation.

The examples below consider how left-truncation can both cause and fix biases.

Example 1: Delayed entry Say a study looks at predicting the time until death for a patient diagnosed with tuberculosis (TB) treated with a novel treatment. The study design uses a convenience sample that means some individuals had TB from the study start and others did not. Left-truncation is present if individuals had TB before the study start. If one were to ignore left truncation, these patients would be treated as if they were diagnosed with TB on entry to the study, which could bias estimates to shorter survival times (Figure 1.3, third row). However, it would also be wrong to exclude this data as that would induce *survivorship bias*: individuals with more aggressive strains are systematically excluded and thus biasing analysis to longer survival times. A common way to account for this bias would be to model the data such that the observation period is reset to time of diagnosis and not the study entry. Specialized methods introduced in Chapter 3 should also be used.

Example 2: Selection bias Consider researchers predicting the probability of miscarriage over time for pregnant people. There will be cases of miscarriage occurring before a person finds out they are pregnant, which means data about their pregnancy will never be collected (Figure 1.3, fourth row). The first consequence of this omission is that the true number of miscarriages will be underestimated. The second consequence is that the time until miscarriage outcome will be overestimated, as earlier miscarriages are not recorded so the outcome time is skewed towards later ones. If a model were trained on this bias data then it is likely to predict the risk of miscarriage being lower than it actually is and occurring later in time.

Whilst both the previous examples involve left-truncation, the mishandling of truncation in the first example results in an analytical bias by mishandling delayed entry and can be fixed using modelling methods. The second example is an unavoidable structural bias (pregnancies/miscarriages are unobserved not just censored) and requires gathering more data or conducting sensitivity analyses.

Example 3: Immortal time bias Immortal time bias occurs when an observation in the data is guaranteed to survive a period of time (hence being ‘immortal’ in that time) by virtue of the study design (Figure 1.3, bottom row). For example, say a randomized controlled trial is conducted to test if a novel chemotherapy treatment improves survival rates from a given cancer. The trial is split into two arms, one for existing treatments and one for the novel treatment, and a patient is eligible for the novel treatment only if they have been living with cancer for two years and no other treatment has been shown to work. Finally, patients are enrolled into the study from the date of diagnosis. This dataset now includes immortal time bias as patients can only be in the novel treatment arm if they have already survived two years, whereas patients in the other arm have no such restriction. This conditioning on survival is mathematically equivalent to left-truncating the treatment arm at the eligibility time (essentially resetting ‘time zero’ to date of treatment), while not applying the same truncation to the control arm.

Hence, even if the novel treatment has no benefit, patients in the novel arm are guaranteed to have a better survival outcome (from diagnosis) as they would not have been included if they died before two years, whereas patients may die (even if by chance) in the control arm before this time (Figure 1.3). To control for this bias, one could apply the same truncation rule to both arms of the study, meaning setting ‘two years’ as the new study start time. Alternatively, patients could be randomly assigned to a treatment group at enrollment with observation throughout the initial two year period, even before treatment is provided. Detecting immortal time bias is vital, especially in randomized controlled trials to ensure novel treatments are not oversold.

Right-truncation is rare as it requires very specific, data collection methods. For example, if studying death from disease using a retrospective dataset, then right-truncation would occur if the dataset was sampled to only include observations who die; excluding observations that survived beyond the observation period.

Censoring is a mechanism to yield more useful results by recording as much data as possible. Truncation is due to the study design and may either create or remove biases in data collection/curation. The first Part of this book will continue to demystify the concepts of censoring, truncation, and prediction types.

1.3 Start to finish

To help make the concepts in this book less abstract, this section outlines what you may consider when undertaking machine learning survival analysis. There are many different ways to break down such an analysis and the following presents one such possibility:

1. Establish the research question
2. Gather relevant data
3. Describe the outcome
4. Identify censoring/truncation in the data and describe strategies for handling them
5. Describe the prediction type
6. Select metrics based on the data
7. Select models based on the data and metrics
8. Split data for model training
9. Evaluate your model

A hypothetical example is given below, it is adapted from Dennis et al. (2020). Terms and methods below will be defined throughout the rest of this book.

1. Research question Say that we are looking to predict the 30-day survival distribution for a patient with Type 2 diabetes being admitted to a critical care setting in England, UK for COVID-19.

2. Data This is clearly a retrospective study as the pandemic is in the past but there are many datasets with relevant information, such as the COVID-19 Hospitalisation in English Surveillance System (CHESS) dataset. To reduce biases that could arise from data collection (such as left-truncation biases), a fixed date of interest is set: 1 March 2020 to 27 July 2020.

3. Outcome The outcome of interest is 30-day in-hospital all-cause mortality, which is

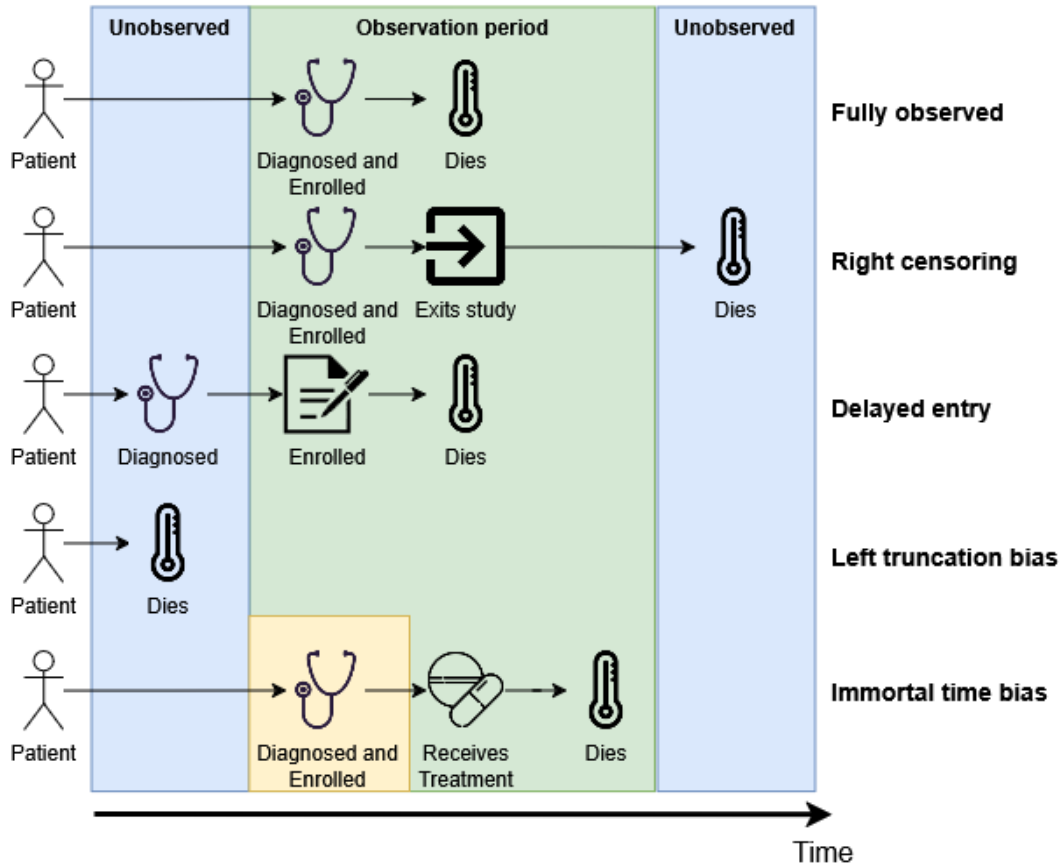


Figure 1.3: Common forms of censoring and truncation with biases. First row (fully observed patient): a patient is diagnosed with a disease and immediately enrolled into study and observed to die during the study period. Second row (right censoring): a patient is diagnosed with a disease and immediately enrolled into study but they drop-out before they die, their true survival time is unknown. Third row (left truncation, delayed entry): a patient is diagnosed before they enter the study but enrolled at a later time, they are erroneously treated as if they were diagnosed on the date of enrolment. Fourth row (left truncation selection bias): a patient dies before they enter the study and are never observed. Fifth row (immortal time bias): a patient is diagnosed with a disease and immediately enrolled into study. However, in contrast to the patient in the top row in the control group who can die at any point from enrolment, the patient in the treatment group (bottom row) cannot die between enrolment and treatment (otherwise they could not have entered the treatment group).

the risk of dying from any cause within 30 days of being admitted to hospital, meaning it can occur at most once (Chapter 3). Other potential outcomes include: discharge, loss to follow-up, patient survives to 30 days.

4. Censoring/truncation The study is focused on admissions during the observation period, thus excludes patients diagnosed with COVID-19 before 1 March 2020. Immortal time bias and survivorship bias are avoided by defining study entry as hospital admission and using a fixed 30-day observation window, with inclusion/exclusion into the study not dependent on any outcomes, treatment, patient age, illness length. Loss to follow-up is assumed to be a random, independent right-censoring event. Surviving to 30 days is an administrative right-censoring event (Chapter 3) – which means the reason for censoring is due to the observation window closing and not the patient (as in the bus example above). Discharge is a competing risk as once a patient is discharged (Chapter 4), they are no longer at risk of ‘in-hospital’ mortality.

5. Prediction types As the goal is survival probability over time, the survival task is to predict a probability distribution over the 30-day horizon (Chapter 5).

6. Metrics The task is to evaluate survival distribution predictions, whilst accounting for competing risks. Proper scoring rules (Chapter 8) are ideal for evaluating distribution predictions and the right-censored logloss is one example of a scoring rule that can be extended to evaluate predictions when competing risks are present.

7. Models The sample of interest from the CHESS dataset has over 20,000 observations with relatively few features. This means that traditional survival models (Chapter 10) can be considered alongside more modern alternatives. Given the focus on survival distribution predictions, one might start by considering a Fine and Gray model with optional boosting to improve predictions (Chapter 13). Additionally, cause-specific random survival forests with log-rank splitting might also be worth exploring (Chapter 11).

8. Data splitting Given the size of the dataset, a simple hold-out splitting strategy might suffice (Chapter 2). For example with a random subset of 15,000 observations to develop models and the rest used to evaluate model predictions. As the rate of censoring is unlikely to be too small or large (can be confirmed with exploratory analysis), stratified sampling of the data is not required.

9. Evaluation Finally, with all the above in place, the models can be trained on the same training data and then evaluated using the metrics outlined above. Once the optimal model has been found, it can be retrained on the complete dataset for feature analysis or deployment.

1.4 Reproducibility and online book

An online open-access (CC BY-NC-SA 4.0) version of this book is available for free at mlsabook.com. This book includes simulations and figures generated in R, the code for any figures or experiments in this book are freely available at <https://github.com/mlsabook/MLSA> under an MIT license.

Part I

Survival Analysis and Machine Learning

2

Machine Learning

TODO (150-200 WORDS)

 Minor changes expected!

This page is a work in progress and minor changes will be made over time.

This chapter covers core concepts in machine learning. This is not intended as a comprehensive introduction and does not cover mathematical theory nor how to run machine learning models using software. Instead, the focus is on introducing important concepts and to provide basic intuition for a general machine learning workflow. This includes the concept of a machine learning task (introduced in a survival context in Chapter 5), data splitting (resampling), model training and prediction, evaluation, and model comparison. Recommendations for more comprehensive introductions are given at the end of this chapter, including books that cover practical implementation in different programming languages.

2.1 Basic workflow

This book focuses on *supervised learning*, in which predictions are made for outcomes based on data with observed dependent and independent variables. For example, predicting someone's height is a supervised learning problem as data can be collected for features (independent variables) such as age and sex, and an observable outcome (dependent variable), which is height. Alternatives to supervised learning include *unsupervised learning*, *semi-supervised learning*, and *reinforcement learning*. This book is primarily concerned with *predictive survival analysis*, i.e., making future predictions based on (partially) observed survival outcomes, which falls naturally within the supervised learning domain.

The basic machine learning workflow is represented in Figure 2.1. Data is split into training and test datasets. A learner is selected and is trained on the training data, inducing a fitted model. The features from the test data are passed to the model which makes predictions for the unseen outcomes (Box 1). The outcomes from the test data are passed to a chosen measure with the predictions, which evaluates the performance of the model (Box 2). The process of repeating this procedure to test different training and test data is called *resampling* and running multiple resampling experiments with different models is called *benchmarking*. All these concepts will be explained in this chapter.

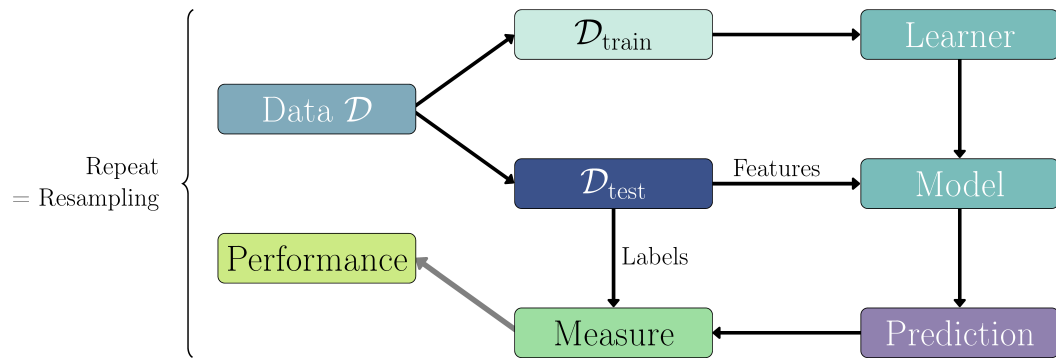


Figure 2.1: Basic machine learning workflow with data splitting, model training, predicting, and evaluating. Image from Foss and Kotthoff (2024) (CC BY-NC-SA 4.0).

2.2 Tasks

A machine learning task is the specification of the mathematical problem that is to be solved by a given algorithm. For example, “predict the height of a male, 13 year old child”, is a machine learning task. Tasks are derived from datasets and one dataset can give rise to many tasks across any machine learning domain. The dataset described by columns: ‘age’, ‘weight’, ‘height’, ‘sex’, ‘diagnosis’, ‘time of death’, ‘clinician notes’, could give rise to any of the following tasks (and more):

- Predict age from weight, height, and sex - supervised regression task
- Predict sex from age and diagnosis - supervised classification task
- Predict time of death from all other features - supervised survival task
- Categorise observations into clusters - unsupervised clustering
- Learn to speak like a clinician depending on client diagnosis - natural language processing, likely with reinforcement learning

As this book is focused on supervised learning, only the first three of these is covered in this chapter and beyond. The specification of a task is vital for interpreting predictions from a model and its subsequent performance. This is particularly true when separating between deterministic and probabilistic predictions, as discussed later in the chapter.

Formally, let $\mathbf{x} \in \mathcal{X} \subseteq \mathbb{R}^{n \times p}$ be a matrix with p features for n observations and let $y \in \mathcal{Y}$ be a vector of labels (or *outcomes* or *targets*) for all observations. A dataset is then given by $\mathcal{D} = ((\mathbf{x}_1, y_1), \dots, (\mathbf{x}_n, y_n))$ where it is assumed $\mathcal{D} \stackrel{i.i.d.}{\sim} (\mathbb{P}_{xy})^n$ for some unknown distribution \mathbb{P} .

A machine learning task is the problem of learning the unknown function $f : \mathcal{X} \rightarrow \mathcal{Y}$ where \mathcal{Y} specifies the nature of the task, for example classification, regression, or survival.

2.2.1 Regression

Regression tasks make continuous predictions, for example someone’s height. Regression may be deterministic, in which case a single continuous value is predicted, or probabilistic, where a probability distribution over the Reals is predicted. For example, predicting an individual’s height as 165cm would be a deterministic regression prediction, whereas predicting their

height follows a $\mathcal{N}(165, 2)$ distribution would be probabilistic.

Formally, a deterministic regression task is specified by $f_{Rd} : \mathcal{X} \rightarrow \mathcal{Y} \subseteq \mathbb{R}^n$, and a probabilistic regression task by $f_{Rp} : \mathcal{X} \rightarrow \mathcal{S}$ where $\mathcal{S} \subset \text{Distr}(\mathcal{Y})$ and $\text{Distr}(\mathcal{Y})$ is the space of distributions over \mathcal{Y} .

In machine learning, deterministic regression is much more common than probabilistic and hence the shorthand ‘regression’ is used to refer to deterministic regression (in contrast to statistical modeling, where regression usually implies probabilistic regression).

2.2.2 Classification

Classification tasks make discrete predictions, for example whether it will rain, snow, or be sunny tomorrow. Similarly to regression, predictions may be deterministic or probabilistic. Deterministic classification predicts which category an observation falls into, whereas probabilistic classification predicts the probability of an observation falling into each category. Predicting it will rain tomorrow is a deterministic prediction whereas predicting $\hat{p}(\text{rain}) = 0.6; \hat{p}(\text{snow}) = 0.1; \hat{p}(\text{sunny}) = 0.3$ is probabilistic.

Formally, a deterministic classification task is given by $f_{Cd} : \mathcal{X} \rightarrow \mathcal{Y} \subseteq \mathbb{N}_0$, and a probabilistic classification task as $f_{Cp} : \mathcal{X} \rightarrow \mathcal{Y} \subseteq [0, 1]^k$ where k is the number of categories an observation may fall into. Practically this latter prediction is estimation of the probability mass function $\hat{p}_Y(y) = P(Y = y)$. If only two categories are possible, these reduce to the *binary classification* tasks: $f_{Bd} : \mathcal{X} \rightarrow \{0, 1\}$ and $f_{Bp} : \mathcal{X} \rightarrow [0, 1]$ for deterministic and probabilistic binary classification respectively.

Note that in the probabilistic binary case it is common to write the task as predicting $[0, 1]$ not $[0, 1]^2$ as the classes are mutually exclusive. The class for which probabilities are predicted is referred to as the *positive class*, and the other as the *negative class*.

2.3 Training and predicting

The terms *algorithm*, *learner*, and *model* are often conflated in machine learning. A *learner* is a description of a learning algorithm, prediction algorithm, parameters, and hyperparameters. The *learning algorithm* is a mathematical strategy to estimate the unknown mapping from features to outcome as represented by a task, $f : \mathcal{X} \rightarrow \mathcal{Y}$. During *training*, data, \mathcal{D} , is fed into the learning algorithm and induces the *model* \hat{f} . Whereas the learner defines the algorithm for training and prediction, the model is the result of training the algorithm on data.

After training the model, new data, \mathbf{x}^* , can be fed to the *prediction algorithm*, which is a mathematical strategy that uses the model to make predictions $\hat{\mathbf{y}} = \hat{f}(\mathbf{x}^*)$. Algorithms can vary from simple linear equations with coefficients to estimate, to complex iterative procedures that differ considerably between training and predicting.

Algorithms usually involve parameters and hyperparameters. Parameters are learned from data whereas hyperparameters are set beforehand to guide the algorithms. Model *parameters* (or *weights*), $\boldsymbol{\theta}$, are coefficients to be estimated during model training. Hyperparameters, $\boldsymbol{\lambda}$, control how the algorithms are run but are not directly updated by them. Hyperparameters can be mathematical, for example the learning rate in a gradient boosting machine (Chapter 13), or structural, for example the depth of a decision tree (Chapter 11). The number of hyperparameters usually increases with learner complexity and affects its predictive

performance. Often hyperparameters need to be tuned (Section 2.5) instead of manually set. Computationally, storing $(\hat{\boldsymbol{\theta}}, \lambda)$ is sufficient to recreate any trained model.

Box 1 (Ridge regression)

Let $f : \mathcal{X} \rightarrow \mathcal{Y}$ be the regression task of interest with $\mathcal{X} \subseteq \mathbb{R}$ and $\mathcal{Y} \subseteq \mathbb{R}$. Let $(\mathbf{x}, \mathbf{y}) = ((x_1, y_1), \dots, (x_n, y_n))$ be data such that $x_i \in \mathcal{X}$ and $y_i \in \mathcal{Y}$ for all $i = 1, \dots, n$. Say the **learner** of interest is a regularized linear regression model with **learning algorithm**:

$$(\hat{\beta}_0, \hat{\beta}_1) := \arg \min_{\beta_0, \beta_1} \left\{ \sum_{i=1}^n (y_i - (\beta_0 + \beta_1 x_i))^2 + \gamma \beta_1^2 \right\}.$$

and **prediction algorithm**:

$$\hat{f}(\phi) = \hat{\beta}_0 + \hat{\beta}_1 \phi$$

The **hyperparameters** are $\lambda = (\gamma \in \mathbb{R}_{>0})$ and the **parameters** are $\boldsymbol{\theta} = (\beta_0, \beta_1)^\top$. Say that $\gamma = 2$ is set and the learner is then trained by passing (\mathbf{x}, \mathbf{y}) to the learning algorithm and thus estimating $\hat{\boldsymbol{\theta}}$ and \hat{f} . A **prediction**, can then be made by passing new data $x^* \in \mathcal{X}$ to the fitted model: $\hat{y} := \hat{f}(x^*) = \hat{\beta}_0 + \hat{\beta}_1 x^*$.

2.4 Evaluating and benchmarking

To understand if a model is ‘good’, its predictions are evaluated with a *loss function*. Loss functions assign a score to the discrepancy between predictions and true values, $L : \mathcal{Y} \times \mathcal{Y} \rightarrow \bar{\mathbb{R}}$. Given (unseen) real-world data, $(\mathbf{X}^*, \mathbf{y}^*)$, and a trained model, \hat{f} , the loss is given by $L(\hat{f}(\mathbf{X}^*), \mathbf{y}^*) = L(\hat{\mathbf{y}}, \mathbf{y}^*)$. For a model to be useful, it should perform well in general, meaning its generalization error should be low. The *generalization error* refers to the model’s performance on new data, rather than just the data encountered during training and development.

A model should only be used to make predictions if its generalization error was estimated to be acceptable for a given context. If a model were to be trained and evaluated on the same data, the resulting loss, known as the *training error*, would be an overoptimistic estimate of the true generalization error (James et al. 2013). This occurs as the model is making predictions for data it has already ‘seen’ and the loss is therefore not evaluating the model’s ability to generalize to new, unseen data. Another reason for data splitting is to help mitigate model overfitting, which occurs when models learn noise in the training data leading them to perform worse on new data. This can be avoided using data splitting methods, feature engineering (manually or using built-in machine learning methods) to remove noisy features, and early stopping which stops training a model once a certain performance has been reached.

Estimation of the generalization error requires *data splitting*, which is the process of splitting available data, \mathcal{D} , into *training data*, $\mathcal{D}_{train} \subset \mathcal{D}$, and *testing data*, $\mathcal{D}_{test} = \mathcal{D} \setminus \mathcal{D}_{train}$.

The simplest method to estimate the generalization error is to use *holdout resampling*, which is the process of partitioning the data into one training dataset and one testing dataset,

with the model trained on the former and predictions made for the latter. Using 2/3 of the data for training and 1/3 for testing is a common splitting ratio (Kohavi 1995). For independent and identically distributed (iid) data, it is generally best practice to partition the data randomly. This ensures that any potential patterns or information encoded in the ordering of the data are removed, as such patterns are unlikely to generalize to new, unseen data. For example, in clinical datasets, the order in which patients enter a study might inadvertently encode latent information such as which doctor was on duty at the time, which could theoretically influence patient outcomes. As this information is not explicitly captured in measured features, it is unlikely to hold predictive value for future patients. Random splitting breaks any spurious associations between the order of data and the outcomes.

When data is not iid, for example spatially correlated or time-series data, then random splitting may not be advisable, see Hornung et al. (2023) for an overview of evaluation strategies in non-standard settings.

Holdout resampling is a quick method to estimate the generalization error, and is particularly useful when very large datasets are available. However, hold-out resampling has a very high variance for small datasets and there is no guarantee that evaluating the model on one hold-out split is indicative of real-world performance.

k-fold cross-validation (CV) can be used as a more robust method to better estimate the generalization error (Hastie, Tibshirani, and Friedman 2001). *k*-fold CV partitions the data into *k* subsets, called *folds*. The training data comprises of $k - 1$ of the folds and the remaining one is used for testing and evaluation. This is repeated *k* times until each of the folds has been used exactly once as the testing data. The performance from each fold is averaged into a final performance estimate (Figure 2.2). It is common to use $k = 5$ or $k = 10$ (Leo Breiman and Spector 1992; Kohavi 1995). This process can be repeated multiple times (*repeated k-fold CV*) and/or *k* can even be set to *n*, which is known as *leave-one-out cross-validation*.

Cross-validation can also be stratified, which ensures that a variable of interest will have the same distribution in each fold as in the original data. This is important, and often recommended, in survival analysis to ensure that the proportion of censoring in each fold is representative of the full dataset (Casalicchio and Burk 2024; Herrmann et al. 2021).

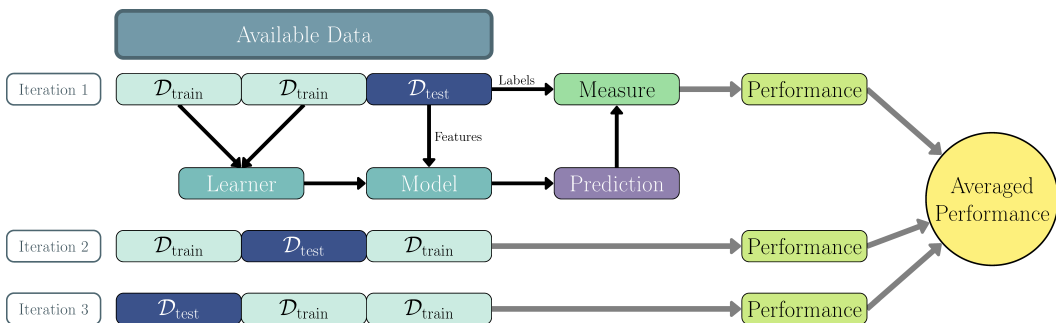


Figure 2.2: Three-fold cross-validation. In each iteration a different dataset is used for predictions and the other two for training. The performance from each iteration is averaged into a final, single metric. Image from Casalicchio and Burk (2024) (CC BY-NC-SA 4.0).

Repeating resampling experiments with multiple models is referred to as a *benchmark experiment*. A benchmark experiment compares models by evaluating their performance on *identical* data, which means the same resampling strategy and folds should be used for all models. Determining if one model is actually better than another is a surprisingly complex

topic (Benavoli et al. 2017; Demšar 2006; Dietterich 1998; Nadeau and Bengio 2003) and is out of scope for this book, instead any benchmark experiments performed in this book are purely for illustrative reasons and no results are expected to generalize outside of these experiments. A common heuristic is to suggest one model outperforms another if it performs better across all folds in a repeated cross-validation benchmark experiment, however this is just a heuristic and without robust hypothesis testing results should be interpreted with caution.

Box 2 (Evaluating ridge regression)

Let $\mathcal{X} \subseteq \mathbb{R}$ and $\mathcal{Y} \subseteq \mathbb{R}$ and let $(\mathbf{x}^*, \mathbf{y}^*) = ((x_1^*, y_1^*), \dots, (x_m^*, y_m^*))$ be data previously unseen by the model trained in Box 1 where $x_i \in \mathcal{X}$ and $y_i \in \mathcal{Y}$ for all $i = 1, \dots, m$.

Predictions are made by passing \mathbf{x}^* to the fitted model yielding $\hat{\mathbf{y}} = (\hat{y}_1, \dots, \hat{y}_m)$ where $\hat{y}_i := \hat{f}(x_i^*) = \hat{\beta}_0 + \hat{\beta}_1 x_i^*$.

Say the mean absolute error is used to evaluate the model, defined by

$$L(\phi, \varphi) = \frac{1}{n} \sum_{i=1}^n |\phi_i - \varphi_i|$$

where $(\phi, \varphi) = ((\phi_1, \varphi_1), \dots, (\phi_n, \varphi_n))$.

The model's predictive performance is then calculated as $L(\hat{\mathbf{y}}, \mathbf{y}^*)$.

2.5 Hyperparameter Optimization

Section 2.3 introduced model hyperparameters, which control how training and prediction algorithms are run. Setting hyperparameters is a critical part of model fitting and can significantly change model performance. *Tuning* is the process of using internal benchmark experiments to automatically select the optimal hyper-parameter configuration. For example, the regularization parameter, γ , in ridge regression is a potential hyperparameter to tune. This hyperparameter may be tuned over a range of values, say $[0.1, 25]$ or over a discrete subset, say $\{0.1, 10, 25\}$, for now assume the latter. Three ridge regression models with $\gamma = 0.1$, $\gamma = 10$, and $\gamma = 25$ respectively are compared in a benchmark experiment. The value of γ that results in the model with the optimal performance is then selected for the hyperparameter value going forward. *Nested resampling* is a common method to reduce bias that could occur from using overlapping data for tuning, training, or testing (R. Simon 2007). Nested resampling is the process of resampling the training set again for tuning and then the optimal model is refit on the entire training data (Figure 2.3).

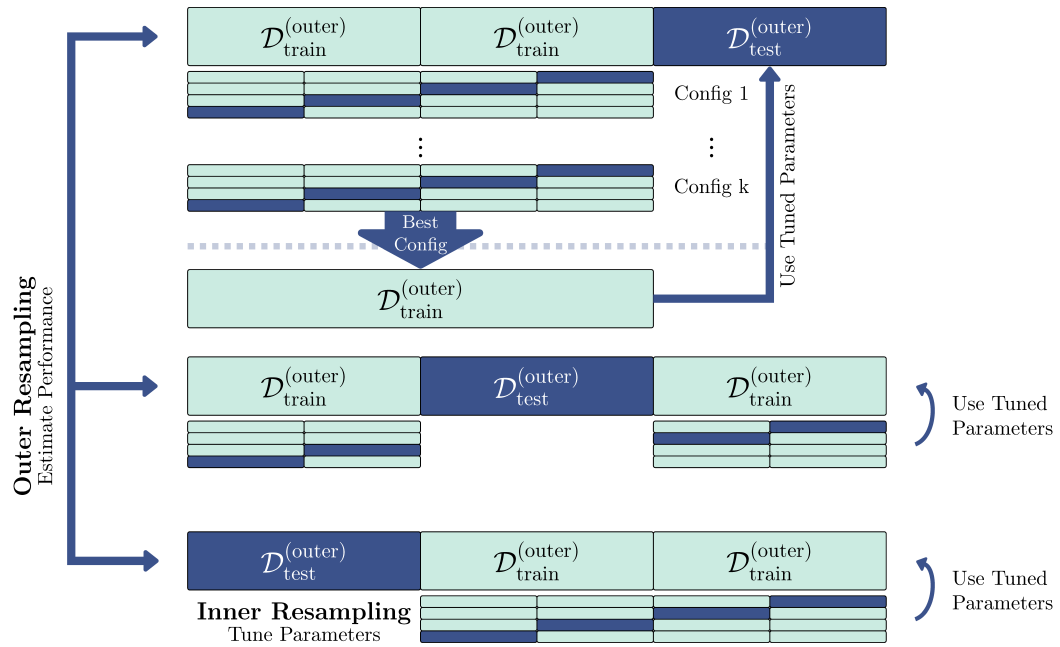


Figure 2.3: An illustration of nested resampling. The large blocks represent three-fold CV for the outer resampling for model evaluation and the small blocks represent four-fold CV for the inner resampling for hyperparameter optimization. The light blue blocks are the training sets and the dark blue blocks are the test sets. Image and caption from Becker, Schneider, and Fischer (2024) (CC BY-NC-SA 4.0).

2.6 Conclusion

Key takeaways

- Machine learning tasks define the predictive problem of interest;
- Regression tasks make predictions for continuous outcomes, such as the amount of rain tomorrow;
- Classification tasks make predictions for discrete outcomes, such as the predicted weather tomorrow;
- Both regression and classification tasks may make deterministic predictions (a single number or category), or probabilistic predictions (the probability of a number or category);
- Models have parameters that are fit during training and hyperparameters that are set or tuned;
- Models should be evaluated on resampled data to estimate the generalization error to understand future performance.

Further reading

- *The Elements of Statistical Learning* (Hastie, Tibshirani, and Friedman 2001), *An Introduction to Statistical Learning* (James et al. 2013), and *Pattern Recognition and Machine Learning* (Bishop 2006) for comprehensive introductions and overviews to machine learning.
- *Applied Machine Learning Using mlr3 in R* (Bischl et al. 2024) and *Tidy Modeling* (Kuhn and Silge 2023) for machine learning in R
- *Hands-on Machine Learning with Scikit-Learn, Keras, and TensorFlow* (Géron 2019) for machine learning in Python.
- Bischl et al. (2012) for discussions about more resampling strategies including bootstrapping and subsampling.

3

Survival Analysis

TODO (150-200 WORDS)

 Minor changes expected!

This page is a work in progress and minor changes will be made over time.

Survival Analysis is concerned with data where the outcome is the time until an event takes place (a ‘time-to-event’). Because the collection of such data takes place in the temporal domain (it takes time to observe a duration), the event of interest is often unobservable, for example because it did not occur by the end of the data collection period. In survival analysis terminology this is referred to as *censoring*.

This chapter defines basic terminology and mathematical definitions in survival analysis, which are used throughout this book. Building upon this chapter, Chapter 4 introduces event-history analysis, which is a generalization to settings with multiple, potentially competing or recurrent events, including multi-state outcomes. Concluding this part of the book, Chapter 5 defines different prediction tasks in survival analysis.

While these definitions and concepts are not new to survival analysis, it is imperative they are understood to build successful models. Evaluation functions (Part II) can identify if one model is better suited than another to minimize a given objective function, however they cannot identify if the objective function itself was specified correctly, which depends on the assumptions about the data generating process. Evaluating models with the wrong objective function yields meaningless results. Hence, it is of utmost importance for machine learning practitioners to be able identify and specify the survival problem present in their data correctly to ensure models are correctly fit and evaluated.

3.1 Quantifying the Distribution of Event Times

This section introduces functions that can be used to fully characterize a probability distribution, particular focus is given to functions that are important in survival analysis.

Note that we can generally distinguish between events taking place in discrete time or continuous time. For example, consider the time a politician serves in parliament. If we consider the number of election cycles they stay in parliament, it would constitute discrete time, as time can only take values, $1, 2, 3, \dots$, that is $Y \in \mathbb{N}_{>0}$. On the other hand, the time

an individual stays in hospital is usually determined as the difference between the admission date-time and discharge date-time, which would constitute a continuous time $Y \in \mathbb{R}_{\geq 0}$.

In practice the differences are often blurred as time-measurement will naturally be discretized at some level and precision beyond some resolution is often not of interest (hospital length of stay might be interesting up to days or hours, but not minutes and seconds). Also discrete-time methods are often applied to continuous time data and vice versa. It is nevertheless important to make the distinction as it informs mathematical treatment and definition of the different quantities introduced below.

3.1.1 Continuous Time

For now, assume a continuous, positive, random variable Y taking values in $\mathbb{R}_{\geq 0}$. A standard representation of the distribution of Y is given by the probability density function (pdf), $f_Y : \mathbb{R}_{\geq 0} \rightarrow \mathbb{R}_{\geq 0}$, and cumulative distribution function (cdf), $F_Y : \mathbb{R}_{\geq 0} \rightarrow [0, 1]$; $F_Y(\tau) = P(Y \leq \tau)$.

In survival analysis, it is more common to describe the distribution of event times Y via the *survival function* and *hazard function* (or *hazard rate*) rather than the pdf or cdf. The survival function is defined as

$$S_Y(\tau) = P(Y > \tau) = \int_{\tau}^{\infty} f_Y(u) \, du, \quad (3.1)$$

which is the probability that an event has not occurred by $\tau \geq 0$ and thus the complement of the cdf: $S_Y(\tau) = 1 - F_Y(\tau)$. By definition, $S_Y(0) = 1$ and $S(\tau) \rightarrow 0$ for $\tau \rightarrow \infty$.

The hazard function is given by

$$\begin{aligned} h_Y(\tau) &= \lim_{d\tau \searrow 0} \frac{P(\tau \leq Y < \tau + d\tau | Y \geq \tau)}{d\tau} \\ &= \lim_{d\tau \searrow 0} \frac{P(Y \in [\tau, \tau + d\tau] | Y \geq \tau)}{d\tau} \\ &= \frac{f_Y(\tau)}{S_Y(\tau)} \end{aligned} \quad (3.2)$$

where $d\tau$ denotes a time-interval. The hazard rate is often interpreted as the instantaneous risk of observing an event at τ , given that the event has not been observed before τ . This is not a probability and h_Y can be greater than one.

The cumulative hazard function can be derived from the hazard function by

$$H_Y(\tau) = \int_0^{\tau} h_Y(u) \, du, \quad (3.3)$$

and relates to the survival function via

$$\begin{aligned} H_Y(\tau) &= \int_0^{\tau} h_Y(u) \, du = \int_0^{\tau} \frac{f_Y(u)}{S_Y(u)} \, du \\ &= \int_0^{\tau} -\frac{S'_Y(u)}{S_Y(u)} \, du = -\log(S_Y(\tau)) \end{aligned}$$

These last relationships are particularly important, as many methods estimate the hazard rate, which is then used to calculate the cumulative hazard and survival probability

$$S_Y(\tau) = \exp(-H_Y(\tau)) = \exp\left(-\int_0^\tau h_Y(u) \, du\right) \quad (3.4)$$

Unless necessary to avoid confusion, subscripts are dropped from S_Y, h_Y etc. going forward and instead these functions are referred to as S, h (and so on).

Usual regression techniques cannot be used to estimate these quantities as Y is only partially observed, due to different types of censoring and truncation (see Section 3.2, Section 3.3, Section 3.4).

3.1.2 Discrete Time

Now let \tilde{Y} be a discrete, positive random variable that represents discrete or discretized time, taking values in $\mathbb{N}_{>0}$; and $\tau \in \mathbb{N}_{>0}$ some time point in discrete time.

The discrete-time hazard rate is defined as

$$h_{\tilde{Y}}^d(\tau) = P(\tilde{Y} = \tau | \tilde{Y} \geq \tau). \quad (3.5)$$

Thus, in contrast to the continuous time hazard 3.2, the discrete time hazard is an actual (conditional) probability, rather than a rate and therefore might be easier to interpret.

The cumulative discrete time hazard is given by

$$H_{\tilde{Y}}^d(\tau) = \sum_{k=1}^{\tau} h_{\tilde{Y}}^d(k) \quad (3.6)$$

We also define the complement of 3.5, the probability to survive beyond τ given survival until τ , as

$$s_{\tilde{Y}}^d(\tau) := 1 - h_{\tilde{Y}}^d(\tau) = P(\tilde{Y} > \tau | \tilde{Y} \geq \tau).$$

It follows that the unconditional probability to survive beyond time point τ is given by

$$S_{\tilde{Y}}^d(\tau) = P(\tilde{Y} > \tau) = \prod_{k \leq \tau} s_{\tilde{Y}}^d(\tau) = \prod_{k \leq \tau} (1 - h_{\tilde{Y}}^d(\tau)), \quad (3.7)$$

and the unconditional probability for an event at time τ is

$$P(\tilde{Y} = \tau) = S_{\tilde{Y}}^d(\tau - 1)h_{\tilde{Y}}^d(\tau). \quad (3.8)$$

When applied to continuous time Y , the follow-up is divided in J disjunct intervals $(a_0, a_1], \dots, (a_{j-1}, a_j] \dots, (a_{J-1}, a_J]$, $j = 1, \dots, J$ such that

$$Y \in (a_{j-1}, a_j] \Leftrightarrow \tilde{Y} = j$$

Thus,

$$h_{\tilde{Y}}^d(j) = P(Y \in (a_{j-1}, a_j] | Y > a_{j-1})$$

and

$$S_{\tilde{Y}}^d(j) = P(Y > a_j) = S_Y(a_j)$$

3.2 Single-event, right-censored data

The complexity of Survival Analysis compared to other fields arises from the fact that the outcome of interest is often only observed partially. In particular, the time-to-event is often unknown at the end of the observation period, as the event has not occurred yet.

Let,

- X taking values in \mathbb{R}^p be the generative random variable representing the data *features/covariates/independent variables*.
- Y taking values in $\mathbb{R}_{\geq 0}$ be the (partially unobservable) *true survival time*.
- C taking values in $\mathbb{R}_{\geq 0}$ be the (partially unobservable) *true censoring time*.

In the presence of censoring C , it is impossible to fully observe the true outcome of interest, Y . Instead, the observable variables are defined by

- $T := \min\{Y, C\}$, the *outcome time* (realizations are referred to as the *observed outcome time*); and
- $\Delta := \mathbb{I}(Y = T) = \mathbb{I}(Y \leq C)$, the *event indicator* (also known as the *censoring or status indicator*).

Together (T, Δ) is referred to as the *survival outcome* or *survival tuple* and they form the dependent variables. The survival outcome provides a concise mechanism for representing the outcome time and indicating which outcome (event or censoring) took place.

A *survival dataset* is a $n \times p$, real-valued matrix defined by $\mathcal{D} = ((\mathbf{x}_1, t_1, \delta_1) \cdots (\mathbf{x}_n, t_n, \delta_n))^{\top}$, where (t_i, δ_i) are realizations of the respective random variables (T_i, Δ_i) and \mathbf{x}_i is a p -dimensional vector, $\mathbf{x}_i = (x_{i,1} \ x_{i,2} \cdots x_{i,p})^{\top}$ of features.

In this book, we will often refer to the unique, ordered event times. For example, given survival data, $(t_1 = 6, \delta_1 = 0), (t_2 = 1, \delta_2 = 1), (t_3 = 10, \delta_3 = 1), (t_4 = 5, \delta_4 = 0), (t_5 = 10, \delta_5 = 1)$ the ordered unique event times are $(t_{(1)}, t_{(2)}) = (1, 10)$ as the censored observations are removed, as are duplicated times.

Let $m \leq n$ be the number of unique, observed event times. We define the **unique, ordered event times** simply as

$$t_{(1)} < \cdots < t_{(m)}, \quad m \leq n. \quad (3.9)$$

A common short-hand in survival analysis is to assume the subscript (k) is an index referring to the observation who experienced the event at time $t_{(k)}$. For example, $(\mathbf{x}_{(k)}, t_{(k)}, \delta_{(k)})$ are the features and outcome for the observation that experienced the event at $t_{(k)}$, the k th ordered event time.

Finally, the following quantities are used frequently throughout this book and survival analysis literature more generally. Let $(t_i, \delta_i) \stackrel{i.i.d.}{\sim} (T, \Delta), i = 1, \dots, n$, be observed survival outcomes.

The **risk set at τ** , is the index-set of observation units at risk for the event just before τ

$$\mathcal{R}_{\tau} := \{i : t_i \geq \tau\} \quad (3.10)$$

where i is the index of an observation in the data. For right-censored data, $\mathcal{R}_0 = \{1, \dots, n\}$ and $\mathcal{R}_\tau \subseteq \mathcal{R}_{\tau'}, \forall \tau > \tau'$. Note that in a continuous setting, ‘just before’ refers to an infinitesimally smaller time than τ , in practice, as this is unobservable the risk set is defined at τ , hence an observation may both be at risk, and experience an event (or be censored) at τ .

The **number of observations at risk at τ** is the cardinality of the risk set at τ ,

$$n_\tau := \sum_i \mathbb{I}(t_i \geq \tau) = |\mathcal{R}_\tau|$$

Finally, the **number of events at τ** is defined by,

$$d_\tau := \sum_i \mathbb{I}(t_i = \tau, \delta_i = 1)$$

For truly continuous variables, one might expect only one event to occur at each observed event time: $d_{t_{(k)}} = 1, \forall k$. In practice, ties are often observed due to finite measurement precision, such that $d_\tau > 1$ occurs frequently in real-world datasets.

The quantities \mathcal{R}_τ , n_τ , and d_τ underlie many models and measures in survival analysis. Several non-parametric and semi-parametric methods (Chapter 10) like the Kaplan-Meier estimator (see Section 3.5.2.1) are based on the ratio d_τ/n_τ .

Table 3.1 exemplifies an observed survival dataset, a subset of the `tumor` data (Bender and Scheipl 2018), which contains the time until death in days after operation ($\delta_i = 1$ if death occurred at the outcome time t_i and $\delta_i = 0$ otherwise).

In this example, the above quantities would be:

- $\mathcal{R}_{\tau=1217} = \{1, 3, 5\}$ (these subjects’ outcome times are greater or equal to $\tau = 1217$ so they are at risk for the event at this time)
- $n_{\tau=1217} = |\mathcal{R}_{1217}| = 3$
- $d_{\tau=1217} = 1$: As only $i = 1$ experienced the event (and not censoring) at this time.

Table 3.1: Subset of the `tumor` (Bender and Scheipl 2018) time-to-event dataset. Rows are individual observations (ID), $\mathbf{x}_{\cdot j}$ columns are features, t is observed time-to-event, δ is the event indicator.

id (i)	age (x_{·1})	sex (x_{·2})	complications (x_{·3})	days (t)	status (δ)
1	71	female	no	1217	1
2	70	male	no	519	0
3	67	female	yes	2414	0
4	58	male	no	397	1
5	39	female	yes	1217	0
6	59	female	no	268	1

3.3 Types of Censoring

Three types of censoring are commonly defined in survival analysis: right-censoring, left-censoring, and interval-censoring. The latter can be viewed as the most general case. Multiple

types of censoring and/or truncation (Section 3.4) can occur in any given data set and it is vital to identify which types are present in order to correctly select and specify models and measures for the data.

3.3.1 Right-censoring

Right-censoring is the most commonly assumed form of censoring in survival data. It occurs when the event of interest was not experienced during the observation period, which may happen because it was no longer observable (for example, due to withdrawal from the study) or because the event did not happen until study end. The exact event time is unknown but it is known that the event is after the observed censoring time, hence *right-censoring* (imagine a timeline from left to right as in Figure 3.1).

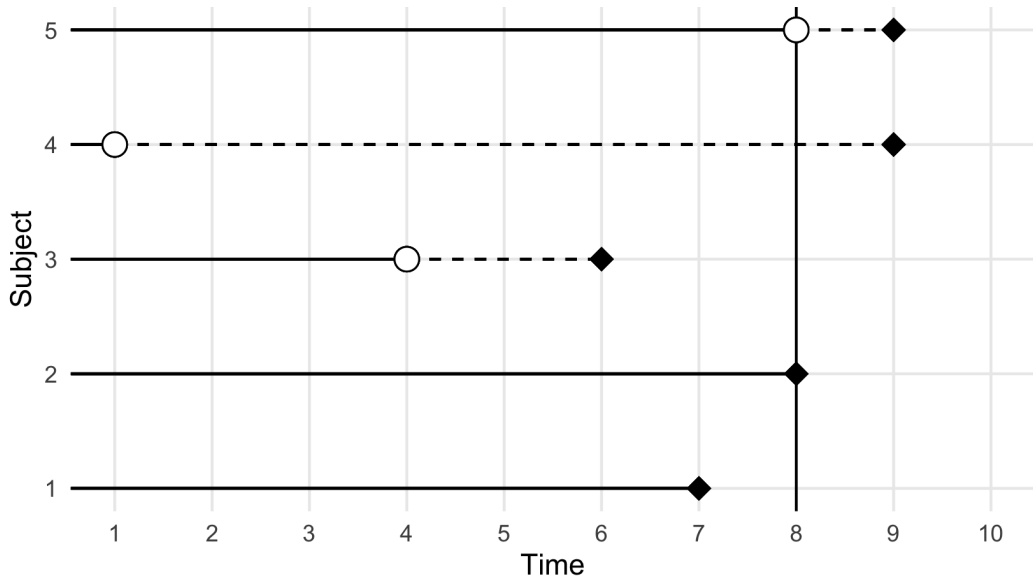


Figure 3.1: Dead and censored subjects (y-axis) over time (x-axis). Black diamonds indicate true death times and white circles indicate censoring times. Diamonds at the end of dashed lines are hypothetical (unknown in reality). Vertical line is the study end time. Subjects 1 and 2 die in the study time. Subject 3 is censored in the study and (unknown) dies within the study time. Subject 4 is censored in the study and (unknown) dies after the study. Subject 5 is censored at study end and (unknown) dies after the end of the study.

Right-censoring can be further divided into Type-I, Type-II and random censoring. Type-I, or *administrative*, censoring occurs at the fixed, pre-defined end of an observation period τ_u , in which case the outcome is given by $(T_i = \min(Y_i, \tau_u), \Delta_i = \mathbb{I}(Y_i \leq \tau_u))$. Censored observations are therefore represented as $(\tau_u, 0)$. Type-II censoring also occurs when the observation period ends. However, in this case the study ends when a pre-defined number of subjects experienced the event of interest and hence τ_u is random.

Random censoring occurs when censoring times *randomly* follow an unknown distribution and one observes $(T_i = \min(Y_i, C_i), \Delta_i = \mathbb{I}(Y_i \leq C_i))$. Different types of right-censoring can, and sometimes do, co-occur in any given data set.

In practice, these different types of right-censoring are usually handled the same during

modeling and evaluation and so this book refers to ‘right-censoring’ generally, which could occur from a combination of the above types.

3.3.2 Left- and Interval-censoring

Left-censoring occurs when the event is known to have happened at some unknown time before observation time, interval-censoring occurs when the event is known to have happened within some time span, but not the exact time.

Consider a survey about phone use where participants are asked: “How old were you when you used a smart phone for the first time?”. The possible answers are:

- exact age of first use
- didn’t use a smart phone yet
- did or does use a phone but doesn’t remember age of first time use
- did or does use a phone, remembers a specific age range

The first case represents an exactly observed event time, the second case the familiar right-censoring, as the event may occur later in life, but it is unknown when. The third case is referred to as left-censoring, we know the event occurred before the interview, but don’t know when. The fourth case is an example of interval-censoring, as we know the event occurred within some age span, but not the exact age.

Interval- and left-censoring often occur in medical contexts. For example, some guidelines suggest annual screenings for skin cancer (starting from a certain age). However, the initial age at which individuals do screenings and regularity of check ups varies widely. If cancer was detected between two screenings, the observation is interval-censored. If cancer is detected at first screening, the observation is left-censored (unless the ‘age’ of the cancer can be narrowed down based on size and other characteristics, in which case it would become interval-censored). Also of note, particularly in a medical context, is that interval censoring may be safely ignored depending on the time scale being modelled. Say a patient is screened in February and March 2025 and cancer is detected in the second screening, then they are technically interval censored as (February 2025, March 2025). However, if this data is modelled at an annual scale, then their outcome is known to be [2025] and they are not considered censored.

Censoring Notation

In the presence of left- or interval-censoring the usual representation of survival outcomes as (t_i, δ_i) is not sufficient to denote the different types of observations in the data set. Instead, we represent the data as intervals in which the event occurs. Formally, let Y_i the random variable for time until the event of interest and L_i, R_i random variables that define an interval $(L_i, R_i]$ with realizations l_i, r_i . Let further t_i the time of observation (for example age at interview in the phone use example) or last-follow up time for subject i . Then the event time of subject i is

- left-censored if $Y_i \in (L_i = 0, R_i = t_i]$;
- right-censored at t_i if $Y_i \in (L_i = t_i, R_i = \infty)$;
- interval-censored $Y_i \in (L_i = l_i, R_i = r_i]$, $l_i < r_i \leq t_i$
- exactly observed if $Y_i \in (L_i = t_i, R_i = t_i]$

In the cancer screening example from above it holds that $r_i = t_i$ and l_i the last check-up before r_i . In the phone use example, the participants might specify any age range between 0 and t_i .

To make this more concrete, consider phone use example data, where t_i is the age at interview. In practice, such data is often stored by creating two variables representing the left (l_i) and right border (r_i) of the respective intervals (t_i is not really needed here to define the outcome, but included for illustration).

id	t_i	l_i	r_i
1	13	13	∞
2	17	15	15
3	16	14	16
4	16	13	15
5	18	0	18

Here, the first subject is right-censored at 13 years ($l_i = t_i = 13, r_i = \infty$), the second subject remembered exactly ($l_i = r_i = 15 < t_i = 17$), the third subject remembers that it was after 14, but not exact age ($l_i = 14 < r_i = 16 = t_i$), fourth subject remembers use after 13 years and latest at 15 years of age ($l_i = 13 < r_i = 15 < t_i$), and the fifth subject uses a smart phone currently at age 18, but cannot specify further ($l_i = 0 < r_i = 18 = t_i$).

From the example above, it is clear, that right- and left-censoring are special cases of interval-censoring. However, if only right- or left-censoring is present, the likelihood and estimation simplifies (see Section 3.5). Also note that in case of left- and interval-censoring the event is known to have occurred, while for right-censoring the event didn't occur during time under observation. For left- and right-censoring one might be tempted to consider it an event $\delta_i = 1$ without exact time, while right-censoring would be consider a non-event $\delta_i = 0$. However, technically it is assumed that the event will always occur, if we wait long enough (for right-censored data in the interval (t_i, ∞)). Censoring therefore means having imprecise information about the time of event rather than information about the event occurring or not occurring.

Dependent vs. Informative Censoring

Censoring is sometimes described as *uninformative* if Y and C are independent, $Y \perp\!\!\!\perp C$, which means that knowing the value of one gives no information about the value of the other. However, this definition could be misleading as the term ‘uninformative’ may imply that C is independent of both X and Y , and not just Y . To avoid misinterpretation, the following definitions are used in this book:

- If $C \perp\!\!\!\perp X$, censoring is *feature-independent*, otherwise censoring is *feature-dependent*.
- If $C \perp\!\!\!\perp Y$, censoring is *event-independent*, otherwise censoring is *event-dependent*.
- If $(C \perp\!\!\!\perp Y)|X$, censoring is conditionally independent of the event given covariates, or *conditionally event-independent*.
- If $C \perp\!\!\!\perp (X, Y)$, censoring is *uninformative*, otherwise censoring is *informative*.

Uninformative censoring can generally be well-handled by models as the true underlying distribution of survival times is not affected by censoring. In fact, in this case one could even use regression models after removing censored observations (if they do not form a high proportion of the data).

In reality, censoring is rarely non-informative as reasons for drop-out or missingness in outcomes tend to be related to the study of interest. Event-dependent censoring is a tricky case that, if not handled appropriately (by a competing-risks framework), can easily lead to poor model development. Imagine a study is interested in predicting the time between relapses of stroke but a patient suffers a brain aneurysm due to some separate neurological condition. There is a high possibility that a stroke may have occurred if the aneurysm had not. A survival model is unlikely to distinguish the censoring event (aneurysm) from the event of interest (stroke) and will confuse predictions.

In practice, the majority of models and measures assume that censoring is conditionally event-independent and hence censoring patterns can be predicted/estimated based on the covariates. For example, if studying the survival time of ill pregnant patients in hospital, then dropping out of the study due to pregnancy is clearly dependent on how many weeks pregnant the patient is when the study starts (for the sake of argument assume no early/late pregnancy due to illness).

3.4 Censoring vs. Truncation

A common confusion is to conflate censoring and truncation, which is problematic as the methods to handle them differ substantially. Outside of time-to-event settings, truncation usually refers to truncating (or removing) an entire subject from a dataset. As discussed in Chapter 1, truncation in survival analysis refers to partially truncating a period of time and is quite common in the more general event history setting (Chapter 4).

While censored observations have incomplete information about the time-to-event, they are still part of the data set. Whereas truncation leads to observations not entering the data set (at least not at time 0). This will usually introduce bias that needs to be accounted for.

3.4.1 Left-truncation

Left-truncation often occurs when inclusion into a study is conditional on the occurrence of another event. Left-truncation plays an important role when modeling recurrent events or multi-state data (Chapter 4), thus the concept will be introduced in more detail.

By example, consider a study from the 18th century (Broström 1987), when childhood and maternal mortality were relatively high. The goal of the study was to establish the effect of a mother's death on the survival of the infant. Since each death was reported to the authorities, an infant was added to the study if and when their mother died. To create a matched cohort, two other infants, whose mothers were alive, were matched into the study based on their age and other relevant features. Thus, groups of three infants within the study had identical features except for the status of the mother (alive or dead). Because of the study design, infants who died before their mothers could never enter into the study. A mother's death is thus referred to as left-truncation event and the infant's age at time of inclusion into the study is referred to as left-truncation time.

More formally, let t_i^L the subject-specific left-truncation time. Then we only observe subjects with $y_i > t_i^L$ and subjects with $y_i < t_i^L$ never enter the data.

This is illustrated in Figure 3.2. Continuing with the example above, say Infant 1 dies at t_1 , while the mother dies at some later time point t_1^L , therefore infant 1 never enters the study.

The mother of Infant 2 dies at t_2^L , at which point the infant is included in the study and experiences an event at t_2 . Finally, say Infant 3 enters the study at t_3^L and is censored at 365 days when the study ends.

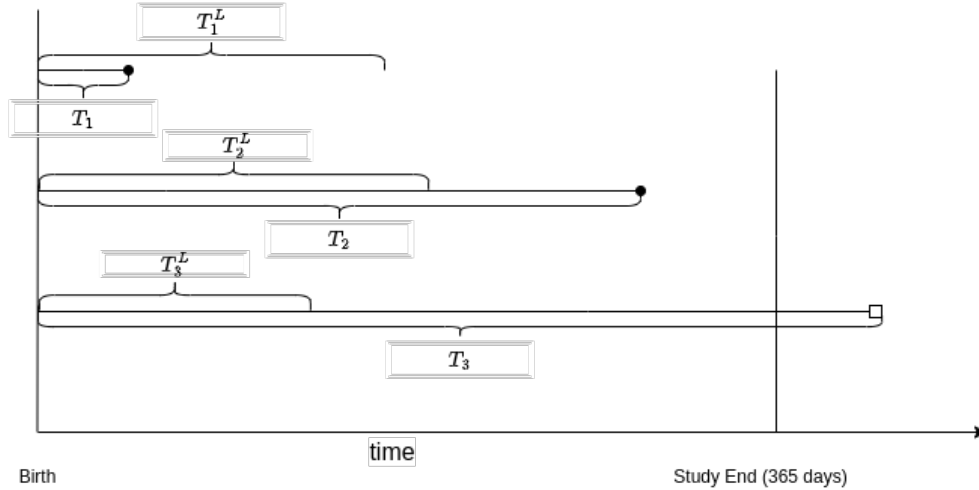


Figure 3.2: Illustration of left-truncation data. Subjects 2 and 3 enter the data set as the study entry condition (mother's death) occurs before the event of interest occurs after the left-truncation time (left-truncation time shorter than event time). Subject 1 on the other hand never enters the data as the event occurs before the study entry condition (left-truncation time longer than event time).

In this example, left-truncation biases the sample towards healthier or more robust infants, as frail infants die earlier and thus on average before their mothers. This would bias the estimates if not properly taken into account (see Section 3.5.2.3).

3.4.2 Right-truncation

Right-truncation often occurs in retrospective sampling based on registry data, when data is queried for cases reported by a certain cut-off time (see for example Vakulenko-Lagun, Mandel, and Betensky (2020)). A common example is the estimation of the incubation period of an infectious disease, which is the time from infection to the disease onset. Only known, symptomatic (and/or tested) cases are entered into the database. At a time τ , one can only observe the subset of the infected population that has already experienced the disease, and not the population that is still incubating the disease, hence biasing the data to shorter incubation periods.

Formally, let t_i^r be the right-truncation time (here time from infection until the time at which the database is queried), then subjects only enter the data set when $t_i < t_i^r$. This is illustrated in Figure 3.3 using three subjects. All three subjects were infected during the observation period, however, the right-truncation time t_2^r of subject 2 is shorter than the incubation period t_2 for this subject, thus at the time of querying the data base, this subject will not be included in the sample, as $t_2 > t_2^r$.

Note the difference to right-censoring. If subject 2 was right-censored, the subject would be in our sample and the time of infection would be known - the time of disease onset would be

censored. In case of right-truncation on the other hand, the subject is not included in the sample at time of data extraction, as subjects are only included in the registry after disease onset. Overall this leads to a bias towards shorter incubation times and potentially feature values that lead to shorter incubation times.

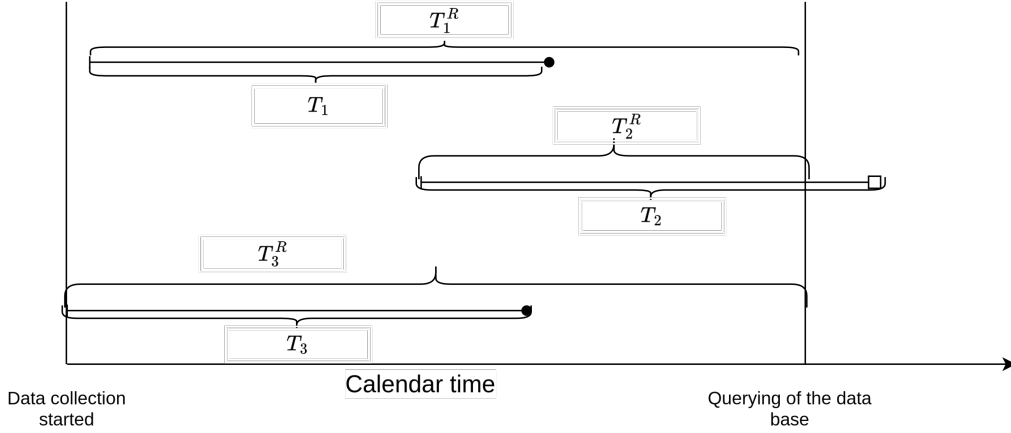


Figure 3.3: Illustration of right-truncation based on registry data. For subjects 1 and 3 the right-truncation time is longer than the incubation period, therefore they are included in the sample when the registry is queried. For subject 2 on the other hand the right-truncation time is shorter, therefore it's excluded from the sample.

As for left-truncation, ignoring right-truncation will lead to biased estimations. While for left-truncated data simple adjustments of the risk set work for non- and semi-parametric methods like the Kaplan-Meier and Cox-type estimators, this is not the case for right-truncated data. However, parametric methods can be employed (see Section 3.5) and generalised product limit estimators for right-truncated data exist (Michael G. Akritas and LaValley 2005).

3.5 Estimation

While details about estimation will be given later, when different models are introduced in Part III and Part IV of the book, it is worthwhile discussing some general concepts here, namely parametric and non-parametric approaches.

3.5.1 Parametric estimation

Consider for now uncensored data $(t_i, \delta_i = 1), i = 1, \dots, n$. A standard approach would be to assume a suitable distribution for the event times $t_i \stackrel{iid}{\sim} F_Y(\boldsymbol{\theta}), \boldsymbol{\theta} = (\theta_1, \theta_2, \dots)^\top$, and define the likelihood of the data as

$$\mathcal{L}(\boldsymbol{\theta}) = \prod_{i=1}^n f_Y(t_i | \boldsymbol{\theta}) \quad (3.11)$$

where f_Y is the pdf of F_Y .

The model parameters can then be obtained by maximizing the likelihood such that

$$\hat{\boldsymbol{\theta}} = \arg \max_{\boldsymbol{\theta}} \mathcal{L}(\boldsymbol{\theta})$$

However, in the presence of censoring 3.11 is incorrect, as the exact event time is only known for some subjects. For example, for right-censored data ($\delta_i = 0$) we only know that the event occurred after observed censoring time t_i . Thus the likelihood contribution for such data points is $P(Y_i > t_i) = S_Y(t_i)$, whereas for observed event times ($\delta_i = 0$) the likelihood contribution is $f_Y(t_i)$ as before.

Let now $\mathcal{O} = \{i : \delta_i = 1\}$ the index set of observed event times and $\mathcal{RC} = \{i : \delta_i = 0\}$ the index set of censored observations. The likelihood of this data can be written as

$$\begin{aligned} \mathcal{L}(\boldsymbol{\theta}) &\propto \prod_{i \in \mathcal{O}} f_Y(t_i | \boldsymbol{\theta}) \prod_{i \in \mathcal{RC}} S_Y(t_i | \boldsymbol{\theta}) \\ &= \prod_{i=1}^n f_y(t_i | \boldsymbol{\theta})^{\delta_i} S_Y(t_i | \boldsymbol{\theta})^{1-\delta_i} \\ &= \prod_{i=1}^n \frac{f_y(t_i | \boldsymbol{\theta})^{\delta_i}}{S_Y(t_i | \boldsymbol{\theta})^{\delta_i}} S_Y(t_i | \boldsymbol{\theta}) \\ &= \prod_{i=1}^n h_Y(t_i | \boldsymbol{\theta})^{\delta_i} S_Y(t_i | \boldsymbol{\theta}), \end{aligned}$$

where the last equality follows from 3.2.

Similar adjustments to the likelihood can be made for other types of censoring and in the presence of truncation. Following Klein and Moeschberger (2003), we can define the individual likelihood contributions for the different types of censoring as

- observed event at t_i : $f_Y(t_i | \boldsymbol{\theta})$
- right-censoring: $P(Y_i > t_i | \boldsymbol{\theta}) = S_Y(t_i | \boldsymbol{\theta})$
- left-censoring: $P(Y_i < t_i | \boldsymbol{\theta}) = F_Y(t_i | \boldsymbol{\theta}) = 1 - S_Y(t_i | \boldsymbol{\theta})$
- interval-censoring: $P(l_i < Y_i \leq r_i | \boldsymbol{\theta}) = S_Y(l_i | \boldsymbol{\theta}) - S_Y(r_i | \boldsymbol{\theta})$

Depending on which of the above contributions occur in the data set, we can now construct our likelihood accordingly. Let $\mathcal{O}, \mathcal{RC}, \mathcal{LC}, \mathcal{IC}$ non-overlapping subsets of the observed data \mathcal{D} for subjects with observed event times, right-censoring, left-censoring and interval-censoring, respectively. Assuming independence between observations and in absence of truncation, the likelihood for the observed data can be defined as

$$\mathcal{L}(\boldsymbol{\theta}) \propto \prod_{i \in \mathcal{O}} f_Y(t_i | \boldsymbol{\theta}) \prod_{i \in \mathcal{RC}} S_Y(t_i | \boldsymbol{\theta}) \prod_{i \in \mathcal{LC}} (1 - S_Y(t_i | \boldsymbol{\theta})) \prod_{i \in \mathcal{IC}} (S_Y(l_i | \boldsymbol{\theta}) - S_Y(r_i | \boldsymbol{\theta})) \quad (3.12)$$

In case of truncation, the adjustments are made to all observations, as we have to condition on the event occurring after/before the truncation time. The truncation adjusted likelihood contributions (assuming independence of truncation and event/censoring times) would thus be given by

- left-truncation:

$$- \text{event: } f(Y_i = t_i | Y_i \geq t_i^L, \boldsymbol{\theta}) = \frac{f_Y(t_i | \boldsymbol{\theta})}{S_Y(t_i^L | \boldsymbol{\theta})}$$

- left-censoring: $P(Y_i < t_i | Y_i \geq t_i^L, \boldsymbol{\theta}) = \frac{S_Y(t_i | \boldsymbol{\theta})}{S_Y(t_i^L | \boldsymbol{\theta})}$
- interval-censoring: $P(l_i < Y_i \leq r_i | Y_i \geq t_i^L, \boldsymbol{\theta}) = \frac{S_Y(l_i | \boldsymbol{\theta}) - S_Y(r_i | \boldsymbol{\theta})}{S_Y(t_i^L | \boldsymbol{\theta})}$
- right-truncation:
 - event: $f(Y_i = t_i | Y_i \leq t_i^R, \boldsymbol{\theta}) = \frac{f_Y(t_i | \boldsymbol{\theta})}{F_Y(t_i^R | \boldsymbol{\theta})}$
 - left-censoring: $P(Y_i < t_i | Y_i \leq t_i^R, \boldsymbol{\theta}) = \frac{S_Y(t_i | \boldsymbol{\theta})}{F_Y(t_i^R | \boldsymbol{\theta})}$
 - interval-censoring: $P(l_i < Y_i \leq r_i | Y_i \leq t_i^R, \boldsymbol{\theta}) = \frac{S_Y(l_i | \boldsymbol{\theta}) - S_Y(r_i | \boldsymbol{\theta})}{F_Y(t_i^R | \boldsymbol{\theta})}$

Note that in practice, data sets will often not contain all types of censoring or truncation, in which case 3.12 will contain only a subset of the product terms. This has been illustrated in 3.12 under absence of truncation and $\mathcal{LC} = \mathcal{IC} = \emptyset$.

3.5.2 Non-parametric estimation

As the name suggests, non-parametric estimation (and semi-parametric estimation) techniques do not make (strong) assumptions about the underlying distribution of event times.

A common principle for such techniques is to partition the follow-up into intervals (or to define specific time-points during the follow-up) and to estimate the continuous (3.2) or discrete time (3.5) hazards for each interval/time-point. Once the respective hazard estimates are obtained, estimates of other quantities, for example the survival probability, can be derived based on the relationship given in Section 3.1.1 or Section 3.1.2.

3.5.2.1 Kaplan-Meier estimator

The Kaplan-Meier estimator (Kaplan and Meier 1958), a simple, non-parametric estimator for the survival function (3.1), is an example for this principle. While it is usually used for continuous time, its construction can be motivated from a discrete time perspective. Recall from Section 3.2 the definition of unique, ordered, event time $t_{(k)}, k = 1, \dots, m$ (3.9). Define $\tilde{Y} = t_{(k)} \Leftrightarrow Y \in (t_{(k-1)}, t_{(k)}]$ as discrete time representation of Y . Using the quantities introduced in Section 3.2, the discrete time hazard 3.5 is estimated as the ratio of the number of events occurring at $t_{(k)}$, to the number of subjects at risk at $t_{(k)}$:

$$h^d(t_{(k)}) = P(Y \in (t_{(k-1)}, t_{(k)}) | Y > t_{(k-1)}) = \frac{d_{t_{(k)}}}{n_{t_{(k)}}}. \quad (3.13)$$

The survival probability and the definition of the Kaplan-Meier estimator (3.14) then follow from 3.7:

$$S(\tau) = \prod_{k: t_{(k)} \leq \tau} \left(1 - \frac{d_{t_{(k)}}}{n_{t_{(k)}}} \right) \quad (3.14)$$

which is a step-function at the observed ordered event times $t_{(k)}, k = 1, \dots, m$ with $S_{KM}(\tau) = 1 \forall \tau < t_{(1)}$. It is usually estimated for all unique event times. In this book, \hat{S}_{KM} specifically refers to the Kaplan-Meier estimator fit on some training data.

For illustration, we consider the `tumor` data set from Section 3.2. Figure 3.4 shows the estimated survival probability obtained by applying the Kaplan-Meier estimator to the full data set, containing observations of $n = 776$ subjects. By definition, the survival function starts at $S(t) = 1$ at $t = 0$ and monotonically decreases towards $S(t) = 0$ for $t \rightarrow \infty$. However, follow-ups are usually not infinite and in the presence of censoring, the survival function may

not reach 0 by the end of the observation period. For the Kaplan-Meier estimator specifically, $\hat{S}_{KM}(t_{(m)}) = 0$ only if the last observed time is an event time and there are no censored observations at the same time.

Dotted lines indicate the median survival, defined as the time at which the survival function reaches $S(t) = 0.5$. In this example, the median survival time is approximately 1500 days. This means that 50% of the subjects are expected die within 1500 days after operation.

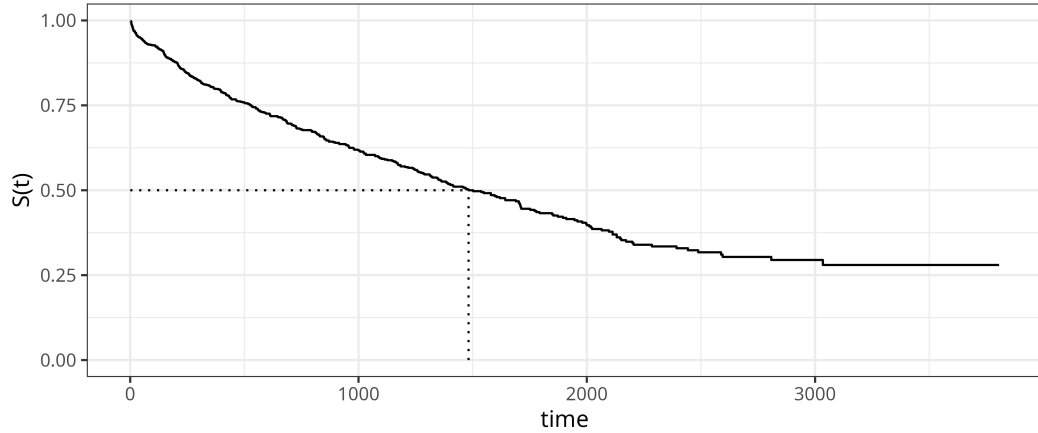


Figure 3.4: Kaplan-Meier estimate for the `tumor` data (Bender and Scheipl 2018). The estimated survival probabilities are given by the solid step-function. Dotted lines indicate the median survival time).

While the Kaplan-Meier estimator does not directly support estimation of covariate effects on the estimated survival probabilities, it is often used for descriptive analysis by applying the estimator to different subgroups (referred to as stratification in survival analysis). For example, Figure 3.5 shows \hat{S}_{KM} separately for subjects aged 50 years or older and subjects younger than 50 years, respectively. Dashed lines again illustrate median survival times. However, note that the median survival time does not exist for the younger age group, as their estimated survival function does not cross 0.5.

3.5.2.2 Nelson-Aalen

As the Kaplan-Meier estimator (Section 3.5.2.1), the Nelson-Aalen estimator (Nelson (1972), O. Aalen (1978)) is based on the discrete time hazards 3.13. Rather than estimating the survival probability, the Nelson-Aalen estimator estimates the discrete time cumulative hazard function 3.6 and is defined as

$$H_{NA}(\tau) = \sum_{k:t_{(k)} \leq \tau} h^d(t_{(k)}) = \sum_{k:t_{(k)} \leq \tau} \frac{d_{t_{(k)}}}{n_{t_{(k)}}}. \quad (3.15)$$

Note that we use a continuous time valued τ for the definition, which implies that $H_{NA,e}(\tau) = H_{NA,e}(t_{(k)}) \forall \tau \in [t_{(k)}, t_{(k+1)})$. In words: For time points between two unique event times we assume the previous value of the estimate.

Based on 3.4 we can also define a survival probability estimator based on the Nelson-Aalen estimator as

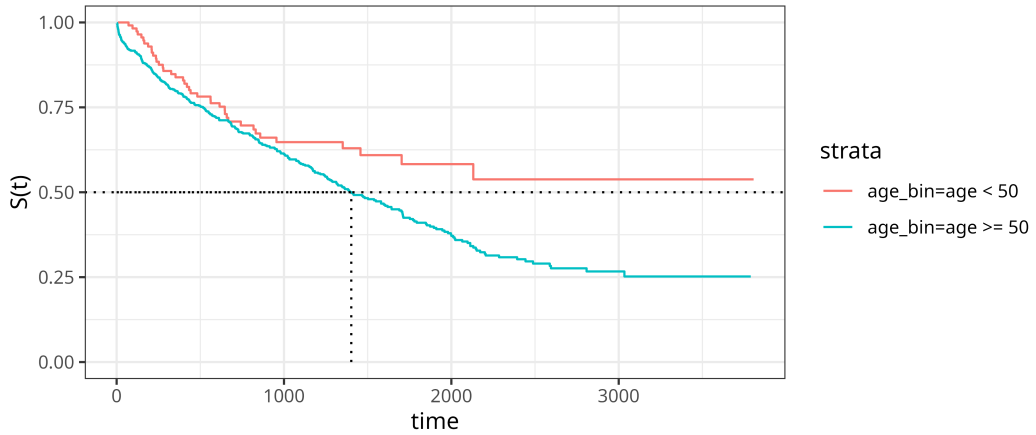


Figure 3.5: Kaplan-Meier estimate for the `tumor` data (Bender and Scheipl 2018) applied to subgroups of subjects of 50 or more years old and less than 50 years old, respectively. The estimated survival probabilities are given by the solid step-function. Dotted lines indicate the median survival time).

$$S_{NA}(\tau) = \exp(-H_{NA}(\tau)). \quad (3.16)$$

Kaplan–Meier and Nelson–Aalen are consistent for survival and cumulative hazard respectively under independent right-censoring. Both these non-parametric estimators can be used as simple predictive methods (Section 10.1), and are often used as informative baseline models, which can be compared to sophisticated alternatives to improve interpretability in model evaluation (Herrmann et al. 2021; Huang et al. 2020a; P. Wang, Li, and Reddy 2019). Both methods can also be used for graphical calibration of models (Section 7.2.1), components of complex models (?@sec-car), and other diagnostic graphical tools (Habibi et al. 2018; Jager et al. 2008; Moghimi-dehkordi et al. 2008).

3.5.2.3 Left truncation

Non-and semi-parametric estimators can be easily extended to deal with left-truncation by adjusting the risk set definition (3.10) to the more general definition (McGough et al. 2021)

$$\mathcal{R}_\tau^L = \{i : t_i^L \leq \tau \leq t_i\}, \quad (3.17)$$

which excludes individuals from the risk set until their left-truncation time has occurred (3.17).

The number of individuals at risk at τ is then

$$n_\tau^L = |\mathcal{R}_\tau^L| = \sum_i \mathbb{I}(t_i^L \leq \tau \leq t_i), \quad (3.18)$$

where t_i, t_i^L are the outcome time and left truncation time of observation i respectively.

The Kaplan-Meier (3.14) and Nelson-Aalen (3.15) estimators can still be used with $n_{t(k)}$ replaced by $n_{t(k)}^L$ and $d_{t(k)}$ calculated in the usual manner.

For illustration consider an excerpt from the infants data in Table 3.3 discussed in Section 3.4.1, where t is the observed event or censoring time and t^L is the left-truncation time.

Table 3.3: Excerpt of the `infants` (Broström 2024) time-to-event dataset. Rows are individual observations (`id`), `group` indicates matched infants, t^L is the left-truncation time (time of inclusion into the study), t is the observed time, δ is the event indicator.

group	id	t^L	t	δ	mother
1	1	55	365	0	dead
1	2	55	365	0	alive
1	3	55	365	0	alive
2	4	13	76	1	dead
2	5	13	365	0	alive
2	6	13	365	0	alive
4	7	2	16	1	dead
4	8	2	365	0	alive
4	9	2	365	0	alive

In Table 3.3, without stratifying according to mother's status, the first observed event time is $t_{(1)} = t_7 = 16$. Then, ignoring left-truncation,

- $\mathcal{R}_{t_{(1)}} = \{1, 2, 3, 4, 5, 6, 7, 8, 9\}$
- $d_{t_{(1)}} = 1$
- $n_{t_{(1)}} = 9$
- $S(t_{(1)}) = 1 - \frac{1}{9} \approx 0.9$

In contrast, when we take left-truncation into account, subjects only enter the risk set for the event after their left-truncation time (we already know they survived until t_i^L so they are not at risk for the event before that time), thus

- $\mathcal{R}_{t_{(1)}}^L = \{4, 5, 6, 7, 8, 9\}$
- $d_{t_{(1)}} = 1$
- $n_{t_{(1)}}^L = 6$
- $S(t_{(1)}) = 1 - \frac{1}{6} \approx 0.8$

Thus, in the presence of left-truncation, $n_{t_{(k)}}^L \leq n_{t_{(k)}}$ and therefore $S(t_{(k)})^L \leq S(t_{(k)})$.

Figure 3.6 shows the difference between estimated survival probabilities when left-truncation is ignored (left panel) and taken into account (right panel), respectively. It is clear that the survival probabilities were underestimated in both groups, but more so in the group of infants whose mother died (thereby underestimating the effect of the mothers' death on infant survival).

Interval-censoring

For interval-censoring, the Kaplan-Meier estimator is replaced by the nonparametric maximum likelihood estimator (NPMLE) (Z. Zhang and Sun 2010), which estimates the likelihood function under the assumption of left- or interval-censored data as in Section 3.5.1. The most common algorithm to compute this is the iterative Turnbull algorithm (Turnbull 1974). The intuition behind this algorithm is that an observation, i , should only contribute to the estimation at a given time-point, τ , if the event could have happened in the censoring interval, $\tau \in (L_i, R_i]$.

In summary (Giolo 2004):

Let $t_{(k)}, k = 1, \dots, m$ be the ordered times at which to evaluate the NPMLE.

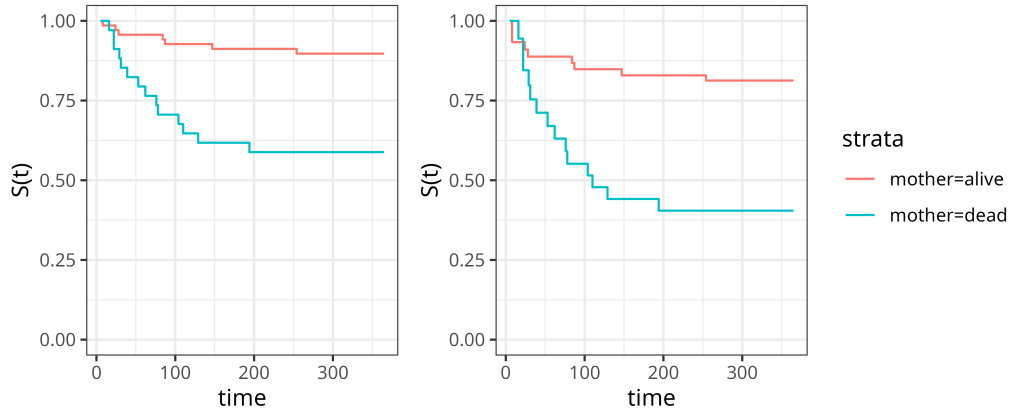


Figure 3.6: Left: Kaplan-Meier estimate of survival probabilities of infants depending on status of the mother ignoring left-truncation. Right: Kaplan-Meier estimate of survival probabilities adjusting for left-truncation.

1. Make an initial guess for $\hat{S}^0(t_{(k)})$, $k = 1, \dots, m$.

Where \hat{S}^0 is the initial guess. Let \hat{S}^j be the estimated survival function at iteration j .

1. **While** $|\hat{S}^j(t_{(k)}) - \hat{S}^{j-1}(t_{(k)})| > \epsilon, \forall k = 1, \dots, m$ **Do:**

- a. Compute the probability of an event at each time-point:

$$p_{t_{(k)}} = \hat{S}^{j-1}(t_{(k-1)}) - \hat{S}^{j-1}(t_{(k)}), \quad k = 1, \dots, m$$

- b. Estimate the number of events at each time-point:

$$d_{t_{(k)}} = \sum_{i=1}^n \frac{w_{ik} p_{t_{(k)}}}{\sum_{l=1}^m w_{il} p_{t_{(l)}}}, \quad k = 1, \dots, m$$

Where $w_{ik} = 1$ if the interval $(t_{(k-1)}, t_{(k)}]$ is contained within $(L_i, R_i]$, and $w_{ik} = 0$ otherwise; and L_i, R_i are the left- and right-censoring times for observations $i = 1, \dots, n$.

- c. Compute the cumulative number of events at or after $t_{(k)}$:

$$n_{t_{(k)}} = \sum_{l=k}^m d_{t_{(l)}}, \quad k = 1, \dots, m$$

This serves a similar role to the usual ‘number at risk’ formula.

- d. Calculate \hat{S}^j using the Kaplan-Meier formula (3.14), substituting the values in Steps 2b and 2c.

Giolo (2004) suggest using the Kaplan-Meier to find the initial guess in Step 1 and to use $\epsilon = 10^{-3}$. A similar algorithm can be used for left-censored data.

3.6 Estimation of the censoring distribution

The techniques discussed in section Section 3.5 can also be used to estimate the distribution of censoring times $(t_i, 1 - \delta_i)$. This is often done in order to calculate the inverse probability of censoring weights (Section 3.6.2) used in the evaluation of survival models (Section 6.1.1) and in order to account for (covariate-)dependent censoring (Willems et al. (2018)).

3.6.1 The Kaplan-Meier estimator for the censoring distribution

The Kaplan-Meier estimator can be used to estimate the distribution of censoring times. The definition of the risk set (3.10) is thus the denominator n_τ in 3.13 remains the same, but the numerator d_τ is now the number of censoring events at τ , which we denote as

$$d_\tau^C = \sum_i \mathbb{I}(t_i = \tau, \delta_i = 0).$$

The Kaplan-Meier estimator for the censoring distribution is then given by

$$G_{KM}(\tau) = \prod_{\ell: t_{(\ell)} < \tau} \left(1 - \frac{d_{t_{(\ell)}}^C}{n_{t_{(\ell)}}} \right), \quad (3.19)$$

where $t_{(\ell)}, l = 1, \dots, g$ are the unique, ordered censoring times. In this book, \hat{G}_{KM} specifically refers to the Kaplan-Meier estimator fit to the observed censoring times $(t_i, 1 - \delta_i)$ from some training data.

3.6.2 Inverse probability of censoring weights (IPCW)

The inverse probability of censoring (IPC) weights are defined as

$$w(\tau|\mathbf{x}) = \frac{1}{S(\tau|\mathbf{x})} \quad (3.20)$$

When no relationship between the censoring time and the covariates is assumed, the IPC weights are in most cases estimated by plugging in the Kaplan-Meier estimate of 3.19 into 3.20, such that

$$\hat{w}(\tau) = \frac{1}{\hat{G}_{KM}(\tau)} \quad (3.21)$$

3.7 Conclusion

Key takeaways

- The first step in any survival analysis is to understand the data and the type of censoring and or truncation present.
- Any data set can have a combination of different types of censoring and truncation
- Non-parametric estimators are well equipped to deal with right-censoring and left-truncation.
- Parametric estimation can naturally deal with different types of censoring and truncation, but requires assumptions about the distribution of the event times.

Further reading

- John D. Kalbfleisch and Prentice (1980) provide an early, theoretical treatment of the main concepts of survival analysis.
- Klein and Moeschberger (2003) is a standard reference for survival analysis and provides a comprehensive overview of the different types of censoring and truncation
- For practical discussion about survival models in the context of right-censoring and left-truncation see McGough et al. (2021)

4

Event-history Analysis

TODO (150-200 WORDS)

! Major changes expected!

This page is a work in progress and major changes will be made over time.

In this chapter we take a more general view on time-to-event data. So far, we only considered a single potentially censored, outcome of interest. Here we explore more complex settings with multiple, potentially mutually exclusive events and recurrences of events. In this generalization, the observed data is sometimes referred to as *event-history data* and its analysis as *event-history analysis*.

One way to think about event history data is in terms of transitions between different states, as illustrated in Figure 4.1. Usually, a subject starts out in an initial state 0 (for example, ‘healthy’) and from there transitions to different states. States from which further transitions are possible are called *transient* (displayed as circles), otherwise a state is called *terminal* or *absorbing* (displayed as squares).

In the *single event* setting (Figure 4.1, upper left panel), a subject can only transition to one state (the event of interest). This setting was the focus of Chapter 3. There, the censoring event was considered independent of the event of interest. In the *competing risks* setting (Figure 4.1, upper right panel, Section 4.2), a subject could transition to any of the q mutually exclusive states, thus the subject is initially *at risk* for a transition to multiple states. Once one of them occurs, the process is considered to have concluded (for the modeling purposes).

In the *recurrent events setting* (Figure 4.1 lower left panel), the same event can be observed multiple times on the same subject (for example recurrent respiratory infections during one year). Two different ways to represent recurrent events are shown: (top) reset the status to 0 after occurrence of an event or (bottom) consider the 1st, 2nd, etc. recurrences of the event as separate states. A detail omitted in the graph: Often recurrent event processes also have a competing, absorbing event. In this more complex setting, but also in general, recurrent events are often represented as multi-state process, which we discuss next. Therefore we forgo detailed discussion of this setting in this book and refer to Cook and Lawless (2007) for a detailed account specific to recurrent events analysis.

In the most general case, the *multi-state* setting (Figure 4.1 lower right panel, Section 4.3), there are multiple transient and terminal states with potential back transitions (for example, moving between different stages of an illness with the possibility of (partial) recovery and death as terminal event).

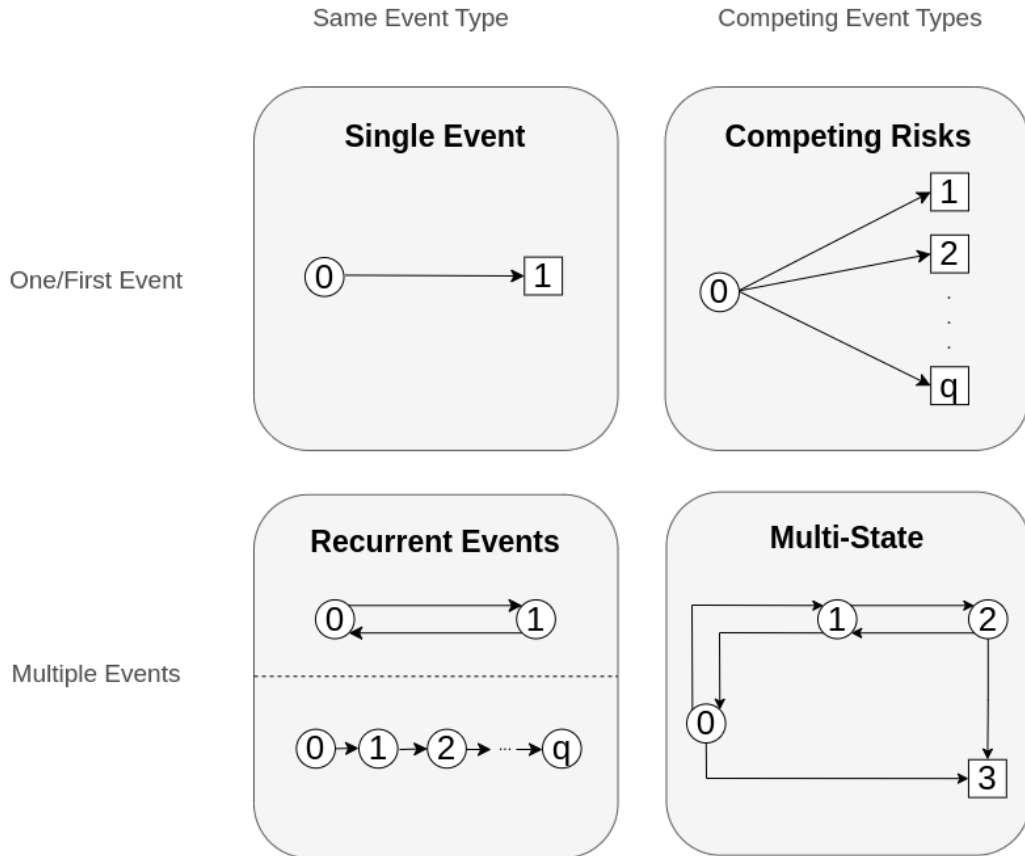


Figure 4.1: Illustration of different types of time-to-event processes. Transient states are displayed as circles, absorbing states are displayed as squares. Top, left: Standard single-event setting with transition from initial state 0 to state 1; Top, right: Competing risks setting with q competing events. The follow-up ends once one of the $\{1, \dots, q\}$ events is observed or the study ends; Bottom, left: Recurrent events setting with multiple occurrences of the same event. Bottom, right: Multi-state setting where subjects can transition between multiple transient states with possible back-transitions or to absorbing states.

Note that the concepts discussed in Section 3.3 and Section 3.4 are still relevant here, as, dependent on the specific process, any transition between two states could be subject to different types of censoring and truncation. In particular, remaining in one of the transient states until the end of follow-up constitutes right-censoring with respect to all possible transitions from that state and left-truncation is particularly important as subjects enter the risk sets for a transition at different time points in context of recurrent events and multi-state settings.

4.1 A process point of view

In order to formalize the different settings more conveniently, we introduce the stochastic process

$$E(\tau) \in \{0, \dots, q\}, \quad \tau \geq 0, \quad (4.1)$$

which indicates the state that is occupied at time τ .

Using this notation in the single-event setting we get $E(\tau) \in \{0, 1\}$ such that the hazard 3.2 could be written as

$$\begin{aligned} h(\tau) &= \lim_{d\tau \searrow 0} \frac{P(Y \in [\tau, \tau + d\tau] | Y \geq \tau)}{d\tau} \\ &= \lim_{d\tau \searrow 0} \frac{P(E(\tau + d\tau) = 1 | E(\tau-) = 0)}{d\tau}, \end{aligned} \quad (4.2)$$

where $\tau-$ indicates the time point immediately before τ .

This notation doesn't yield many advantages in the single-event setting, but will shorten notation later on, particularly in the multi-state setting. While not further pursued here beyond notational convenience, we refer to O. Aalen, Borgan, and Gjessing (2008) for an excellent treatment of event-history analysis derived from the point of view of stochastic processes.

4.2 Competing Risks

In contrast to single-event survival analysis, competing risks are concerned with the time to the first of multiple, mutually exclusive events.

Table 4.1. shows an excerpt of the `sir.adm` data (Allignol, Beyersmann, and Schumacher 2008) of patients on an intensive care unit (ICU). Time under observation (`time`) could end in one of three outcomes: 1 (discharge alive), 2 (death on ICU) or 0 (neither discharge nor death at the end of follow-up, which constitutes right-censoring at the end of study). The interest was in how pneumonia status (`pneumonia`) at admission to the ICU affects mortality.

Table 4.1: Subset of the `sir.adm` dataset (Allignol, Beyersmann, and Schumacher 2008). Each row represent one subject, `time` is the time under observation, `status` indicates the outcome observed (0: censored at the end of the study, 1: discharged alive from the ICU, 2: death in the ICU). `pneumonia` indicates whether a subject already had pneumonia at ICU admission.

time	status	pneumonia
8	0	no
8	0	no
31	1	yes
5	1	no
9	2	no
5	2	no

Contrast this data to the `tumor` data example in Section 3.5.2.1. There, patients were followed even after hospital discharge, thus loss to follow-up could be considered reasonably independent of the event of interest (death). In this study, follow-up stopped once patients were discharged. As discharged patients are healthier compared to the ones who remain on ICU, assuming independence between the time until discharge and time until death is unrealistic. Analysis of this data and how the different assumptions (independent censoring vs. competing risks) affects the estimates is discussed in Section 4.2.2 and Section 4.2.4.

4.2.1 Notation and Definitions

In the competing risks setting, everyone starts out in the initial state 0 and can progress to one of the absorbing states

$$e \in \{1, \dots, q\} \quad (4.3)$$

These absorbing states are also often referred to as *competing events*, *event types*, or *causes* (as in cause that ended the observation). State $e = 0$ is the initial state and a subject that remains in state 0 until the end of the follow up is considered censored.

The goal is to characterize the process $E(\tau) \in \{0, \dots, q\}$ in terms of transition hazards and probabilities. In extension of 4.2, we define *cause-specific* hazards

$$h_e(\tau) = \lim_{d\tau \rightarrow 0} \frac{P(E(\tau + d\tau) = e | E(\tau) = 0)}{d\tau}. \quad (4.4)$$

Analogous to the single-event case, we can also define the cause-specific cumulative hazard

$$H_e(\tau) = \int_0^\tau h_e(u) du \quad (4.5)$$

As competing events are mutually exclusive at any time τ , it is possible to define the *all-cause hazard* which is the hazard of any event occurring as the sum of all cause-specific hazards

$$h(\tau) = \sum_{e=1}^q h_e(\tau), \quad (4.6)$$

as well as the *all-cause cumulative hazard*, which can be obtained either via the integral over the all-cause hazard (4.6) or as sum of cause-specific cumulative hazards (4.5):

$$\begin{aligned}
H(\tau) &= \sum_{e=1}^q H_e(\tau) = \sum_{e=1}^q \int_0^\tau h_e(u) \, du \\
&= \int_0^\tau \sum_{e=1}^q h_e(u) \, du = \int_0^\tau h(u) \, du
\end{aligned} \tag{4.7}$$

The *all-cause survival probability* gives the probability that *none* of the events occurred before τ . This is usually not estimated directly but calculated from the cause specific hazards instead via 4.7 and 4.8:

$$S(\tau) = P(Y > \tau) = \exp(-H(\tau)) \tag{4.8}$$

Finally, the probability of experiencing an event e before time τ , *which is often referred to as Cumulative Incidence Function (CIF)*, is given by

$$\begin{aligned}
F_e(\tau) &= P(Y \leq \tau, E(Y) = e) \\
&= \int_0^\tau f_e(u) \, du = \int_0^\tau S(u-)h_e(u) \, du,
\end{aligned} \tag{4.9}$$

where

- $S(u-)$ is the probability of surviving (not experiencing any of the competing events) until the time-point shortly before u
- $f_e(u)du = S(u-)h_e(u)du$ is the probability of experiencing event e at time point u (which follows analogously to 3.2).

Note that here we use the notation $S(u-)$ rather than $S(u)$ to make explicit that we want the probability to survive until the time point immediately before u . This doesn't make much difference in continuous time where $P(T > t) = P(T \geq t)$, but may be important in (discrete) approximations (as in Section 4.2.2).

$F_e(\tau)$ can be interpreted as the proportion of subjects who experienced event of type e until time τ . Because the events are mutually exclusive, it holds that

$$S(\tau) + \sum_{e=1}^q F_e(\tau) = S(\tau) + F(\tau) = 1$$

where $F(\tau)$ is the probability that an event of any type occurring before τ and $S(\tau)$ the probability that no event occurs (4.8).

Note that all terms of 4.9 can be calculated from the individual hazards (4.4). Many estimation procedures for the CIF take this approach, consequently referred to as cause-specific hazards approach.

4.2.2 Non-parametric estimators

Non-parametric estimators for the cause-specific (cumulative) hazard (4.5) in the competing risks setting are derived analogously to the single event case (Section 3.5.2). The non-parametric estimate for the CIF is obtained by plugging in the non-parametric estimates of $S(t)$ and $h(t)$ into (4.9) as follows.

First, recall from Section 3.2 the definitions of the unique ordered event times $t_{(k)}, k = 1 \dots, m$, the risk-set at time $t_{(k)}$, $\mathcal{R}_{t_{(k)}}$, the number of events, $d_{t_{(k)}}$, and number of observations at risk $n_{t_{(k)}}$. Assume partitioning of the follow-up into m disjoint intervals $(t_{(k-1)}, t_{(k)}], k = 1, \dots, m$, such that $Y \in (t_{(k-1)}, t_{(k)}] \Leftrightarrow \tilde{Y} = t_{(k)}$, with \tilde{Y} defined as in Section 3.1.2.

An estimate for the *cause-specific* hazard is derived by updating the numerator in 3.13 to $d_{e,t_{(k)}}$ (the number of events of type e at time $t_{(k)}$):

$$h_e^d(t_{(k)}) := \frac{d_{e,t_{(k)}}}{n_{t_{(k)}}}, \quad e \in \{1, \dots, q\}. \quad (4.10)$$

Finally, the Aalen-Johansen (AJ) estimator (O. O. Aalen and Johansen (1978)) for the CIF is obtained by plugging in the Kaplan-Meier estimate (3.14) for the all-cause survival probability (probability that none of the competing events occurred) and the cause-specific hazard (4.10) for cause e into (4.9):

$$F_{AJ,e}(\tau) = \sum_{k:t_{(k)} \leq \tau} \hat{S}_{KM}(\tau-) \hat{h}_e^d(\tau) = \sum_{k:t_{(k)} \leq \tau} \hat{S}_{KM}(t_{(k-1)}) \frac{d_{e,t_{(k)}}}{n_{t_{(k)}}} \quad (4.11)$$

4.2.3 Application to mortality of ICU patients

For illustration of the AJ estimator and the interpretation of the CIFs consider the analysis conducted in Beyersmann, Allignol, and Schumacher (2012), based on the data from Table 4.1. Recall that one is interested in estimation of the mortality conditional on pneumonia status at admission, while accounting for discharge from the ICU as competing risk ($E(\tau) \in \{0, 1, 2\}$, where 0 indicates being alive in ICU (the initial state), 1 indicates discharge from ICU and 2 indicates death). While the AJ estimator cannot naturally incorporate feature information, it can be applied to subgroups of the data (here based on the pneumonia status $x_{\text{pneu}} \in \{0, 1\}$). Note that this will yield different sets of unique event times in each group, thus the AJ can have jumps at different time-points for the two groups.

Figure 4.2 shows the AJ estimates of the CIFs for each event type (discharge/death) stratified by pneumonia status. For example, the proportion of subjects with pneumonia being discharged until $\tau = 120$ days is approximately 75% ($\hat{F}_1(120|x_{\text{pneu}} = 1) = \hat{P}(Y \leq 120, E(Y) = 1|x_{\text{pneu}} = 1) \approx 0.75$), while approximately 25% died in the ICU ($\hat{F}_2(120|x_{\text{pneu}} = 1) = \hat{P}(Y \leq 120, E(Y) = 2|x_{\text{pneu}} = 1) \approx 0.25$). For patients without pneumonia we have $\hat{F}_1(120|x_{\text{pneu}} = 0) \approx 0.91$ and $\hat{F}_2(120|x_{\text{pneu}} = 0) \approx 0.09$. In this example, $\hat{F}_1 + \hat{F}_2 \approx 1$ for both pneumonia groups, as only 14 of 747 patients were censored (neither discharge nor death) at the end of the follow-up and thus the all-cause survival probability $\hat{S}(120) \approx 0$.

4.2.4 Independent Censoring vs. Competing Risks

It is worth spending some time to consider the difference between independent right-censoring and competing risks. Note that for the estimation of the hazard (4.10), occurrences of competing events are implicitly assumed right-censored (as $d_{e,t_{(k)}}$) only counts events of type e and $n_{t_{(k)}}$ contains the same subjects that would remain if events of type $\tilde{e} \neq e$ were considered censored before $t_{(k)}$. Nevertheless, competing risks are taken into account in the definition of the CIFs (4.9) and thus also in the AJ estimator (4.11), as the all-cause survival probability (4.8) depends on all cause-specific hazards.

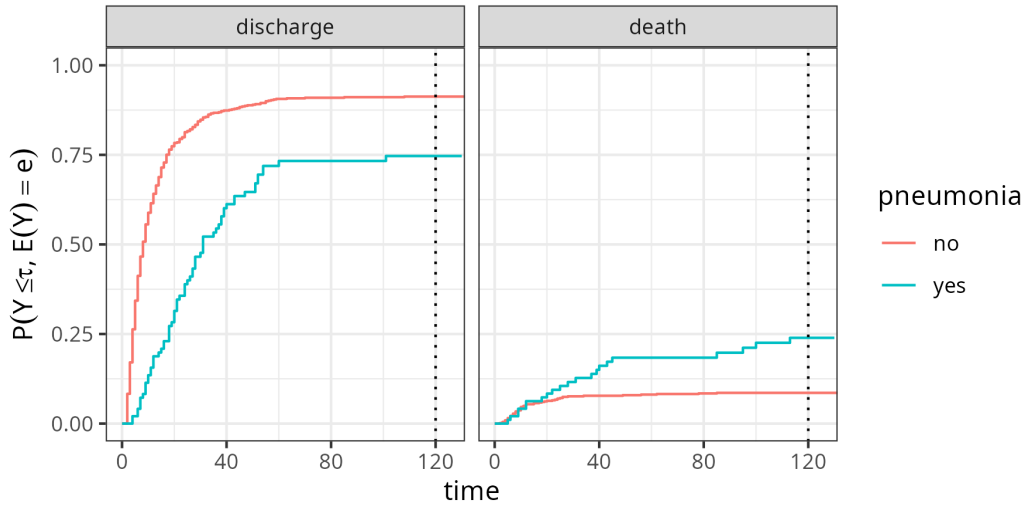


Figure 4.2: Aalen-Johansen estimator for the `sir.adm` data (Allignol, Beyersmann, and Schumacher 2008), stratified by pneumonia status at admission to the ICU. Left panel: Proportion of subjects discharged alive from the ICU. Right panel: Proportion of subjects who died in the ICU.

In contrast, assume that in our analysis of the `sir.adm` data we would consider time of discharge as independent right-censoring. As we only have one other event (death), the data could be treated as single-event, right-censored data as in Chapter 3 and therefore analyzed using the Nelson-Aalen estimator (3.16). The probability of death before some time-point τ could thus be obtained via $P(Y \leq \tau) = F(\tau) = 1 - S_{NA}(\tau)$.

Figure 4.3 shows the estimates obtained under the two assumptions. Solid lines indicate the probabilities under the competing risks assumption (identical to the right-hand side of Figure 4.2). Dashed lines are obtained under the independent right-censoring assumption. Clearly, the probabilities of dying at time $\tau = 120$ are greater when independent censoring is assumed ($\approx 75\%$ vs. $\approx 25\%$ in the pneumonia group and $\approx 62\%$ vs. $\approx 13\%$ in the no pneumonia group).

4.3 Multi-state Models

The multi-state process can be considered the most general type of time-to-event process, as other types (single-event, competing risks, recurrent events) can be viewed as special cases. Multi-state modeling allows realistic depiction of complex processes where subjects can start in different states and transition back and forth between them.

For illustration consider the `prothr` dataset (de Wreede, Fiocco, and Putter 2011) of liver cirrhosis patients from a randomized clinical trial with possible transitions depicted in Figure 4.4. Patients may have normal (state 0) or abnormal (state 1) levels of prothrombin (a protein important for blood clotting, produced by the liver) at the beginning of the trial. Some patients were treated with prednisone (which suppresses immune response and reduces inflammation) and others received a placebo. Death (state 2) constitutes an

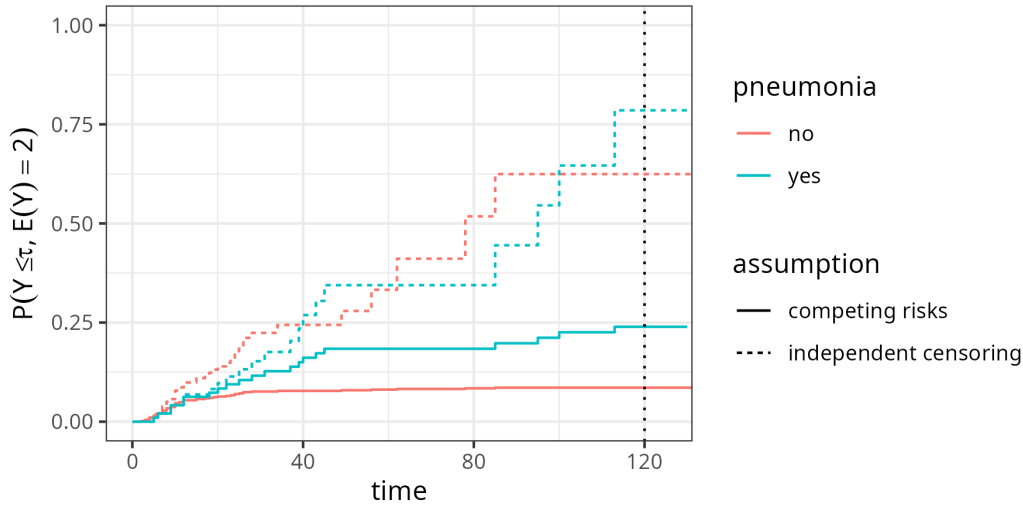


Figure 4.3: Estimation of the probability of dying in the ICU conditional on pneumonia status at admission. Dashed lines give the probabilities under assumption of right-censoring. Solid lines give the probabilities when taking into account discharge as competing risk.

absorbing state.

The goal of the trial was to investigate if treatment (prednisone) slows down or reverses disease progression (transitions $0 \rightarrow 1$ and $1 \rightarrow 0$) and reduces mortality (transitions $0 \rightarrow 2$ and $1 \rightarrow 2$).

Table 4.2 shows a subset of the data set and contains for each subject (`id`) one row for each transition for which the subject was at risk for. In this example, this includes transitions that were possible, but didn't happen (counterfactual transitions). The columns `from` and `to` indicate the initial state and the possible end state. `tstart` indicates the time at which the subject entered the risk set for said transitions and `tstop` the time point at which the subjects exited the `from` state (or were censored for any transition). The variable `status` indicates whether the transition was actually made (`status = 1`) or not (`status = 0`). This is necessary, as all possible transitions are listed, so we need an indicator for which transition actually occurred. If `status=0` for all possible transitions, the subject is censored for further transitions. Finally, `treatment` indicates whether a patient was assigned the treatment or placebo group.

Concretely, subject `id=1` already had abnormal prothrombin levels at the beginning of the trial, thus started in state 1 with possible transitions $1 \rightarrow 0$ and $1 \rightarrow 2$. In this case, the patient died, thus transition $1 \rightarrow 2$ was realized after 151 days, while the transition $1 \rightarrow 0$ is a ‘counterfactual’ transition that could have happened in the time-span between `tstart=0` and `tend=151`, but didn't. Patient `id=8` also started in state 1, but made a back transition to normal prothrombin levels after 211 days at which time they entered the risk set for transitions $0 \rightarrow 1$ and $0 \rightarrow 2$. Neither of the transitions occurred, as `status=0` for both transitions, which means the subject remained in status 0 until the end of their follow-up at 2770 days (that is was right-censored at 2770 days). Finally, subject `id=46` started in state 0 (normal prothrombin levels), transitioned to state 1 (abnormal levels) after 415 days and then died (transition $1 \rightarrow 2$) two days later. This also illustrates the importance of left-truncation (Section 3.4) in multi-state processes. For example, subjects `id=1` and `id=8`

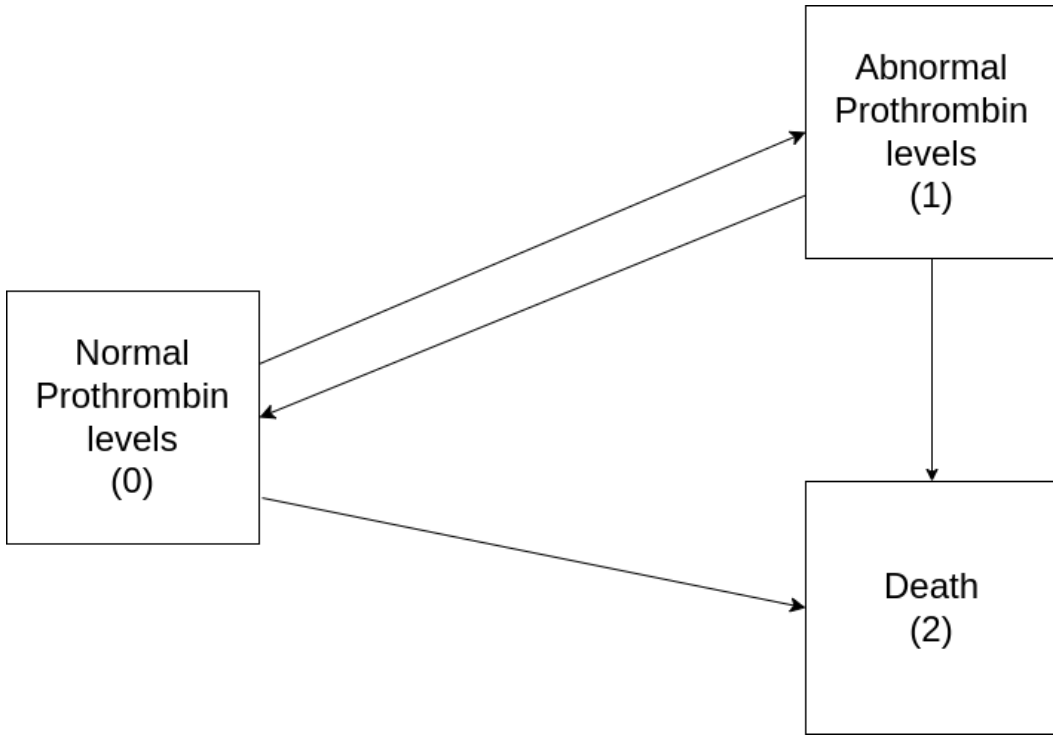


Figure 4.4: Transition graph for the liver cirrhosis patients.

are at risk for the transitions $1 \rightarrow 0$ and $1 \rightarrow 2$ from the beginning of the trial ($tstart = 0$). Subject `id=46` on the other hand starts in state 0 and only enters state 1 (and thus the risk set for the transitions $1 \rightarrow 0$ and $1 \rightarrow 2$) after 415 days ($tstart = 415$). Other subjects in the data may never enter the risk set for these transitions by remaining in state 0 until the end of follow up or by directly transitioning to state 2. The fact that subjects enter the risk sets for different transitions at different time points technically constitutes left-truncation and thus should be taken into account accordingly (Section 4.3.4).

Table 4.2: Subset of the `prothr` dataset (de Wreede, Fiocco, and Putter 2011).

id	from	to	trans	tstart	tstop	status	treatment
1	1	0	3	0	151	0	Placebo
1	1	2	4	0	151	1	Placebo
8	1	0	3	0	211	1	Prednisone
8	1	2	4	0	211	0	Prednisone
8	0	1	1	211	2770	0	Prednisone
8	0	2	2	211	2770	0	Prednisone
46	0	1	1	0	415	1	Prednisone
46	0	2	2	0	415	0	Prednisone
46	1	0	3	415	417	0	Prednisone
46	1	2	4	415	417	1	Prednisone

4.3.1 Notation and Definitions

In the competing risks setting, we characterized the data generating process by cause-specific transitions hazards $h_e(\tau)$ (4.4). Implicitly these are transitions from starting state 0 to end state e , however, since everyone starts in state 0 this is ignored notationally. In the multi-state setting on the other hand, subjects can be in different states at different time points. Transitions between different states are therefore characterized by transition-specific hazards, denoted by $h_{\ell \rightarrow e}(\tau)$ or short $h_{\ell e}(\tau)$, where ℓ is the starting state and e the end state.

Let $E(\tau) \in \{0, \dots, q\}$ be the state of the process at time τ as before (4.1). Then, the transition-specific hazard can be defined as

$$h_{\ell e}(\tau) = \lim_{d\tau \rightarrow 0} \frac{P(E(\tau + d\tau) = e | E(\tau-) = \ell)}{d\tau} \quad (4.12)$$

Transition hazards 4.12 indicate the instantaneous risk to enter state e at time τ given occupation of state ℓ at $\tau-$, which is the instant before τ .

Analogous to the competing risks setting, we can define the transition specific cumulative hazards

$$H_{\ell e}(\tau) = \int_0^\tau h_{\ell e}(u) du \quad (4.13)$$

The probability to transition from state ℓ to e between two time-points depends on all transitions possible from ℓ and potentially the transitions that have taken place in the past. Thus, other quantities of interest in the multi-state setting are the transition probabilities $P_{\ell e}(\zeta, \tau) := P(E(\tau) = e | E(\zeta) = \ell)$, that is the probability to transition from state ℓ to state e between time points $\zeta < \tau$. Implicitly, this notation assumes that the process is Markovian: the transition probability depends only on the state at ζ and not any additional past states. Extensions do exist that relax this assumption, for example by including information about the past, but are not relevant for now.

Transition probabilities of a multi-state process are often summarized in a matrix

$$\mathbf{P}(\zeta, \tau) := \begin{pmatrix} P_{00}(\zeta, \tau) & \cdots & P_{0q}(\zeta, \tau) \\ \vdots & \ddots & \vdots \\ P_{q0}(\zeta, \tau) & \cdots & P_{qq}(\zeta, \tau) \end{pmatrix}, \quad (4.14)$$

where rows indicate starting states and columns indicate end states. Some of the elements of \mathbf{P} might be zero or one depending on the specific process, presence of absorbing states and possible pathways between states. As subjects can only be in one of the $q + 1$ states at τ , rows sum to 1:

$$\sum_{e=0}^q P_{\ell e} = 1, \forall \ell \in \{0, \dots, q\}. \quad (4.15)$$

4.3.2 Transition probabilities

In this section we briefly motivate how transition probabilities between two non-consecutive time points can be expressed as the product (integral) of transition probabilities between intermediate, subsequent time points.

For illustration, consider what is often referred to as an illness-death model depicted in Figure 4.5 (similar to Figure 4.4, but without back-transition), where subjects can transition from healthy state 0 to absorbing death state 2 either directly or via intermediate state 1.

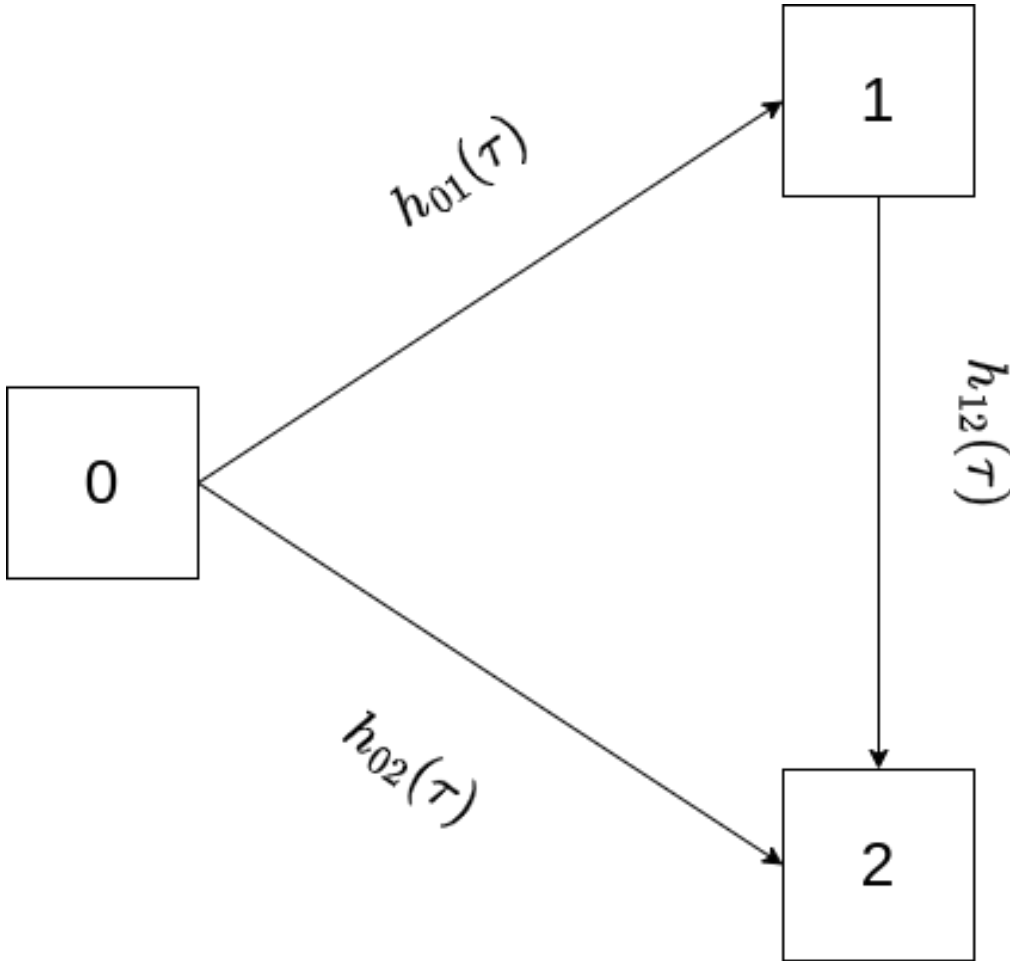


Figure 4.5: An *illness-death model* where subjects can transition from healthy state (0) to death (2) directly or via intermediate illness state (1)

In this example, back-transitions are not possible, therefore the lower triangle of the matrix is filled with zeros and $P_{22}(\zeta, \tau) = 1, \forall \zeta < \tau$ by virtue of being an absorbing state. The matrix of transition probabilities is thus given as

$$\mathbf{P}(\zeta, \tau) = \begin{pmatrix} P_{00}(\zeta, \tau) & P_{01}(\zeta, \tau) & P_{02}(\zeta, \tau) \\ 0 & P_{11}(\zeta, \tau) & P_{12}(\zeta, \tau) \\ 0 & 0 & 1 \end{pmatrix} \quad (4.16)$$

First, assume that data is collected in discrete time, that is $\zeta, \tau \in \{0, 1, 2, \dots\}, \zeta < \tau$ and transitions only occur at these discrete time points and not in between. Say we are interested in transition probability $P_{02}(4, 6)$, that is the probability to transition from state 0 to state 2 between time points $\zeta = 4$ and $\tau = 6$, given we are in state 0 at time $\zeta = 4$. This is possible in the three ways depicted in Figure 4.6.

$t = 4$ $t = 5$ $t = 6$

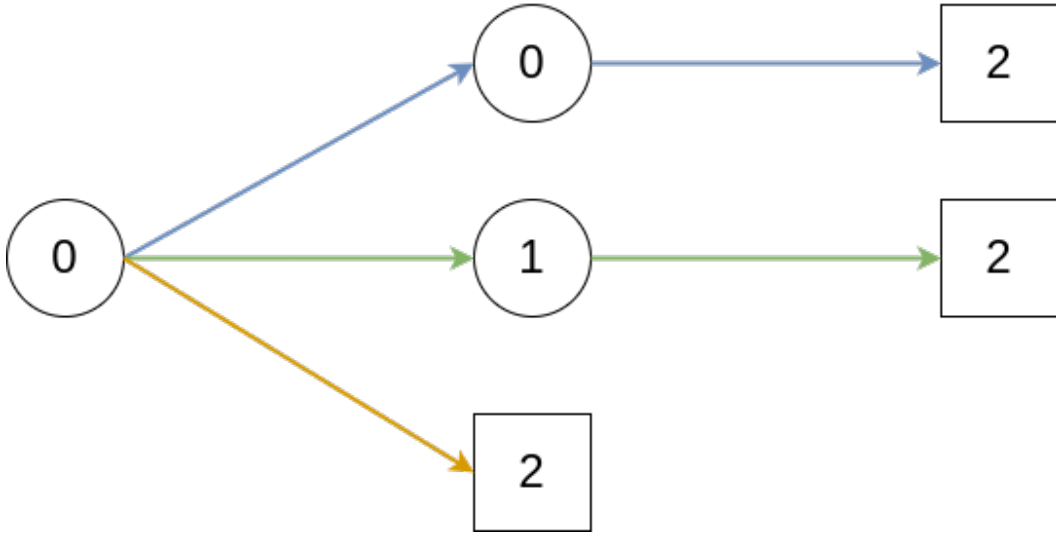


Figure 4.6: Possible paths to transition from state 0 to state 2 between time points 4 and 6

Thus, $P_{02}(4, 6) = p_{00}(5)p_{02}(6) + p_{01}(5)p_{12}(6) + p_{02}(5)$, where $p_{\ell e}(\tau) = P(E(\tau) = e | E(\tau-1) = \ell)$ are the probabilities for transitions $\ell \rightarrow e$ between two subsequent discrete time points. Thus, in discrete time, the matrix of transition probabilities can be represented as a finite matrix product

$$\mathbf{P}(\zeta, \tau) = \prod_{j=\zeta+1}^{\tau} \begin{pmatrix} p_{00}(j) & p_{01}(j) & p_{02}(j) \\ 0 & p_{11}(j) & p_{12}(j) \\ 0 & 0 & 1 \end{pmatrix}. \quad (4.17)$$

For the concrete example we thus have

$$\begin{aligned}
 \mathbf{P}(4, 6) &= \begin{pmatrix} P_{00}(4, 6) & P_{01}(4, 6) & P_{02}(4, 6) \\ 0 & P_{11}(4, 6) & P_{12}(4, 6) \\ 0 & 0 & 1 \end{pmatrix} = \prod_{j=5}^6 \begin{pmatrix} p_{00}(j) & p_{01}(j) & p_{02}(j) \\ 0 & p_{11}(j) & p_{12}(j) \\ 0 & 0 & 1 \end{pmatrix} \\
 &= \begin{pmatrix} p_{00}(5) & p_{01}(5) & p_{02}(5) \\ 0 & p_{11}(5) & p_{12}(5) \\ 0 & 0 & 1 \end{pmatrix} \begin{pmatrix} p_{00}(6) & p_{01}(6) & p_{02}(6) \\ 0 & p_{11}(6) & p_{12}(6) \\ 0 & 0 & 1 \end{pmatrix} \\
 &= \begin{pmatrix} p_{00}(5)p_{00}(6) & p_{00}(5)p_{01}(6) + p_{01}(5)p_{11}(6) & p_{00}(5)p_{02}(6) + p_{01}(5)p_{12}(6) + p_{02}(5) \\ 0 & p_{11}(5)p_{11}(6) & p_{11}(5)p_{12}(6) + p_{12}(5) \\ 0 & 0 & 1 \end{pmatrix},
 \end{aligned}$$

where the quantity of interest, $P_{02}(4, 6)$ is given in the top right corner, but other transition probabilities are also readily available. For example, the probability to transition from state 1 to 2 between time points $\zeta = 4$ and $\tau = 6$ is given as $P_{12}(4, 6) = p_{11}(5)p_{12}(6) + p_{12}(5)$.

Returning to the continuous time setting where transitions can occur at any time point, ideas from the discrete time setting still hold. Imagine dividing the interval $(\zeta, \tau]$ into J intervals such that $\zeta = t_0 < t_1 < \dots < t_j < \dots < t_J = \tau$, assuming that no events occur between time points $t_j \in \mathbb{R}_+, j = 1, \dots, J$. Then 4.17 still holds when replacing $p_{\ell e}(j)$ with $p_{\ell e}(t_j)$.

4.3.3 Transition probabilities and hazards

Increasing the number of intervals to infinity or equivalently, reducing the interval size to infinitesimally small intervals we can define the transition probability matrix as a product integral over the instantaneous transition probabilities $p_{\ell e}(u)$, expressed in terms of transition-specific (cumulative) hazards.

To do so, we use, somewhat informally, the following relationships

- From equations 4.12 and 4.13 we can equate the instantaneous transition probabilities to increments of the cumulative hazard (that is the increase in the cumulative hazard within a (fixed, infinitesimally) small interval du): $dH_{\ell e}(u) = P(E(u + du) = e | E(u-) = \ell) =: p_{\ell e}(u)$,
- because of relationship 4.15, diagonal elements (transitions into the same state) are set to $dH_{\ell\ell}(u) := -\sum_{e \neq \ell} dH_{\ell e}(u)$ such that $1 + dH_{\ell\ell}(u) = 1 - \sum_{e \neq \ell} dH_{\ell e}(u) = 1 - \sum_{e \neq \ell} p_{\ell e}(u) = p_{\ell\ell}(u)$.

Consequently, the transition probability matrix can be written as

$$\mathbf{P}(\zeta, \tau) = \mathcal{P}_{u \in (\zeta, \tau]} \begin{pmatrix} p_{00}(u) = 1 + dH_{00}(u) & \cdots & p_{0q}(u) = dH_{0q}(u) \\ \vdots & \ddots & \vdots \\ p_{q0}(u) = dH_{q0}(u) & \cdots & p_{qq}(u) = 1 + dH_{qq}(u) \end{pmatrix}$$

$$= \mathcal{P}_{u \in (\zeta, \tau]} (\mathbf{I} + d\mathbf{H}(u)),$$

where \mathcal{P} is the product integral operator, \mathbf{I} is a $(q+1) \times (q+1)$ identity matrix and $d\mathbf{H}(u)$ is the matrix of increments of the cumulative hazard within infinitesimally small intervals. Thus, similar to the competing risks setting, relationship 4.18 implies that knowledge of the transition specific (cumulative) hazards is sufficient to fully specify the multi-state process.

As analytical solutions of 4.18 only exist for specific models, in practice, the transition probabilities are often once again approximated numerically via a finite matrix product on a discrete time grid $\zeta = t_0 < t_1 < \dots < t_{J-1} < t_J = \tau$

$$\mathbf{P}(\zeta, \tau) \approx \prod_{j=1}^J (\mathbf{I} + \Delta \mathbf{H}_{\ell e}(t_j)), \quad (4.18)$$

where $\Delta H_{\ell e}(t_j) = H_{\ell e}(t_j) - H_{\ell e}(t_{j-1})$ is the increment of the cumulative hazards between consecutive time points.

4.3.4 Non-parametric estimation of transition probabilities

From 4.18, it follows that transition probabilities can be estimated by first computing the transition-specific cumulative hazards, $H_{\ell e}(\tau)$. Similarly to the competing risks setting (Section 4.2.2), we can first define the transition specific hazards

$$h_{\ell e}^d(t_{(k)}) := \frac{d_{\ell e, t_{(k)}}}{n_{\ell; t_{(k)}}},$$

where

- $d_{\ell e, t_{(k)}}$ is the number of subjects that made the transition $\ell \rightarrow e$ at time $t_{(k)}$ and
- $n_{\ell; t_{(k)}}$ is the number of subjects in state ℓ immediately before $t_{(k)}$.

The cumulative transition-specific hazards follow as

$$H_{NA, \ell e}(\tau) = \sum_{k: t_{(k)} \leq \tau} h_{\ell e}^d(t_{(k)}) = \sum_{k: t_{(k)} \leq \tau} \frac{d_{\ell e, t_{(k)}}}{n_{\ell; t_{(k)}}},$$

and transition probabilities are obtained via 4.18 as

$$\mathbf{P}(\zeta, \tau) = \prod_{j=1}^J (\mathbf{I} + \Delta \mathbf{H}_{NA, \ell e}(t_{(j)})). \quad (4.19)$$

4.3.5 Application to liver cirrhosis patients

For illustration, consider again the `prothr` data set (Table 4.2), with possible transitions summarized in Figure 4.4. In contrast to the illness-death model in Figure 4.5, back transitions are possible and some subjects already start in the “abnormal” state at the beginning of the study.

Figure 4.7 shows the transition probabilities for the four possible transitions over time for subjects who received treatment and placebo, respectively. In this example back-transitions are possible, therefore, in contrast to the cumulative incidence functions in the competing risks setting, transition probabilities (to transient states) are not monotonously increasing over time. While the probabilities to transition from normal or abnormal state to death ($0 \rightarrow 2$, $1 \rightarrow 2$) increase over time for both groups, probabilities for transitions between the transient states (normal to abnormal and vice versa) increase in the beginning but eventually decreases over time. Overall, prednisone doesn’t appear to have a strong protective effect. Although there appears to be a reduction in $0 \rightarrow 2$ transitions and an increase in $1 \rightarrow 0$ transitions between time points 1000 and 3000, this effect doesn’t seem to persist until the end of the follow up.

4.4 Conclusion

Key takeaways

- Defining the state diagram of the data generating process can be helpful to understand the dynamics in the data and to select an appropriate framework (and model) for the analysis.
- Non-parametric estimators like the Aalen-Johanson estimator can be used as first step in the analysis of competing risks and multi-state settings.
- The empirical transition matrix provides a general procedure to obtain estimates of transition probabilities based on any learner that can estimate transition-specific hazards.

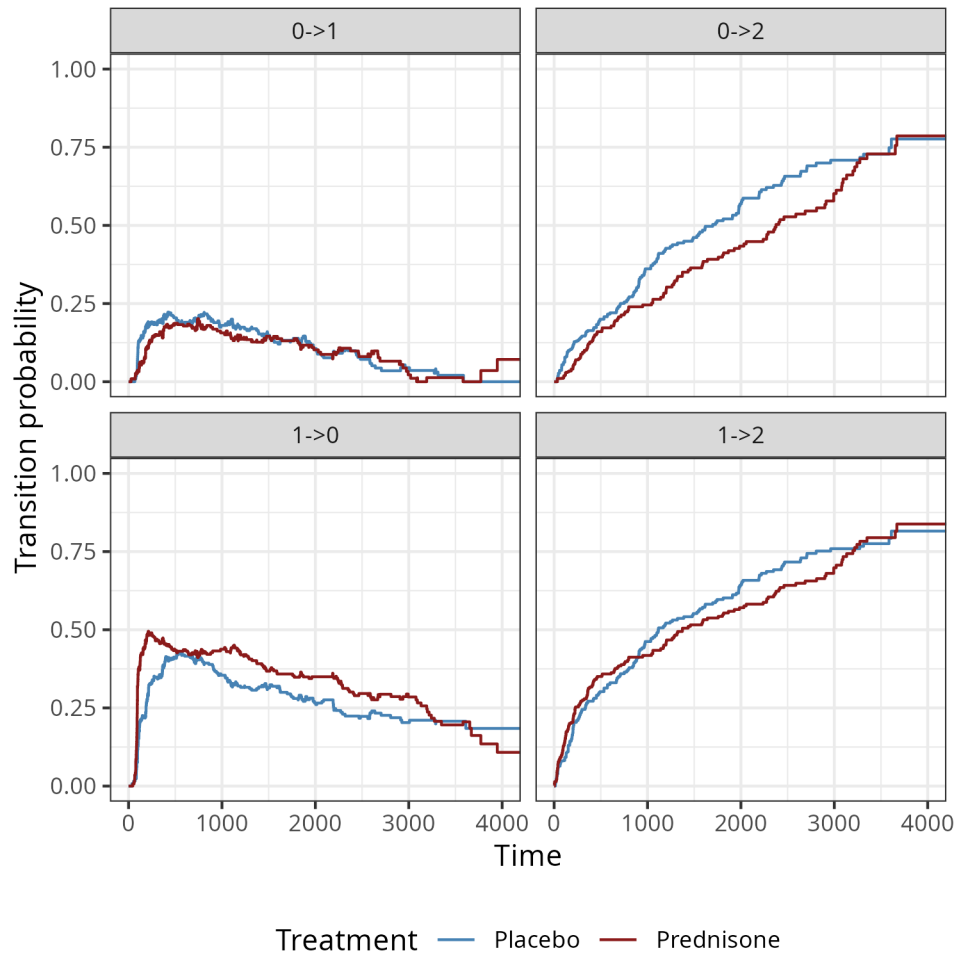


Figure 4.7: Estimated transition probabilities for the different transitions of the prothrombin data example .

Further reading

- O. Aalen, Borgan, and Gjessing (2008) introduces different approaches for event-history analysis motivated from the point of view of the counting process.
- Beyersmann, Allignol, and Schumacher (2012) provide an accessible overview of important concepts for competing risks and multi-state modelling, particularly non-parametric estimation.

5

Survival Task

This chapter introduces the different survival problems and formalizes them as survival tasks. There are four prediction types in survival analysis: relative risks - predicting the risk of an event compared to others in the sample; survival times - predicting the time until an event happens; prognostic index - predicting a linear predictor to assess outcomes based on risk factors; and survival distributions - predicting the probability of an event taking place over time. These reduce to three formal survival tasks: deterministic (survival time), ranking (risks and prognostic index), and probabilistic (distribution). This separation of tasks helps create a taxonomy of survival models and losses that is used throughout the book.

 Minor changes expected!

This page is a work in progress and minor changes will be made over time.

A machine learning task specifies a mathematical problem to be solved by an algorithm (Section 2.2). Formally, a task is a mapping $f : \mathcal{X} \rightarrow \mathcal{Y}$ with three components: a description of the input space \mathcal{X} , a description of the target space \mathcal{Y} , and a description of the estimation procedure that learns f from data. A *survival task* is a machine learning task in which the target space \mathcal{Y}_S corresponds to a *survival prediction type* (Section 5.1), and the learning algorithm f_S is designed to handle censoring and/or truncation while targeting that prediction type (as in the methods introduced in Part III).

Throughout this chapter let $\mathcal{X} \subseteq \mathbb{R}^{n \times p}$ be a set representing the covariate matrix. The censoring mechanism does not affect the definition of the prediction types, hence this chapter does not distinguish between right-, left-, or interval-censoring when defining \mathcal{Y}_S .

5.1 Survival prediction types

Survival prediction types describe the codomain \mathcal{Y}_S , four are commonly defined:

1. Survival distribution: Probability of the event occurring over time;
2. Relative risk: A scalar quantity representing the risk of event that is meaningful only in comparison to other individuals in the sample;
3. Survival time or time-to-event: A point prediction of the time at which the event of interest will occur;
4. Prognostic index: A risk score usually based on a linear predictor.

Survival distribution predictions are *probabilistic* as they return a full distribution over time. Survival time predictions are *deterministic* point predictions in the sense that they return a single scalar value, though uncertainty remains due to underlying variance. Relative risk and prognostic index predictions do not directly predict when or if the event of interest will occur, instead they produce scores that can be used to rank or compare an individual's risk to others in the same cohort.

To distinguish the types of 'risk', it may be helpful to view survival distribution predictions as a form of *absolute risk* prediction. Derived summaries from distributions, such as the probability of experiencing the event at a given time, have a direct probabilistic interpretation and can be meaningfully understood without comparison to others in the sample. By contrast, the other prediction types are *relative risk* predictions: their scale is directly tied to others in the sample and are most (in some cases *only*) interpretable through comparisons.

These prediction types are closely related. Relative risks and survival time predictions can be derived from a predicted survival distribution, though the reverse does not hold in general as a single survival time or risk score does not uniquely determine a probability distribution. Both prognostic index and time-to-event predictions can usually be interpreted as a type of relative risk prediction. Under (often strict) assumptions, prediction types can be converted between each other. In fact, many algorithms target a single prediction type but internally compute another as an intermediate step, this pattern will appear throughout Part III, for example with the prognostic index being computed in linear models before being transformed into a survival distribution prediction (some algorithmic examples in Chapter 10).

Despite their close connection, it is essential to keep discussion of prediction types distinct as they are not directly comparable. For example, it is not meaningful to compare a relative risk score from one model to a survival distribution prediction of another without first transforming the distribution prediction. Even within a single prediction type, interpretations can be confused. For example, in some literature a larger value of a risk score implies higher risk of event, whereas in other sources, a larger value implies lower risk. Distinction of prediction types is also critical for evaluation as each prediction type naturally aligns with different types of metrics, a topic returned to throughout Part II.

In applied predictive modelling, *direct* survival time prediction is uncommon as time-to-event predictions are difficult to interpret and evaluate under censoring. Instead, practitioners often report distribution-derived summaries such as τ -year survival probabilities or the predicted median survival time. Similarly, the prognostic index is more commonly used for model interpretation or inference, whereas relative risk predictions are common in applications such as resource allocation and risk stratification. Though, as will be seen below, a prognostic index can usually be interpreted as a relative risk.

Figure 5.1 illustrates the different information provided by the different prediction types; the prognostic index is omitted as it would visually look the same as the relative risk prediction type. An example of tabular survival data is in the top-left panel. The top-right panel shows predicted survival times, for each observation this is a single scalar value representing the estimated time the event will take place. The bottom-left panel visualizes relative risk predictions, each subject's score is defined relative to a baseline (an individual with covariates set to zero) and scores can be compared in direction and magnitude. Finally, the bottom-right panel shows survival distribution predictions, where each observation's survival probability is estimated over time.

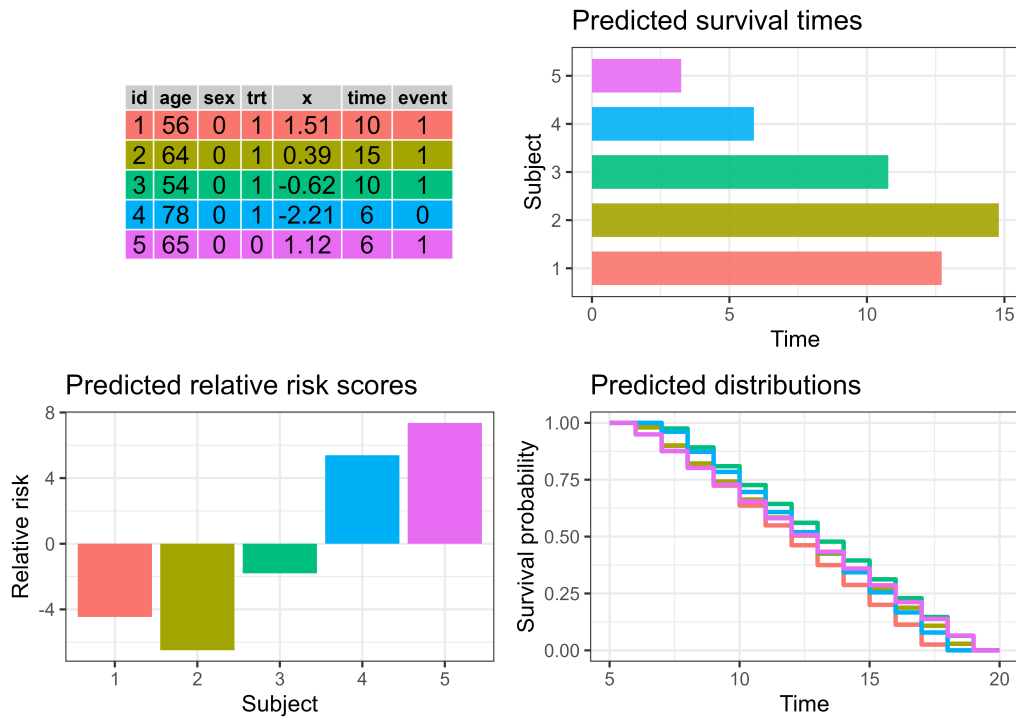


Figure 5.1: Illustration of prediction types. Tabular survival data (top-left) can be used by an algorithm to make various prediction types, each conveying different information. Survival times (top-right) provide a single number estimating the time until an event takes place. Relative risk scores (bottom-left) compare the risk of event between subjects within the same sample. Survival distributions (bottom-right) estimate the probability of the event taking place over time.

5.2 Predicting distributions

Predicting a survival distribution means estimating the probability of an individual experiencing the event of interest from time-point 0 to ∞ . In principle, such predictions are defined over the continuous $\mathbb{R}_{\geq 0}$. However, in practice it is more common for predictions to be made over the discrete \mathbb{N}_0 . This reflects the fact that many algorithms rely on discrete, non-parametric estimators or piecewise-constant representations of the underlying distribution prediction.

Theoretically, distributional prediction can target any of the distribution defining functions introduced in Section 3.1, though predicting $S(t)$ or $h(t)$ is most common. Mathematically, the survival task associated with the distribution prediction type is defined by $f_S : \mathcal{X} \rightarrow \mathcal{S}$, where $\mathcal{S} \subseteq \text{Distr}(\mathbb{R}_{\geq 0})$ denotes a set of distributions on $\mathbb{R}_{\geq 0}$. In the most general multi-state setting, this generalizes to $f_S : \mathcal{X} \rightarrow [0, 1]^{q \times q}$ for q different states, this simplifies to $f_S : \mathcal{X} \rightarrow \mathcal{S}^q$ in the competing risks setting.

In applied settings, communicating a predicted distribution over time is a daunting task for both clinician and patient. Instead, distribution predictions are commonly used to derive time-specific survival probabilities, which represent the probability of surviving beyond a relevant time point, for example the probability of being alive ten years after a diagnosis of Huntingdon's disease. Predicting ‘ τ -year survival probabilities’ is sometimes mistakenly framed as a classification problem, in which a model predicts whether an event will occur by a fixed time. This is misleading as traditional classification models cannot incorporate observations censored before the time horizon of interest, and discarding such observations would bias any results (Loh et al. 2025).

Survival distributions can also be used for decision making by establishing thresholds on survival probabilities. For example, in an engineering context, a survival model might be used to estimate the reliability of a jet engine over time, with a maintenance rule defined such that the engine is serviced once the predicted survival probability falls below a predefined reliability threshold (which could be as high as 0.95).

Another source of potential confusion can arise when trying to interpret a survival distribution prediction for an individual in the single-event setting. In reality, an event either does or does not occur at a specific time, so it is natural to ask what it means to predict an individual's survival probability distribution. Figure 5.2 visualizes what the survival distribution prediction aims to achieve. The top-left panel shows the idealized ‘real-world’ survival curves for multiple individuals, each represented by a Heaviside step function that drops from 1 to 0 when the individual experiences the event. The top-right panel highlights a curve for a single event. The bottom-left panel shows the goal of survival distribution predictions: a smooth survival function that captures the average behavior of these individual events across the population. Finally, the bottom-right panel shows the same events stratified by a single binary covariate, producing one survival distribution prediction for each subgroup. In a machine learning task, this stratification process is generalized by conditioning on the full covariate vector, yielding one predicted survival distribution for each individual.

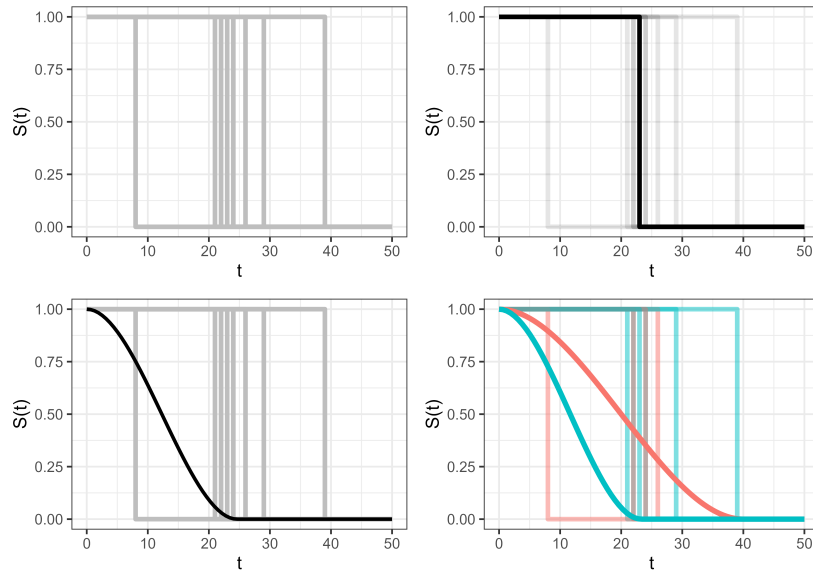


Figure 5.2: Demonstrating the relationship from theoretical real-world event curves to survival distribution predictions.

5.3 Predicting relative risks

Predicting relative risk scores refers to estimating a value that ranks individuals in a cohort according to their predicted risk of experiencing the event. These scores are meaningful only in comparison to other individuals in the same cohort used to train the model; they cannot be interpreted in isolation, nor can they be compared to scores produced by a different model, except under very strong assumptions. The interpretation of these scores can also differ across model classes, parameterizations, and even software implementations. For example, some models produce scores where larger values correspond to higher risk, whereas others produce scores where smaller values correspond to higher risk. To avoid ambiguity, throughout this book larger values always correspond to higher risk and smaller values correspond to lower risk. In machine learning terms, the relative risks prediction is the problem of estimating $f_S : \mathcal{X} \rightarrow \mathbb{R}$.

As an example of this prediction type, consider three individuals, $\{i, j, k\}$ with predicted risks $\{0.5, 10, 0.1\}$, respectively. From these values, two broad types of conclusion can be drawn.

1. Conclusions comparing individuals

- The corresponding ranks for $\{i, j, k\}$ are $\{2, 3, 1\}$.
- k has the lowest risk and j the highest risk.
- The risk of i is slightly higher than that of k , whereas j 's risk is substantially higher than both.

2. Conclusions comparing risk groups:

- Thresholding at 0.4 classifies k as low-risk and i and j as high-risk.
- Thresholding at 1.0 classifies i and k as low-risk and j as high-risk.

As in other domains, differences in relative risks should always be interpreted cautiously. In the example above, j 's relative risk is 100 times that of k ; however, if k 's absolute probability of experiencing the event is 0.0001, then j 's absolute probability remains small at 0.01.

Estimation and interpretation of risks in the competing risks settings follows similar principles. Though, one must take care to clearly identify if the task of interest is to predict risks for each of the q causes, $f_S : \mathcal{X} \rightarrow \mathbb{R}^q$, or a single all-cause risk. In multi-state models, the notion of a single scalar 'risk' is less clearly defined and any risk-based summaries derived from survival probabilities should be interpreted with caution.

5.3.1 Distributions and risks

In general it is not possible to uniquely recover a survival distribution from a relative risk score, except in very specific cases (discussed in Section 5.5). The reverse direction, deriving a risk score from a predicted survival distribution, is more common. One stable approach to compute a risk score is by calculating the 'ensemble mortality' or 'expected mortality' (B. H. Ishwaran et al. 2008). The expected mortality for an individual i is defined as

$$\sum_{\tau \in \mathcal{T}} -\log(\hat{S}_i(\tau)) = \sum_{\tau \in \mathcal{T}} \hat{H}_i(\tau),$$

where \hat{S}_i is the predicted survival function, \hat{H}_i is the corresponding cumulative hazard, and \mathcal{T} is the set of observed time points. This quantity represents the expected number of events among individuals with similar covariate profiles to i . A larger value therefore indicates that i has a higher risk profile, hence being a suitable quantity to represent a relative risk score. As a concrete example, consider two individuals, i and j , with predicted survival probabilities at times $\mathcal{T} = \{0, 1, 2, 3\}$:

$$\begin{aligned} (\tau, \hat{S}_i(\tau)) &= (0, 1), (1, 0.8), (2, 0.4), (3, 0.15), \\ (\tau, \hat{S}_j(\tau)) &= (0, 1), (1, 0.6), (2, 0.4), (3, 0.35). \end{aligned}$$

From these values alone, it is not immediately obvious which individual would be considered at higher risk. The corresponding cumulative hazards are

$$\begin{aligned} (\tau, \hat{H}_i(\tau)) &= (0, 0), (1, 0.10), (2, 0.40), (3, 0.82), \\ (\tau, \hat{H}_j(\tau)) &= (0, 0), (1, 0.22), (2, 0.40), (3, 0.46). \end{aligned}$$

Using the ensemble mortality approach, this yields relative risk scores of

$$\begin{aligned} \sum_{\tau \in \mathcal{T}} \hat{H}_i(\tau) &= 0 + 0.10 + 0.40 + 0.82 = 1.32, \\ \sum_{\tau \in \mathcal{T}} \hat{H}_j(\tau) &= 0 + 0.22 + 0.40 + 0.46 = 1.08. \end{aligned}$$

Under this method, individual i is considered to be at 1.2 times higher risk than individual j .

5.4 Predicting survival times

Predicting a survival time refers to estimating when an individual will experience the event of interest. Mathematically, this corresponds to estimating $f_S : \mathcal{X} \rightarrow \mathbb{R}_{>0}$, that is, predicting a single non-negative value on $[0, \infty]$.

From a practical perspective, the expected time-to-event may appear to be an attractive prediction type as it initially appears intuitive and easy to interpret. However, evaluating survival time point predictions is limited and generally ill-advised and reliance on such predictions is therefore challenging. To illustrate this, consider an individual censored at time $t = 5$. There is no way to know if the event would have occurred at $\tau = 6$ or $\tau = 600$; all that is known is that the event did not occur before $t = 5$. As a result, it is impossible to assess how close a time prediction is to the true, unobserved event time.

Even when a prediction is clearly incorrect, the magnitude of its error cannot be quantified. For the same individual censored at $t = 5$, suppose a model predicts a survival time of $\hat{t} = 3$. This prediction is clearly wrong as the event did not occur before $t = 5$. However, the prediction might only be slightly wrong if the true event time were $\tau = 6$, or extremely wrong if the true event time were $\tau = 600$.

For these reasons, this book recommends predicting and evaluating survival distributions and then deriving time-oriented summaries.

In the event history analysis setting, a single ‘survival time’ is even more ill-defined as it is ambiguous whether this refers to the time until a specific event or until any event takes place. For multi-state models, one could estimate *sojourn times*, which represent the expected time spent in a given state and can be derived from estimated transition probabilities. Sojourn times are particularly well defined in Markov and semi-Markov models, where they follow from stochastic process theory. These derivations are beyond the scope of this book; for further details, see, for example, Ibe (2013).

5.4.1 Times and risks

Converting a survival time prediction to a risk prediction is conceptually straightforward, as survival times encode natural ordering. An individual predicted to survive longer is, by definition, at lower overall risk. Formally, if \hat{t}_i, \hat{t}_j denote predicted survival times and \hat{r}_i, \hat{r}_j are associated rankings, then

$$\hat{t}_i > \hat{t}_j \Rightarrow \hat{r}_i < \hat{r}_j.$$

The reverse transformation, from ranking to survival time, is generally not possible without strong assumptions as relative risk scores are usually abstract quantities that do not map directly to meaningful survival times.

5.4.2 Times and distributions

Moving from a survival time to a distribution prediction is uncommon for the reasons just discussed. Given the availability of survival models that directly predict distributions, and the difficulties in evaluating survival time predictions, there is little practical value in constructing a survival distribution from a predicted survival time. Although, as in regression

settings, it is certainly *possible* to construct a distribution around a central estimate by assuming a parametric form, for example $\text{TruncatedNormal}(\hat{\mu}, \sigma, a = 0, b = \infty)$ where σ represents an assumed or estimated standard deviation; such approaches rely on strong assumptions and are rarely used in practice.

It is more common to reduce a prediction from a probability distribution to a survival time by *attempting* to compute the mean or median of the distribution. When there is no censoring, the expected survival time can be computed from the survival function using the ‘Darth Vader rule’ (Muldowney, Ostaszewski, and Wojdowski 2012):

$$\mathbb{E}[Y] = \int_0^\infty S_Y(y) \, dy \quad (5.1)$$

However, this rule is often unusable in survival datasets as censoring can lead to estimated survival distributions that are *improper*. A valid probability distribution for a random variable Y must satisfy: $\int f_Y dy = 1$, $S_Y(0) = 1$ and $S_Y(\infty) = 0$. This last condition is often violated in survival distribution predictions, particularly when non-parametric estimators are used as intermediate steps before constructing full distribution predictions (some examples in Section 10.2). To see why this is the case, recall from Section 3.5.2.1 that the Kaplan-Meier estimator is defined as:

$$\hat{S}_{KM}(\tau) = \prod_{k:t_{(k)} \leq \tau} \left(1 - \frac{d_{t_{(k)}}}{n_{t_{(k)}}}\right).$$

This estimator reaches zero only if all individuals at risk at the final observed time-point experience the event: $d_{t_{(k)}} = n_{t_{(k)}}$. In practice, there is almost always administrative censoring at the final time-point and as such $d_{t_{(k)}} < n_{t_{(k)}}$ and hence $\hat{S}(\infty) > 0$.

Heuristics have been proposed to address this issue, including linear extrapolation of the survival curve to zero, or an immediate drop to zero at the final time-point. However, these can introduce bias into estimated survival times (K. Han and Jung 2022; R. Sonabend, Bender, and Vollmer 2022). The survival time could also be reported as the median survival time, defined as the time at which the predicted survival probability drops to 0.5. However, this quantity is only defined if the survival curves falls below 0.5 within the observed follow-up period, which is never guaranteed.

An alternative approach is to summarize the predicted distribution with the *restricted mean survival time* (RMST) (K. Han and Jung 2022; Andersen, Hansen, and Klein 2004). Rather than integrating over the entire time axis as in (5.1), the RMST truncates the integral at a finite horizon:

$$\text{RMST}(\tau) = \int_0^\tau S_Y(y) \, dy.$$

It follows from (5.1) that $\text{RMST}(\infty) = \mathbb{E}[Y]$. Whereas (5.1) represents the average survival time over $[0, \infty)$, the RMST represents the average survival time up to τ . Equivalently,

$$\text{RMST}(\tau) = \mathbb{E}[\min(Y, \tau)], \quad (5.2)$$

which treats all events occurring after τ as if they occurred at τ . The RMST is well-defined even when the predicted distribution is improper, provided that τ lies within the range of observed follow-up times.

Say individuals are observed over a five-year time period and administrative censoring is present so that $\mathbb{E}[Y]$ cannot be reliably computed. One *can* compute RMST(5) to provide an interpretable lower bound on the mean survival time: $\text{RMST}(5) \leq \mathbb{E}[Y]$. This results in a meaningful statement such as: “the average survival time is at least RMST(5)” (Figure 5.3).

The RMST is commonly used to understand the effect of covariates, particularly treatments when in a healthcare context. For example, suppose a clinician is interested in understanding how a specific treatment affects two-year and five-year survival for a given disease. Assume patient i received the treatment and patient j did not, and that their predicted survival curves are

$$\begin{aligned}(\tau, \hat{S}_i(\tau)) &= (0, 1.00), (1, 0.80), (2, 0.75), (3, 0.75), (4, 0.70), (5, 0.60), \\(\tau, \hat{S}_j(\tau)) &= (0, 1.00), (1, 0.90), (2, 0.85), (3, 0.60), (4, 0.50), (5, 0.00).\end{aligned}$$

The corresponding RMSTs at $\tau = 2$ and $\tau = 5$ are (using discrete sum approximations over unit time intervals)

$$\begin{aligned}\text{RMST}_i(2) &\approx 1.00 + 0.80 + 0.75 = 2.55, \\ \text{RMST}_j(2) &\approx 1.00 + 0.90 + 0.85 = 2.75, \\ \text{RMST}_i(5) &\approx 1.00 + 0.80 + 0.75 + 0.75 + 0.70 + 0.60 = 4.60, \\ \text{RMST}_j(5) &\approx 1.00 + 0.90 + 0.85 + 0.60 + 0.50 + 0.00 = 3.85.\end{aligned}$$

Over the two-year follow-up period, patient j is expected to remain event-free for approximately 0.20 years (2.4 months) longer than patient i . In contrast, over the five-year interval, patient i is expected to remain event-free for approximately 0.75 years (9 months) longer than patient j . Computing the RMST at these two thresholds provides interpretable summaries: the treatment offers no short-term benefit within two years (and may even bring some risks) but confers a meaningful advantage over a longer five-year horizon.

These results (visualized in Figure 5.3) illustrate a key feature of the RMST. By fixing the time horizon τ , the contribution of survival differences after τ is ignored. In the above example, although patient j 's survival probability drops sharply to zero, this late drop in survival probability contributes relatively little to the area under the curve up to $\tau = 5$. Even if patient i were to survive many years longer than patient j , the RMST at $\tau = 5$ treats all events occurring after five years as if they occurred at that time, a consequence of (5.2). As a result, the RMST difference over the five-year horizon remains modest, even though the long term survival difference, if it were estimable, could be substantial.

5.5 Prognostic index predictions

In medical terminology (often used in survival analysis), a *prognostic index* is a quantity that summarizes an individual's risk of experiencing the event of interest based on observed risk factors. Given covariates, $\mathbf{X} \in \mathbb{R}^{n \times p}$, and coefficients, $\boldsymbol{\beta} \in \mathbb{R}^p$, the *linear predictor* is defined as $\eta := \mathbf{X}\boldsymbol{\beta}$. Applying a transformation g , which could simply be the identity function

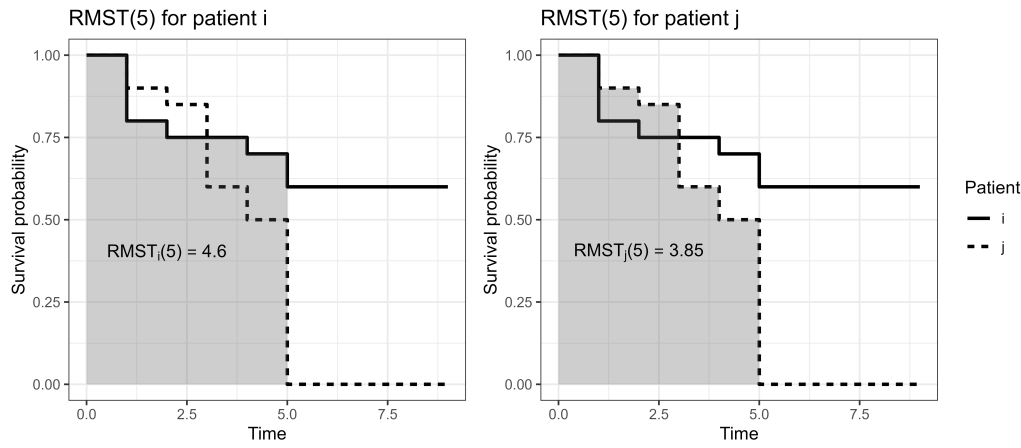


Figure 5.3: Illustrating the RMST at $\tau = 5$. The RMST is the area under the survival curve up to the point of interest. The solid line shows the survival curve for one patient and the dashed line for another. The left panel shows the RMST at $\tau = 5$ for patient i and the right panel for patient j . The figure illustrates how the difference in RMST is marginal at this point as the tail behavior of the patients is ignored.

$g(x) = x$, yields a *prognostic index*, $g(\boldsymbol{\eta})$. A prognostic index can serve several purposes, including:

1. Scaling and/or normalization: simple transformation can improve interpretability and visualization;
2. Ensuring meaningful results: for example, $g(\boldsymbol{\eta}) = \exp(\boldsymbol{\eta})$ transforms covariates to act multiplicatively on the resulting prognostic score, which is appropriate for models in which the covariates rescale the underlying risk instead of inducing additive shifts (explored further in Section 10.2);
3. Interpretability conventions: for example, $g(\boldsymbol{\eta}) = -\boldsymbol{\eta}$ might be sufficient to larger values correspond to higher risk.

In event history analysis, prognostic indices are defined analogously, but with a cause-specific interpretation.

5.5.1 Prognostic index, risks, and times

A prognostic index is naturally interpreted as a relative risk score. When used in this way, it is essential that both the magnitude and sign of the index align with the convention adopted above, meaning that larger values must correspond to a higher risk of experiencing the event.

The reverse transformation, from risk score to prognostic index, does not hold in general. For example, models introduced in Chapter 13 and Chapter 12 directly predict risk scores that cannot be expressed as transformations of covariates. Therefore, reporting a prognostic index emphasizes that the predicted quantity is interpretable in its own right, much like a survival time prediction.

There is no direct mapping between a prognostic index and survival time. However, a prognostic index may be used to construct a distribution prediction, from which a time-based

summary can be derived.

5.5.2 Prognostic index and distributions

In general, a prognostic index cannot be uniquely recovered from a predicted survival distribution without additional modeling assumptions. By contrast, constructing a survival distribution conditional on a prognostic index is very common in survival analysis. Many survival models predict survival distributions by first estimating a group-wise survival distribution, often using nonparametric estimators (Section 3.5.2), then combine this estimate with an individual's prognostic index. The manner in which these components are combined is algorithm-specific and discussed in detail in Part III.

As a concrete illustration, one class of model known as ‘proportional hazards models’, construct survival predictions of the form

$$S(\tau \mid \mathbf{x}) = S_0(\tau)^{\exp(\eta)},$$

where $S_0(\tau)$ is known as the baseline survival function, and η is the individual’s prognostic index.

5.6 Conclusion

Key takeaways

- There are four main prediction types in survival analysis: probability distributions, survival times, relative risks, and prognostic indices.
- The choice of prediction type determines both what a model learns and how its outputs should be interpreted. Prediction types are not directly comparable nor evaluated in the same way.
- Distribution predictions are the most informative and under suitable assumptions may be used to derive other prediction types.
- Ranking predictions are widely used in practice and often easier to evaluate. However, their interpretation is relative and restricted to comparisons within the given cohort.

Limitations

- Transformations between prediction types typically rely on modeling assumptions that may be strong, untestable, or context dependent.
- Survival time predictions, while appearing intuitive, are difficult to evaluate under censoring and can easily lead to misleading interpretations.
- Extensions of prediction types to event history analysis are not always straightforward as key quantities such as “risk” or “time-to-event” may be poorly defined.
- In real-world applications, the choice of prediction type may be constrained by software implementations or end-user (for example, clinicians) rather than theoretical considerations.

Further reading

- R. Sonabend, Bender, and Vollmer (2022) and Haider et al. (2020) discuss methods for transforming survival distribution predictions into relative risks and survival times.
- For deeper discussion of the restricted mean survival time, see Uno et al. (2014), K. Han and Jung (2022), and Royston and Parmar (2011).
- Van Houwelingen (2007) provides a comprehensive overview of dynamic survival prediction settings in which models are updated over time.
- John D. Kalbfleisch and Prentice (1980) offer a more theoretical perspective on the relationships between prediction types.
- See Candido dos Reis et al. (2017) for a real-world example of how survival distribution predictions can be computed in a healthcare setting.

Part II

Evaluation

6

Discrimination

TODO (150-200 WORDS)

 Minor changes expected!

This page is a work in progress and minor changes will be made over time.

This chapter discusses ‘discrimination measures’, which evaluate how well models separate observations into different risk groups. A model is said to have good discrimination if it correctly predicts that one observation is at higher risk of the event of interest than another, where the prediction is ‘correct’ if the observation predicted to be at higher risk does indeed experience the event sooner.

In the survival setting, the ‘risk’ is taken to be the continuous ranking prediction. All discrimination measures are ranking measures, which means that the exact predicted value is irrelevant, only its relative ordering is required. For example given predictions {100, 2, 299.3}, only their rankings, {2, 1, 3}, are used by measures of discrimination.

This chapter begins with time-independent measures (Section 6.1), which measure concordance between pairs of observations at a single observed time point. The next section focuses on time-dependent measures (Section 6.2), which are primarily AUC-type measures that evaluate discrimination over all possible unique time-points and integrate the results for a single metric.

6.1 Time-Independent Measures

The simplest form of discrimination measures are concordance indices, which, in general, measure the proportion of cases in which the model correctly ranks a pair of observations according to their risk. These measures may be best understood in terms of two key definitions: ‘comparable’, and ‘concordant’.

Definition 6.1 (Concordance). Let (i, j) be a pair of observations with outcomes $\{(t_i, \delta_i), (t_j, \delta_j)\}$ and let $r_i, r_j \in \mathbb{R}$ be their respective risk predictions. Then (i, j) are called (F. E. J. Harrell et al. 1984; F. E. Harrell, Califff, and Pryor 1982):

- *Comparable* if $t_i < t_j$ and $\delta_i = 1$;
- *Concordant* if $r_i > r_j$.

Note that this book defines risk rankings such that a higher value implies higher risk of event and thus lower expected survival time (Chapter 5), hence a pair is concordant if $\mathbb{I}(t_i < t_j, r_i > r_j)$. Other sources may instead assume that higher values imply lower risk of event and hence a pair would be concordant if $\mathbb{I}(t_i < t_j, r_i < r_j)$.

Concordance measures then estimate the probability of a pair being concordant, given that they are comparable:

$$P(r_i > r_j | t_i < t_j \cap \delta_i) \quad (6.1)$$

These measures are referred to as time *independent* when r_i, r_j is not a function of time as once the observations are organized into comparable pairs, the observed survival times can be ignored. The time-dependent case is covered in Section 6.2.1.

While various definitions of a ‘Concordance index’ (C-index) exist (discussed in the next section), they all represent a weighted proportion of the number of concordant pairs over the number of comparable pairs. As such, a C-index value will always be between [0, 1] with 1 indicating perfect separation, 0.5 indicating no separation, and 0 being separation in the ‘wrong direction’, i.e. all high risk observations being ranked lower than all low risk observations.

Concordance measures may either be reported as a value in [0, 1], a percentage, or as ‘discriminatory power’, which refers to the percentage improvement of a model’s discrimination above the baseline value of 0.5. For example, if a model has a concordance of 0.8 then its discriminatory power is $(0.8 - 0.5)/0.5 = 60\%$. This representation of discrimination provides more information by encoding the model’s improvement over some baseline although is often confused with reporting concordance as a percentage (e.g. reporting a concordance of 0.8 as 80%). In theory this representation could result in a negative value, however this would indicate that $C < 0.5$, which would indicate serious problems with the model that should be addressed before proceeding with further analysis. Representing measures as a percentage over a baseline is a common method to improve measure interpretability and closely relates to the ERV representation of scoring rules (Section 8.4).

6.1.1 Concordance Indices

Common concordance indices in survival analysis can be expressed as a general measure:

Let $\hat{\mathbf{r}} = (\hat{r}_1 \ \hat{r}_2 \ \dots \ \hat{r}_n)^\top$ be predicted risks, $(\mathbf{t}, \boldsymbol{\delta}) = ((t_1, \delta_1) \ (t_2, \delta_2) \ \dots \ (t_n, \delta_n))^\top$ be observed outcomes, let W be some weighting function, and let τ be a cut-off time. Then, the time-independent (‘ind’) *survival concordance index* is defined by,

$$C_{ind}(\hat{\mathbf{r}}, \mathbf{t}, \boldsymbol{\delta} | \tau) = \frac{\sum_{i \neq j} W(t_i) \mathbb{I}(t_i < t_j, \hat{r}_i > \hat{r}_j, t_i < \tau) \delta_i}{\sum_{i \neq j} W(t_i) \mathbb{I}(t_i < t_j, t_i < \tau) \delta_i} \quad (6.2)$$

The choice of W specifies a particular variation of the c-index (see below). The use of the cut-off τ mitigates against decreased sample size (and therefore high variance) over time due to the removal of censored observations (see Figure 6.1). For τ to be comparable across datasets, a common choice would be to set τ as the time at which 80%, or perhaps 90% of the data have been censored or experienced the event.

There are multiple methods for dealing with tied predictions and times. Strictly, tied times are incomparable given the definition of ‘comparable’ given above and hence are usually

ignored in the numerator. On the other hand, ties in the prediction are more problematic but a common method is to set a value of 0.5 for observations when $r_i = r_j$ (Therneau and Atkinson 2024). Specific concordance indices can be constructed by assigning a weighting scheme for W which generally depends on the Kaplan-Meier estimate of the survival function of the censoring distribution fit on training data, \hat{G}_{KM} , or the Kaplan-Meier estimate for the survival function of the survival distribution fit on training data, \hat{S}_{KM} , or both. Measures that use \hat{G}_{KM} are referred to as Inverse Probability of Censoring Weighted (IPCW) measures as the estimated censoring distribution is utilised to weight the measure in order to compensate for removed censored observations. This is visualised in Figure 6.1 where \hat{G}_{KM} , \hat{G}_{KM}^{-2} , and \hat{S}_{KM} are computed based on the `whas` dataset (Hosmer Jr, Lemeshow, and May 2011).

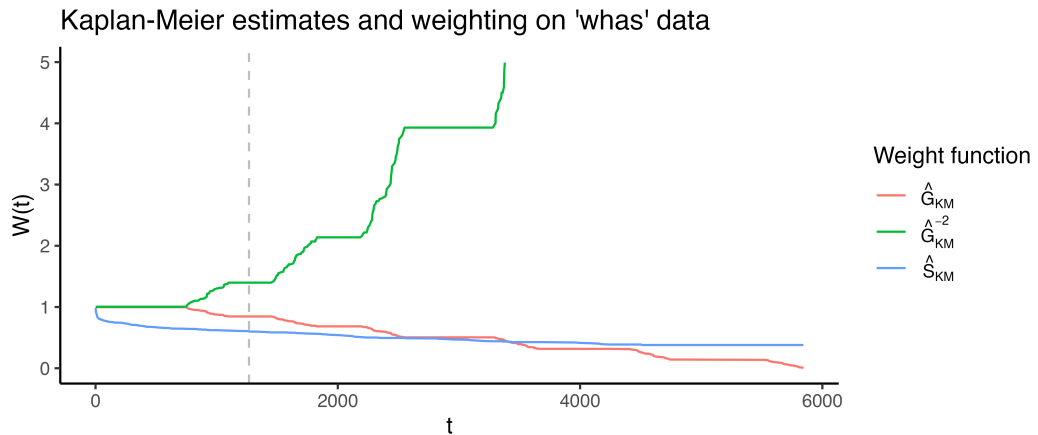


Figure 6.1: Weighting functions obtained on the `whas` dataset. x-axis is follow-up time. y-axis is outputs from one of three weighting functions: \hat{G}_{KM} , survival function based on the censoring distribution of the `whas` dataset (red), and \hat{G}_{KM}^{-2} (green), \hat{S}_{KM} , marginal survival function based on original `whas` dataset (blue). The vertical gray line at $t = \tau = 1267$ represents the point at which $\hat{G}(t) < 0.6$.

The following are a few of the weights that have been proposed for the concordance index:

- $W(t_i) = 1$: Harrell's concordance index, C_H (F. E. J. Harrell et al. 1984; F. E. Harrell, Calif, and Pryor 1982), which is widely accepted to be the most common survival measure and imposes no weighting on the definition of concordance. The original measure given by Harrell has no cut-off, $\tau = \infty$, however applying a cut-off is now more widely accepted in practice.
- $W(t_i) = [\hat{G}_{KM}(t_i)]^{-2}$: Uno's C, C_U (Uno et al. 2011).
- $W(t_i) = \hat{S}_{KM}(t_i)$ (Therneau and Atkinson 2024)
- $W(t_i) = \hat{S}_{KM}(t_i)/\hat{G}_{KM}(t_i)$ (Schemper, Wakounig, and Heinze 2009)

All methods assume that censoring is conditionally-independent of the event given the features (Section 3.3), otherwise weighting by \hat{S}_{KM} or \hat{G}_{KM} would not be applicable. It is assumed here that \hat{S}_{KM} and \hat{G}_{KM} are estimated on the training data and not the testing data (though the latter may be seen in some implementations, e.g. Therneau (2015)).

6.1.2 Choosing a C-index

With multiple choices of weighting available, choosing a specific measure might seem daunting. Matters are only made worse by debate in the literature, reflecting uncertainty in measure choice and interpretation. In practice, when a suitable cut-off τ is chosen, all these weightings perform very similarly (Rahman et al. 2017; Schmid and Potapov 2012). For example, Table 6.1 uses the `whas` data again to compare Harrell's C with measures that include IPCW weighting, when no cutoff is applied (top row) and when a cutoff is applied when $\hat{G}(t) = 0.6$ (grey line in Figure 6.1). The results are almost identical when the cutoff is applied but still not massively different without the cutoff.

Table 6.1: Comparing C-index measures (calculated on the `whas` dataset using a Cox model with three-fold cross-validation) with no cut-off (top) and a cut-off when $\hat{G}(t) = 0.6$ (bottom). First column is Harrell's C, second is the weighting $1/\hat{G}(t)$, third is Uno's C.

	$W = 1$	$W = G^{-1}$	$W = G^{-2}$
$\tau = \infty$	0.74	0.73	0.71
$\tau = 1267$	0.76	0.75	0.75

On the other hand, if a poor choice is selected for τ (cutting off too late) then IPCW measures can be highly unstable (Rahman et al. 2017), for example the variance of Uno's C drastically increases with increased censoring (Schmid and Potapov 2012).

In practice, all C-index metrics provide an intuitive measure of discrimination and as such the choice of C-index is less important than the transparency in reporting. ‘C-hacking’ (R. Sonabend, Bender, and Vollmer 2022) is the deliberate, unethical procedure of calculating multiple C-indices and to selectively report one or more results to promote a particular model or result, whilst ignoring any negative findings. For example, calculating Harrell's C and Uno's C but only reporting the measure that shows a particular model of interest is better than another (even if the other metric shows the reverse effect). To avoid ‘C-hacking’:

- i) the choice of C-index should be made before experiments have begun and the choice of C-index should be clearly reported;
- ii) when ranking predictions are composed (`?@sec-car`) from distribution predictions, the composition method should be chosen and clearly described before experiments have begun.

As the C-index is highly dependent on censoring within a dataset, C-index values between experiments are not directly comparable, instead comparisons are limited to comparing model rankings, for example conclusions such as “model A outperformed model B with respect to Harrell's C in this experiment”.

6.2 Time-Dependent Measures

In the time-dependent case, where the metrics are computed based on specific survival times, the majority of measures are based on the Area Under the Curve, with one exception which is a simpler concordance index.

6.2.1 Concordance Indices

In contrast to the measures described above, Antolini's C (Antolini, Boracchi, and Biganzoli 2005) provides a time-dependent ('dep') formula for the concordance index. The definition of 'comparable' is the same for Antolini's C, however, concordance is now determined using the individual predicted survival probabilities calculated at the smaller event time in the pair:

$$P(\hat{S}_i(t_i) < \hat{S}_j(t_i) | t_i < t_j \cap \delta_i)$$

Note that observations are concordant when $\hat{S}_i(t_i) < \hat{S}_j(t_i)$ as at the time t_i , observation i has experienced the event and observation j has not, hence the expected survival probability for $\hat{S}_i(t_i)$ should be as close to 0 as possible (noting inherent randomness may prevent the perfect $\hat{S}_i(t_i) = 0$ prediction) but otherwise should be less than $\hat{S}_j(t_i)$ as j is still 'alive'. Once again this probability is estimated with a metric that could include a cut-off and different weighting schemes (though this is not included in Antolini's original definition):

$$C_{dep}(\hat{\mathbf{S}}, \mathbf{t}, \boldsymbol{\delta} | \tau) = \frac{\sum_{i \neq j} W(t_i) \mathbb{I}(t_i < t_j, \hat{S}_i(t_i) < \hat{S}_j(t_i), t_i < \tau) \delta_i}{\sum_{i \neq j} W(t_i) \mathbb{I}(t_i < t_j, t_i < \tau) \delta_i}$$

where $\hat{\mathbf{S}} = (\hat{S}_1 \ \hat{S}_2 \cdots \hat{S}_n)^\top$.

Antolini's C provides an intuitive method to evaluate the discrimination of a model based on distribution predictions without depending on compositions to ranking predictions.

6.2.2 Area Under the Curve

AUC, or AUROC, measures calculate the Area Under the Receiver Operating Characteristic (ROC) Curve, which is a plot of the *sensitivity* (or true positive rate (TPR)) against $1 - specificity$ (or true negative rate (TNR)) at varying thresholds (described below) for the predicted probability (or risk) of event. Figure 6.2 visualises ROC curves for two classification models. The blue line is a featureless baseline that has no discrimination. The red line is a decision tree with better discrimination as it comes closer to the top-left corner.

In a classification setting with no censoring, the AUC has the same interpretation as Harrell's C (Uno et al. 2011). AUC measures for survival analysis were developed to provide a time-dependent measure of discriminatory ability (Patrick J. Heagerty, Lumley, and Pepe 2000). In a survival setting it can reasonably be expected for a model to perform differently over time and therefore time-dependent measures are advantageous. Computation of AUC estimators is complex and as such there are limited accessible metrics available off-shelf.

The AUC, TPR, and TNR are derived from the *confusion matrix* in a binary classification setting. Let $y_i, \hat{y}_i \in \{0, 1\}$ be the true and predicted binary outcomes respectively for some observation i . The confusion matrix is then given by:

	$y_i = 1$	$y_i = 0$
$\hat{y}_i = 1$	TP	FP
$\hat{y}_i = 0$	FN	TN

where $TN := \sum_i \mathbb{I}(y_i = 0, \hat{y}_i = 0)$ is the number of true negatives, $TP := \sum_i \mathbb{I}(y_i = 1, \hat{y}_i = 1)$ is the number true positives, $FP := \sum_i \mathbb{I}(y_i = 0, \hat{y}_i = 1)$ is the number of false positives, and $FN := \sum_i \mathbb{I}(y_i = 1, \hat{y}_i = 0)$ is the number of false negatives. From these are derived

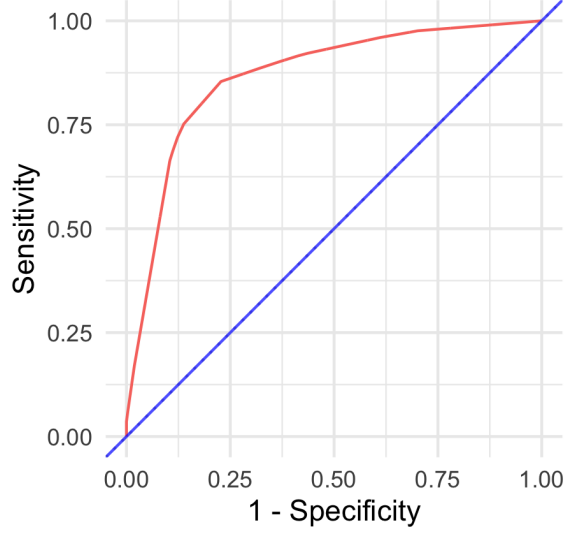


Figure 6.2: ROC Curves for a classification example. Red is a decision tree with good discrimination as it ‘hugs’ the top-left corner. Blue is a featureless baseline with no discrimination as it sits on $y = x$.

$$\begin{aligned} TPR &:= \frac{TP}{TP + FN} \\ TNR &:= \frac{TN}{TN + FP} \end{aligned}$$

In classification, a probabilistic prediction of an event can be *thresholded* to obtain a deterministic prediction. For a predicted $\hat{p} := \hat{P}(b = 1)$, and threshold α , the thresholded binary prediction is $\hat{b} := \mathbb{I}(\hat{p} > \alpha)$. This is achieved in survival analysis by thresholding the linear predictor at a given time for different values of the threshold and different values of the time. All measures of TPR, TNR and AUC are in the range $[0, 1]$ with larger values preferred.

Weighting the linear predictor was proposed by Uno *et al.* (2007) (Uno et al. 2007) and provides a method for estimating TPR and TNR via

$$TPR_U(\hat{\eta}, \mathbf{t}, \boldsymbol{\delta} | \tau, \alpha) = \frac{\sum_{i=1}^n \delta_i \mathbb{I}(k(\hat{\eta}_i) > \alpha, t_i \leq \tau) [\hat{G}_{KM}(t_i)]^{-1}}{\sum_{i=1}^n \delta_i \mathbb{I}(t_i \leq \tau) [\hat{G}_{KM}(t_i)]^{-1}}$$

and

$$TNR_U(\hat{\eta}, \mathbf{t} | \tau, \alpha) = \frac{\sum_{i=1}^n \mathbb{I}(k(\hat{\eta}_i) \leq \alpha, t_i > \tau)}{\sum_{i=1}^n \mathbb{I}(t_i > \tau)}$$

where $\hat{\eta} = (\hat{\eta}_1 \ \hat{\eta}_2 \ \cdots \ \hat{\eta}_n)^\top$ is a vector of estimated linear predictors, τ is the time at which to evaluate the measure, α is a cut-off for the linear predictor, and k is a known, strictly

increasing, differentiable function. k is chosen depending on the model choice, for example if the fitted model is PH then $k(x) = 1 - \exp(-\exp(x))$ (Uno et al. 2007). Similarities can be drawn between these equations and Uno's concordance index, in particular the use of IPCW. Censoring is again assumed to be at least random once conditioned on features. Plotting TPR_U against $1 - TNR_U$ for varying values of α provides the ROC.

The second method, which appears to be more prominent in the literature, is derived from Heagerty and Zheng (2005) (Patrick J. Heagerty and Zheng 2005). They define four distinct classes, in which observations are split into controls and cases.

An observation is a *case* at a given time-point if they are dead, otherwise they are a *control*. These definitions imply that all observations begin as controls and (hypothetically) become cases over time. Cases are then split into *incident* or *cumulative* and controls are split into *static* or *dynamic*. The choice between modelling static or dynamic controls is dependent on the question of interest. Modelling static controls implies that a 'subject does not change disease status' (Patrick J. Heagerty and Zheng 2005), and few methods have been developed for this setting (Kamarudin, Cox, and Kolamunnage-Dona 2017), as such the focus here is on *dynamic* controls. The incident/cumulative cases choice is discussed in more detail below.¹

The TNR for dynamic cases is defined as

$$TNR_D(\hat{\mathbf{r}}, N|\alpha, \tau) = P(\hat{r}_i \leq \alpha | t_i > \tau)$$

where $\hat{\mathbf{r}} = (\hat{r}_1 \ \hat{r}_2 \ \dots \ \hat{r}_n)^\top$ is some prediction, which is usually deterministic, often the linear predictor $\hat{\eta}$, however could be a predicted survival probability – though in the latter case there is not necessarily an advantage over Antolini's C. Cumulative and incident versions of the TPR are respectively defined by

$$TPR_C(\hat{\mathbf{r}}, N|\alpha, \tau) = P(\hat{r}_i > \alpha | t_i \leq \tau)$$

and

$$TPR_I(\hat{\mathbf{r}}, N|\alpha, \tau) = P(\hat{r}_i > \alpha | t_i = \tau)$$

A 'true negative' occurs when the risk is below a certain threshold and the event has yet to occur, in contrast a 'true positive' occurs when the event has already occurred and therefore the risk is expected to be above the threshold. Estimation of these quantities depends on non-parametric estimators, such as the Kaplan-Meier and Akritas estimator (`?@sec-surv-models-uncond`), further details are not provided here.

The choice between the incident/dynamic (I/D) and cumulative/dynamic (C/D) measures primarily relates to the use-case. The C/D measures are preferred if a specific time-point is of interest (Patrick J. Heagerty and Zheng 2005) and is implemented in several applications for this purpose (Kamarudin, Cox, and Kolamunnage-Dona 2017). The I/D measures are preferred when the true survival time is known and discrimination is desired at the given event time (Patrick J. Heagerty and Zheng 2005).

Defining a time-specific AUC is now possible with

¹All measures discussed in this section evaluate model discrimination from 'markers', which may be a *predictive* marker (model predictions) or a *prognostic* marker (a single covariate). This section always defines a marker as a ranking prediction, which is valid for all measures discussed here with the exception of one given at the end.

$$AUC(\hat{\mathbf{r}}, N|\tau) = \int_0^1 TPR(\hat{\mathbf{r}}, N|1 - TNR^{-1}(p|\tau), \tau) dp$$

Finally, integrating over all time-points produces a time-dependent AUC and as usual a cut-off is applied for the upper limit,

$$AUC^*(\hat{\mathbf{r}}, N|\tau^*) = \int_0^{\tau^*} AUC(\hat{\mathbf{r}}, N|\tau) \frac{2\hat{p}_{KM}(\tau)\hat{S}_{KM}(\tau)}{1 - \hat{S}_{KM}^2(\tau^*)} d\tau$$

where $\hat{S}_{KM}, \hat{p}_{KM}$ are survival and mass functions estimated with a Kaplan-Meier model on training data.

Since Heagerty and Zheng's paper, other methods for calculating the time-dependent AUC have been devised, including by Chambliss and Diao (Chambliss and Diao 2006), Song and Zhou (Song and Zhou 2008), and Hung and Chiang (Hung and Chiang 2010). These either stem from the Heagerty and Zheng paper or ignore the case/control distinction and derive the AUC via different estimation methods of TPR and TNR. Blanche *et al.* (2012) (Blanche, Latouche, and Viallon 2012) surveyed these and concluded "regarding the choice of the retained definition for cases and controls, no clear guidance has really emerged in the literature", but agree with Heagerty and Zeng on the use of C/D for clinical trials and I/D for 'pure' evaluation of the marker. Blanche *et al.* (2013) (Blanche, Dartigues, and Jacqmin-Gadda 2013) published a survey of C/D AUC measures with an emphasis on non-parametric estimators with marker-dependent censoring, including their own Conditional IPCW (CIPCW) AUC, which is not discussed further here as it cannot be used for evaluating predictions (R. E. B. Sonabend 2021).

Reviews of AUC measures have produced (sometimes markedly) different results (Blanche, Latouche, and Viallon 2012; L. Li, Greene, and Hu 2018; Kamarudin, Cox, and Kolamunnage-Dona 2017) with no clear consensus on how and when these measures should be used. The primary advantage of these measures is to extend discrimination metrics to be time-dependent. However, it is unclear how to interpret a threshold of a linear predictor and moreover if this is even the 'correct' quantity to threshold, especially when survival distribution predictions are the more natural object to evaluate over time.

6.3 Extensions

6.3.1 Competing risks

Discrimination measures are usually extended to the competing risk setting by evaluating cause-specific probabilities individually and then potentially summing or averaging over cause-specific measures (Geloven *et al.* 2022; C. Lee *et al.* 2018; Bender *et al.* 2021; Alberge *et al.* 2025).

To recap formulae from Chapter 4, given q possible events then the cause-specific hazard for an event is defined as h_e :

$$h_e(\tau) = \lim_{\Delta\tau \rightarrow 0} \frac{P(\tau \leq Y \leq \tau + \Delta\tau, E = e \mid Y \geq \tau)}{\Delta\tau}, \quad e = 1, \dots, q.$$

where Y is the random variable representing the time-to-event and $E \in \{1, \dots, k\}$ is the random variable with realizations e , which denotes one of k competing events that can occur at event time Y .

In a single-event setting, a pair of observations, (i, j) , with outcomes $\{(t_i, \delta_i), (t_j, \delta_j)\}$, and predicted risk predictions, $r_i, r_j \in \mathbb{R}$, are called comparable if $t_i < t_j$ and $\delta_i = 1$; and concordant if also $r_i > r_j$. In a competing risks setting, for an event of interest e , the observations are (Geloven et al. 2022):

- *Comparable* if $t_i < t_j$ and $\delta_{ie} = 1$; and
- *Concordant* if $r_i > r_j$

Where $\delta_{ie} = 1$ is equivalent to $\mathbb{I}(Y_i \leq C_i \wedge E_i = e)$.

The usual definition of concordance measures then follow given this additional conditioning on the event of interest e . In practice, given that competing risks models often estimate cause-specific hazard functions, it is a variation of Antolini's time-dependent concordance measure that suits the competing risks setting best. Hence for an event e , the measure is given by:

$$C(\hat{\mathbf{h}}_e, \mathbf{t}, \boldsymbol{\delta} | \tau) = \frac{\sum_{i \neq j} W(t_i) \mathbb{I}(t_i < t_j, \hat{h}_{e_i}(t_i) > \hat{h}_{e_j}(t_i), t_i < \tau) \delta_{ie}}{\sum_{i \neq j} W(t_i) \mathbb{I}(t_i < t_j, t_i < \tau) \delta_{ie}}$$

where $\hat{\mathbf{h}}_e = (\hat{h}_{e_1} \ \hat{h}_{e_2} \ \dots \ \hat{h}_{e_n})^\top$ are cause specific hazards for individual observations risk of event e .

6.3.2 Other censoring and truncation types

AUC and concordance indices are designed to rank observations, or at least evaluate how well a model discriminates between two risk groups. This is a substantial challenge when there is interval censoring in the data as the ‘true’ ranks of observations are unknown. Let i, j be two observations with interval censoring times $(l_i, r_i), (l_j, r_j)$ respectively. Given valid combinations ($r > l$) then these observations may coincide with one of six combinations:

1. $l_i < r_i < l_j < r_j$
2. $l_i < l_j < r_i < r_j$
3. $l_i < l_j < r_j < r_i$
4. $l_j < r_j < l_i < r_i$
5. $l_j < l_i < r_j < r_i$
6. $l_j < l_i < r_i < r_j$

Of these, only case (1) and (4) can be used in a standard concordance index as the intervals are non-overlapping. For all other cases, conditional probabilities have to be substituted or imputation used to estimate when in an interval the event takes place (Tsouprou 2015; Ying Wu and Cook 2020). After such estimation, interpretation of any metric is difficult, as it’s unclear if the original prediction is being evaluated or the guesswork that went into the evaluation measure. In this case it is likely better to use more straightforward methods that do not require these extra steps.

When it comes to time-dependent AUC measures, the TNR and TPR can be extended to accommodate interval-censoring, by updating the equations to only include contributions

from observations when the event is guaranteed to have occurred ($r_i \leq \tau$) or not ($l_i > \tau$) (J. Li and Ma 2011):

$$TNR_D(\hat{\mathbf{r}}, N | \alpha, \tau) = P(\hat{r}_i \leq \alpha | l_i > \tau)$$

and

$$TPR_C(\hat{\mathbf{r}}, N | \alpha, \tau) = P(\hat{r}_i > \alpha | r_i \leq \tau)$$

In the presence of interval censoring, estimation depends on more complex estimators such as the nonparametric maximum likelihood estimator, which can be challenging to fit and splines could be used instead (Yuan Wu et al. 2020). However, splines themselves require modelling and any metric that requires modelling to estimate introduces significant difficulties in its interpretation. As a more simplistic (yet sometimes realistic on average) alternative, one could impute the outcome time as the midpoint between the interval margins, $t_i = (l_i + r_i)/2$ (Jacqmin-Gadda et al. 2016).

As left-censoring is a specialised case of interval-censoring (with $l_i = 0$) the above formulae can be used to handle left-censored data as well.

6.3.3 Truncation

When only right-censoring is present, the objective of concordance measures is to estimate the probability that the ranking of two observations' risk is correctly specified (6.1). The naive method to deal with left-truncation is to simply ignore it and use 6.2 as usual. Doing so yields an estimator, C_N , that converges in probability to

$$P(r_i > r_j | \delta_i, t_i < t_j, t_i \geq t_i^L, t_j \geq t_j^L) \quad (6.3)$$

where t_i^L, t_j^L are the left-truncation times for i and j respectively (which are 0 if the observation is not left-truncated). This is considered a 'naive' estimator as it may introduce bias (Hartman et al. 2022), to see why this is the case consider that the right-hand-side of 6.3 is true in one of two cases (ignoring ties):

1. $t_i < t_j^L < t_j$;
2. $t_j^L < t_i < t_j$.

In the first case, j enters the study after i has experienced the outcome and the observations never overlap in the data at the same time Hartman et al. (2022) demonstrate that evaluating discrimination in the presence of these 'nonoverlapping intervals' creates bias if truncation is dependent on the predictors (for the same reason, methods for estimation need to be adapted as well). Therefore, the data should be further restricted to overlapping intervals, yielding the estimator

$$C_{LT}(\hat{\mathbf{r}}, \mathbf{t}, \boldsymbol{\delta}, \mathbf{t}^L | \tau) = \frac{\sum_{i \neq j} \mathbb{I}(t_i < t_j, \hat{r}_i > \hat{r}_j, t_i < \tau, t_i \geq t_j^L) \delta_i}{\sum_{i \neq j} \mathbb{I}(t_i < t_j, t_i < \tau, t_i \geq t_j^L) \delta_i}$$

In contrast to 6.2, no generic weighting term is included, which is due to the complexity of estimating IPC weights in the context of left-truncation (Therneau and Atkinson 2024).

Interestingly, experiments have shown that naively applying Harrell's C (6.2 with $W = 1$) may be a better estimator than C_{LT} with lower bias (Hartman et al. 2022). Whilst more complex IPC measures have been proposed, they do not seem to be in common usage anywhere whereas C_N and C_{LT} are both used in published research and software (McGough et al. 2021; Therneau 2015). As has been seen throughout this book, left-truncation research is still nascent. No evidence of methods for right-truncation could be found.

7

Calibration

TODO (150-200 WORDS)

 Minor changes expected!

This page is a work in progress and minor changes will be made over time.

Calibration measures evaluate the ‘average’ quality of survival distribution predictions. In general there is a trade-off between discrimination and calibration. A model that makes perfect individual predictions (good discrimination) might be overfit to the data and make poor predictions on new, unseen data. Whereas a model that makes perfect population predictions (good calibration) might not be able to separate between individual observations. The literature around survival analysis calibration measures is scarce (Rahman et al. 2017), potentially due to the complexity of even defining calibration in a survival context (Van Houwelingen 2000). Though this meaning does become clearer as specific metrics are introduced. As with other measure classes, only measures that can generalize beyond Cox PH models are included here but note that several calibration measures for re-calibrating PH models have been discussed in the literature (Demler, Paynter, and Cook 2015; Van Houwelingen 2000).

Calibration measures can be grouped (Andres et al. 2018) into those that evaluate distributions at a single time-point, ‘1-Calibration’ or ‘Point Calibration’ measures, and those that evaluate distributions at all time-points ‘distributional-calibration’ or ‘probabilistic calibration’ measures. A point-calibration measure will evaluate a function of the predicted distribution at a single time-point whereas a probabilistic measure evaluates the distribution over a range of time-points; in both cases the evaluated quantity is compared to the observed outcome, (t, δ) .

7.1 Point Calibration

Point calibration measures can be further divided into metrics that evaluate calibration at a single time-point (by reduction) and measures that evaluate an entire distribution by only considering the event time. The difference may sound subtle but it affects conclusions that can be drawn. In the first case, a calibration measure can only draw conclusions at that one time-point, whereas the second case can draw conclusions about the calibration of the entire distribution. This is the same caveat as using prediction error curves for scoring rules (Section 8.3).

7.1.1 Calibration by Reduction

Point calibration measures are implicitly reduction methods as they use classification methods to evaluate a full distribution based on a single point only ([?@sec-car](#)). For example, given a predicted survival function \hat{S} , one could calculate the survival function at a single time point, $\hat{S}\tau$ and then use probabilistic classification calibration measures. Using this approach one may employ common calibration methods such as the Hosmer–Lemeshow test (Hosmer and Lemeshow 1980). Measuring calibration in this way can have significant drawbacks as a model may be well-calibrated at one time-point but poorly calibrated at all others (Haider et al. 2020). To mitigate this, one could perform the Hosmer–Lemeshow test (or other applicable tests) multiple times with multiple testing correction at many (or all possible) time points, however this would be less efficient and more difficult to interpret than other measures discussed in this chapter.

7.1.2 Houwelingen's α

As opposed to evaluating distributions at one or more arbitrary time points, one could instead evaluate distribution predictions at meaningful times. van Houwelingen proposed several measures (Van Houwelingen 2000) for calibration but only one generalises to all probabilistic survival models, termed here ‘Houwelingen's α ’. The measure assesses if the model correctly estimates the theoretical ‘true’ cumulative hazard function of the underlying data generating process, $H = \hat{H}$.

The statistic is derived by noting the closely related nature of survival analysis and counting processes. In brief, for an observation i one could define the counting process $N_i(\tau) = \mathbb{I}(T_i \leq \tau, \Delta_i = 1)$, which represents the number of events i has experienced at τ . Clearly in single-event survival analysis this will be 0 before the event has been experienced or 1 at or after the event. An important quantity in counting process is the ‘intensity process’, which is the instantaneous rate at which events occur *given* past information. This is related to, but distinct from the hazard rate. The core difference is that the intensity process incorporates real-world information via the individual risk indicator, $R_i(\tau) = \mathbb{I}(T_i \geq \tau)$. Hence the hazard and intensity are related via $\lambda_i(\tau) = R_i(\tau)h(\tau|\mathbf{x}_i)$. The intensity process can itself be thought of as the expected number of events at t , which is 0 if the event has already occurred at $R_i(\tau) = 0$ or equal to $h(\tau|\mathbf{x}_i)$ otherwise (Hosmer Jr, Lemeshow, and May 2011). Therefore the expected number of events between $[0, \tau]$ can be obtained by the cumulative intensity process

$$\Lambda_i(\tau) = \int_0^\tau \lambda_i(s) \, ds = \int_0^\tau R_i(s) h(s|\mathbf{x}_i) \, ds = \int_0^{\min\{\tau, t_i\}} h(s|\mathbf{x}_i) \, ds = H(\min\{\tau, t_i\}, \mathbf{x}_i) \quad (7.1)$$

A particularly useful quantity is the expected number of events for individual i in $[0, t_i]$, which can be seen from (7.1) reduces to $H(t_i|\mathbf{x}_i)$. In a perfect model one would expect $\hat{H}(t_i|\mathbf{x}_i) = 1$ if $\delta_i = 1$ and 0 otherwise. Hence summing over all observations, $\sum_i \hat{H}(t_i|\mathbf{x}_i)$ gives the total number of expected events in the dataset. Houwelingen's α exploits this result to provide a simple method for assessing calibration by comparing the actual and expected number of events:

$$H_\alpha(\boldsymbol{\delta}, \hat{\mathbf{H}}, \mathbf{t}) = \frac{\sum_i \delta_i}{\sum_i \hat{H}(t_i|\mathbf{x}_i)}$$

with standard error $SE(H_\alpha) = \exp(1/\sqrt{\sum_i \delta_i})$ (Van Houwelingen 2000). A slightly more useful metric is given by $H_\alpha(\boldsymbol{\delta}, \hat{\mathbf{H}}, \mathbf{t}) - 1$ which is lower-bounded at 0 and can therefore be minimized in automated tuning processes. A model is then well-calibrated if $H_\alpha = 0$.

The next metrics we look at evaluate models across a spectrum of points to assess calibration over time.

7.2 Probabilistic Calibration

Calibration over a range of time points may be assessed quantitatively or qualitatively, with graphical methods often favoured. Graphical methods compare the average predicted distribution to the expected distribution, which can be estimated with the Kaplan-Meier curve, discussed next.

7.2.1 Kaplan-Meier Comparison

The simplest graphical comparison compares the average predicted survival curve to the Kaplan-Meier curve estimated on the testing data. Let $\hat{S}_1, \dots, \hat{S}_n$ be predicted survival functions, then the average predicted survival function is the mixture: $\hat{S} = \frac{1}{n} \sum_{i=1}^n \hat{S}_i(\tau)$. This estimate can be plotted next to the Kaplan-Meier estimate of the survival distribution in a test dataset (i.e., the true data for model evaluation), allowing for visual comparison of how closely these curves align. An example is given in Figure 7.1, a Cox model (CPH), random survival forest, and relative risk tree, are all compared to the Kaplan-Meier estimator. This figure highlights the advantages and disadvantages of this method. The relative risk tree is clearly poorly calibrated as it increasingly diverges from the Kaplan-Meier. In contrast, the Cox model and random forest cannot be directly compared to one another, as both models frequently overlap with each other and the Kaplan-Meier estimator. Hence it is possible to say that the Cox and forests models are better calibrated than the risk tree, however it is not possible to say which of those two is better calibrated and whether their distance from the Kaplan-Meier is significant or not at a given time (when not clearly overlapping).

This method is useful for making broad statements such as “model X is clearly better calibrated than model Y” or “model X appears to make average predictions close to the Kaplan-Meier estimate”, but that is the limit in terms of useful conclusions. One could refine this method for more fine-grained information by instead using predictions to create ‘risk groups’ that can be plotted against a stratified Kaplan-Meier (Austin, Harrell Jr, and Klaveren 2020), however this method is harder to interpret and adds even more subjectivity around how many risk groups to create and how to create them (Royston and Altman 2013; Austin, Harrell Jr, and Klaveren 2020). The next measure we consider includes a graphical method as well as a quantitative interpretation.

7.2.2 D-Calibration

Recall that calibration measures assess whether model predictions align with population-level outcomes. In probabilistic classification, this means testing if predicted probabilities align with observed frequencies. For example, among all instances where a model predicts a 70% probability of the event happening, approximately 70% of the corresponding observations should actually experience the event. In survival analysis, calibration is extended by examining

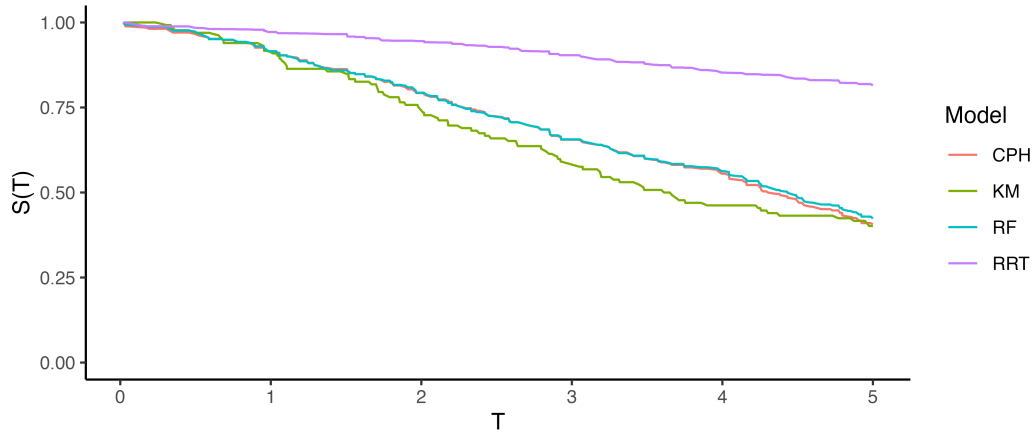


Figure 7.1: Comparing the calibration of a Cox PH (CPH), random forest (RF), and relative risk tree (RRT) to the Kaplan-Meier estimate of the survival function calculated on a test set. The calibration of RRT notably decreases over time whereas RF and CPH are closer to the Kaplan-Meier curve.

if predicted survival probabilities align with the actual distribution of event times. This is motivated by a well-known result: for any continuous random variable X , it holds that $S_X(X) \sim \mathcal{U}(0, 1)$ (Angus 1994). This means that, regardless of whether the true outcome times, T , follow a Weibull, Gompertz, or any other continuous distribution, the survival probabilities evaluated at those times should be uniformly distributed in a well-calibrated model, $\hat{S}_i(T) \sim \mathcal{U}(0, 1)$.

D-Calibration (Andres et al. 2018; Haider et al. 2020) leverages the fact that the event times, t_i , are i.i.d. randomly sampled event times from a distribution T , which justifies replacing T with t_i (Lemma B.2 Haider et al. 2020) and so a survival model is considered well-calibrated if the predicted survival probabilities at observed event times follow a standard Uniform distribution: $\hat{S}_i(t_i) \sim \mathcal{U}(0, 1)$.

The χ^2 test-statistic is used to test if random variables follow a particular distribution:

$$\chi^2 := \sum_{g=1}^G \frac{(o_g - e_g)^2}{e_g}$$

where o_g, e_g are respectively the number of observed and expected events in groups $g = 1, \dots, G$. In this case, the χ^2 statistic is testing if there is an even distribution of predicted survival probabilities across the $[0, 1]$ range. In practice the test is simplified to instead compare if $\hat{S}_i(t_i) \sim \text{DiscreteUniform}(0, 1)$. To do so the $[0, 1]$ range is cut into G equal width bins. Now let n be the total number of observations, then, under the null hypothesis, the expected number of events in each bin is equal: $e_i = n/G$.

To calculate the observed number of events in each bin, first define which observations are in each bin. The observations in the g th bin are defined by the set:

$$\mathcal{B}_g := \{i = 1, \dots, n : \lceil \hat{S}_i(t_i) \times G \rceil = g\}$$

where $i = 1, \dots, n$ are the indices of the observations, \hat{S}_i are predicted survival functions, t_i are observed outcome times, and $\lceil \cdot \rceil$ is the ceiling function. For example, if there are 5 bins then the bins are $\{[0, 0.2], (0.2, 0.4], (0.4, 0.6], (0.6, 0.8], (0.8, 1]\}$. So observation i would be in the fourth bin if $\hat{S}_i(t_i) = 0.7$ as $[0.7 \times 5] = [3.5] = 4$. Finally, the observed number of events is the number of observations in the corresponding set: $o_g = |\mathcal{B}_g|$.

The D-Calibration measure, or χ^2 statistic, is then defined by:

$$D_{\chi^2}(\hat{\mathbf{S}}, \mathbf{t}) := \frac{\sum_{i=1}^B (o_i - \frac{n}{G})^2}{n/G}$$

where $\hat{\mathbf{S}} = (\hat{S}_1 \ \hat{S}_2 \cdots \hat{S}_n)^\top$ and $\mathbf{t} = (t_1 \ t_2 \cdots t_n)^\top$.

This measure has several useful properties. Firstly, one can test the null hypothesis that a model is ‘D-calibrated’ by deriving a p -value from comparison to χ^2_{B-1} . Secondly, D_{χ^2} tends to zero as a model is increasingly well-calibrated, hence the measure can be used for model comparison. Finally, the theory lends itself to an intuitive graphical calibration method, known as reliability diagrams (Wilks 1990). A D-calibrated model implies:

$$p = \frac{\sum_i \mathbb{I}(t_i \leq \hat{F}_i^{-1}(p))}{n}$$

where p is some value in $[0, 1]$, \hat{F}_i^{-1} is the i th predicted inverse cumulative distribution function, and n is again the number of observations. In words, the number of events occurring at or before each quantile should be equal to the quantile itself, for example 50% of events should occur before their predicted median survival time. Therefore, one can plot p on the x-axis and the right hand side of the above equation on the y-axis. A D-calibrated model should result in a straight line on $x = y$. This is visualized in Figure 7.2 for the same models as in Figure 7.1. This figure supports the previous findings that the relative risk tree is poorly calibrated in contrast to the Cox model and random forest but again no direct comparison between the latter models is possible.

Whilst D-calibration has the same problems as the Kaplan-Meier method with respect to visual comparison, at least in this case there are quantities to help draw more concrete solutions. For the models in Figure 7.2, it is clear that the relative risk tree is not D-calibrated with $p < 0.01$ indicating the null hypothesis of D-calibration (predicted survival probabilities follow $\mathcal{U}(0, 1)$) can be comfortably rejected. Whilst the D-calibration for the Cox model is smaller than that of the random forest, the difference is unlikely to be significant, as is seen in the overlapping curves in the figure.

7.3 Extensions

7.3.1 Competing risks

Numerical methods have been proposed for calibration in a competing risk setting, including using pseudo-measures (Schoop, Schumacher, and Graf 2011) and overall calibration ratios (Geloven et al. 2022). However, these are complex to implement and interpret and therefore graphical methods are more often used in practice (Monterrubio-Gómez, Constantine-Cooke, and Vallejos 2024).

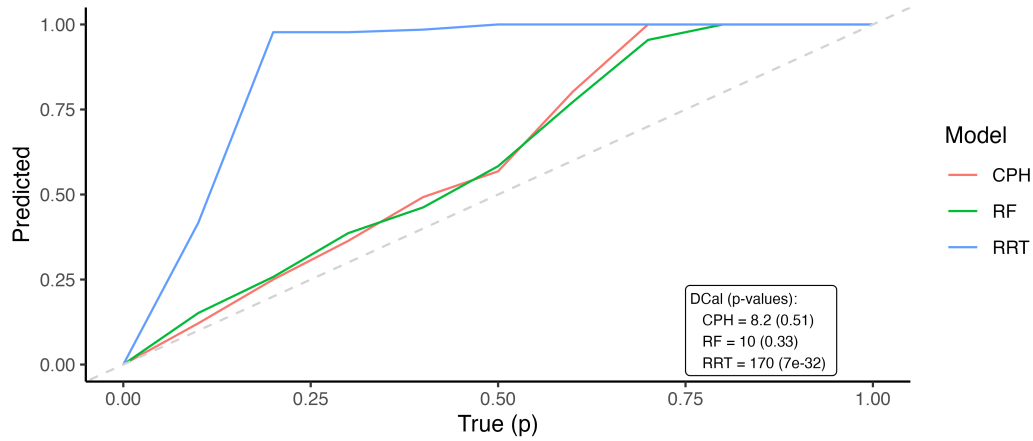


Figure 7.2: Comparing the D-calibration of a Cox PH (CPH), random forest (RF), and relative risk tree (RRT) to the expected distribution on $y=x$. As with Figure 7.1, the relative risk tree is clearly not D-calibrated (as supported by the figures in the bottom-right). The CPH and RF are closer to the $y=x$ however neither follow it perfectly.

As there is not a *single* survival curve in the competing risks setting, instead one can estimate the ‘true’ CIF using the Aalen-Joahnson estimator (Section 4.2.2) and plot this against the average prediction in the same way as in Section 7.2.1.

As discussed earlier in this chapter, interpreting and using calibration measures is complex enough in the single event setting. Extending this to multiple plots, one for each event, makes interpretation even more complex. Using scoring rules to capture calibration performance in the competing risks setting is likely to be more straightforward (Section 8.5).

7.3.2 Other censoring and truncation types

Using graphical plots is simplest for measuring calibration when left-censoring, interval-censoring, and/or truncation are involved. In these contexts, predicted survival functions can be compared to the ‘true’ survival probability estimated with the Kaplan-Meier (Section 7.2.1) by using non-parametric estimators that can incorporate other censoring and truncation types as required. For example the NPMLE for interval censoring and the left-truncated risk set definition for left-truncation, see Section 3.5.2 for more.

8

Scoring Rules

TODO (150-200 WORDS)

 Minor changes expected!

This page is a work in progress and minor changes will be made over time.

Scoring rules evaluate probabilistic predictions and (attempt to) measure the overall predictive ability of a model in terms of both calibration and discrimination (Gneiting and Raftery 2007; Murphy 1973). In contrast to calibration measures, which assess the average performance across all observations on a population level, scoring rules evaluate the sample mean of individual predictions across all observations in a test set. As well as being able to provide information at an individual level, scoring rules are also popular as probabilistic forecasts are widely recognized to be superior to deterministic predictions for capturing uncertainty in predictions (A. P. Dawid 1984; A. Philip Dawid 1986). Formalisation and development of scoring rules has primarily been due to Dawid (A. P. Dawid 1984; A. Philip Dawid 1986; A. Philip Dawid and Musio 2014) and Gneiting and Raftery (Gneiting and Raftery 2007); though the earliest measures promoting “rational” and “honest” decision making date back to the 1950s (Brier 1950; Good 1952). Few scoring rules have been proposed in survival analysis, although the past few years have seen an increase in popularity in these measures. Before delving into these measures, we will first describe scoring rules in the simpler classification setting.

Scoring rules are pointwise losses, which means a loss is calculated for all observations and the sample mean is taken as the final score. To simplify notation, we only discuss scoring rules in the context of a single observation where $L_i(\hat{S}_i, t_i, \delta_i)$ would be the loss calculated for some observation i where \hat{S}_i is the predicted survival function (from which other distribution functions can be derived), and (t_i, δ_i) is the observed survival outcome.

8.1 Classification Losses

In the simplest terms, a scoring rule compares two values and assigns them a score (hence ‘scoring rule’), formally we’d write $L : \mathbb{R} \times \mathbb{R} \rightarrow \bar{\mathbb{R}}$. In machine learning, this usually means comparing a prediction for an observation to the ground truth, so $L : \mathbb{R} \times \mathcal{P} \rightarrow \bar{\mathbb{R}}$ where \mathcal{P} is a set of distributions. Crucially, scoring rules usually refer to comparisons of true and

predicted *distributions*. As an example, take the Brier score (Brier 1950) defined by:

$$L_{\text{Brier}}(\hat{p}_i, y_i) = (y_i - \hat{p}_i(y_i))^2$$

This scoring rule compares the ground truth to the predicted probability distribution by testing if the difference between the observed event and the truth is minimized. This is intuitive as if the event occurs and $y_i = 1$, then $\hat{p}_i(y_i)$ should be as close to one as possible to minimize the loss. On the other hand, if $y_i = 0$ then the better prediction would be $\hat{p}_i(y_i) = 0$.

This demonstrates an important property of the scoring rule, *properness*. A loss is *proper*, if it is minimized by the correct prediction. In contrast, the loss $L_{\text{improper}}(\hat{p}_i, y_i) = 1 - L_{\text{Brier}}(\hat{p}_i, y_i)$ is still a scoring rule as it compares the ground truth to the prediction probability distribution, but it is clearly improper as the perfect prediction ($\hat{p}_i(y_i) = y_i$) would result in a score of 1 whereas the worst prediction would result in a score of 0. Proper losses provide a method of model comparison as, by definition, predictions closest to the true distribution will result in lower expected losses.

Another important property is *strict properness*. A loss is *strictly proper* if the loss is uniquely minimized by the ‘correct’ prediction. For example, the Brier score is minimized by only one value, which is the optimal prediction (Figure 8.1). Strictly proper losses are particularly important for automated model optimization, as minimization of the loss will result in the ‘optimum score estimator based on the scoring rule’ (Gneiting and Raftery 2007).

Mathematically, a classification loss $L : \mathcal{P} \times \mathcal{Y} \rightarrow \bar{\mathbb{R}}$ is *proper* if for any distributions p_Y, p in \mathcal{P} and for any random variables $Y \sim p_Y$, it holds that $\mathbb{E}[L(p_Y, Y)] \leq \mathbb{E}[L(p, Y)]$. The loss is *strictly proper* if, in addition, $p = p_Y$ uniquely minimizes the loss.

As well as the Brier score, which was defined above, another widely used loss is the log loss (Good 1952), defined by

$$L_{\text{logloss}}(\hat{p}_i, y_i) = -\log \hat{p}_i(y_i) \tag{8.1}$$

These losses are visualised in Figure 8.1, which highlights that both losses are strictly proper (A. Philip Dawid and Musio 2014) as they are minimized when the true prediction is made, and converge to the minimum as predictions are increasingly improved. It can also be seen from the scale of the plots that the log-loss penalizes wrong predictions stronger than the Brier score, which may be beneficial or not depending on the given use-case.

8.2 Survival Losses

Analogously to classification losses, a survival loss $L : \mathcal{P} \times \mathbb{R}_{>0} \times \{0, 1\} \rightarrow \bar{\mathbb{R}}$ is *proper* if for any distributions p_Y, p in \mathcal{P} , and for any random variables $Y \sim p_Y$, and C taking values in $\mathbb{R}_{>0}$; with $T := \min(Y, C)$ and $\Delta := \mathbb{I}(T = Y)$; it holds that, $\mathbb{E}[L(p_Y, T, \Delta)] \leq \mathbb{E}[L(p, T, \Delta)]$. The loss is *strictly proper* if, in addition, $p = p_Y$ uniquely minimizes the loss. A survival loss is referred to as outcome-independent (strictly) proper if it is only (strictly) proper when C and Y are independent.

With these definitions, the rest of this chapter lists common scoring rules in survival analysis and discusses some of their properties. As with other chapters, this list is likely not exhaustive

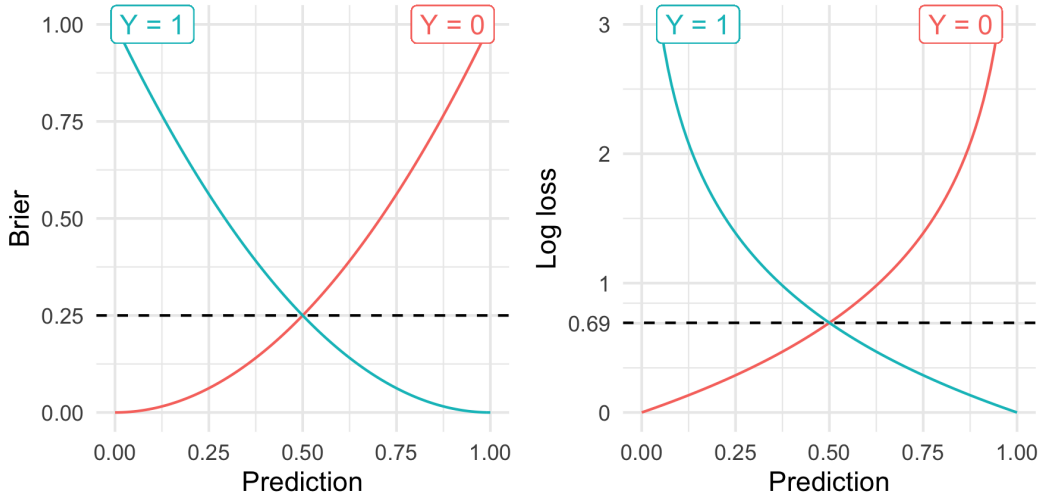


Figure 8.1: Brier and log loss scoring rules for a binary outcome and varying probabilistic predictions. x-axis is a probabilistic prediction in $[0, 1]$, y-axis is Brier score (left) and log loss (right). Blue lines are varying Brier score/log loss over different predicted probabilities when the true outcome is 1. Red lines are varying Brier score/log loss over different predicted probabilities when the true outcome is 0. Both losses are minimized when $\hat{p}_i(y_i) = y_i$.

but will cover commonly used losses. The losses are grouped into squared losses, absolute losses, and logarithmic losses, which respectively estimate the mean squared error, mean absolute error, and logloss in uncensored settings.

8.2.1 Squared Losses

The Integrated Survival Brier Score (ISBS) was introduced by Graf (Graf and Schumacher 1995; Graf et al. 1999) as an analogue to the integrated brier score in regression. It is likely the most commonly used scoring rule in survival analysis, possibly due to its intuitive interpretation.

The loss is defined by

$$L_{ISBS}(\tau^*, \hat{S}_i, t_i, \delta_i | \hat{G}_{KM}) = \int_0^{\tau^*} \frac{\hat{S}_i^2(\tau) \mathbb{I}(t_i \leq \tau, \delta_i = 1)}{\hat{G}_{KM}(t_i)} + \frac{\hat{F}_i^2(\tau) \mathbb{I}(t_i > \tau)}{\hat{G}_{KM}(\tau)} d\tau \quad (8.2)$$

where $\hat{S}_i^2(\tau) = (\hat{S}_i(\tau))^2$ and $\hat{F}_i^2(\tau) = (1 - \hat{S}_i(\tau))^2$, and $\tau^* \in \mathbb{R}_{\geq 0}$ is an upper threshold to compute the loss up to, and \hat{G}_{KM} is the Kaplan-Meier trained on the censoring distribution for IPCW (Section 6.1).

At first glance this might seem intimidating but it is worth taking the time to understand the intuition behind the loss. Recall the classification Brier score, $L(\hat{p}_i, y_i) = (y_i - \hat{p}_i)^2$, this provides a method to evaluate a probability mass function at one point. In a regression setting, the *integrated Brier score*, also known as the continuous ranked probability score, is the integral of the Brier score for all real-valued thresholds (Gneiting and Raftery 2007) and hence allows predictions to be evaluated over multiple points as

$$L(\hat{F}_i, y_i) = \int (\mathbb{I}(y_i \leq \tau) - \hat{F}_i(\tau))^2 d\tau \quad (8.3)$$

where \hat{F}_i is the predicted cumulative distribution function and τ is some meaningful threshold. As the left-hand indicator can only take one of two values 8.3 can be represented as two distinct cases, now using t instead of y to represent time:

$$L(\hat{F}_i, t_i) = \begin{cases} (1 - \hat{F}_i(\tau))^2 = \hat{S}_i^2(\tau), & \text{if } t_i \leq \tau \\ (0 - \hat{F}_i(\tau))^2 = \hat{F}_i^2(\tau), & \text{if } t_i > \tau \end{cases} \quad (8.4)$$

In the first case, the observation experienced the event before τ , hence the optimal prediction for $\hat{F}(\tau)$ (the probability of experiencing the event before τ) is 1, and therefore the optimal $\hat{S}(\tau)$ is 0. Conversely, in the second case has not experienced the event yet, the optimal $\hat{F}(\tau)$ is 0. The loss therefore meaningfully represents the ideal predictions in the two possible real-world scenarios.

The final component of the loss is accommodating for censoring. At τ an observation will either have:

1. Not experienced any outcome: $t_i > \tau$;
2. Experienced the event: $t_i \leq \tau \wedge \delta_i = 1$; or
3. Been censored: $t_i \leq \tau \wedge \delta_i = 0$

Censored observations are discarded after the censoring time as evaluating predictions after this time is impossible as the ground truth is unknown. To compensate for removing observations, IPCW (Section 6.1.1) is again used to upweight predictions as τ increases. IPC weights, W_i are defined such that observations are either weighted by $\hat{G}_{KM}(\tau)$ when they have not yet experienced the event or by their final observed time, $\hat{G}_{KM}(t_i)$, otherwise (Table 8.1).

Table 8.1: IPC weighting scheme for the ISBS.

$W_i := W(t_i, \delta_i)$	$t_i > \tau$	$t_i \leq \tau$
$\delta_i = 1$	$\hat{G}_{KM}^{-1}(\tau)$	$\hat{G}_{KM}^{-1}(t_i)$
$\delta_i = 0$	$\hat{G}_{KM}^{-1}(\tau)$	0

When censoring is uninformative, the Graf score consistently estimates the mean square error (Gerdts and Schumacher 2006). Despite this, the score is not strictly proper and even its properness is in doubt (in doubt not proven due to their being open debate in the literature about how to define properness in a survival context) (Rindt et al. 2022). Fortunately, as the score is deeply embedded in the literature, experiments have demonstrated that scores generated from using the ISBS only differ very slightly to a strictly proper alternative (R. Sonabend et al. 2025).

8.2.2 Logarithmic losses

The development of logarithmic losses follows from adapting the negative likelihood for censored datasets. Consider the usual negative likelihood in a regression setting, which is a standard measure for evaluating a model's performance:

$$L_{NLL}(\hat{f}_i, y_i) = -\log[\hat{f}(y_i)]$$

for a predicted density function \hat{f}_i and true outcome y_i . Note this is analogous to the classification log loss in (8.1) with the probably mass function replaced with the density function.

Now recall (3.12) from Section 3.5.1, which gives the contribution from a single observation as

$$\mathcal{L}(t_i) \propto \begin{cases} f(t_i), & \text{if } i \text{ is uncensored} \\ S(t_i), & \text{if } i \text{ is right-censored} \\ F(t_i), & \text{if } i \text{ is left-censored} \\ S(l_i) - S(r_i), & \text{if } i \text{ is interval-censored} \end{cases}$$

where r_i, l_i are the boundaries of the censoring interval (adaptations in the presence of left-truncation as described in Section 3.5.1 may also be applied).

The log-loss can then be constructed depending on what type of censoring or truncation is present in the data. For example, if only right-censoring is present then the right-censored logloss (RCLL) is defined as:

$$L_{RCLL}(\hat{S}_i, t_i, \delta_i) = -\log(\delta_i \hat{f}_i(t_i) + (1 - \delta_i) \hat{S}_i(t_i)) \quad (8.5)$$

If censoring is independent of the event (Section 3.3) then this scoring rule is strictly proper (Avati et al. 2020). The loss is also highly interpretable as a measure of predictive performance when broken down into its two halves:

1. An observation censored at t_i has not experienced the event and hence the ideal prediction would be close to $S(t_i) = 1$; correspondingly (8.5) becomes $-\log(1) = 0$.
2. If an observation experiences the event at t_i , then the ideal prediction would be close to $f(t_i) = \infty$ or $p(t_i) = 1$ in the discrete case; therefore (8.5) equals $-\infty$ or 0 for continuous and discrete time respectively.

Analogous losses follow when left- and/or interval-censoring is present by using the objective functions in Section 3.5.1.

Other logarithmic losses have also been proposed, such as the integrated survival log loss (ISLL) in Graf et al. (1999). The ISLL is similar to the ISBS except \hat{S}_i^2 and \hat{F}_i^2 are replaced with $\log(\hat{F}_i)$ and $\log(\hat{S}_i)$ respectively. To our knowledge, the ISLL does not appear used in practice and nor is there a practical benefit over other losses – though we note the work of Alberge et al. (2025) discussed in Section 8.5.

8.2.3 Absolute Losses

The final class of losses considered here can be viewed as analogs of the mean absolute error in an uncensored setting. The absolute survival loss, developed over time by Schemper and Henderson (2000) and Schmid et al. (2011) is similar to the ISBS but removes the squared term:

$$L_{ASL}(\hat{S}_i, t_i, \delta_i | \hat{G}_{KM}) = \int_0^{\tau^*} \frac{\hat{S}_i(\tau) \mathbb{I}(t_i \leq \tau, \delta_i = 1)}{\hat{G}_{KM}(t_i)} + \frac{\hat{F}_i(\tau) \mathbb{I}(t_i > \tau)}{\hat{G}_{KM}(\tau)} d\tau$$

where \hat{G}_{KM} and τ^* are as defined above. Analogously to the ISBS, the absolute survival loss consistently estimates the mean absolute error when censoring is uninformative (Schmid et al. 2011) but there are also no proofs or claims of properness. The absolute survival loss and ISBS tend to yield similar results (Schmid et al. 2011) but in practice the former does not appear to be widely used.

8.3 Prediction Error Curves

As well as evaluating probabilistic outcomes with integrated scoring rules, non-integrated scoring rules can be utilized for evaluating distributions at a single point. For example, instead of evaluating a probabilistic prediction with the ISBS over $\mathbb{R}_{\geq 0}$, one could compute the Brier score at a single time-point, $\tau \in \mathbb{R}_{\geq 0}$, only. Plotting these for varying values of τ results in *prediction error curves*, which provide a simple visualization for how predictions vary over time. Prediction error curves are mostly used as a graphical guide when comparing few models, rather than as a formal tool for model comparison. Example prediction error curves are provided in Figure 8.2 for the ISBS where the the Cox PH consistently outperforms the SVM.

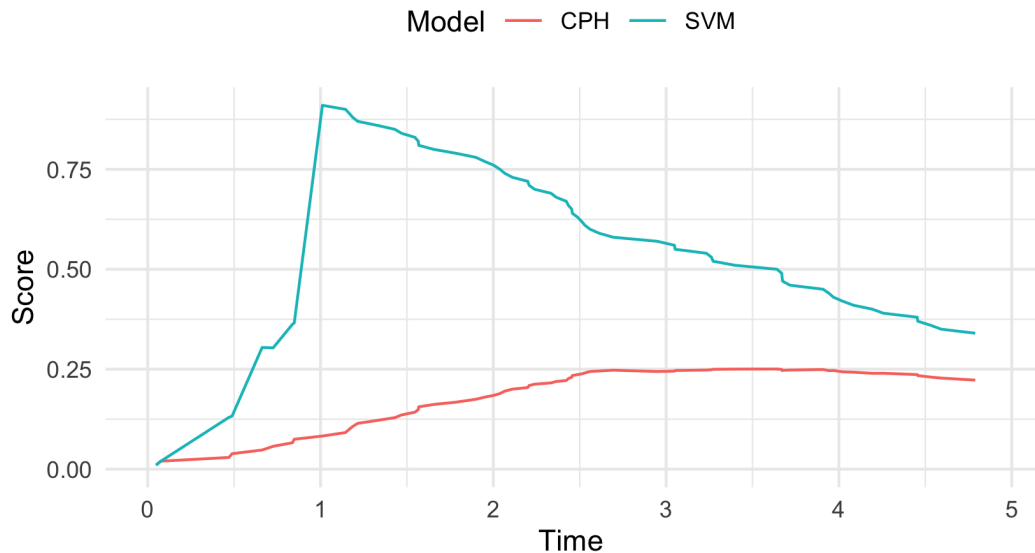


Figure 8.2: Prediction error curves for the CPH and SVM models from Chapter 7. x-axis is time and y-axis is the ISBS computed at different time-points. The CPH (red) performs better than the SVM (blue) as it scores consistently lower. Trained and tested on randomly simulated data from **mlr3proba**.

8.4 Baselines and ERV

A common criticism of scoring rules is a lack of interpretability, for example, an ISBS of 0.5 or 0.0005 has no meaning by itself, so below we present two methods to help overcome this problem.

The first method is to make use of baselines for model comparison, which are models or values that can be utilized to provide a reference for a loss and provide a universal method to judge all models of the same class (Gressmann et al. 2018). In classification, it is possible to derive analytical baseline values, for example a Brier score is considered ‘bad’ if it is above 0.25 or a log loss if it is above 0.693 (Figure 8.1), this is because these are the values obtained if you always predicted probabilities as 0.5, which is the best un-informed (i.e., data independent) baseline in a binary classification problem. In survival analysis, simple analytical expressions are not possible as losses are dependent on the unknown distributions of both the survival and censoring time. For this reason it is advisable to include baselines models for model comparison. Common baselines include the Kaplan-Meier estimator (Section 3.5.2.1) and Cox PH ([?@sec-surv-models-crack](#)). As a rule of thumb, if a model performs worse than the Kaplan-Meier than it’s considered ‘bad’, whereas if it outperforms the Cox PH then it is considered ‘good’.

As well as directly comparing losses from a ‘sophisticated’ model to a baseline, one can also compute the percentage increase in performance between the sophisticated and baseline models, which produces a measure of explained residual variation (ERV) (Edward L. Korn and Simon 1990; Edward L. Korn and Simon 1991). For any survival loss L , the ERV is,

$$R_L(S, B) = 1 - \frac{L_{|S}}{L_{|B}}$$

where $L_{|S}$ and $L_{|B}$ is the loss computed with respect to predictions from the sophisticated and baseline models respectively.

The ERV interpretation makes reporting of scoring rules easier within and between experiments. For example, say in experiment A we have $L_{|S} = 0.004$ and $L_{|B} = 0.006$, and in experiment B we have $L_{|S} = 4$ and $L_{|B} = 6$. The sophisticated model may appear worse at first glance in experiment A (as the losses are very close) but when considering the ERV we see that the performance increase is identical (both $R_L = 33\%$), thus providing a clearer way to compare models.

8.5 Extensions

8.5.1 Competing risks

Similarly to discrimination measures, scoring rules are primarily used with competing risks by evaluating cause-specific probabilities individually (Geloven et al. 2022; C. Lee et al. 2018; Bender et al. 2021).

For example, given the cause-specific survival, S_e , density, f_e , and cumulative distribution function, F_e , the right-censored log-loss for event e is defined as

$$L_{RCLL;i}^e(\hat{S}_{i;e}, t_i, \delta_i) = -\log[\delta_i \hat{f}_{i;e}(t_i) + (1 - \delta_i) \hat{S}_{i;e}(t_i)]$$

Similar logic can be applied to the ISBS and other scoring rules.

Recently, an all-cause logarithmic scoring rule has been proposed which makes use of the IPC weighting in the ISBS (Alberge et al. 2024, 2025):

$$L_{AC;i}(\hat{S}_i, t_i, \delta_i) = \sum_{e=1}^k \frac{\mathbb{I}(t_i \leq \tau, \delta_i = e) \log(\hat{F}_{i;e})}{\hat{G}(t_i)} + \frac{\mathbb{I}(t_i > \tau) \log(\hat{S}_i(\tau))}{\hat{G}(\tau)}$$

This ‘all-cause’ loss is an adaptation of the ISLL (Section 8.2.2) with an adaptation to the weights to handle competing risks. Comparing this loss to the decomposition in Section 8.2.1, we can see observations either: experience the event of interest, in which case their cause-specific CIF is evaluated; do not experience any event and so the all-cause survival is evaluated; or experience a different event and contribute nothing to the loss.

This ‘all-cause’ loss could be minimized in an automated procedure and/or used for model comparison more easily than cause-specific losses. However, doing so may hide cause-specific patterns, for example a model might have better performance for some causes than others. If performance in individual causes is important, then cause-specific losses may be preferred, optionally with multi-objective optimization methods (Morales-Hernández, Van Nieuwenhuyse, and Rojas Gonzalez 2023).

8.5.2 Other censoring and truncation types

We have already seen in Section 8.2.2 how logarithmic losses can be extended to handle more diverse censoring and truncation types by updating the likelihood function as necessary. For squared losses there has been substantially less development in this area, a notable extension is an adaptation to the Brier score for administrative censoring (Kvamme and Borgan 2023). There is potential to extend the ISBS to handle interval censoring by estimating the probability of survival within the interval (Tsouprou 2015), however research is sparse and there is no evidence of use in practice.

8.6 Conclusion

Key takeaways

- Scoring rules are a useful tool for measuring a model’s overall predictive ability, taking into account calibration and discrimination.
- Strictly proper scoring rules allow models to be compared to one another, which is important when choosing models in a benchmark experiment.
- Many scoring rules for censored data are *not* strictly proper, however experiments suggest that improper rules still provide useful and trustworthy results (R. Sonabend et al. 2025)

Limitations

- Scoring rules can be difficult to interpret but ERV representations can be a helpful way to overcome this.
- There is no consensus about which scoring rule to use and when so in practice multiple scoring rules may have to be reported in experiments to ensure transparency and fairness of results.
- For non- and semi-parametric survival models that return distribution predictions, estimates of $f(t)$ are not readily available and require approximations (Rindt et al. 2022), hence logarithmic losses such as RCLL can often not be directly used in practice.

Further reading

- A. Philip Dawid and Musio (2014) and Gneiting and Raftery (2007) provide a comprehensive summary of scoring rules in regression and classification settings.
- Rindt et al. (2022), R. Sonabend et al. (2025) and Yanagisawa (2023) review survival scoring rules, including loss forms not discussed in this chapter such as pinball losses.
- Choodari-Oskooei, Royston, and Parmar (2012a), Choodari-Oskooei, Royston, and Parmar (2012b), and Rahman et al. (2017) compare measures for external validation including some scoring rules.

9

Distance Measures

This chapter discusses evaluation of distance measures for evaluating the distance between survival time predictions and the ground truth. The chapter explains why such evaluations are fundamentally problematic in the presence of censoring.

As discussed in Chapter 5, evaluating the distance between survival time point predictions and the ground truth event times is fundamentally problematic when censoring is present. In particular, there is no principled way to define a metric that accurately reflects the average discrepancy between predicted survival times and all event times. Restricting evaluation to uncensored observations and applying standard regression measures such as the mean absolute error (MAE) can introduce substantial bias (P. Wang, Li, and Reddy 2019). Moreover, S.-A. Qi et al. (2023) show that naïvely applying the MAE to survival data can induce model performance rankings that are inconsistent with those obtained from the oracle MAE computed using fully observed event times; this remains true even when using inverse probability of censoring–weighted variants of the MAE. A pseudo-observation–based approach has been shown, under controlled simulation settings, to induce the same model rankings as the oracle MAE (S.-A. Qi et al. 2023). However, this approach is not intended to, nor does it, recover a meaningful measure of absolute distance between predicted survival times and the ground truth event times.

Given these limitations, this book recommends avoiding distance-based evaluation of survival time predictions. Instead, discrimination-based measures (Chapter 6) may be used to evaluate survival time predictions whilst being clear this is an evaluation of the relative risk of event only and not an attempt to quantify the distance between predictions and truth.

9.1 Conclusion

Key takeaways

- Survival time point predictions should not evaluated using standard distance-based error measures in a principled way when censoring is present.
- Existing approaches can support relative comparison of models but do not resolve the fundamental ambiguity of unobserved event times.
- As a result, discrimination-based evaluation should be preferred, with careful interpretation of what is, and is not, being evaluated.

Part III

Models

10

Traditional Survival Models

TODO (150-200 WORDS)

 Minor changes expected!

This page is a work in progress and minor changes will be made over time.

In a predictive setting it can be easy to dismiss ‘traditional models’ and favour testing of more modern ‘machine learning’ tools; this would be a mistake. Firstly, on low dimensional data (small number of variables), traditional methods often outperform machine learning models (Burk et al. 2024; Beaulac et al. 2020). Secondly, even on high-dimensional data, several papers have demonstrated that augmenting traditional models (Section 10.6) can yield models that outperform machine learning alternatives (Yunwei Zhang et al. 2021; Spooner et al. 2020). Finally, the majority of machine learning survival algorithms make use of these traditional models, for example by using non-parametric estimators (Section 10.1) and/or assuming a proportional hazards form (Section 10.2), as a central component to construct an algorithm around. Therefore, a robust understanding of these models is imperative to fairly construct and evaluate machine learning survival models. This chapter begins with demonstrating non-parametric estimators as predictive tools, including a recap of some estimators in Chapter 3. Semi- and fully-parametric models are then introduced, most notably the Cox proportional hazards model and the accelerated failure time model. Finally, methods to improve traditional models through machine learning methodology is presented.

10.1 Non-Parametric Estimators

Non-parametric estimators have already been introduced in Section 3.5.2, therefore this section is brief and focuses only on how these estimators can be used as predictive models.

10.1.1 Unconditional estimators

Recall from Section 3.5.2 the Kaplan-Meier and Nelson-Aalen estimators respectively defined by

$$S_{KM}(\tau) = \prod_{k:t_{(k)} \leq \tau} \left(1 - \frac{d_{t_{(k)}}}{t_{(k)}}\right) \quad (10.1)$$

and

$$H_{NA}(\tau) = \sum_{k:t_{(k)} \leq \tau} \frac{d_{t_{(k)}}}{n_{t_{(k)}}}$$

where $d_{t_{(k)}}$ and $n_{t_{(k)}}$ are the number of events and observations at risk at the k th ordered event time, $t_{(k)}$ respectively.

For example, Figure 10.1 shows the Kaplan-Meier estimator fit on the **rats** (Mantel, Bohidar, and Ciminera 1977) dataset. The top image displays how the estimator is a step function with steps occurring at event times (some examples in green dashed lines). At censoring times, the estimator stays constant (examples in blue dotted lines). The bottom image displays how to use the estimator as a predictive tool. To predict the survival probability of a new rat, one can find the estimated survival probability at a given time from the trained estimator, without needing any more details about the rat in question (as covariates are ignored). This provides a quick tool that tends to be well-calibrated to the average observation.

As predictive models, these can also be extended to other censoring and truncation types as well as event history analysis more generally from using the estimators defined in Section 3.5.2, Section 4.2.2, and Section 4.3.4.

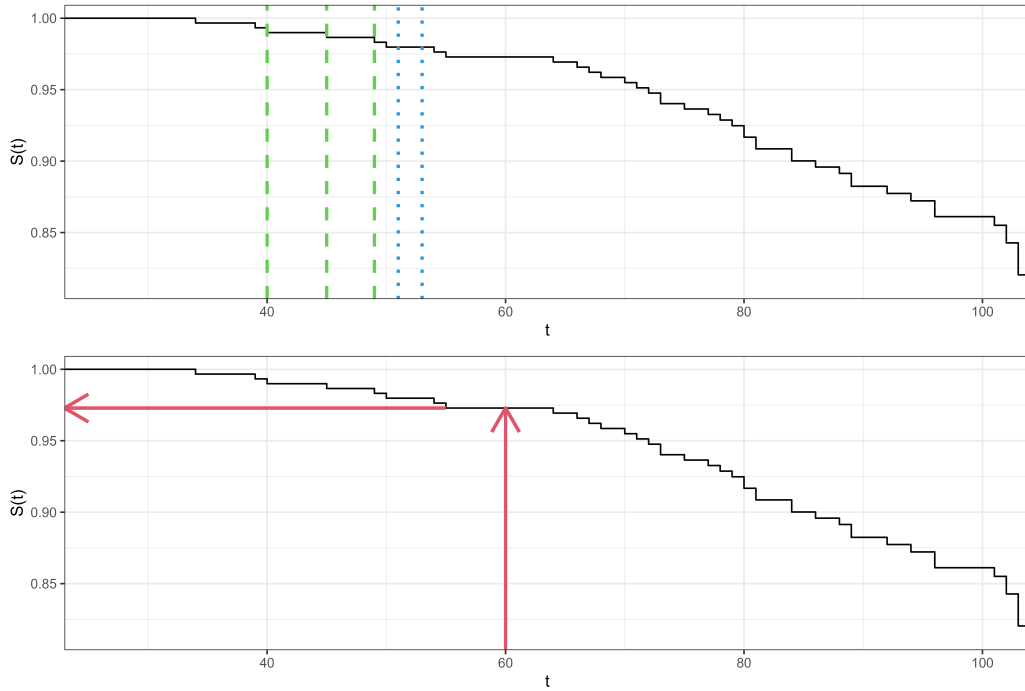


Figure 10.1: Using the Kaplan-Meier estimator as a predictive tool. The top image shows the estimator fit to data, the green dashed lines so steps in the function at event times and the blue dotted lines are censoring times in the training data and no steps occur. The bottom image demonstrates using the estimator as a predictive tool by reading off the survival probability at given times.

10.1.2 Conditional estimators

As well as unconditional estimators, which do not account for covariates, an alternative is the conditional Akritas estimator (Michael G. Akritas 1994) usually defined by (Blanche, Dartigues, and Jacqmin-Gadda 2013):

$$S(\tau|\mathbf{x}^*, \lambda) = \prod_{k:t_{(k)} \leq \tau} \left(1 - \frac{\sum_{i=1}^n K(\mathbf{x}^*, \mathbf{x}_i | \lambda) \mathbb{I}(t_i = t_{(k)}, \delta_i = 1)}{\sum_{i=1}^n K(\mathbf{x}^*, \mathbf{x}_i | \lambda) \mathbb{I}(t_i \geq t_{(k)})} \right) \quad (10.2)$$

where K is a kernel function, usually $K(x, y | \lambda) = \mathbb{I}(|\hat{F}_X(x) - \hat{F}_X(y)| < \lambda)$, $\lambda \in (0, 1]$, \hat{F}_X is the empirical distribution function of the data, and λ is a hyper-parameter. The estimator can be interpreted as a conditional Kaplan-Meier estimator which is computed on a neighbourhood of subjects closest to \mathbf{x}^* . In fact, if $\lambda = 1$ then $K(\cdot | \lambda) = 1$ and (10.2) is identical to (10.1).

The formulation in (10.2) includes fitting and predicting in one step as the usual application of the model is as a non-parametric estimator. By first estimating \hat{F}_X on separate training data, the estimator can be used as a baseline predictive model.

10.2 Proportional Hazards

This section begins with an introduction to the proportional hazards concept, introduces estimation with the Cox PH model, and then moves to fully parametric proportional hazards models, with the Weibull model as a motivating example.

Let $\eta_i = \mathbf{x}_i^\top \boldsymbol{\beta}$ be the linear predictor for some observation i with covariates \mathbf{x}_i and model coefficients $\boldsymbol{\beta} \in \mathbb{R}^p$, then proportional hazards (PH) models assume that the hazard function for i follows the form

$$h_{PH}(\tau | \mathbf{x}_i) = h_0(\tau) \exp(\eta_i) \quad (10.3)$$

or equivalently:

$$H_{PH}(\tau | \mathbf{x}_i) = H_0(\tau) \exp(\eta_i) \quad (10.4)$$

and

$$S_{PH}(\tau | \mathbf{x}_i) = S_0(\tau)^{\exp(\eta_i)} \quad (10.5)$$

h_0, H_0, S_0 are referred to as the baseline hazard, cumulative hazard, and survival function respectively. Instead of modelling a separate intercept, the baseline hazard represents the hazard when the linear predictor is zero, hence the term ‘baseline’. Note that the baseline hazard may not have a meaningful interpretation, unless the covariates are all centered around zero or reference coded in case of categorical covariates (similar to the intercept β_0 in linear regression).

It can be seen from (10.3) that time is only incorporated via the baseline hazard (ignoring adaptations to time-varying models). Therefore, PH models estimate the baseline risk of an event at a given time, and modulate this risk according to the specification of covariates.

This represents the eponymous ‘proportional hazards’ assumption as the individual’s hazard at time τ is directly proportional to a multiplicative function of their own covariates: $h(\tau|x_i) \propto \exp(\eta_i)$. In other words, a unit change in a covariate acts multiplicatively on the estimated hazard. Further, the hazard ratio, which is a measure of the difference in risk, between two different subjects, depends solely on the value of their (linear) predictors and not on time. For a single covariate x :

$$\frac{h_{PH}(\tau|x_i)}{h_{PH}(\tau|x_j)} = \frac{h_0(\tau) \exp(x_i\beta)}{h_0(\tau) \exp(x_j\beta)} = \exp(\beta(x_i - x_j))$$

Equivalently:

$$h_{PH}(\tau|x_i) = \exp(\beta(x_i - x_j))h_{PH}(\tau|x_j) \quad (10.6)$$

So in the case where the covariate differs between subjects by 1, the hazard ratio increases multiplicatively by $\exp(\beta)$. This yields an interpretable model, in which hazard ratios are constant over time and don’t depend on τ . That is, the covariates effect on the hazard is independent of time. Note that this doesn’t imply that the effect of covariates on the survival function is constant over time (a constant difference in hazards at each time point will accumulate over time and the difference between the survival functions will increase).

We next consider how to fit the β parameters semi-parametrically (Section 10.2.1) and fully parametrically (Section 10.2.2).

10.2.1 Semi-Parametric PH

The Cox Proportional Hazards (Cox PH) (Cox 1972), or Cox model, is likely the most widely known semi-parametric model and the most studied survival model (Reid 1994; P. Wang, Li, and Reddy 2019). Often, it is considered synonymous with proportional hazards and the functional form of the hazard given in (10.3). However, the main contribution of Cox’s work was to develop a method to estimate β without making any assumptions about the baseline hazard. We derive the estimation of the parameters in some detail as the objective function of the Cox model is also used by many machine learning methods like boosting (Chapter 13) and neural networks (Chapter 14).

Recall from Section 3.5, to estimate the distribution of event times one either needs to make distributional assumptions and accordingly define the likelihood of observing the data (given model parameters), or to use non-parametric estimators, which usually do not incorporate covariate information. Let $i_{(k)}$ denote the subject who experienced the event at ordered event time $t_{(k)}$. Cox noted the contribution of an individual could be defined as the probability of a particular subject $i_{(k)}$ experiencing the event at $t_{(k)}$ given that *someone* in the risk set experienced the event at that time. The likelihood contribution of this k th event is given by

$$\ell_{i_{(k)}}^{Cox} = \frac{h_0(t_{(k)}) \exp(\eta_{i_{(k)}})}{\sum_{j \in \mathcal{R}_{t_{(k)}}} h_0(t_{(k)}) \exp(\eta_j)} = \frac{\exp(\eta_{i_{(k)}})}{\sum_{j \in \mathcal{R}_{t_{(k)}}} \exp(\eta_j)},$$

which depends on β via $\eta = \mathbf{x}^\top \beta$. Note how the baseline hazard h_0 cancels out in the likelihood contribution and thus doesn’t depend on time anymore. Thus, for the estimation of β , the baseline hazard can be considered a ‘nuisance parameter’ and the likelihood for the entire data set can be defined as:

$$\mathcal{L}_{PL}(\beta) = \prod_{k=1}^m \ell_{i_{(k)}}^{Cox} = \prod_{k=1}^m \left(\frac{\exp(\eta_{i_{(k)}})}{\sum_{j \in \mathcal{R}_{t_{(k)}}} \exp(\eta_j)} \right). \quad (10.7)$$

Information about the event times only contributes to (1) through the index of the product and sum, thus preserving rankings, i.e., the product is taken from first to last observed event time. The baseline hazard, and thus information about the exact event time is absent from the function. Moreover, censored observations only contribute in the denominator of the calculation. (1) is therefore referred to as a *partial likelihood* (Cox 1975) function, as it does not make use of all the observed data.

- (1) also assumes that there are no ties in the event time, that is, no two subjects have an event at the same time. In practice, ties can be common and several methods have been proposed to handle them, namely an exact method (J. D. Kalbfleisch and Prentice 1973) (which is computationally expensive), the Breslow approximation (Breslow 1974), and the Efron approximation (Efron 1977); further details are not discussed here but all three methods are readily available in openly available software.

The log-partial likelihood, usually preferred for optimization, is given by

$$\hat{\gamma}_{PL}(\beta) = \sum_{k=1}^m \left(\eta_{i_{(k)}} - \log \left(\sum_{j \in \mathcal{R}_{t_{(k)}}} \exp(\eta_j) \right) \right), \quad (10.8)$$

such that

$$\hat{\beta} = \arg \max_{\beta} \hat{\gamma}_{PL}(\beta). \quad (10.9)$$

Traditionally, $\hat{\beta}$ is obtained using numerical optimization methods, such as Newton-Raphson or Fisher-Scoring, which require derivation of the first and second derivatives of 10.8.

Importantly, the partial likelihood allows us to estimate covariate effects (and interpret them in terms of hazard ratios) without making any assumptions about the underlying distribution of event times. Obtaining $\hat{\beta}$ also gives us enough information to make predictions in the form of relative risks (Chapter 5).

At this point, however, we don't have an estimate of the baseline hazard h_0 and thus cannot make survival distribution predictions. The Breslow estimator (Breslow 1972; Lin 2007) provides a way to obtain an estimate of the cumulative baseline hazard, H_0 , using the parameters from the Cox model:

$$H_{Bres}(\tau) = H_0(\tau) = \sum_{k: t_{(k)} \leq \tau} \frac{d_{t_{(k)}}}{\sum_{j \in \mathcal{R}_{t_{(k)}}} \exp(\eta_j)}. \quad (10.10)$$

Note that if the value for all covariates or their effects was zero, or if there were no covariates, then the Breslow estimator is identical to the Nelson-Aalen estimator (Section 3.5.2.2):

$$H_{Bres}(\tau) = \sum_{k: t_{(k)} \leq \tau} \frac{d_{t_{(k)}}}{\sum_{j \in \mathcal{R}_{t_{(k)}}} 1} = \sum_{t_{(k)} \leq \tau} \frac{d_{t_{(k)}}}{n_{t_{(k)}}} = H_{NA}(\tau).$$

With these formulae, the Cox PH model can be used as a predictive model by using training data to estimate $\hat{\beta}$ via (10.9). These fitted coefficients are used to predict $\hat{\eta}$ for new observations and finally the cumulative baseline hazard is computed with (10.10) to return a predicted distribution, for example the survival probability (10.5).

The Cox model is highly interpretable and has a long history of usage in clinical prediction modelling and analysis. However, the proportional hazards assumption is often violated in real life, leaving the model to be a questionable choice when used for data analysis or inference. Over the years, extensions to the Cox model have been developed (Therneau and Grambsch 2001) to incorporate stratified baseline hazards (the PH assumption only has to hold within strata), time-varying effects (the effects of time-constant covariates change over time) and time-varying covariates (the values of covariates change over time). However, especially in case of time-varying covariates, it is difficult to make meaningful and interpretable predictions (as the values of covariates might not be known at the time of prediction). Whilst violation of the PH assumption can be problematic, especially for interpretation of covariate effects, it doesn't appear to cause problems in terms of prediction accuracy. In fact, the Cox model often outperforms machine learning alternatives, including those that relax the PH assumption (Burk et al. 2024; Michael F. Gensheimer and Narasimhan 2018; Luxhoj and Shyur 1997; Van Belle et al. 2011).

10.2.2 Parametric PH

Semi-parametric approaches (like the Cox model) are popular because they don't make an assumption about the underlying distribution of event times, leaving the baseline hazard unspecified. However, there are some cases where modelling a particular distribution may make sense. On these occasions, a particular probability distribution of the event times is assumed, with three common choices (**Kalbfleisch2011?**; P. Wang, Li, and Reddy 2019) being the Exponential, Gompertz, and Weibull distributions. The Weibull distribution is particularly important as it reduces to the Exponential distribution when the shape parameter equals 1. Moreover, it is unique (and Exponential as a special case) in that it has both the PH and AFT (**?@sec-aft**) property (technically a less known representation of Gompertz also has this property).

Assuming a PH model one can plug in the hazard and survival functions from the Weibull distribution into (10.3) and (10.5) respectively. First recall for a Weibull(γ, λ) distribution with shape parameter γ and scale parameter λ , the relevant functions can be given by (John D. Kalbfleisch and Prentice 1980):

$$h(\tau) = \lambda\gamma\tau^{\gamma-1}$$

and

$$S(\tau) = \exp(-\lambda\tau^\gamma)$$

Taking these to be the baseline hazard and survival functions respectively, they can be substituted into the Cox model as follows:

$$h_{WeibullPH}(\tau|\mathbf{x}_i) = (\lambda\gamma\tau^{\gamma-1}) \exp(\eta_i) \quad (10.11)$$

or equivalently

$$S_{WeibullPH}(\tau|\mathbf{x}_i) = (\exp(-\lambda\tau^\gamma))^{\exp(\eta_i)}$$

Finally, these formulae can be used to define the full likelihood (Section 3.5.1) for the WeibullPH model (here for right-censored data):

$$\begin{aligned}\mathcal{L}(\boldsymbol{\theta}) &= \prod_{i=1}^n h_Y(t_i | \mathbf{x}_i, \boldsymbol{\theta})^{\delta_i} S_Y(t_i | \mathbf{x}_i, \boldsymbol{\theta}) \\ &= \prod_{i=1}^n \left((\lambda \gamma t_i^{\gamma-1} \exp(\eta_i))^{\delta_i} \right) \left(\exp(-\lambda t_i^\gamma \exp(\eta_i)) \right)\end{aligned}$$

with log-likelihood

$$\begin{aligned}\hat{\mathcal{L}}(\boldsymbol{\theta}) &= \sum_{i=1}^n \delta_i [\log(\lambda\gamma) + (\gamma - 1) \log(t_i) + \eta_i] - \lambda t_i^\gamma \exp(\eta_i) \\ &\propto \sum_{i=1}^n \delta_i [\log(\lambda\gamma) + \gamma \log(t_i) + \eta_i] - \lambda t_i^\gamma \exp(\eta_i)\end{aligned}$$

Parameters can then be fit using maximum likelihood estimation (MLE) with respect to all unknown parameters $\boldsymbol{\theta} = \{\boldsymbol{\beta}, \gamma, \lambda\}$. Expansion to other censoring types and truncation follows by using other likelihood forms presented in Section 3.5.

When considering which probability distributions to model in predictive experiments, Weibull is a common starting choice (Hielscher et al. 2010; R. and J. 1968; Rahman et al. 2017), its two parameters make it a flexible fit to data but on the other hand it can be easily reduced to Exponential when $\gamma = 1$. Gompertz (Gompertz 1825) is commonly used in medical domains, especially when describing adult lifespans. In a machine learning context, one can select the optimal distribution for future predictive performance by running a benchmark experiment. In contrast to the semi-parametric Cox model, fully parametric PH models can predict absolutely continuous survival distributions, they do not treat the baseline hazard as a nuisance, and in general will result in more precise and interpretable predictions if the distribution is correctly specified (Reid 1994; Royston and Parmar 2002).

10.2.3 Competing risks

There are two common methods to extend the Cox model to the competing risks setting. The first makes use of the cause-specific hazard to fit a cause-specific Cox model, the second fits a ‘subdistribution’ hazard.

Cause-specific PH models

In cause-specific models we define the hazard for cause e as:

$$h_e(\tau | \mathbf{x}_{e;i}) = h_{e;0}(\tau) \exp(\eta_{e;i}), \quad (10.12)$$

where $h_{e;0}$ is a cause-specific baseline hazard and $\mathbf{x}_{e;i}$ is a set of cause-specific covariates (although in practice often the same covariates are used for all causes), and $\eta_{e;i}$ is the cause-specific linear predictor:

$$\eta_{e;i} = \mathbf{x}_{e;i}^T \boldsymbol{\beta}_e.$$

In order to estimate $\boldsymbol{\beta}_e$, let $t_{e;(k)}, k = 1, \dots, m(e)$ be the unique, ordered event times at which events of cause e occur and let $i_{e;(k)}$ be the index of the observation that experiences

the k th event of cause e . Then the cause-specific partial likelihood is given by:

$$\mathcal{L}_{PL}(\boldsymbol{\beta}_e) = \prod_{k=1}^{m(e)} \left(\frac{\exp(\eta_{e;i_{e;(k)}})}{\sum_{j \in \mathcal{R}_{t_{e;(k)}}} \exp(\eta_{e;j})} \right), \quad (10.13)$$

This is identical to the single-event partial likelihood in (1), with the only difference being that the product and sum are over the unique, ordered event times for cause e . The risk-set definition is unaltered such that $\mathcal{R}_{t_{e;(k)}}$ is the set of observations that have not experienced an event of *any* cause or censoring by $t_{e;(k)}$.

Using the same logic, the Breslow estimator follows from (10.10):

$$H_{Bres;e}(\tau) = \sum_{k:t_{e;(k)} \leq \tau} \frac{d_{t_{e;(k)}}}{\sum_{j \in \mathcal{R}_{t_{e;(k)}}} \exp(\eta_{e;j})}, \quad (10.14)$$

and the feature-dependent, cause-specific cumulative hazard (10.4) as

$$H_e(\tau|\mathbf{x}) = H_{Bres;e}(\tau) \exp(\mathbf{x}^T \boldsymbol{\beta}_e) \quad (10.15)$$

Finally, in order to obtain an estimate of the cumulative incidence function $F_e(\tau)$ (4.9), we need an estimate of the all cause survival probability and an estimate of the cause-specific hazard (which is not directly available in the Cox model as the Breslow estimator only provides an estimate of the cause-specific *cumulative* baseline hazard). The all cause survival probability is obtained using 10.15 and the usual relationships (4.7, 3.4) as

$$S(\tau|\mathbf{x}) = \exp \left(- \sum_{e=1}^q H_e(\tau|\mathbf{x}) \right) \quad (10.16)$$

and an estimate of the cause-specific hazard is obtained via

$$\begin{aligned} h_e(\tau|\mathbf{x}) &= \Delta H_e(\tau|\mathbf{x}) = \Delta H_{Bres;e}(\tau) \exp(\mathbf{x}^T \boldsymbol{\beta}_e) \\ &= \frac{d_{t_{e;(k)}}}{\sum_{j \in \mathcal{R}_{t_{e;(k)}}} \exp(\eta_{e;j})} \exp(\mathbf{x}^T \boldsymbol{\beta}_e), \end{aligned} \quad (10.17)$$

where $\Delta H_{Bres;e}(\tau)$ is the increment of the cause-specific cumulative baseline hazard between successive time points (note the missing sum over different time points compared to 10.14). With 10.16 and 10.17, the CIF is approximated by

$$F_e(\tau|\mathbf{x}) = \sum_{k:t_{(k)} \leq \tau} S(\tau|\mathbf{x}) h_e(\tau|\mathbf{x}). \quad (10.18)$$

Subdistribution PH models

The methods discussed thus far estimate cause-specific hazards (4.4), which represent the instantaneous risk of an individual experiencing the cause of interest, given that they have not yet experienced *any* event. An alternative approach is to model subdistribution hazards, which model the risk of an individual experiencing the cause of interest, given they have not yet experienced the event of interest, but may have experienced a competing event. As will be shown below, the benefit of the subdistribution model is the ability to directly predict the cumulative incidence function (CIF) under a PH model, rather than using the indirect

calculation in Equation (10.18). The subdistribution hazard approach also provides a direct relationship between covariates and the CIF for an event of interest (Austin, Lee, and Fine 2016).

Mathematically, the difference between cause-specific and subdistribution hazards comes from the definition of the risk set. The subdistribution risk set is defined as:

$$\mathcal{R}_{e;\tau} := \{i : t_i \geq \tau \vee [t_i < \tau \wedge e_i \neq e \wedge \delta_i = 1]\} \quad (10.19)$$

Observe that in this definition the left-hand side is the same as the standard risk set definition (3.10) and the right-hand side additionally includes those that have experienced a different event already. Anyone that has been censored ($e = e_0$) before τ is removed from the risk set.

The definition of the subdistribution risk (10.19) is equivalent to defining the subdistribution hazard for cause e as:

$$h_e^{SD}(\tau) = \lim_{d\tau \rightarrow 0} \frac{P(\tau \leq Y \leq \tau + d\tau, E = e \mid Y \geq \tau \vee (E \neq e \wedge \Delta = 1))}{d\tau}. \quad (10.20)$$

Fine and Gray (Fine and Gray 1999) proposed a proportional hazards formulation of the subdistribution hazard (10.20) as

$$h_{FG;e}(\tau | \mathbf{x}_i) = h_{e;0}^{SD}(\tau) \exp(\eta_i), \quad (10.21)$$

with subdistribution baseline hazard $h_{e;0}^{SD}(\tau)$ (we add the superscript here in order to make explicit that this baseline hazard will differ from the one obtained from the Cox model (10.4) due to differences in risk set definition).

While the subdistribution hazards model is different from the proportional hazards Cox model, Fine and Gray (1999) showed that its parameters could be estimated using a weighted partial likelihood, which is otherwise identical to the cause-specific partial likelihood (10.13):

$$\mathcal{L}_{PL}^{SD}(\beta) = \prod_{k=1}^m \left(\frac{\exp(\eta_{e;i_{e;(k)}})}{\sum_{j \in \mathcal{R}_{e;t_{e;(k)}}} w_{kj} \exp(\eta_{e;j})} \right), \quad (10.22)$$

In (10.22), $t_{e;(k)}$ is the same as in the cause-specific case and weights w_{kj} account for the fact that the subdistribution risk set is different from the cause-specific risk set. The weights are defined as

$$w_{kj} := \frac{G_{KM}(t_{e;(k)})}{G_{KM}(\min\{t_{e;(k)}, t_j\})},$$

where G_{KM} is the Kaplan-Meier estimator fit on the censoring distribution (Section 3.5.2.1). Because of the way the subdistribution risk set is defined in (10.19), the denominator of (10.22) is a weighted sum over individuals, $j \in \mathcal{R}_{e;t_{e;(k)}}$, at time $t_{e;(k)}$ who have either yet to experience an event ($t_j \geq t_{e;(k)}$) or experienced a different event ($t_j < t_{e;(k)} \wedge e_i \neq e \wedge \delta_i = 1$). The weighting function handles these cases as follows:

1. If $t_j \geq t_{e;(k)}$ then $w_{kj} = 1$ and thus observations that have not experienced any event contribute fully to the denominator.
2. If $t_j < t_{e;(k)}$ then $w_{kj} < 1$ as G_{KM} is a monotonically decreasing function and w_{kj} continues to decrease as the distance between t_j and $t_{e;(k)}$ increases. Thus the contribution from observations that have experienced competing events reduces over time.

Whilst modelling the subdistribution can seem unintuitive, note that if there is only one event of interest then $w_{kj} = 1$ for all k and j and further $e_i \neq e$ must always be false, meaning (10.19) reduces to the standard risk set definition (3.10) as only the left condition can ever be true and by the same logic the subdistribution hazard reduces to the usual hazard definition. Therefore the standard Cox PH for single events is perfectly recovered.

Instead of interpreting the subdistribution hazards directly, Austin and Fine (2017) recommend interpreting the fitted coefficients via the cause-specific CIF and cumulative hazard forms of (10.21), which can be obtained in the ‘usual’ way by first integrating to obtain the cumulative hazard form:

$$H_{FG;e}(\tau | \mathbf{x}_i) = H_{e;0}^{SD}(\tau) \exp(\eta_i) \quad (10.23)$$

where $H_{e;0}^{SD}$ is the cause-specific baseline cumulative hazard for cause e . Then using (3.4) to relate the survival and hazard functions and representing this in terms of the CIF:

$$F_{FG;e}(\tau | \mathbf{x}_i) = 1 - \exp(-H_{e;0}^{SD}(\tau))^{\exp(\eta_i)} \quad (10.24)$$

Or more simply:

$$F_{FG;e}(\tau | \mathbf{x}_i) = 1 - (1 - F_{e;0}^{SD}(\tau))^{\exp(\eta_i)} \quad (10.25)$$

where $F_{e;0}^{SD}$ is the cause-specific baseline cumulative incidence function for cause e . The model in (10.25) is fit by estimating the baseline cumulative hazard function and substituting into (10.24). Similarly to how the subdistribution hazard was created, estimation of \hat{H}^{SD} follows by updating (10.10) to use the subdistribution risk set definition and applying the same weighting to compensate for multiple events:

$$\hat{H}_{Bres;e}^{SD}(\tau) = \sum_{k:t_{e;(k)} \leq \tau} \frac{d_{t_{e;(k)}}}{\sum_{j \in \mathcal{R}_{e;t_{e;(k)}}} w_{kj} \exp(\hat{\eta}_j)} \quad (10.26)$$

Use of the Fine-Gray model has to be carefully considered before model fitting. The subdistribution risk set definition, which includes competing events, treats all causes as non-terminal (even if realistically impossible), which means an observation could be considered at risk of the event of interest even after experiencing a terminal event (like death). Moreover, combining subdistribution CIF estimates across causes can result in probabilities that exceed 1, which should be impossible as events are mutually exclusive and exhaustive (Austin et al. 2022). The cause-specific hazards approach for the estimation of the CIF (Section 4.2.1 and Equations 10.16, 10.18) is often preferred (Austin et al. 2022) as fitting subdistribution models requires model assumptions to hold for all causes simultaneously, which is not possible (Bonneville, de Wreede, and Putter (2024)).

The Fine-Gray model is most appropriate when one is only interested in analyzing one of the causes. In this case, interpretation of coefficients from a subdistribution model can be more intuitive as they represent the magnitude of the effect on the incidence, rather than the hazard, which is often of more interest, for example in clinical settings (Austin and Fine 2017).

10.3 Accelerated Failure Time

Whilst the proportional hazards models is a powerful model, it often does not represent real-world phenomena well. The accelerated failure time (AFT) model is a popular alternative which models the effect of covariates as ‘acceleration factors’ that act multiplicatively on time. In contrast to the PH model, AFT models are all fully-parametric. A semi-parametric model has been suggested (Buckley and James 1979) however this is not widely used as it lacks ‘theoretical justification’ and is ‘not reliable’ (Wei 1992). Similarly, whilst its theoretically possible to fit cause-specific AFT models for the competing risks setting, this does not appear common in practice.

10.3.1 Understanding acceleration

Moving from a PH to AFT framework can be confusing, so to elucidate this, take the following example adapted from Kleinbaum and Klein (1996). Consider the lifespans of humans and small dogs. In this example we are taking species to be a modifier and we’re looking at what survival would look like under AFT (time scaling) versus PH (hazard scaling).

Suppose small dogs age five times faster than humans. Under AFT (time-scaling modifier), a dog’s survival at age τ matches a human’s at 5τ :

$$S_{dog}(\tau) = S_{human}(5\tau)$$

For example, at age 10, a small dog has the same probability of being alive as a human at age 50. The dog’s survival curve is *accelerated* by a factor of 5, as shown in the bottom, red curve in Figure 10.2.

If instead, one assumes a constant hazard ratio then at age τ , the dog’s risk is five times the humans (10.5):

$$S_{dog}(\tau) = S_{human}(\tau)^5$$

the middle, blue curve in Figure 10.2.

These illustrative curves demonstrate how the same modifier yields different behaviour under PH and AFT assumptions.

More generally, the accelerated failure time model estimates survival functions as

$$S_{AFT}(\tau|\mathbf{x}_i) = S_0(\tau e^{-\eta_i}) \tag{10.27}$$

with respective hazard function

$$h_{AFT}(\tau|\mathbf{x}_i) = e^{-\eta_i} h_0(\tau e^{-\eta_i}) \tag{10.28}$$

Note three key differences compared to the PH model. Firstly, $\exp(-\eta_i)$ is modelled instead of $\exp(\eta_i)$, hence in a PH model $h_{PH}(\eta_i + 1) > h_{PH}(\eta_i)$ whereas in an AFT model $h_{AFT}(\eta_i + 1) < h_{AFT}(\eta_i)$. Secondly, the baseline risk now clearly depends on both time and the linear

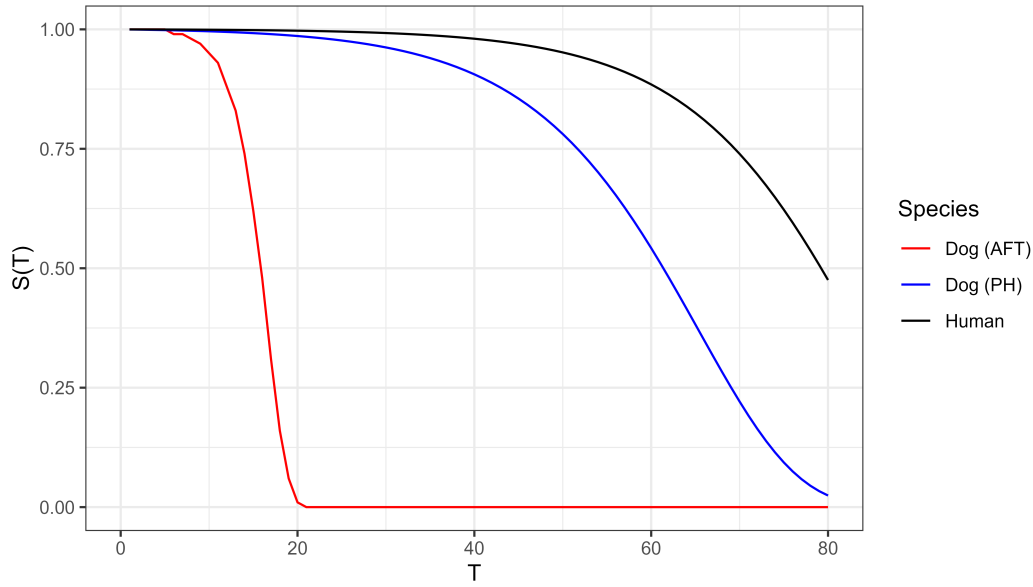


Figure 10.2: Comparing human (black) and dog lifespans where the latter is modelled using an AFT model (red) versus a PH model (blue). Clearly the AFT model is (sadly) a better reflection of reality. Human lifespan modelled with Gompertz(0.09, 0.00005).

predictor. Thirdly, an increase in a covariate results in a multiplicative increase over *time* compared to the PH model in which the hazard is increased – this is often seen as more intuitive to understand than hazard ratio, especially to clinicians who may be more interested in survival times and not abstract relative risks.

This third point is visualised in Figure 10.3 in which a covariate is increased by $\log(2)$. The left panel shows that the estimated hazard function from a PH model is double the baseline at all time points – the multiplicative effect is seen on the y-axis (risk). In contrast, the right panel shows how the survival function from an AFT model decreases at double the speed to the baseline – the multiplicative effects is now on the x-axis (time). Another way to demonstrate this effect is through the log-linear form of the accelerated failure time model:

$$\log(t_i) = \mu + \eta_i + \sigma\epsilon_i \quad (10.29)$$

where σ is a scale parameter, ϵ_i is an error term, and μ is an intercept. Now consider the difference in t_i when η_i is increased by one (assuming just one covariate):

$$\log(t_i|x_i + 1) - \log(t_i|x_i) = (\mu + \beta(x_i + 1) + \sigma\epsilon_i) - (\mu + \beta x_i + \sigma\epsilon_i) = \beta$$

Taking exponentials

$$\frac{t_i|x_i + 1}{t_i|x_i} = \exp(\beta)$$

Hence increasing a covariate effectively multiplies the survival time by $\exp(\beta)$:

$$t_i|x_i + 1 = e^\beta t_i|x_i$$

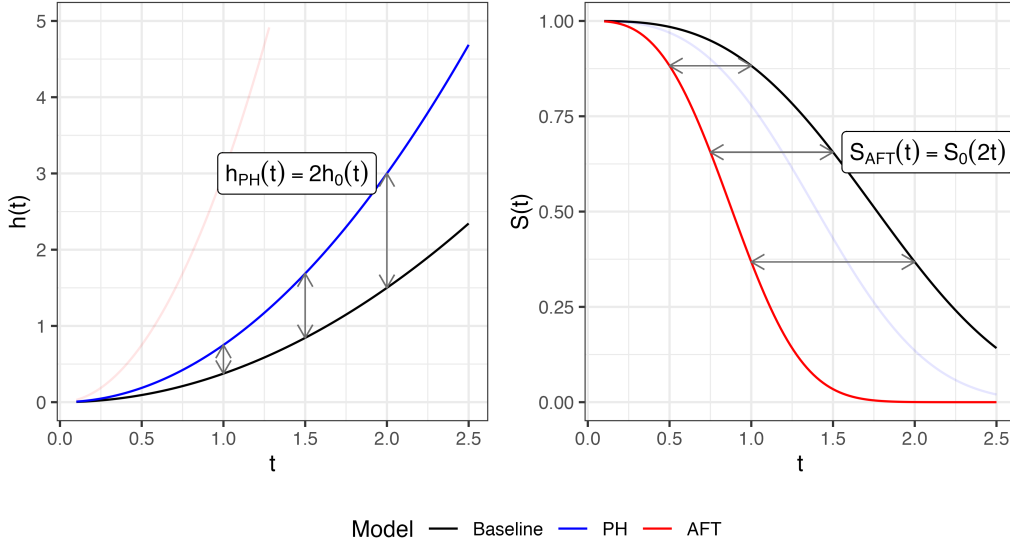


Figure 10.3: Comparing increasing a covariate x_i between PH (left) and AFT (right) models. An increase of $x_i + \log(2)$ multiplies $h(t)$ by $\exp(\log(2)) = 2$ in a PH model. Whereas the result in the AFT is to multiply time t by 2, hence for any t , the AFT model reaches $S(t)$ in half the time as the baseline.

10.3.2 Parametric AFTs

As stated, AFTs are usually fully parametric, which means S_0 and h_0 are chosen according to some specific distribution. Common distribution choices include Weibull, Exponential, Log-logistic, and Log-Normal (Kalbfleisch2011?; P. Wang, Li, and Reddy 2019). The hazard function of the log-logistic distribution is plotted in Figure 10.4, note the hazard is non-monotonic, allowing non-PH representations to be modelled where the risk of an event may increase before decreasing, or vice versa. When distributions are well-specified and the PH assumption is violated, AFTs can outperform PH alternatives (Patel, Kay, and Rowell 2006; J. Qi 2009; Zare et al. 2015).

As with the PH model, AFT models can be fit using maximum likelihood estimation of the full-likelihood by plugging in distribution defining functions into (10.27) and (10.27) and likelihoods defined in (Section 3.5.1). Using Exponential this time as an example (the maths is a bit more friendly), first recall that if $X \sim \text{Exp}(\lambda)$ then $h_X(\tau) = \lambda$ and $S_X(\tau) = \exp(-\lambda\tau)$. Then:

$$h_{\text{ExpAFT}}(\tau|\mathbf{x}_i) = \lambda e^{-\eta_i}$$

and

$$S_{\text{ExpAFT}}(\tau|\mathbf{x}_i) = \exp(-\lambda\tau e^{-\eta_i})$$

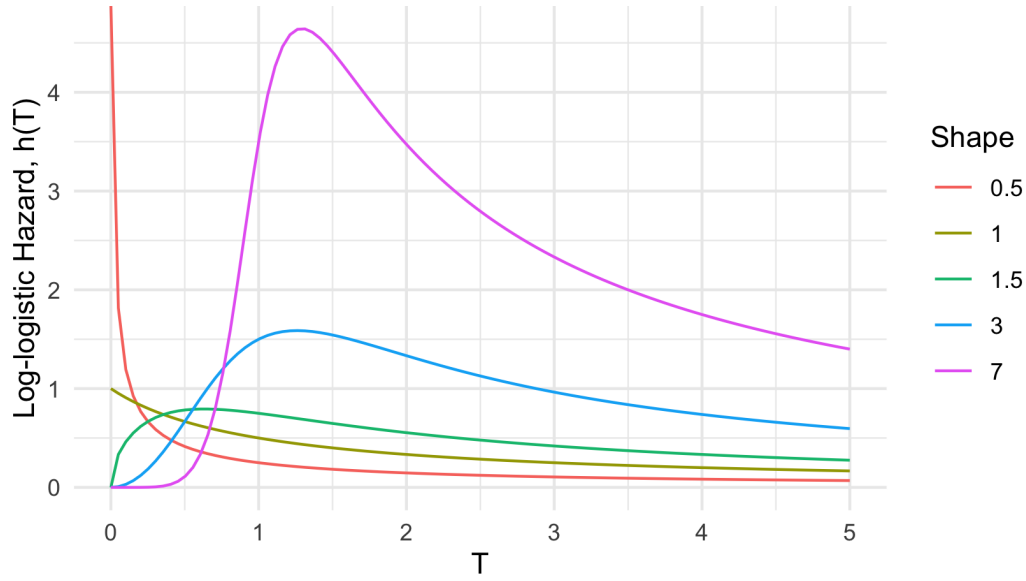


Figure 10.4: Log-logistic hazard curves with a fixed scale parameter of 1 and a changing shape parameter. x-axis is time and y-axis is the log-logistic hazard as a function of time.

Giving the ExpAFT likelihood (Section 3.5.1):

$$\begin{aligned}\mathcal{L}(\boldsymbol{\theta}) &= \prod_{i=1}^n h_Y(t_i|\boldsymbol{\theta})^{\delta_i} S_Y(t_i|\boldsymbol{\theta}) \\ &= \prod_{i=1}^n (\lambda e^{-\eta_i})^{\delta_i} \left(\exp(-\lambda t_i e^{-\eta_i}) \right) \\ &= \prod_{i=1}^n \lambda^{\delta_i} \exp(-\lambda t_i e^{-\eta_i} - \delta_i \eta_i)\end{aligned}$$

with log-likelihood

$$\begin{aligned}\hat{\mathcal{L}}(\boldsymbol{\theta}) &= \sum_{i=1}^n \log(\lambda^{\delta_i} \exp(-\lambda t_i e^{-\eta_i} - \delta_i \eta_i)) \\ &= \sum_{i=1}^n \delta_i \log(\lambda) - \lambda t_i e^{-\eta_i} - \delta_i \eta_i\end{aligned}$$

Likelihoods can also be derived using the log-linear form in (10.29) however these are beyond the scope of this book. As before, extensions to other censoring types and truncation follows by specifying the correct likelihood form from Section 3.5.1.

10.4 Proportional Odds

Proportional odds models (Bennett 1983) are the final of the three major linear model classes in survival analysis. In contrast to the PH and AFT models just discussed, proportional models are rarely, if ever, used on their own to make inferences about underlying data or as predictive models. Instead they are more commonly found as components within neural networks (Chapter 14) or in flexible parametric models (discussed next). Therefore this section very briefly describes the motivation for the model and its key properties.

As the name may suggest, the proportional odds model is analogous to the proportional hazards model except with the goal of modelling odds instead of hazards. For a given time τ , the odds of an event happening at **at** τ are

$$O(\tau) = \frac{p(\tau)}{1 - p(\tau)}$$

Where $p(\tau)$ is the probability of the event happening at τ . Of course as has been seen throughout this book the general interest is centered around the survival probability and therefore a more relevant quantity is the odds of the event not happening **before** τ :

$$O(\tau) = \frac{S(\tau)}{1 - S(\tau)} = \frac{S(\tau)}{F(\tau)}$$

By considering the same functional form as in the proportional hazards model, the proportional odds model follows analogously, substituting odds in place of the hazards:

$$O_{PO}(\tau|\mathbf{x}_i) = O_0(\tau) \exp(\eta_i)$$

where O_0 is the baseline odds.

By the same logic as the proportional hazards model, this model assumes $O(\tau|\mathbf{x}_i) \propto \exp(\eta_i)$ and that a unit increase in a covariate multiplies the odds of surviving past t by $\exp(\eta_i)$. A useful implication is the convergence of hazard functions, which states $h_i(\tau)/h_0(\tau) \rightarrow 1$ as $\tau \rightarrow \infty$ (Kirmani and Gupta 2001). To see this note that the PO model can be represented in terms of the hazard function via (Collett 2014)

$$h_{PO}(\tau|\mathbf{x}_i) = h_0(\tau) \left(1 - \frac{S_0(\tau)}{(\exp(\eta_i) - 1)^{-1} + S_0(\tau)} \right) \quad (10.30)$$

Dividing by the baseline hazard yields

$$\frac{h_{PO}(\tau|\mathbf{x}_i)}{h_0(\tau)} = \left(1 - \frac{S_0(\tau)}{(\exp(\eta_i) - 1)^{-1} + S_0(\tau)} \right) = \frac{(\exp(\eta_i) - 1)^{-1}}{(\exp(\eta_i) - 1)^{-1} + S_0(\tau)}$$

Simplifying gives $(1 + S_0(\tau)(\exp(\eta_i) - 1))^{-1}$. As $S_0(\tau) \rightarrow 0$ when $\tau \rightarrow \infty$, it follows that the hazard ratio tends to 1 as τ increases.

This means that for any individual, their individual hazard approaches the baseline hazard over a long period of time. This assumption holds in several contexts, commonly in medical domains in which death is the event of interest. For example, take two patients with a disease, patient i receives treatment and patient j does not. Let $\exp(\eta_i) = 4$, $\exp(\eta_j) = 1$, $S_0(0) = 1$, and $S_0(5) = 0.01$. Following (10.30), we have for patient i

$$h_{PO}(0|\mathbf{x}_i) = 0.25h_0(0); \quad h_{PO}(\tau|\mathbf{x}_i) = 0.97h_0(5)$$

and for patient j

$$h_{PO}(0|\mathbf{x}_j) = h_0(0); \quad h_{PO}(5|\mathbf{x}_j) = h_0(5)$$

The treatment effect reduces the hazard for observation i at early time-points. However, at the later time-point, the hazard is very similar for both observations.

There is no simple closed form expression for the partial likelihood of a semi-parametric proportional odds model and hence in practice a Log-logistic distribution is usually assumed for the baseline odds and the model is fit by maximum likelihood estimation on the full likelihood (Bennett 1983), discussed further in the next section.

10.5 Flexible Parametric Models

Royston-Parmar flexible parametric models (Royston and Parmar 2002) extend PH and PO models by estimating the baseline hazard with natural cubic splines. The model was designed to keep the form of the PH or PO methods but without being forced to estimate a misleading baseline hazard (for semi-parametric models) or misspecifying the survival distribution (for fully-parametric models). This is achieved by fitting natural cubic splines in place of the baseline hazard.

The crux of the method is to use splines to model time on a log-scale and to either estimate the log cumulative Hazard for PH models, or the log Odds for PO models. For the flexible PH model, a Weibull distribution is the basis for the baseline distribution, whereas a Log-logistic distribution is assumed for the baseline odds in the flexible PO model. The exact derivation of the model requires a lot of mathematical exposition which is not included here, a very good summary of the model is given in Collett (2014). Instead, below is the model in its full form with an explanation of the variables and figures that demonstrate cubic splines.

The flexible parametric Royston-Parmar (RP) proportional hazards and proportional odds model are respectively defined by

$$\log H_{RP}(\tau|\mathbf{x}_i) = s(\tau|\boldsymbol{\gamma}, \mathbf{k}) + \eta_i \quad (10.31)$$

$$\log O_{RP}(\tau|\mathbf{x}_i) = s(\tau|\boldsymbol{\gamma}, \mathbf{k}) + \eta_i \quad (10.32)$$

where $\boldsymbol{\gamma}$ are spline coefficients to be estimated by maximum likelihood estimation, \mathbf{k} are the positions of K knots, and s is the restricted cubic spline function in log time defined by

$$s(\tau|\gamma, \mathbf{k}) = \gamma_0 + \gamma_1 \log(\tau) + \gamma_2 \nu_1(\log(\tau)) + \dots + \gamma_K \nu_K(\log(\tau))$$

ν_j is the basis function at knot k_j defined by

$$\nu_j(x) = (x - k_j)_+^3 - \lambda_j(x - k_{min})_+^3 - (1 - \lambda_j)(x - k_{max})_+^3$$

where

$$\lambda_j = \frac{k_{max} - k_j}{k_{max} - k_{min}}$$

and $(x - y)_+ = \max\{0, (x - y)\}$ for any x, y , and where k_{min} and k_{max} are the boundaries of the cubic spline, meaning the curve is linear when $\log(t) < k_{min}$ or $\log(t) > k_{max}$.

To see how the proportional hazards RP model relates to the Weibull distribution, first we integrate and take logs of the Weibull-PH hazard function from equation (10.11):

$$\log(H_{WeibullPH}(\tau|\mathbf{x}_i)) = \log((\lambda\tau^\gamma) \exp(\eta_i)) = \log(\lambda) + \gamma \log(\tau) + \eta_i$$

Setting $\gamma_0 = \log(\lambda)$ and $\gamma_1 = \gamma$ yields (10.31) when there are no knots. Analogous results can be shown between (10.32) and the Log-logistic distribution.

To fit the model, the number and position of knots are theoretically tunable, although Royston and Parmar advised against tuning and suggest often only one internal knot is required and the placement of the knot does not make a significant difference to performance (Royston and Parmar 2002). Increasing knots can increase model overfitting however Bower et al. (2019) showed up to seven knots does not significantly increase model bias. The model's primary advantage is it's flexibility to model non-linear effects and can also be extended to time-dependent covariates. Moreover, the model can be fit via maximum likelihood estimation and thus many standard off-shelf routines for estimating a smooth survival time function. Despite advantages, the model appears to be limited in common use which makes it difficult to verify the model's utility across different contexts (Ng et al. 2018).

In the same manner as other proportional hazards models, the Royston-Parmar model can be extended to competing risks by modelling cause-specific hazards, considering only one event at a time and censoring competing events (Hinchliffe and Lambert 2013).

10.6 Improving traditional models

A number of model-agnostic algorithms have been created to improve a model's predictive ability. When applied to traditional algorithms, these methods can be used to create powerful models that outperform other machine learning. As each could be the subject of a whole book, this section remains brief and just covers the general overview. These are split into methods for:

1. modelling non-linear data effects;
2. reducing the number of variables in a dataset; and
3. combining predictions from multiple models.

10.6.1 Non-linear effects

One of the major limitations of the models discussed so far is the assumption of a linear relationship between covariates and outcomes (on the scale of the predictor). At first one might view the Cox model as non-linear due to the presence of the exponential function. However, the linearity becomes clear when the model is equivalently expressed as:

$$\log \left(\frac{h(\tau | \mathbf{x}_i)}{h_0(\tau)} \right) = x_1\beta_1 + \dots x_p\beta_p$$

Consider modelling the time until disease progression with covariates age (continuous) and treatment (binary):

$$\log \left(\frac{h(\tau | \mathbf{x}_i)}{h_0(\tau)} \right) = x_{age_i}\beta_{age} + x_{trt_i}\beta_{trt}$$

In this form, increasing age from 1 to 21 or 81 to 101 has the same effect on the log hazard ratio; this is clearly not realistic. There are many approaches to relaxing linearity; these are discussed extensively elsewhere and not repeated here, we recommend (James et al. 2013) which covers non-linear modelling in detail.

In brief, PH and AFT can be extended to *generalised additive models* (GAM) in the ‘usual’ way. For example for the Cox model,

$$\log \left(\frac{h_i(\tau | \mathbf{x}_i)}{h_0(\tau)} \right) = f_1(x_1) + \dots + f_p(x_p)$$

where each f_j is a smooth, possibly non-linear function of its covariate. If all f_j are the identity function then this reduces to the standard Cox model. The functions f_j are often chosen to be natural splines, but step functions, polynomial bases, or any other transformation can also be used. The Royston-Parmar model (Section 10.5) is a special case of a GAM where splines are used to model the baseline hazard.

10.6.2 Dimension reduction and feature selection

In a predictive modelling problem, only a small subset of variables in datasets tend to be relevant for correctly predicting the outcome. Other variables are either redundant – they provide no more information than their counterparts – or irrelevant – they do not influence the outcome. In these cases, using all variables for modelling results in worse interpretability, increased computational complexity, and often inferior model performance as model’s tend to overfit the training data and generalise poorly to new data.

To improve model performance, one can therefore ‘help’ models by applying feature selection methods to reduce the number of variables in the dataset. Feature selection is often grouped into three categories: 1) filters; 2) wrappers; and 3) embedded methods. Wrappers fit multiple models on subsets of variables and select the best performing subsets, this is often computationally infeasible in the context of very large datasets, and as such have less relevance in survival analysis which often tackles very high-dimensional datasets such as genomic datasets and detailed time-series economic data. This section only looks at methods specific to survival analysis and does not consider general algorithms such as PCA, see further reading below for suggested additional material that covers these areas.

Embedded methods

Embedded methods refers to those that are incorporated during model fitting. The vast majority of machine learning models incorporate embedded methods and thus reduce a dataset's size as part of the training process. In contrast, models that do not apply any form of feature selection will perform poorly when there is a large number of variables in a dataset. One model that straddles the line of 'traditional' and 'machine learning' methodology is the elastic Cox model, which incorporates the 'lasso' and 'ridge' regularization methods. Given a generic learning algorithm, lasso and ridge regularization constrain the model coefficients subject to the $\|\cdot\|^\infty$ -norm and $\|\cdot\|^\epsilon$ -norm respectively. The Lasso-Cox (Tibshirani 1997) model fits the Cox model by estimating β as

$$\hat{\beta} = \arg \max \mathcal{L}(\beta); \text{ subject to } \sum |\beta_j| \leq \gamma$$

where \mathcal{L} is the likelihood defined in (1) and $\gamma > 0$ is a hyper-parameter.

In contrast, the Ridge-Cox model estimates β as

$$\hat{\beta} = \arg \max \mathcal{L}(\beta); \text{ subject to } \sum \beta_j^2 \leq \gamma$$

Ridge and lasso are both shrinkage methods, which are used to reduce model variance and overfitting, especially in the context of multi-collinearity. However, the $\|\cdot\|^1$ norm in Lasso regression can also shrink coefficients to zero and thus performs variable selection as well. It is therefore possible to incorporate a feature selection method first and then pass the results to a Ridge-Cox model – though experiments have shown Ridge-Cox on its own is already a powerful tool (Spooner et al. 2020). Alternatively, as with many machine learning algorithms, deciding between lasso and ridge can be performed in empirical benchmark experiments by using elastic net (N. Simon et al. 2011; Zou and Hastie 2005), which is a convex combination of $\|\cdot\|^1$ and $\|\cdot\|^2$ penalties such that β is estimated as

$$\hat{\beta} = \arg \max \mathcal{L}(\beta); \text{ subject to } \alpha \sum |\beta_j| + (1 - \alpha) \sum \beta_j^2 \leq \gamma$$

where α is a hyper-parameter to be tuned.

Filter methods

Filter methods are a two-step process that score features according to some metric and then select either a given number of top-performing features (i.e., have the best score) or those where the score exceeds some threshold. Once again determining the number of features to select, or the threshold to exceed, can be performed via hyperparameter optimisation. Bommert et al. (2021) compared 14 filter methods for high-dimensional survival data by extending existing methods, making use of tools seen throughout this book including non-parametric estimators, martingale residuals, and inverse probability of censoring weighting. However, the authors found that the method that outperformed all others was a simple variance filter:

$$V(\mathbf{x}_{\cdot j}) = \text{Var}(\mathbf{x}_{\cdot j})$$

where $\mathbf{x}_{\cdot j}$ is the j th variable in the data and V is the resulting score. The filter measures the amount of variance in the feature and removes features that have little variation.

Another common filter method is to train another model and make use of its embedded feature selection and pass these results to a simpler model. This allows a traditional model to be trained on relevant features without loss to interpretability or performance. Common choices for models to use in the first step of the pipeline include random forests (Chapter 11) and gradient boosting machines (Chapter 13).

10.6.3 Ensemble methods

Ensemble methods fit multiple models and combine the result into a single prediction. Common ensemble methods include boosting, bagging, and stacking. These are briefly explained below and can be applied to any model, whether machine learning or a simple linear model. Note that nested cross-validation should be used when fitting any of the models below in order to ensure no data is ‘leaked’ between training and predictions (Section 2.5).

Bagging and averaging

The simplest ensemble method is to fit multiple models on the same data and make predictions by taking an average over the individual model predictions. The average over predictions could be uniform, weighted with weights selected through expert knowledge, or weighted with weights optimised as hyper-parameters. Ensemble methods perform best when there is high variance between models as each then captures unique information about the underlying data. Therefore ensemble averaging is more common after first subsetting the training data and training each model on a different subset.

Whilst increasing variance is beneficial, too much variance may result in worse predictions. Hence, bagging (Bootstrap AGGregatING) is a common approach to increase variance without losing predictive accuracy. Bootstrapping is the process of sampling data with replacement, meaning the rows may be duplicated in each subset – this is discussed further in Chapter 11. After sampling the process is the same with predictions made and averaged.

Model-based boosting

Model-based boosting fits a sequence of models that iteratively improve model performance by correcting the previous model’s mistakes. The initial model is trained as usual on a testing dataset, and subsequent models are fit on the same features but using ‘pseudo-residuals’ as targets (a regression problem). These pseudo-residuals are the negative gradient of a chosen loss from the previous iteration – this is discussed in detail in Chapter 13. The result is a gradual increase in improvement as each model captures patterns missed previously. In a survival analysis context, many of the losses discussed in Part II can be used in this pipeline, with the choice of loss dependent on the task of interest. Model-based boosting is a generic pipeline which may underperform the purpose-built algorithms discussed in Chapter 13.

Stacking

Stacking can improve model performance by fitting multiple models and aggregating the predictions using a meta-model. Fitting a meta-model, often a simple linear model, results in fitted coefficients that weight the input models according to how close or far they were from the truth.

Training data is partitioned (once or several times) and the first partition is used to train several independent models, a meta-model is fit using the outputs (predictions) from the base models as features and the targets (t_i, δ_i) from the second partition as targets.

As an example, take stacking three Cox models with a Cox meta-model. Let $\mathcal{D} = \{(\mathbf{x}_i, t_i, \delta_i)\}$

be a dataset. Partition \mathcal{D} into two disjoint datasets \mathcal{D}_1 of size n and \mathcal{D}_2 of size m . Three Cox base models are fit on \mathcal{D}_1 and linear predictors are obtained (predicted) for all m observations in \mathcal{D}_2 :

$$Z = \begin{bmatrix} \hat{\eta}_1^{(1)} & \dots & \hat{\eta}_1^{(3)} \\ \vdots & \ddots & \vdots \\ \hat{\eta}_m^{(1)} & \dots & \hat{\eta}_m^{(3)} \end{bmatrix}$$

where $\hat{\eta}_i^{(j)}$ is the linear predictor for the i th observation in the validation set from the j th base model.

Fit the meta-Cox model on $(Z, (t_i, \delta_i)_{i \in \mathcal{D}_2})$:

$$h_M(\tau | \hat{\eta}_i) = h_0^{(M)}(\tau) \exp(\beta_1^{(M)} \hat{\eta}_i^{(1)} + \beta_2^{(M)} \hat{\eta}_i^{(2)} + \beta_3^{(M)} \hat{\eta}_i^{(3)}), \quad i \in \mathcal{D}_2$$

Finally, the base learners are refit on all \mathcal{D} but keeping $\hat{\beta}^{(M)}$ and $\hat{h}_0^{(M)}$ from the meta-model fixed.

Predictions for a new observation, \mathbf{x}^* are made by first predicting $(\hat{\eta}_*^{(1)}, \hat{\eta}_*^{(2)}, \hat{\eta}_*^{(3)})$ from the trained base models and passing those to h_M using the fitted $\hat{\beta}^{(M)}$ coefficients and $\hat{h}_0^{(M)}$.

In the above example, Cox models are used throughout. However, any machine learning models with the same prediction types can be stacked, including combinations of models.

10.7 Conclusion

Key takeaways

- Traditional statistical models broadly fall into three categories: non-parametric estimators, semi-parametric models that include a baseline estimate, and fully-parametric estimates. Each has its own advantages and disadvantages.
- Non-parametric estimators are used throughout survival analysis, often as components in more complex machine learning models.
- Proportional hazards and accelerated failure time models encode different assumptions but both are powerful tools for learning patterns from data and even in prediction problems.
- The boundary between machine learning and statistical models is fuzzy, and simpler survival models can outperform more complex machine learning alternatives.

Limitations

- Several models can be extended to time-dependent covariates however these are not well-developed for predictive problems.
- Simpler (linear) models encode assumptions that are rarely met in practice, for example the proportional hazards assumption. However, even if assumptions are violated, these could still generalise well to new data and are therefore worth including

in benchmark experiments.

- Unregularized models perform badly on high-dimensional data without some form of pre-processing, however this is relatively simple with modern off-shelf software such as **sklearn** and **mlr3**.

Further reading

- To learn more about hazard ratios from Cox models and complexities in interpretation, we recommend Sasheyi and Ferry (2017) and Spruance et al. (2004).
- Collett (2014) and John D. Kalbfleisch and Prentice (1980) both provide comprehensive reading for traditional statistical models. The former is slightly less technical and covers extensions to multiple settings.
- For more abstract feature selection algorithms that can be applied to any data (survival or otherwise), see Chandrashekhar and Sahin (2014) and Guyon and Elisseeff (2003).
- Kernel-based approaches have been suggested for smooth non-parametric estimates of the baseline hazard, these do not appear commonly used in practice but details can be found in Gefeller and Dette (1992) and Müller and Wang (1994).

11

Random Forests

TODO (150-200 WORDS)

 Minor changes expected!

This page is a work in progress and minor changes will be made over time.

Random forests are a composite (or ensemble) algorithm built by fitting many simpler component models, *decision trees*, and then averaging the results of predictions from these trees. Due to in-built variable importance properties, random forests are commonly used in high-dimensional settings when the number of variables in a dataset far exceeds the number of rows. High-dimensional datasets are very common in survival analysis, especially when considering omics, genetic and financial data. It is therefore no surprise that *random survival forests*, remain a popular and well-performing model in the survival setting.

11.1 Random Forests for Regression

Training of decision trees can include a large number of hyper-parameters and different training steps including ‘growing’ and subsequently ‘pruning’. However, when utilised in random forests, many of these parameters and steps can be safely ignored, hence this section only focuses on the components that primarily influence the resulting random forest. This section will start by discussing decision trees and will then introduce the *bagging* algorithm used to create random forests.

11.1.1 Decision Trees

Decision trees are a (relatively) simple machine learning model that are comparatively easy to implement in software and are highly interpretable. The decision tree algorithm takes an input, a dataset, selects a variable that is used to partition the data according to some *splitting rule* into distinct non-overlapping datasets or *nodes* or *leaves*, and repeats this step for the resulting partitions, or *branches*, until some criterion has been reached. The final nodes are referred to as *terminal nodes*.

By example, (Figure 11.1) demonstrates a decision tree predicting the price that a car sells for in India (price in thousands of dollars). The dataset includes as variables the registration year, kilometers driven, fuel type (petrol or automatic), seller type (individual or dealer), transmission type (manual or automatic), and number of owners. The decision tree was

trained with a maximum depth of 2 (the number of rows excluding the top), and it can be seen that with this restriction only the transmission type, registration year, and fuel type were selected variables. During training, the algorithm identified that the first optimal variable to split the data was transmission type, partitioning the data into manual and automatic cars. Manual cars are further subset by registration year whereas automatic cars are split by fuel type. It can also be seen how the average sale price (top value in each leaf) diverges between leaves as the tree splits – the average sale prices in the final leaves are the terminal node predictions.

The graphic highlights several core features of decision trees:

1. They can model non-linear and interaction effects: The hierarchical structure allows for complex interactions between variables with some variables being used to separate all observations (transmission) and others only applied to subsets (year and fuel);
2. They are highly interpretable: it is easy to visualise the tree and see how predictions are made;
3. They perform variable selection: not all variables were used to train the model.

To understand how random forests work, it is worth looking a bit more into the most important components of decision trees: splitting rules, stopping rules, and terminal node predictions.

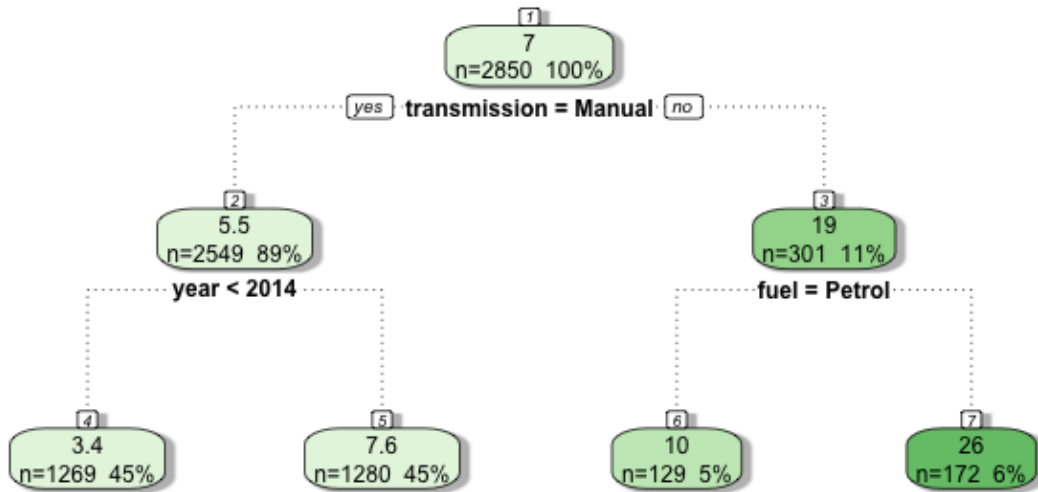


Figure 11.1: Predicting the price a vehicle is sold for in India using a regression tree, dataset from kaggle.com/datasets/nehalbirla/vehicle-dataset-from-cardekho. Rounded rectangles are leaves, which indicate the variable that is being split. Edges are branches, which indicate the cut-off at which the variable is split. Variables are car transmission type (manual or automatic), fuel type (petrol or diesel) and registration year. The number at the top of each leaf is the average selling price in thousands of dollars for all observations in that leaf. The numbers at the bottom of each leaf are the number of observations in the leaf, and the proportion of data contained in the leaf.

Splitting and Stopping Rules

Precisely how the data partitions/splits are derived and which variables are utilised is determined by the *splitting rule*. The goal in each partition is to find two resulting leaves/nodes that have the greatest difference between them and thus the maximal homogeneity within each leaf, hence with each split, the data in each node should become increasingly similar. The splitting rule provides a way to measure the homogeneity within the resulting nodes. In regression, the most common splitting rule is to select a variable and cut-off (a threshold on the variable at which to separate observations) that minimises the mean squared error in the two potential resulting leaves.

For all decision tree and random forest algorithms going forward, let L denote some leaf, then let L_{xy}, L_x, L_y respectively be the set of observations, features, and outcomes in leaf L . Let $L_{y;i}$ be the i th outcome in L_y and finally let $\bar{y}_L = \frac{1}{|L_y|} \sum_{i=1}^{|L_y|} L_{y;i}$ be the mean outcome in leaf L .

Let $j = 1, \dots, p$ be the index of features and let c_j be a possible cutoff value for feature $\mathbf{x}_{\cdot j}$. Define

$$\begin{aligned} L_{xy}^a(j, c_j) &:= \{(\mathbf{x}_i, y_i) | x_{i,j} < c_j, i = 1, \dots, n\} \\ L_{xy}^b(j, c_j) &:= \{(\mathbf{x}_i, y_i) | x_{i,j} \geq c_j, i = 1, \dots, n\} \end{aligned}$$

as the two leaves containing the set of observations resulting from partitioning variable j at cutoff c_j . To simplify equations let L^a, L^b be shorthands for $L^a(j, c_j)$ and $L^b(j, c_j)$. Then a split is determined by finding the arguments, $(j^*, c_{j^*}^*)$ that minimise the residual sum of squares across both leaves (James et al. 2013),

$$(j^*, c_{j^*}^*) = \arg \min_{j, c_j} \sum_{y \in L_y^a} (y - \bar{y}_{L^a})^2 + \sum_{y \in L_y^b} (y - \bar{y}_{L^b})^2 \quad (11.1)$$

This method is repeated from the first leaf to the last such that observations are included in a given leaf L if they satisfy all conditions from all previous branches (splits); features may be considered multiple times in the growing process allowing complex interaction effects to be captured.

Leaves are repeatedly split until a *stopping rule* has been triggered – a criterion that tells the algorithm to stop partitioning data. The stopping rule is usually a condition on the number of observations in each leaf such that leaves will continue to be split until some minimum number of observations has been reached in a leaf. Other conditions may be on the depth of the tree (as in Figure 11.1 which is restricted to a maximum depth of 2), which corresponds to the number of levels of splitting. Stopping rules are often used together, for example by setting a maximum tree depth *and* determining a minimum number of observations per leaf. Deciding the number of minimum observations and/or the maximum depth can be performed with automated hyper-parameter optimisation.

Terminal Node Predictions

The final major component of decision trees are *terminal node predictions*. As the name suggests, this is the part of the algorithm that determines how to actually make a prediction for a new observation. A prediction is made by ‘dropping’ the new data ‘down’ the tree according to the optimal splits that were found during training. The resulting prediction is then a simple baseline statistic computed from the training data that fell into the corresponding node. In regression, this is commonly the sample mean of the training outcome data.

Returning to Figure 11.1, say a new data point is {transmission = Manual, fuel = Diesel, year = 2015}, then in the first split the left branch is taken as ‘transmission = Manual’, in the second split the right branch is taken as ‘year’ = 2015 ≥ 2014, hence the new data point lands in the second terminal leaf and is predicted to sell for \$7,600. The ‘fuel’ variable is ignored as it is only considered for automatic vehicles. As the final predictions are simple statistics based on training data, all potential predictions can be saved in the original trained model and no complex computations are required in the prediction algorithm.

11.1.2 Random Forests

Decision trees often overfit the training data, hence they have high variance, perform poorly on new data, and are not robust to even small changes in the original training data. Moreover, important variables can end up being ignored as only subsets of dominant variables are selected for splitting.

To counter these problems, *random forests* are designed to improve prediction accuracy and decrease variance. Random forests utilise bootstrap aggregation, or *bagging* (Leo Breiman 1996), to aggregate many decision trees. Bagging is a relatively simple algorithm, as follows:

1. **For** $b = 1, \dots, B$:
2. $D_b \leftarrow$ Randomly sample with replacement \mathcal{D}_{train}
3. $\hat{g}_b \leftarrow$ Train a decision tree on D_b
4. **end For**
5. **return** $\{\hat{g}_b\}_{b=1}^B$

Step 2 is known as *bootstrapping*, which is the process of sampling a dataset *with* replacement – which is in contrast to more standard subsampling where data is sampled *without* replacement. Commonly, the bootstrapped sample size is the same as the original. However, as the same value may be sampled multiple times, on average the resulting data only contains around 63.2% unique observations (Efron and Tibshirani 1997). Randomness is further injected to decorrelate the trees by randomly subsetting the candidates of features to consider at each split of a tree. Therefore, every split of every tree may consider a different subset of variables. This process is repeated for B trees, with the final output being a collection of trained decision trees.

Prediction from a random forest for new data \mathbf{x}^* follows by making predictions from the individual trees and aggregating the results by some function σ , which is usually the sample mean for regression:

$$\hat{g}(\mathbf{x}^*) = \sigma(\hat{g}_1(\mathbf{x}^*), \dots, \hat{g}_B(\mathbf{x}^*)) = \frac{1}{B} \sum_{b=1}^B \hat{g}_b(\mathbf{x}^*)$$

where $\hat{g}_b(\mathbf{x}^*)$ is the prediction from the b th tree for some new data \mathbf{x}^* and B are the total number of grown trees.

As discussed above, individual decision trees result in predictions with high variance that are not robust to small changes in the underlying data. Random forests decrease this variance by aggregating predictions over a large sample of decorrelated trees, where a high degree of difference between trees is promoted through the use of bootstrapped samples and random candidate feature selection at each split.

Usually many (hundreds or thousands) trees are grown, which makes random forests robust to changes in data and ‘confident’ about individual predictions. Other advantages include having tunable and meaningful hyper-parameters, including: the number of variables to consider for a single tree, the splitting rule, and the stopping rule. Random forests treat trees as *weak learners*, which are not intended to be individually optimized. Instead, each tree captures a small amount of information about the data, which are combined to form a powerful representation of the dataset.

Whilst random forests are considered a ‘black-box’, in that one cannot be reasonably expected to inspect thousands of individual trees, variable importance can still be aggregated across trees, for example by counting the frequency a variable was selected across trees, calculating the minimal depth at which a variable was used for splitting, or via permutation based feature importance. Hence the model remains more interpretable than many alternative methods. Finally, random forests are less prone to overfitting and this can be relatively easily controlled by using *early-stopping* methods, for example by continually growing trees until the performance of the model stops improving.

11.2 Random Survival Forests

Unlike other machine learning methods that may require complex changes to underlying algorithms, random forests can be relatively simply adapted to *random survival forests* by updating the splitting rules and terminal node predictions to those that can handle censoring and can make survival predictions. This chapter is therefore focused on outlining different choices of splitting rules and terminal node predictions, which can then be flexibly combined into different models.

11.2.1 Splitting Rules

Survival trees and RSFs have been studied for the past four decades and whilst there are many possible splitting rules (Bou-Hamad, Larocque, and Ben-Ameur 2011), only two broad classes are commonly utilised (as judged by number of available implementations, e.g., Pölsterl (2020); Wright and Ziegler (2017); H. Ishwaran et al. (2011)). The first class rely on hypothesis tests, and primarily the log-rank test, to maximise dissimilarity between splits, the second class utilises likelihood-based measures. The first is discussed in more detail as this is common in practice and is relatively straightforward to implement and understand, moreover it has been demonstrated to outperform other splitting rules (Bou-Hamad, Larocque, and Ben-Ameur 2011). Likelihood rules are more complex and require assumptions that may not be realistic, these are discussed briefly.

Hypothesis Tests

The log-rank test statistic has been widely utilized as a splitting-rule for survival analysis (Ciampi et al. 1986; B. H. Ishwaran et al. 2008; LeBlanc and Crowley 1993; Segal 1988). The log-rank test compares the survival distributions of two groups under the null-hypothesis that both groups have the same underlying risk of (immediate) events, with the hazard function used to compare underlying risk.

Let L^a and L^b be two leaves and let h^a, h^b be the (theoretical, true) hazard functions in the two leaves respectively and let $i \in L$ be a shorthand for the indices of the observations in

leaf L so that $i = 1, \dots, |L|$. Define:

- n_τ^a , the number of observations at risk at τ in leaf a

$$n_\tau^a = \sum_{i \in L^a} \mathbb{I}(t_i \geq \tau)$$

- o_τ^a , the observed number of events in leaf a at τ

$$o_\tau^a = \sum_{i \in L^a} \mathbb{I}(t_i = \tau, \delta_i = 1)$$

- $n_\tau = n_\tau^a + n_\tau^b$, the number of observations at risk at τ in both leaves
- $o_\tau = o_\tau^a + o_\tau^b$, the observed number of events at τ in both leaves

Recall $t_{(k)}$ is the k th ordered event time. Then, the log-rank hypothesis test is given by $H_0 : h^a = h^b$ with test statistic (Segal 1988),

$$LR(L^a) = \frac{\sum_{k=1}^m (o_{t_{(k)}}^a - e_{t_{(k)}}^a)}{\sqrt{\sum_{k=1}^m v_{t_{(k)}}^a}}$$

where:

- e_τ^a is the expected number of events in leaf a at τ

$$e_\tau^a := \frac{n_\tau^a o_\tau}{n_\tau}$$

- v_τ^a is the variance of the number of events in leaf a at τ

$$v_\tau^a := e_\tau^a \left(\frac{n_\tau - o_\tau}{n_\tau} \right) \left(\frac{n_\tau - n_\tau^a}{n_\tau - 1} \right)$$

These results follow as under the assumption of equal hazards in both leaves, the number of events at each unique event time is distributed according to a Hypergeometric distribution. The same statistic results if L^b is instead considered.

The higher the log-rank statistic, the greater the dissimilarity between the two groups (Figure 11.2), thereby making it a sensible splitting rule for survival, moreover it has been shown that it works well for splitting censored data (LeBlanc and Crowley 1993). Additionally, the log-rank test requires no knowledge about the shape of the survival curves or distribution of the outcomes in either group (Bland and Altman 2004), making it ideal for an automated process that requires no user intervention.

The log-rank *score* rule (Hothorn and Lausen 2003) is a standardized version of the log-rank rule that could be considered as a splitting rule, though simulation studies have demonstrated non-significant improvements in predictive performance when comparing the two (B. H. Ishwaran et al. 2008). Alternative dissimilarity measures and tests have also been suggested as splitting rules, including modified Kolmogorov-Smirnov test and Gehan-Wilcoxon tests (Ciampi et al. 1988). Simulation studies have demonstrated that both of these may have higher power and produce ‘better’ results than the log-rank statistic (Fleming et al. 1980), however neither appears to be commonly used.

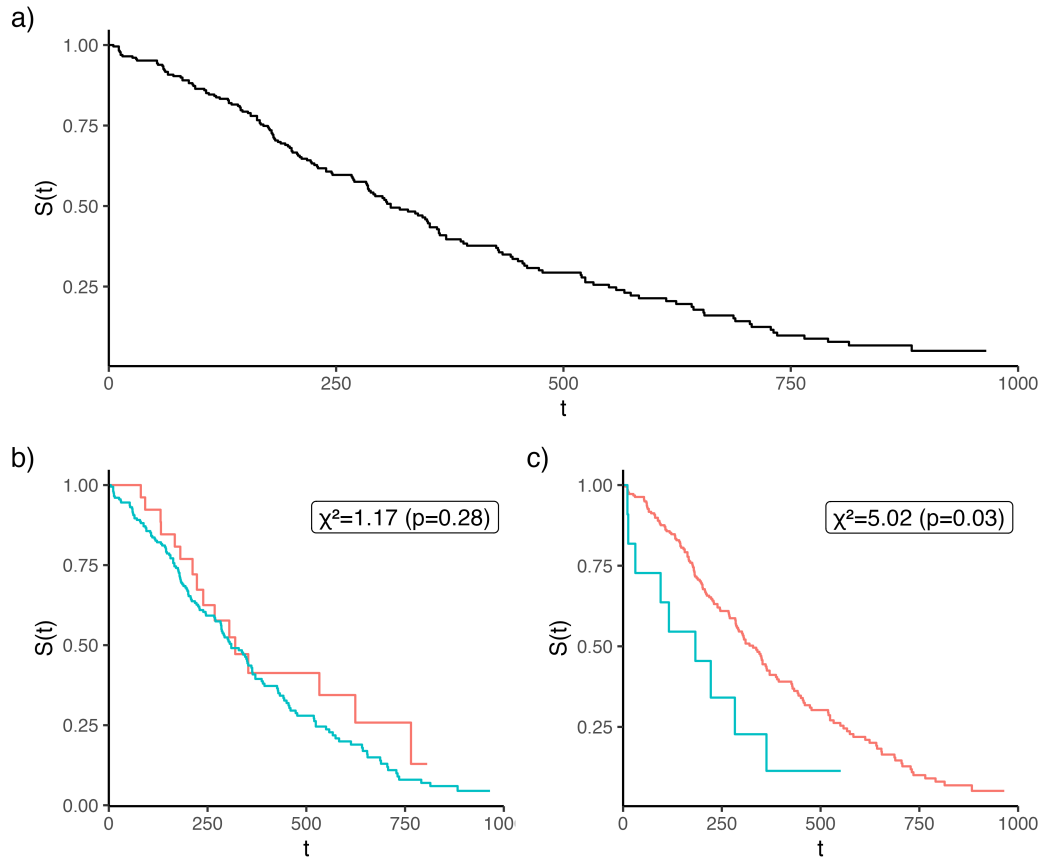


Figure 11.2: Panel (a) is the Kaplan-Meier estimator fit on the complete `lung` dataset from the R package **survival**. (b-c) is the same data stratified according to whether ‘age’ is greater or less than 50 (panel b) or 75 (panel c). The higher χ^2 statistic (panel c) results in a lower p -value and a greater difference between the stratified Kaplan-Meier curves. Hence splitting age at 75 results in a greater dissimilarity between the resulting branches and thus makes a better choice for splitting the variable.

In a competing risk setting, Gray's test (Gray 1988) can be used instead of the log-rank test, as it compares cumulative incidence functions rather than all-cause hazards. Similarly to the log-rank test, Gray's test also compares survival distributions using hypothesis tests to determine if there are significant differences between the groups, thus making it a suitable option to build competing risk RSFs.

Alternative Splitting Rules

A common alternative to the log-rank test is to instead use *likelihood ratio*, or *deviance*, statistics. When building RSFs, the likelihood-ratio statistic can be used to test if the model fit is improved or worsened with each split, thus providing a way to partition data. However, as discussed in Section 3.5.1, there are many different likelihoods that can be assumed for survival data, and there is no obvious way to determine if one is more sensible than another. Furthermore the choice of likelihood must fit the underlying model assumptions. For example, one could assume the data fits the proportional hazards assumption and in each split one could calculate the likelihood-ratio using the Cox PH partial likelihood. Alternatively, a parametric form could be assumed and a likelihood proposed by LeBlanc and Crowley (1992) may be calculated to test model fit. While potentially useful, these methods are implemented in very few off-shelf software packages, thus empirical comparisons to other splitting rules are lacking.

Other rules have also been studied including comparison of residuals (Therneau, Grambsch, and Fleming 1990), scoring rules (H. Ishwaran and Kogalur 2018), distance metrics (Gordon and Olshen 1985), and concordance metrics (Schmid, Wright, and Ziegler 2016). Experiments have shown different splitting rules may perform better or worse depending on the underlying data (Schmid, Wright, and Ziegler 2016), hence one could even consider treating the splitting rule as a hyper-parameter for tuning. However, if there is a clear goal in prediction, then the choice of splitting rule can be informed by the prediction type. For example, if the goal is to maximise separation, then a log-rank splitting rule to maximise homogeneity in terminal nodes is a natural starting point. Whereas if the goal is to accurately rank observations, then a concordance splitting rule may be optimal.

11.2.2 Terminal Node Prediction

As in the regression setting, the usual strategy for predictions is to create a simple estimate based on the training data that lands in the terminal nodes. However, as seen throughout this book, the choice of estimator in the survival setting depends on the prediction task of interest, which are now considered in turn. First, note that all terminal node predictions can only yield useful results if there are a sufficient number of uncensored observations in each terminal node. Hence, a common RSF stopping rule is the minimum number of *uncensored* observations per leaf, meaning a leaf is not split if that would result in too few uncensored observations in the resulting leaves.

Probabilistic Predictions

Starting with the most common survival prediction type, the algorithm requires a simple estimate for the underlying survival distribution in each of the terminal nodes, which can be estimated using the Kaplan-Meier or Nelson-Aalen methods (Hothorn et al. 2004; B. H. Ishwaran et al. 2008; LeBlanc and Crowley 1993; Segal 1988).

Denote b as a decision tree and $L^{b(h)}$ as the terminal node h in tree b . Then the predicted survival function and cumulative hazard for a new observation \mathbf{x}^* is,

$$\hat{S}_{b(h)}(\tau | \mathbf{x}^*) = \prod_{k:t_{(k)} \leq \tau} 1 - \frac{d_{t_{(k)}}}{n_{t_{(k)}}}, \quad \{k \in L^{b(h)} : \mathbf{x}^* \in L^{b(h)}\} \quad (11.2)$$

$$\hat{H}_{b(h)}(\tau | \mathbf{x}^*) = \sum_{k:t_{(k)} \leq \tau} \frac{d_{t_{(k)}}}{n_{t_{(k)}}}, \quad \{k \in L^{b(h)} : \mathbf{x}^* \in L^{b(h)}\} \quad (11.3)$$

where $d_{t_{(k)}}$ and $n_{t_{(k)}}$ are the observed number of events, and the number of observations at risk, respectively at the k th ordered event time. See Figure 11.3 for an example using the `lung` dataset (Therneau 2015).

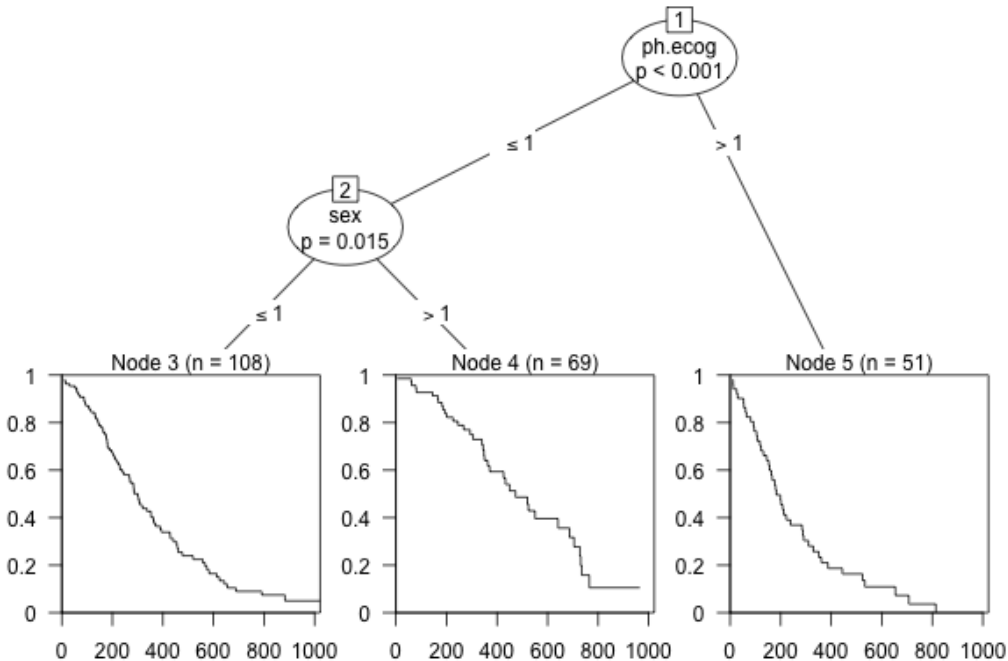


Figure 11.3: Survival tree trained on the `lung` dataset from the R package **survival**. The terminal node predictions are survival curves.

The bootstrapped prediction is the cumulative hazard function or survival function averaged over individual trees. Note that understanding what these bootstrapped functions represents depends on how they are calculated. By definition, a mixture of n distributions with cumulative distribution functions $F_i, i = 1, \dots, n$ is given by

$$F(x) = \sum_{i=1}^n w_i F_i(x)$$

Substituting $F = 1 - S$ and noting $\sum w_i = 1$ gives the computation $S(x) = \sum_{i=1}^n w_i S_i(x)$, allowing the bootstrapped survival function to exactly represent the mixture distribution averaged over all trees:

$$\hat{S}_{Boot}(\tau|\mathbf{x}^*) = \frac{1}{B} \sum_{b=1}^B w_i \hat{S}_b(\tau|\mathbf{x}^*) \quad (11.4)$$

usually with $w_i = 1/B$ where B is the number of trees.

In contrast, if one were to instead substitute $F = 1 - \exp(-H)$, then the mixture distribution depends on a logarithmic function that can only be approximately computed if predicted survival probabilities are close to one, which is an assumption that deteriorates over time. Therefore, to ensure the bootstrapped prediction accurately represents the underlying mixed probability distribution, the bootstrapped cumulative hazard function should be computed as:

$$\hat{H}_{Boot}(\tau|\mathbf{x}^*) = -\log(\hat{S}_{Boot}(\tau|\mathbf{x}^*)) \quad (11.5)$$

Another practical consideration to take into account is how to average the survival probabilities over the decision trees as each individual Kaplan-Meier estimate may have been trained on different time points. This is overcome by recognising that the Kaplan-Meier estimation results in a piece-wise function that can be linearly interpolated between training data. Figure 11.4 demonstrates this process for three decision trees (panel a), where the survival probability is calculated at all possible time points (panels b-c), and the average is computed with linear interpolation added between time-points (panel d).

Extensions to competing risks follow naturally using bootstrapped cause-specific cumulative incidence functions.

Deterministic Predictions

As discussed in Chapter 9, predicting and evaluating survival times is a complex and fairly under-researched area. For RSFs, there is an inclination to estimate survival times based on the mean or median survival times of observations in terminal nodes, however this would lead to biased estimations. Therefore, research has tended to focus on relative risk predictions.

As discussed, relative risks are arbitrary values where only the resulting rank matters when comparing observations. In RSFs, each terminal node should be as homogeneous as possible, hence within a terminal node, the risk between observations should be the same. The most common method to estimate average risk appears to be a transformation from the Nelson-Aalen method (B. H. Ishwaran et al. 2008), which exploits results from counting process to provide a measure of expected mortality (Hosmer Jr, Lemeshow, and May 2011) – the same result is used in the van Houwelingen calibration measure discussed in Section 7.1.2. Given new data, \mathbf{x}^* , falling into terminal node $b(h)$, the relative risk prediction is the sum of the predicted cumulative hazard, $\hat{H}_{b(h)}$, computed at each observation's observed outcome time:

$$\phi_{b(h)}(\mathbf{x}^*) = \sum_{i=1}^m \hat{H}_{b(h)}(t_i|\mathbf{x}^*)$$

where $\hat{H}_{b(h)}$ is the terminal node prediction as in 11.3. This is interpreted as the number of expected events in $b(h)$ and the assumption is that a terminal node with more expected events is a higher risk group than a node with less expected events. The bootstrapped risk prediction is the sample mean over all trees:

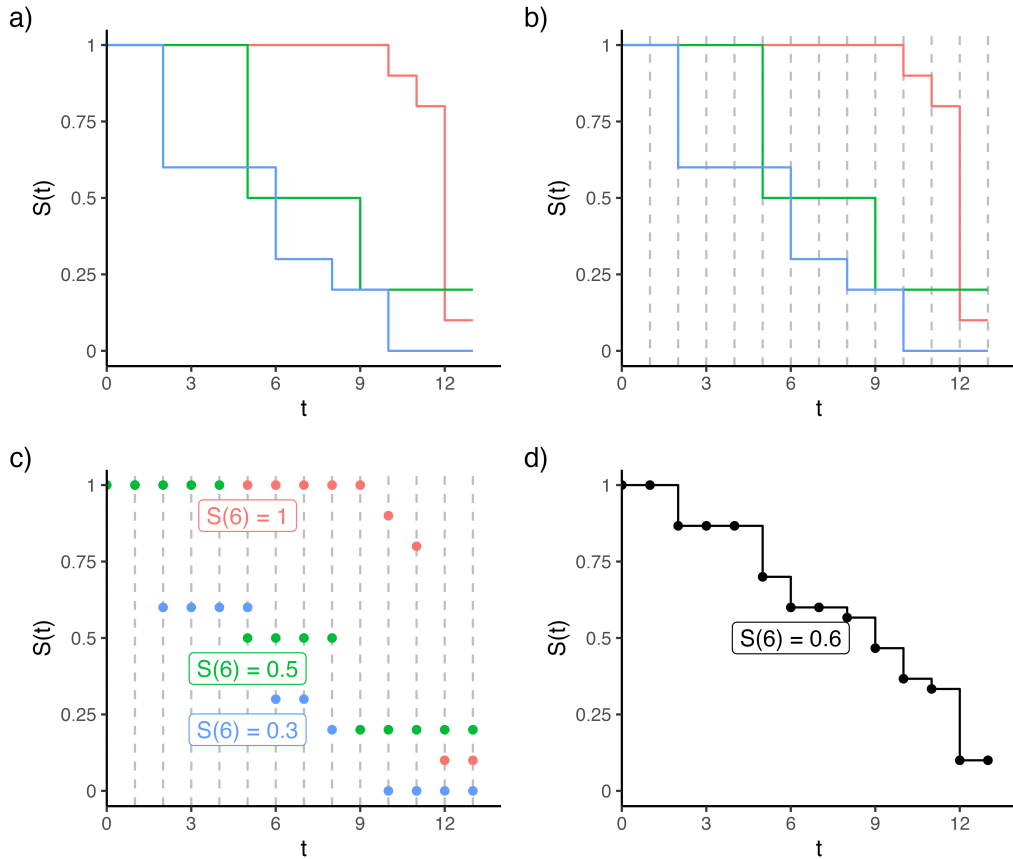


Figure 11.4: Bootstrapping Kaplan-Meier estimators across three decision trees (red, blue, green). Panel a) shows the individual estimates, b) shows the time points to aggregate the trees over, c) is the predicted survival probability from each tree at the desired time points, and d) is the average survival probabilities connected by a step function.

$$\phi_{Boot}(\mathbf{x}^*) = \frac{1}{B} \sum_{b=1}^B \phi_{b(h)}(\mathbf{x}^*)$$

More complex methods have also been proposed that are based on the likelihood-based splitting rule and assume a PH model form (H. Ishwaran et al. 2004; LeBlanc and Crowley 1992). However, these do not appear to be in wide-spread usage.

11.3 Conclusion

Key takeaways

- Random forests are a highly flexible algorithm that allow the various components to be adapted and altered without major changes to the underlying algorithm. This allows random survival forests (RSFs) to be readily available ‘off-shelf’ in many open-source packages;
- RSFs have in-built variable selection methods that mean they tend to perform well on high-dimensional data, routinely outperforming other models (**Burk2024?**);
- Despite having many potential hyper-parameters to tune, all are intuitive and many can even be ignored as sensible defaults exist in most off-shelf software implementations.

Limitations

- Due to the number of trees and the constant bootstrapping procedures, RSFs can be more computationally intensive than other models, though still much less intensive than neural networks and other deep learning methods.
- Despite having some in-built methods for model interpretation, RSFs are still black-boxes that can be difficult to fully interpret.
- With too few trees random forests can have similar limitations to decision trees and with too many random forests can overfit the data. Though most software has sensible defaults to prevent either scenario.

Further reading

- A comprehensive review of random survival forests (RSFs) is provided in Bou-Hamad (2011) (Bou-Hamad, Larocque, and Ben-Ameur 2011), which includes extensions to time-varying covariates and different censoring types.
- The discussion of decision trees omitted many methods for growing and pruning trees, if you are interest in those technical details see L. Breiman et al. (1984).
- RSFs have been shown to perform well in benchmark experiments on high-dimensional data, see Herrmann et al. (2021) and Spooner et al. (2020) for examples.
- This chapter considered the most ‘traditional’ forms of RSFs. Conditional inference forests are popular in the regression setting and whilst they are under-researched in survival, see Hothorn et al. (2005) for literature on the topic. A more recent method that seems to perform well is the (accelerated) oblique random survival

forest discussed in (**Jaeger2024?**).

12

Support Vector Machines

This chapter introduces support vector machines (SVMs) for regression and then describes the extensions to survival analysis. Regression SVMs extend simple linear methods by estimating flexible, non-linear hyperplanes that minimise the difference between predictions and the truth for individual observations. In survival analysis, SVMs may make survival time or ranking predictions, however there is no current formulation for survival distribution predictions. The chapter begins by discussing survival time SVMs and then ranking models before concluding with a hybrid formulation that combines both model forms. This primarily covers the work of Shivaswamy and Van Belle. SVMs are a powerful method for estimating non-linear relationships in data and have proven to be well-performing models in regression and classification. However, SVMs are less developed in survival analysis and have been shown to perform worse than other models in experiments.

 Minor changes expected!

This page is a work in progress and minor changes will be made over time.

Support vector machines are a popular class of models in regression and classification settings due to their ability to make accurate predictions for complex high-dimensional, non-linear data. Survival support vector machines (SSVMs) predict continuous responses that can be used as ranking predictions with some formulations that provide survival time interpretations. This chapter starts with SVMs in the regression setting before moving to adaptions for survival analysis.

12.1 SVMs for Regression

In simple linear regression, the aim is to estimate the line $y = \alpha + x\beta_1$ by estimating the α, β_1 coefficients. As the number of coefficients increases, the goal is to instead estimate the *hyperplane*, which divides the higher-dimensional space into two separate parts. To visualize a hyperplane, imagine looking at a room from a birds eye view that has a dividing wall cutting the room into two halves (Figure 12.1). In this view, the room appears to have two dimensions (x =left-right, y =top-bottom) and the divider is a simple line of the form $y = \alpha + x\beta_1$. In reality, this room is actually three dimensional and has a third dimension (z =up-down) and the divider is therefore a hyperplane of the form $y = \alpha + x\beta_1 + z\beta_2$.

Continuing the linear regression example, consider a simple model where the objective is to find the $\beta = (\beta_1 \ \beta_2 \cdots \beta_p)^\top$ coefficients that minimize $\sum_{i=1}^n (g(\mathbf{x}_i) - y_i)^2$ where



Figure 12.1: Visualising a hyperplane by viewing a 3D room in two-dimensions with a wall that is now seen as a simple line. When standing in this room, the wall will clearly exist in three dimensional space.

$g(\mathbf{x}_i) = \alpha + \mathbf{x}_i^\top \boldsymbol{\beta}$ and (\mathbf{X}, \mathbf{y}) is training data such that $\mathbf{X} \in \mathbb{R}^{n \times p}$ and $\mathbf{y} \in \mathbb{R}^n$. In a higher-dimensional space, a penalty term can be added for variable selection to reduce model complexity, commonly of the form

$$\frac{1}{2} \sum_{i=1}^n (g(\mathbf{x}_i) - y_i)^2 + \frac{\lambda}{2} \|\boldsymbol{\beta}\|^2$$

for some penalty term $\lambda \in \mathbb{R}$. Minimizing this error function effectively minimizes the *average* difference between all predictions and true outcomes, resulting in a hyperplane that represents the best *linear* relationship between coefficients and outcomes.

Similarly to linear regression, support vector machines (SVMs) (Cortes and Vapnik 1995) also fit a hyperplane, g , on given training data, \mathbf{X} . However, in SVMs, the goal is to fit a *flexible* (non-linear) hyperplane that minimizes the difference between predictions and the truth for *individual* observations. A core feature of SVMs is that one does not try to fit a hyperplane that makes perfect predictions as this would overfit the training data and is unlikely to perform well on unseen data. Instead, SVMs use a regularized error function, which allows incorrect predictions (errors) for some observations, with the magnitude of error controlled by an $\epsilon > 0$ parameter as well as slack parameters, $\xi' = (\xi'_1 \ \xi'_2 \cdots \xi'_n)^\top$ and $\xi^* = (\xi^*_1 \ \xi^*_2 \cdots \xi^*_n)^\top$:

$$\begin{aligned} \min_{\boldsymbol{\beta}, \alpha, \xi', \xi^*} \quad & \frac{1}{2} \|\boldsymbol{\beta}\|^2 + C \sum_{i=1}^n (\xi'_i + \xi^*_i) \\ \text{subject to} \quad & \begin{cases} g(\mathbf{x}_i) \geq y_i - \epsilon - \xi'_i \\ g(\mathbf{x}_i) \leq y_i + \epsilon + \xi^*_i \\ \xi'_i, \xi^*_i \geq 0 \end{cases} \end{aligned} \tag{12.1}$$

$\forall i \in 1, \dots, n$ where $g(\mathbf{x}_i) = \alpha + \mathbf{x}_i^\top \boldsymbol{\beta}$ for model weights $\boldsymbol{\beta} \in \mathbb{R}^p$ and $\alpha \in \mathbb{R}$ and the same training data (\mathbf{X}, \mathbf{y}) as above.

Figure 12.2 visualizes a support vector regression model in two dimensions. The red circles are values within the ϵ -tube and are thus considered to have a negligible error. In fact, the red circles do not affect the fitting of the optimal line g and even if they moved around, as long as they remain within the tube, the shape of g would not change. In contrast the blue diamonds have an unacceptable margin of error – as an example the top blue diamond will have $\xi'_i = 0$ but $\xi^*_i > 0$, thus influencing the estimation of g . Points on or outside the epsilon tube are referred to as *support vectors* as they affect the construction of the hyperplane. The $C \in \mathbb{R}_{>0}$ hyperparameter controls the slack parameters and thus as C increases, the number of errors (and subsequently support vectors) is allowed to increase resulting in low variance but higher bias, in contrast a lower C is more likely to introduce overfitting with low bias but high variance (Hastie, Tibshirani, and Friedman 2001). C should be tuned to control this trade-off.

The other core feature of SVMs is exploiting the *kernel trick*, which uses functions known as *kernels* to allow the model to learn a non-linear hyperplane whilst keeping the computations limited to lower-dimensional settings. Once the model coefficients have been estimated using the optimization above, predictions for a new observation \mathbf{x}^* can be made using a function of the form

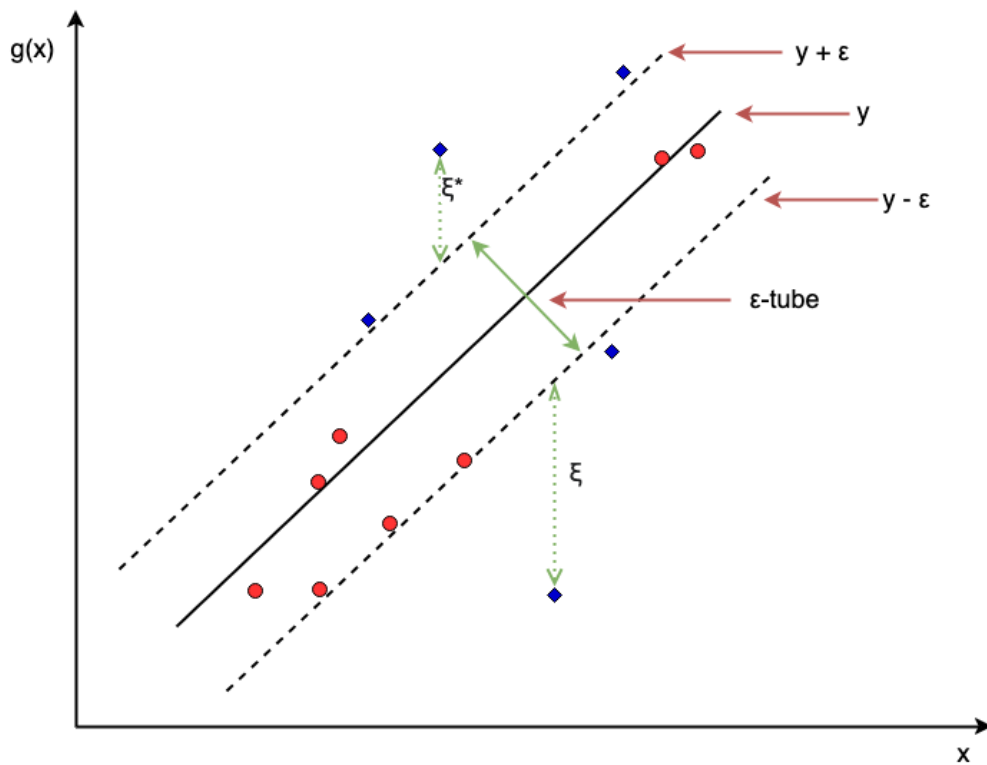


Figure 12.2: Visualising a support vector machine with an ε -tube and slack parameters ξ' and ξ^* . Red circles are values within the ε -tube and blue diamonds are support vectors on and outside the tube. x-axis is single covariate, x , and y-axis is $g(x) = x\beta_1 + \alpha$.

$$\hat{g}(\mathbf{x}^*) = \sum_{i=1}^n \mu_i K(\mathbf{x}^*, \mathbf{x}_i) + \alpha \quad (12.2)$$

Details (including estimation) of the μ_i Lagrange multipliers are beyond the scope of this book, references are given at the end of this chapter for the interested reader. K is a kernel function, with common functions including the linear kernel, $K(x^*, x_i) = \sum_{j=1}^p x_{ij}x_j^*$, radial kernel, $K(x^*, x_i) = \exp(-\omega \sum_{j=1}^p (x_{ij} - x_j^*)^2)$ for some $\omega \in \mathbb{R}_{>0}$, and polynomial kernel, $K(x^*, x_i) = (1 + \sum_{j=1}^p x_{ij}x_j^*)^d$ for some $d \in \mathbb{N}_{>0}$.

The choice of kernel and its parameters, the regularization parameter C , and the acceptable error ϵ , are all tunable hyper-parameters, which makes the support vector machine a highly adaptable and often well-performing machine learning method. The parameters C and ϵ often have no clear apriori meaning (especially true in the survival setting predicting abstract rankings) and thus require tuning over a great range of values; no tuning usually results in a poor model fit (Probst, Boulesteix, and Bischl 2019).

12.2 SVMs for Survival Analysis

Extending SVMs to the survival domain (SSVMs) is a case of: i) identifying the quantity to predict; and ii) updating the optimization problem (12.1) and prediction function (12.2) to accommodate for censoring. In the first case, SSVMs can be used to either make survival time or ranking predictions, which are discussed in turn. The notation above is reused below for SSVMs, with additional notation introduced when required and now using the survival training data $(\mathbf{X}, \mathbf{t}, \boldsymbol{\delta})$.

12.2.1 Survival time SSVMs

To begin, consider the objective for support vector regression with the y variable replaced with the usual survival time outcome t , for all $i \in 1, \dots, n$:

$$\begin{aligned} & \min_{\beta, \alpha, \xi', \xi^*} \frac{1}{2} \|\beta\|^2 + C \sum_{i=1}^n (\xi'_i + \xi^*_i) \\ & \text{subject to } \begin{cases} g(\mathbf{x}_i) \geq t_i - \epsilon - \xi'_i \\ g(\mathbf{x}_i) \leq t_i + \epsilon + \xi^*_i \\ \xi'_i, \xi^*_i \geq 0 \end{cases} \end{aligned} \quad (12.3)$$

In survival analysis, this translates to fitting a hyperplane in order to predict the true survival time. However, as with all adaptations from regression to survival analysis, there needs to be a method for incorporating censoring.

Recall the (t_l, t_u) notation to describe censoring as introduced in Chapter 3 such that the outcome occurs within the range (t_l, t_u) . Let $\tau \in \mathbb{R}_{>0}$ be some known time-point, then an observation is:

- left-censored if the survival time is less than τ : $(t_l, t_u) = (-\infty, \tau)$;
- right-censored if the true survival time is greater than τ : $(t_l, t_u) = (\tau, \infty)$; or

- uncensored if the true survival time is known to be τ : $(t_l, t_u) = (\tau, \tau)$.

Define $\mathcal{L} = \{i : t_i > -\infty\}$ as the set of observations with a finite lower-bounded time, which can be seen above to be those that are right-censored or uncensored. Define $\mathcal{U} = \{i : t_i < \infty\}$ as the analogous set of observations with a finite upper-bounded time, which are those that are left-censored or uncensored.

Consider these definitions in the context of the constraints in 12.3. The first constraint ensures the hyperplane is greater than some lower-bound created by subtracting the slack parameter from the true outcome – given the set definitions above this constraint only has meaning for observations with a finite lower-bound, $i \in \mathcal{L}$, otherwise the constraint would include $g(\mathbf{x}_i) \geq -\infty$, which is clearly not useful. Similarly the second constraint ensures the hyperplane is less than some upper-bound, which again can only be meaningful for observations $i \in \mathcal{U}$. Restricting the constraints in this way leads to the optimization problem (Shivaswamy, Chu, and Jansche 2007) below and visualised in Figure 12.3:

$$\begin{aligned} & \min_{\beta, \alpha, \xi', \xi^*} \frac{1}{2} \|\beta\|^2 + C \left(\sum_{i \in \mathcal{U}} \xi_i + \sum_{i \in \mathcal{L}} \xi_i^* \right) \\ \text{subject to } & \begin{cases} g(\mathbf{x}_i) & \geq t_i - \xi'_i, i \in \mathcal{L} \\ g(\mathbf{x}_i) & \leq t_i + \xi_i^*, i \in \mathcal{U} \\ \xi'_i \geq 0, \forall i \in \mathcal{L}; \xi_i^* \geq 0, \forall i \in \mathcal{U} \end{cases} \end{aligned}$$

If no observations are censored then the optimization becomes the regression optimization in (12.1). Note that in SSVMs, the ϵ parameters are typically removed to better accommodate censoring and to help prevent the same penalization of over- and under-predictions. In contrast to this formulation, one *could* introduce more ϵ and C parameters to separate between under- and over-predictions and to separate right- and left-censoring, however this leads to eight tunable hyperparameters, which is inefficient and may increase overfitting (Fouodo et al. 2018; Land et al. 2011). The algorithm can be simplified to right-censoring only by removing the second constraint completely for anyone censored:

$$\begin{aligned} & \min_{\beta, \alpha, \xi', \xi^*} \frac{1}{2} \|\beta\|^2 + C \sum_{i=1}^n (\xi'_i + \xi_i^*) \\ \text{subject to } & \begin{cases} g(\mathbf{x}_i) & \geq t_i - \xi_i^* \\ g(\mathbf{x}_i) & \leq t_i + \xi'_i, i : \delta_i = 1 \\ \xi'_i, \xi_i^* & \geq 0 \end{cases} \end{aligned}$$

$\forall i \in 1, \dots, n$. With the prediction for a new observation \mathbf{x}^* calculated as,

$$\hat{g}(\mathbf{x}^*) = \sum_{i=1}^n \mu_i^* K(\mathbf{x}_i, \mathbf{x}^*) - \delta_i \mu'_i K(\mathbf{x}_i, \mathbf{x}^*) + \alpha$$

Where again K is a kernel function and the calculation of the Lagrange multipliers is beyond the scope of this book.

12.2.2 Ranking SSVMs

Support vector machines can be used to estimate rankings by penalizing predictions that result in discordant predictions. Recall the definition of concordance from Chapter 6:

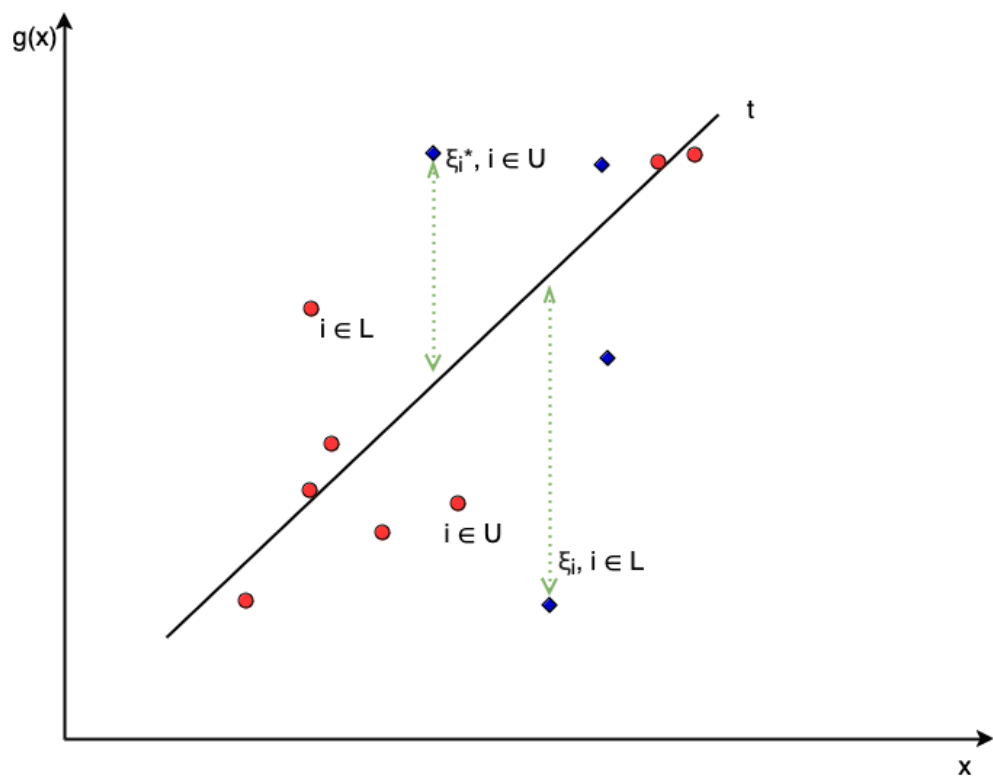


Figure 12.3: Visualising a survival time SVM. Blue diamonds are influential support vectors, which are uncensored or left-censored when $g(\mathbf{x}) < t$ or uncensored or right-censored when $g(\mathbf{x}) > t$. Red circles are non-influential observations.

ranking predictions for a pair of comparable observations (i, j) where $t_i < t_j \cap \delta_i = 1$, are called concordant if $r_i > r_j$ where r_i, r_j are the predicted ranks for observations i and j respectively and a higher value implies greater risk. Using the prognostic index as a ranking prediction (Section 5.5), a pair of observations is concordant if $g(\mathbf{x}_i) > g(\mathbf{x}_j)$ when $t_i < t_j$, leading to:

$$\begin{aligned} & \min_{\beta, \alpha, \xi} \frac{1}{2} \|\beta\|^2 + \gamma \sum_{i=1}^n \xi_i \\ & \text{subject to } \begin{cases} g(\mathbf{x}_i) - g(\mathbf{x}_j) \geq \xi_i, \forall i, j \in CP \\ \xi_i \geq 0, i = 1, \dots, n \end{cases} \end{aligned}$$

where CP is the set of comparable pairs defined by $CP = \{(i, j) : t_i < t_j \wedge \delta_i = 1\}$. Given the number of pairs, the optimization problem quickly becomes difficult to solve with a very long runtime. To solve this problem Van Belle et al. (2011) found an efficient reduction that sorts observations in order of outcome time and then compares each data point i with the observation that has the next smallest *survival* time, skipping over censored observations, in maths: $j(i) := \arg \max_{j \in 1, \dots, n} \{t_j : t_j < t_i\}$. This is visualized in Figure 12.4 where six observations are sorted by outcome time from smallest (left) to largest (right). Starting from right to left, the first pair is made by matching the observation to the first uncensored outcome to the left, this continues to the end. In order for all observations to be used in the optimisation, the algorithm sets the first outcome to be uncensored hence observation 2 being compared to observation 1.

Using this reduction, the algorithm becomes

$$\begin{aligned} & \min_{\beta, \alpha, \xi} \frac{1}{2} \|\beta\|^2 + \gamma \sum_{i=1}^n \xi_i \\ & \text{subject to } \begin{cases} g(\mathbf{x}_i) - g(\mathbf{x}_{j(i)}) \geq t_i - t_{j(i)} - \xi_i \\ \xi_i \geq 0 \end{cases} \end{aligned}$$

$\forall i = 1, \dots, n$. Note the updated right hand side of the constraint, which plays a similar role to the ϵ parameter by allowing ‘mistakes’ in predictions without penalty.

Predictions for a new observation \mathbf{x}^* are calculated as,

$$\hat{g}(\mathbf{x}^*) = \sum_{i=1}^n \mu_i (K(\mathbf{x}_i, \mathbf{x}^*) - K(\mathbf{x}_{j(i)}, \mathbf{x}^*)) + \alpha$$

Where μ_i are again Lagrange multipliers.

12.2.3 Hybrid SSVMs

Finally, Van Belle et al. (2011) noted that the ranking algorithm could be updated to add the constraints of the regression model, thus providing a model that simultaneously optimizes for ranking whilst providing continuous values that can be interpreted as survival time predictions. This results in the hybrid SSVM with constraints $\forall i = 1, \dots, n$:

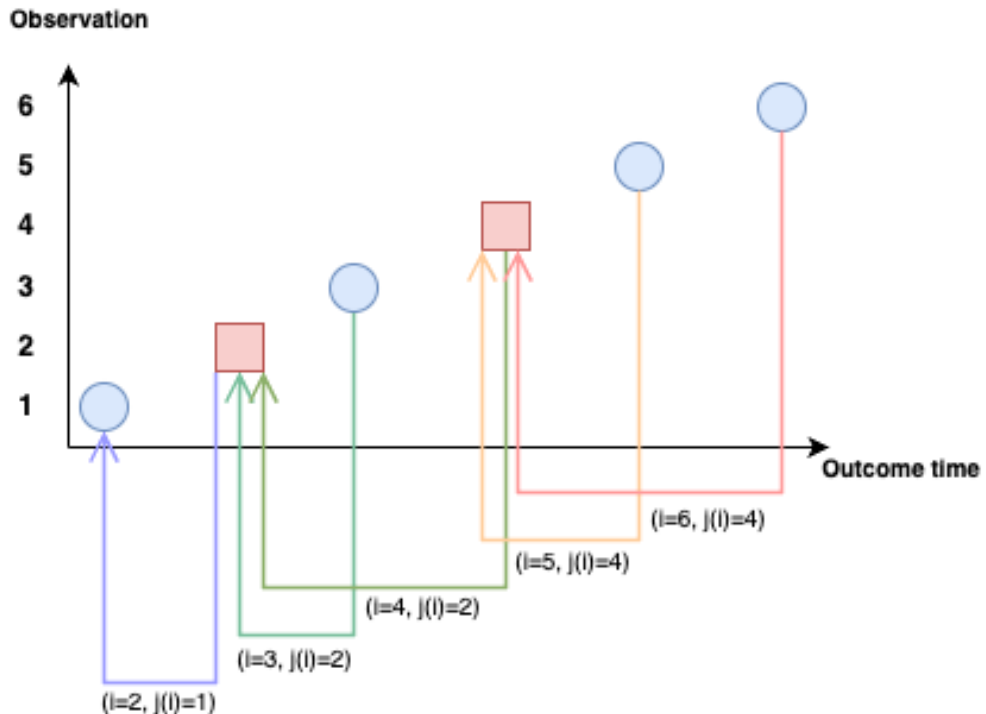


Figure 12.4: Van Belle SVM nearest neighbors reduction. Sorted observations are paired with the nearest uncensored outcome ‘to the left’. Red squares are uncensored observations and blue circles are censored. The observation with the smallest outcome time is always treated as uncensored.

$$\begin{aligned} & \min_{\beta, \alpha, \xi, \xi', \xi^*} \frac{1}{2} \|\beta\|^2 + \gamma \sum_{i=1}^n \xi_i + C \sum_{i=1}^n (\xi'_i + \xi_i^*) \\ \text{subject to } & \begin{cases} g(\mathbf{x}_i) - g(\mathbf{x}_{j(i)}) & \geq t_i - t_{j(i)} - \xi_i \\ g(\mathbf{x}_i) & \leq t_i + \xi_i^*, i : \delta_i = 1 \\ g(\mathbf{x}_i) & \geq t_i - \xi'_i \\ \xi_i, \xi'_i, \xi_i^* & \geq 0 \end{cases} \end{aligned}$$

The blue parts of the equation make up the ranking model and the red parts are the regression model. γ is the penalty associated with the regression method and C is the penalty associated with the ranking method. Setting $\gamma = 0$ results in the regression SVM and $C = 0$ results in the ranking SSVM. Hence, fitting the hybrid model and tuning these parameters is an efficient way to automatically detect which SSVM is best suited to a given task.

Once the model is fit, a prediction from given features $\mathbf{x}^* \in \mathbb{R}^p$, can be made using the equation below, again with the ranking and regression contributions highlighted in blue and red respectively.

$$\hat{g}(\mathbf{x}^*) = \sum_{i=1}^n \mu_i (K(\mathbf{x}_i, \mathbf{x}^*) - K(\mathbf{x}_{j(i)}, \mathbf{x}^*)) + \mu_i^* K(\mathbf{x}_i, \mathbf{x}^*) - \delta_i \mu_i' K(\mathbf{x}_i, \mathbf{x}^*) + \alpha$$

where μ_i, μ_i^*, μ_i' are Lagrange multipliers and K is a chosen kernel function, which may have further hyper-parameters to select or tune.

12.3 Conclusion

Key takeaways

- Support vector machines (SVMs) are a highly flexible machine learning method that can use the ‘kernel trick’ to represent infinite dimensional spaces in finite domains;
- Survival SVMs (SSVMs) extend regression SVMs by either making survival time predictions, ranking predictions, or a combination of the two;
- The hybrid SSVM provides an efficient method that encapsulates all the elements of regression and ranking SSVMs and is therefore a good model to include in benchmark experiments to test the potential of SSVMs.

Limitations

- SSVMs can only perform well with extensive tuning of hyper-parameters over a wide parameter space. To-date, no papers have experimented with the tuning range for the γ and C parameters, we note (Fouodo et al. 2018) tune over $(2^{-5}, 2^5)$.
- Even using the regression or hybrid model, the authors’ experiments with the SSVM have consistently shown ‘survival time’ estimates tend to be unrealistically large.
- Due to the above limitation, regression estimates cannot be meaningful interpreted and as a consequence there is no sensible composition to create a distribution

prediction from an SSVM. Hence, we are hesitant to suggest usage of SSVMs outside of ranking-based problems.

Further reading

- Shivaswamy, Chu, and Jansche (2007), Khan and Bayer Zubek (2008), Land et al. (2011), and Van Belle et al. (2011) to learn more about regression SSVMs.
- Evers and Messow (2008), Van Belle et al. (2007), Van Belle et al. (2008), and Van Belle et al. (2011) for more information about ranking SSVMs.
- Goli, Mahjub, Faradmal, and Soltanian (2016) and Goli, Mahjub, Faradmal, Mashayekhi, et al. (2016) introduce mean residual lifetime optimization SSVMs.
- Fouodo et al. (2018) surveys and benchmarks SSVMs.

13

Boosting Methods

TODO (150-200 WORDS)

! Major changes expected!

This page is a work in progress and major changes will be made over time.

Boosting is a machine learning strategy that can be applied to any model class. Similarly to random forests, boosting is an ensemble method that creates a model from a ‘committee’ of learners. The committee is formed of *weak* learners that make poor predictions individually, which creates a *slow learning* approach (as opposed to ‘greedy’) that requires many iterations for a model to be a good fit to the data. Boosting models are similar to random forests in that both make predictions from a large committee of learners. However the two differ in how the members of the committee are correlated and in how they are combined to make a prediction. In random forests, each decision tree is grown independently and their predictions are combined by a simple mean calculation. In contrast, weak learners in a boosting model are fit sequentially with errors from one learner used to train the next, predictions are then made by a linear combination of predictions from each learner (Figure 13.1).

13.1 GBMs for Regression

One of the earliest boosting algorithms is AdaBoost (Freund and Schapire 1996), which is more generally a Forward Stagewise Additive Model (FSAM) with an exponential loss (Hastie, Tibshirani, and Friedman 2001). Today, the most widely used boosting model is the Gradient Boosting Machine (GBM) (J. H. Friedman 2001) or extensions thereof.

Figure 13.1 illustrates the process of training a GBM in a least-squares regression setting:

1. A weak learner, f_1 , often a decision tree of shallow depth is fit on the training data (\mathbf{X}, \mathbf{y}) .
2. Predictions from the learner, $f_1(\mathbf{X})$, are compared to the ground truth, \mathbf{y} , and the residuals are calculated as $\mathbf{r}_1 = f_1(\mathbf{X}) - \mathbf{y}$.
3. The next weak learner, f_2 , uses the previous residuals for the target prediction, $(\mathbf{X}, \mathbf{r}_1)$
4. This is repeated to train M learners, f_1, \dots, f_M

Predictions are then made as $\hat{\mathbf{y}} = f_1(\mathbf{X}) + f_2(\mathbf{X}) + \dots + f_M(\mathbf{X})$.

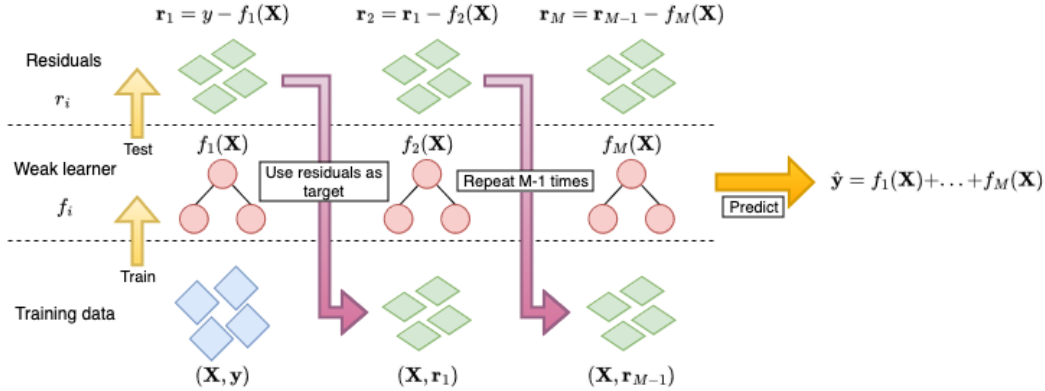


Figure 13.1: Least squares regression Boosting algorithm where the gradient is calculated as the difference between ground truth and predictions.

This is a simplification of the general gradient boosting algorithm, where the residuals are used to train the next model. More generally, a suitable, differentiable loss function relating to the problem of interest is chosen and the negative gradient is computed by comparing the predictions in each iteration with the ground truth. Residuals can be used in the regression case as these are proportional to the negative gradient of the mean squared error.

The algorithm above is also a simplification as no hyper-parameters other than M were included for controlling the algorithm. In order to reduce overfitting, three common hyper-parameters are utilised:

Number of iterations, M : The number of iterations is often claimed to be the most important hyper-parameter in GBMs and it has been demonstrated that as the number of iterations increases, so too does the model performance (with respect to a given loss on test data) up to a certain point of overfitting (Buhlmann 2006; Hastie, Tibshirani, and Friedman 2001; Schmid and Hothorn 2008a). This makes sense as the foundation of boosting rests on the idea that weak learners can slowly be combined to form a single powerful model. Finding the optimal value of M is critical as a value too small will result in poor predictions, whilst a value too large will result in model overfitting.

Subsampling proportion, ϕ : Sampling a fraction, ϕ , of the training data at each iteration can improve performance and reduce runtime (Hastie, Tibshirani, and Friedman 2001), with $\phi = 0.5$ often used. Motivated by the success of bagging in random forests, stochastic gradient boosting (J. Friedman 1999) randomly samples the data in each iteration. It appears that subsampling performs best when also combined with shrinkage (Hastie, Tibshirani, and Friedman 2001) and as with the other hyper-parameters, selection of ϕ is usually performed by nested cross-validation.

Step-size, ν : The step-size parameter is a shrinkage parameter that controls the contribution of each weak learner at each iteration. Several studies have demonstrated that GBMs perform better when shrinkage is applied and a value of $\nu = 0.1$ is often suggested (Buhlmann and Hothorn 2007; Hastie, Tibshirani, and Friedman 2001; J. H. Friedman 2001; D. K. K. Lee, Chen, and Ishwaran 2019; Schmid and Hothorn 2008a). The optimal values of ν and M depend on each other, such that smaller values of ν require larger values of M , and vice versa. This is intuitive as smaller ν results in a slower learning algorithm and therefore more iterations are required to fit the model. Accurately selecting the M parameter is generally

considered to be of more importance, and therefore a value of ν is often chosen heuristically (e.g. the common value of 0.1) and then M is tuned by cross-validation and/or early-stopping, which is the process of monitoring the model's training performance and stopping when a set performance is reached or when performance stagnates (i.e., no improvement over a set number of rounds).

As well as these parameters, the underlying weak learner hyper-parameters are also commonly tuned. If using a decision tree, then it is usual to restrict the number of terminal nodes in the tree to be between 4 and 8, which corresponds to two or three splits in the tree. Including these hyper-parameters, the general gradient boosting machine algorithm is as follows:

1. $g_0 \leftarrow$ Initial guess
2. **For** $m = 1, \dots, M$:
3. $\mathcal{D}_{train}^* \leftarrow$ Randomly sample \mathcal{D}_{train} with probability ϕ
4. $r_{im} \leftarrow -[\frac{\partial L(y_i, g_{m-1}(X_i))}{\partial g_{m-1}(X_i)}], \forall i \in \{i : X_i \in \mathcal{D}_{train}^*\}$
5. Fit a weak learner, h_m , to $(\mathbf{X}, \mathbf{r}_m)$
6. $g_m \leftarrow g_{m-1} + \nu h_m$
7. **end For**
8. **return** $\hat{g} = g_M$

Note:

1. The initial guess, g_0 , is often the mean of y for regression problems but can also simply be 0.
2. Line 4 is the calculation of the negative gradient, which is equivalent to calculating the residuals in a regression problem with the mean squared error loss.
3. Lines 5-6 differ between implementations, with some fitting multiple weak learners and selecting the one that minimizes a simple optimization problem. The version above is simplest to implement and quickest to run, whilst still providing good model performance.

Once the model is trained, predictions are made for new data, \mathbf{X}_{test} with

$$\hat{Y} = \hat{g}(\mathbf{X}_{test}) = g_0(\mathbf{X}_{test}) + \nu \sum_{i=1}^M g_i(\mathbf{X}_{test})$$

GBMs provide a flexible, modular algorithm, primarily comprised of a differentiable loss to minimise, L , and the selection of weak learners. This chapter focuses on tree-based weak learners, though other weak learners are possible. Perhaps the most common alternatives are linear least squares (J. H. Friedman 2001) and smoothing splines (Bühlmann and Yu 2003), we will not discuss these further here as decision trees are primarily used for survival analysis, due the flexibility demonstrated in Chapter 11. See references at the end of the chapter for other weak learners. Extension to survival analysis therefore follows by considering alternative losses.

13.2 GBMs for Survival Analysis

Unlike other machine learning algorithms that historically ignored survival analysis, early GBM papers considered boosting in a survival context (Ridgeway 1999); though there appears to be a decade gap before further considerations were made in the survival setting. After that period, developments, discussed in this chapter, by Binder, Schmid, and Hothorn, adapted GBMs to a framework suitable for survival analysis.

All survival GBMs make ranking predictions and none are able to directly predict survival distributions. However, depending on the underlying model, the predictions may be indirectly composed into a survival distribution, for example algorithms that assume a proportional hazards (PH) or accelerated failure time (AFT) form. This section starts with those models with simpler underlying forms, then explores more complex alternatives.

13.2.1 PH and AFT GBMs

The negative log-likelihood of the semi-parametric PH and fully-parametric AFT models can be derived from the (partial) likelihoods presented in Section 3.5.1. Given the likelihoods measure the goodness of fit of model parameters, algorithms that use these losses use boosting to train the model coefficients, β , hence at each iteration in the algorithm, $g_m(\mathbf{x}_i) = \mathbf{x}_i\beta^{(m)}$, where $\beta^{(m)}$ are the updated coefficients in iteration m .

The Cox partial likelihood (Cox 1972, 1975) is given by

$$L^{PH}(\beta) = \prod_{i:\delta_i=1}^n \frac{\exp(\eta_i)}{\sum_{j \in \mathcal{R}_{t_i}} \exp(\eta_j)}$$

with corresponding negative log-likelihood

$$-l^{PH}(\beta) = - \sum_{i=1}^n \delta_i \left[\eta_i - \log \left(\sum_{j \in \mathcal{R}_{t_i}} \exp(\eta_j) \right) \right] \quad (13.1)$$

where \mathcal{R}_{t_i} is the set of patients at risk at time t_i and $\eta_i = \mathbf{x}_i\beta$.

The gradient of $-l^{PH}$ at iteration m is then

$$r_{im} := \delta_i - \sum_{j=1}^n \delta_j \frac{\mathbb{I}(t_i \geq t_j) \exp(g_{m-1}(\mathbf{x}_i))}{\sum_{k \in \mathcal{R}_{t_j}} \exp(g_{m-1}(\mathbf{x}_k))} \quad (13.2)$$

where $g_{m-1}(\mathbf{x}_i) = \mathbf{x}_i\beta^{(m-1)}$.

For non-PH data, boosting an AFT model can outperform boosted PH models (Schmid and Hothorn 2008b). The AFT is defined by

$$\log \mathbf{y} = \boldsymbol{\eta} + \sigma W$$

where W is a random noise variable independent of X , and σ is a scale parameter controlling the amount of noise; again $\boldsymbol{\eta} = \mathbf{X}\beta$. By assuming a distribution on W , a distribution is assumed for the full parametric model. The model is boosted by simultaneously estimating

σ and β . Assuming a location-scale distribution with location $g(\mathbf{x}_i)$ and scale σ , one can derive the negative log-likelihood in the m th iteration as (Klein and Moeschberger 2003)

$$\begin{aligned} -l_m^{AFT}(\beta) = & -\sum_{i=1}^n \delta_i \left[-\log \sigma + \log f_W \left(\frac{\log(t_i) - \hat{g}_{m-1}(\mathbf{x}_i)}{\hat{\sigma}_{m-1}} \right) \right] + \\ & (1 - \delta_i) \left[\log S_W \left(\frac{\log(t_i) - \hat{g}_{m-1}(\mathbf{x}_i)}{\hat{\sigma}_{m-1}} \right) \right] \end{aligned}$$

where $\hat{g}_{m-1}, \hat{\sigma}_{m-1}$ are the location-scale parameters estimated in the previous iteration. Note this key difference to other GBM methods in which two estimates are made in each iteration step. After updating \hat{g}_m , the scale parameter, $\hat{\sigma}_m$, is updated as

$$\hat{\sigma}_m := \arg \min_{\sigma} -l_m^{AFT}(\beta)$$

σ_0 is commonly initialized as 1 (Schmid and Hothorn 2008b).

As well as boosting fully-parametric AFTs, one could also consider boosting semi-parametric AFTs, for example using the Gehan loss (Johnson and Long 2011) or using Buckley-James imputation (Z. Wang and Wang 2010). However, known problems with semi-parametric AFT models and the Buckley-James procedure (Wei 1992), as well as a lack of off-shelf implementation, mean that these methods are rarely used in practice.

13.2.2 Discrimination Boosting

Instead of optimising models based on a given model form, one could instead estimate $\hat{\eta}$ by optimizing a concordance index, such as Uno's or Harrell's C (Y. Chen et al. 2013; Mayr and Schmid 2014). Consider Uno's C (Section 6.1):

$$C_U(\hat{g}, \mathcal{D}_{train}) = \frac{\sum_{i \neq j} \delta_i \{\hat{G}_{KM}(t_i)\}^{-2} \mathbb{I}(t_i < t_j) \mathbb{I}(\hat{g}(\mathbf{x}_i) > \hat{g}(\mathbf{x}_j))}{\sum_{i \neq j} \delta_i \{\hat{G}_{KM}(t_i)\}^{-2} \mathbb{I}(t_i < t_j)}$$

The GBM algorithm requires that the chosen loss, here C_U , be differentiable with respect to $\hat{g}(X)$, which is not the case here due to the indicator term, $\mathbb{I}(\hat{g}(X_i) > \hat{g}(X_j))$, however this term can be replaced with a sigmoid function to create a differentiable loss (Ma and Huang 2006)

$$K(u|\omega) = \frac{1}{1 + \exp(-u/\omega)}$$

where ω is a tunable hyper-parameter controlling the smoothness of the approximation. The measure to optimise is then,

$$C_{USmooth}(\beta|\omega) = \sum_{i \neq j} \frac{k_{ij}}{1 + \exp[(\hat{g}(X_j) - \hat{g}(X_i))/\omega]} \quad (13.3)$$

with

$$k_{ij} = \frac{\Delta_i (\hat{G}_{KM}(T_i))^{-2} \mathbb{I}(T_i < T_j)}{\sum_{i \neq j} \Delta_i (\hat{G}_{KM}(T_i))^{-2} \mathbb{I}(T_i < T_j)}$$

The negative gradient at iteration m for observation i is then calculated as,

$$r_{im} := - \sum_{j=1}^n k_{ij} \frac{-\exp(\frac{\hat{g}_{m-1}(\mathbf{x}_j) - \hat{g}_{m-1}(\mathbf{x}_i)}{\omega})}{\omega(1 + \exp(\frac{\hat{g}_{m-1}(\mathbf{x}_j) - \hat{g}_{m-1}(\mathbf{x}_i)}{\omega}))} \quad (13.4)$$

The GBM algorithm is then followed as normal with the above loss and gradient. This algorithm may be more insensitive to overfitting than others (Mayr, Hofner, and Schmid 2016), however stability selection (Meinshausen and Bühlmann 2010), which is implemented in off-shelf software packages (Hothorn et al. 2020), can be considered for variable selection.

13.2.3 CoxBoost

Finally, ‘CoxBoost’ is an alternative method to boost Cox models and has been demonstrated to perform well in experiments. This algorithm boosts the Cox PH by optimising the penalized partial-log likelihood; additionally the algorithm allows for mandatory (or ‘forced’) covariates (Binder and Schumacher 2008). In medical domains the inclusion of mandatory covariates may be essential, either for model interpretability, or due to prior expert knowledge. CoxBoost deviates from the algorithm presented above by instead using an offset-based approach for generalized linear models (Tutz and Binder 2007).

Let $\mathcal{I} = \{1, \dots, p\}$ be the indices of the covariates, let \mathcal{I}_{mand} be the indices of the mandatory covariates that must be included in all iterations, and let $\mathcal{I}_{opt} = \mathcal{I} \setminus \mathcal{I}_{mand}$ be the indices of the optional covariates that may be included in any iteration. In the m th iteration, the algorithm fits a weak learner on all mandatory covariates and *one* optional covariate:

$$\mathcal{I}_m = \mathcal{I}_{mand} \cup \{x | x \in \mathcal{I}_{opt}\}$$

In addition, a penalty matrix $\mathbf{P} \in \mathbb{R}^{p \times p}$ is considered such that $P_{ii} > 0$ implies that covariate i is penalized and $P_{ii} = 0$ means no penalization. In practice, this is usually a diagonal matrix (Binder and Schumacher 2008) and by setting $P_{ii} = 0, i \in \mathcal{I}_{mand}$ and $P_{ii} > 0, i \notin \mathcal{I}_{mand}$, only optional (non-mandatory) covariates are penalized. The penalty matrix can be allowed to vary with each iteration, which allows for a highly flexible approach, however in implementation a simpler approach is to either select a single penalty to be applied in each iteration step or to have a single penalty matrix (Binder 2013).

At the m th iteration and the k th set of indices to consider ($k = 1, \dots, p$), the loss to optimize is the penalized partial-log likelihood given by

$$l_{pen}(\gamma_{mk}) = \sum_{i=1}^n \delta_i \left[\eta_{i,m-1} + \mathbf{x}_{i,\mathcal{I}_{mk}} \gamma_{mk}^\top \right] - \delta_i \log \left(\sum_{j=1}^n \mathbb{I}(t_j \leq t_i) \exp(\eta_{i,m-1} + \mathbf{x}_{i,\mathcal{I}_{mk}} \gamma_{mk}^\top) \right) - \lambda \gamma_{mk} \mathbf{P}_{mk} \gamma_{mk}^\top$$

where $\eta_{i,m} = \mathbf{x}_i \beta_m$, γ_{mk} are the coefficients corresponding to the covariates in \mathcal{I}_{mk} which is the possible set of candidates for a subset of total candidates $k = 1, \dots, p$; \mathbf{P}_{mk} is the penalty matrix; and λ is a penalty hyper-parameter to be tuned or selected.¹

¹On notation, note that \mathbf{P}_{ij} refers to the penalty matrix in the i th iteration for the j th set of indices, whereas P_{ij} is the (i, j) th element in the matrix \mathbf{P} .

In each iteration, all potential candidate sets (the union of mandatory covariates and one other covariate) are updated by

$$\hat{\gamma}_{mk} = \mathbf{I}_{pen}^{-1}(\hat{\gamma}_{(m-1)k})U(\hat{\gamma}_{(m-1)k})$$

where $U(\gamma) = \partial l / \partial \gamma(\gamma)$ and $\mathbf{I}_{pen}^{-1} = \partial^2 l / \partial \gamma \partial \gamma^T (\gamma + \lambda \mathbf{P}_{(m-1)k})$ are the first and second derivatives of the unpenalized partial-log-likelihood. The optimal set is then found as

$$k^* := \arg \max_k l_{pen}(\hat{\gamma}_{mk})$$

and the estimated coefficients are updated with

$$\hat{\beta}_m = \hat{\beta}_{m-1} + \hat{\gamma}_{mk^*}, \quad k^* \in \mathcal{I}_{mk}$$

This deviates from the standard GBM algorithm by directly optimizing l_{pen} and not its gradient, additionally model coefficients are iteratively updated instead of a more general model form.

13.3 Conclusion

Key takeaways

- GBMs are a highly flexible and powerful machine learning tool. They have proven particularly useful in survival analysis as minimal adjustments are required to make use of off-shelf software.
- The flexibility of the algorithm allows all the models above to be implemented in relatively few open-source packages.
- There is evidence that boosting models can outperform the Cox PH even in low-dimensional settings (Schmid and Hothorn 2008b), which is not something all ML models can claim.

Limitations

- Boosting, especially with tree learners, is viewed as a black-box model that is increasingly difficult to interpret as the number of iterations increase. However, there are several methods for increasing interpretability, such as variable importance and SHAPs (Lundberg and Lee 2017).
- Boosting often relies on intensive computing power, however, dedicated packages such as **xgboost** (T. Chen et al. 2020), exist to push CPU/GPUs to their limits in order to optimise predictive performance.

Further reading

- Bühlmann and Yu (2003); Hothorn et al. (2020); Z. Wang and Wang (2010) for more general information and background on componentwise GBMs
- J. H. Friedman (2001); Z. Wang and Wang (2010) for linear least squares weak learners

- Bühlmann and Yu (2003); J. H. Friedman (2001) for decision tree weak learners
- Ridgeway (1999) for early research into GBMs for survival analysis
- Johnson and Long (2011) and Z. Wang and Wang (2010) for semi-parametric AFT boosting

14

Neural Networks

TODO (150-200 WORDS)

! Major changes expected!

This page is a work in progress and major changes will be made over time.

Before starting the survey on neural networks, first a comment about their transparency and accessibility. Neural networks are infamously difficult to interpret and train, with some calling building and training neural networks an ‘art’ (Hastie, Tibshirani, and Friedman 2001). As discussed in the introduction of this book, whilst neural networks are not transparent with respect to their predictions, they are transparent with respect to implementation. In fact the simplest form of neural network, as seen below, is no more complex than a simple linear model. With regard to accessibility, whilst it is true that defining a custom neural network architecture is complex and highly subjective, established models are implemented with a default architecture and are therefore accessible ‘off-shelf’.

14.0.1 Neural Networks for Regression

(Artificial) Neural networks (ANNs) are a class of model that fall within the greater paradigm of *deep learning*. The simplest form of ANN, a feed-forward single-hidden-layer network, is a relatively simple algorithm that relies on linear models, basic activation functions, and simple derivatives. A short introduction to feed-forward regression ANNs is provided to motivate the survival models. This focuses on single-hidden-layer models and increasing this to multiple hidden layers follows relatively simply.

The single hidden-layer network is defined through three equations

$$\begin{aligned} Z_m &= \sigma(\alpha_{0m} + \alpha_m^T X_i), \quad m = 1, \dots, M \\ T &= \beta_{0k} + \beta_k^T Z, \quad k = 1, \dots, K \\ g_k(X_i) &= \phi_k(T) \end{aligned}$$

where $(X_1, \dots, X_n) \stackrel{i.i.d.}{\sim} X$ are the usual training data, α_{0m}, β_0 are bias parameters, and $\theta = \{\alpha_m, \beta\}$ ($m = 1, \dots, M$) are model weights where M is the number of hidden units. K is the number of classes in the output, which for regression is usually $K = 1$. The function ϕ is a ‘link’ or ‘activation function’, which transforms the predictions in order to provide an outcome of the correct return type; usually in regression, $\phi(x) = x$. σ is the ‘activation function’, which transforms outputs from each layer. The α_m parameters are often referred

to as ‘activations’. Different activation functions may be used in each layer or the same used throughout, the choice is down to expert knowledge. Common activation functions seen in this section include the sigmoid function,

$$\sigma(v) = (1 + \exp(-v))^{-1}$$

tanh function,

$$\sigma(v) = \frac{\exp(v) - \exp(-v)}{\exp(v) + \exp(-v)} \quad (14.1)$$

and ReLU (Nair and Hinton 2010)

$$\sigma(v) = \max(0, v) \quad (14.2)$$

A single-hidden-layer model can also be expressed in a single equation, which highlights the relative simplicity of what may appear a complex algorithm.

$$g_k(X_i) = \sigma_0(\beta_{k0} + \sum_{h=1}^H (\beta_{kh}\sigma_h(\beta_{h0} + \sum_{m=1}^M \beta_{hm}X_{i;m})) \quad (14.3)$$

where H are the number of hidden units, β are the model weights, σ_h is the activation function in unit h , also σ_0 is the output unit activation, and $X_{i;m}$ is the i th observation features in the m th hidden unit.

An example feed-forward single-hidden-layer regression ANN is displayed in (Figure 14.1). This model has 10 input units, 13 hidden units, and one output unit; two bias parameters are fit. The model is described as ‘feed-forward’ as there are no cycles in the node and information is passed forward from the input nodes (left) to the output node (right).

Back-Propagation

The model weights, θ , in this section are commonly fit by ‘back-propagation’ although this method is often considered inefficient compared to more recent advances. A brief pseudo-algorithm for the process is provided below.

Let L be a chosen loss function for model fitting, let $\theta = (\alpha, \beta)$ be model weights, and let $J \in \mathbb{N}_{>0}$ be the number of iterations to train the model over. Then the back-propagation method is given by,

- **For** $j = 1, \dots, J$: // Forward Pass [i.] Fix weights $\theta^{(j-1)}$. [ii.] Compute predictions $\hat{Y} := \hat{g}_k^{(j)}(X_i|\theta^{(j-1)})$ with (14.3). [] Backward Pass [iii.] Calculate the gradients of the loss $L(\hat{Y}|\mathcal{D}_{train})$. [] Update *[iv.] Update $\alpha^{(r)}, \beta^{(r)}$ with gradient descent.
- **End For**

In regression, a common choice for L is the squared loss,

$$L(\hat{g}, \theta|\mathcal{D}_{train}) = \sum_{i=1}^n (Y_i - \hat{g}(X_i|\theta))^2$$

which may help illustrate how the training outcome, $(Y_1, \dots, Y_n) \stackrel{i.i.d.}{\sim} Y$, is utilised for model fitting.

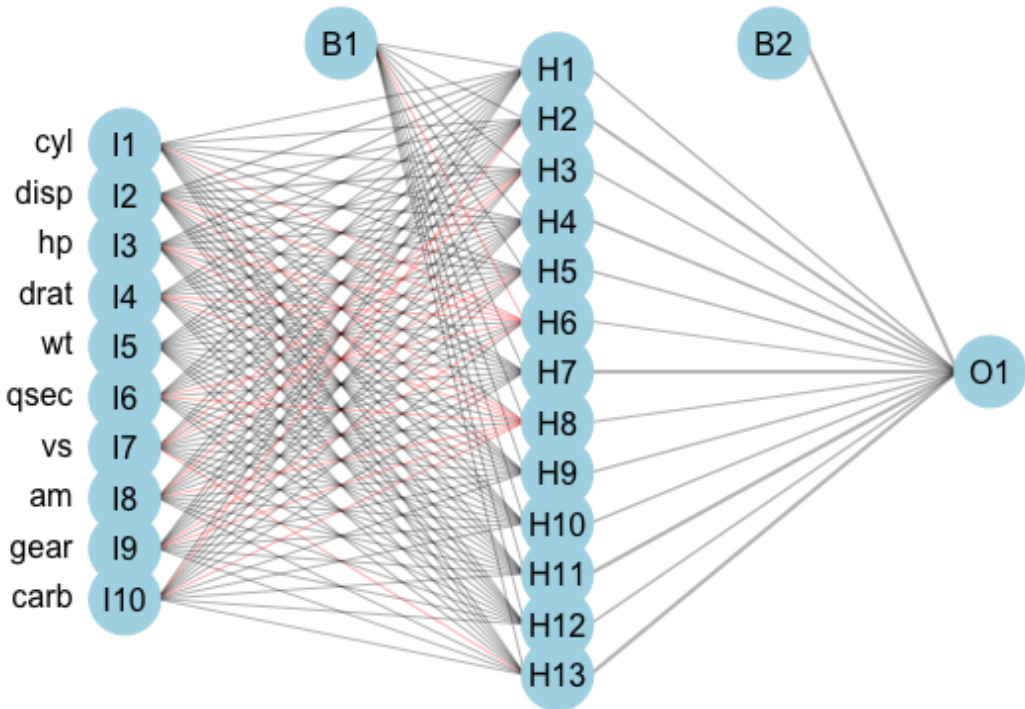


Figure 14.1: Single-hidden-layer artificial neural network with 13 hidden units fit on the `mtcars` (Henderson and Velleman 1981) dataset using the `nnet` (N. Venables and D. Ripley 2002) package, and `gamlss.add` (Stasinopoulos et al. 2020) for plotting. Left column are input variables, I1-I10, second column are 13 hidden units, H1-H13, right column is single output variable, O1. B1 and B2 are bias parameters.

Making Predictions

Once the model is fitted, predictions for new data follow by passing the testing data as inputs to the model with fitted weights,

$$g_k(X^*) = \sigma_0(\hat{\beta}_{k0} + \sum_{h=1}^H (\hat{\beta}_{kh}\sigma_h(\hat{\beta}_{h0} + \sum_{m=1}^M \hat{\beta}_{hm}X_m^*)))$$

Hyper-Parameters

In practice, a regularization parameter, λ , is usually added to the loss function in order to help avoid overfitting. This parameter has the effect of shrinking model weights towards zero and hence in the context of ANNs regularization is usually referred to as ‘weight decay’. The value of λ is one of three important hyper-parameters in all ANNs, the other two are: the range of values to simulate initial weights from, and the number of hidden units, M .

The range of values for initial weights is usually not tuned but instead a consistent range is specified and the neural network is trained multiple times to account for randomness in initialization.

The regularization parameter and number of hidden units, M , depend on each other and have a similar relationship to the learning rate and number of iterations in the GBMs (`?@sec-surv-ml-models-boost`). Like the GBMs, it is simplest to set a high number of hidden units and then tune the regularization parameter (Bishop 2006; Hastie, Tibshirani, and Friedman 2001). Determining how many hidden layers to include, and how to connect them, is informed by expert knowledge and well beyond the scope of this book; decades of research has been required to derive sensible new configurations.

Training Batches

ANNs can either be trained using complete data, in batches, or online. This decision is usually data-driven and will affect the maximum number of iterations used to train the algorithm; as such this will also often be chosen by expert-knowledge and not empirical methods such as cross-validation.

Neural Terminology

Neural network terminology often reflects the structures of the brain. Therefore ANN units are referred to as nodes or neurons and sometimes the connections between neurons are referred to as synapses. Neurons are said to be ‘fired’ if they are ‘activated’. The simplest example of activating a neuron is with the Heaviside activation function with a threshold of 0: $\sigma(v) = \mathbb{I}(v \geq 0)$. Then a node is activated and passes its output to the next layer if its value is positive, otherwise it contributes no value to the next layer.

14.0.2 Neural Networks for Survival Analysis

Surveying neural networks is a non-trivial task as there has been a long history in machine learning of publishing very specific data-driven neural networks with limited applications; this is also true in survival analysis. This does mean however that where limited developments for survival were made in other machine learning classes, ANN survival adaptations have been around for several decades. A review in 2000 by Schwarzer *et al.* surveyed 43 ANNs for diagnosis and prognosis published in the first half of the 90s, however only up to ten

of these are specifically for survival data.¹ Of those, Schwarzer *et al.* deemed three to be ‘na”ive applications to survival data’, and recommended for future research models developed by Liestøl *et al.* (1994) (Liestøl, Andersen, and Andersen 1994), Faraggi and Simon (1995) (Faraggi and Simon 1995), and Biganzoli *et al.* (1998) (E. Biganzoli *et al.* 1998).

This survey will not be as comprehensive as the 2000 survey, and nor has any survey since, although there have been several ANN reviews (B. D. Ripley and Ripley 2001; Huang et al. 2020b; Ohno-Machado 1996; Yang 2010; W. Zhu et al. 2020). ANNs are considered to be a black-box model, with interpretability decreasing steeply as the number of hidden layers and nodes increases. In terms of accessibility there have been relatively few open-source packages developed for survival ANNs; where these are available the focus has historically been in Python, with no R implementations. The new **survivalmodels** (R. Sonabend 2020) package,² implements these Python models via **reticulate** (Ushey, Allaire, and Tang 2020). No recurrent neural networks are included in this survey though the survival models SRN (Oh et al. 2018) and RNN-Surv (Giunchiglia, Nemchenko, and Schaar 2018) are acknowledged.

This survey is made slightly more difficult as neural networks are often proposed for many different tasks, which are not necessarily clearly advertised in a paper’s title or abstract. For example, many papers claim to use neural networks for survival analysis and make comparisons to Cox models, whereas the task tends to be death at a particular (usually 5-year) time-point (classification) (I. Han *et al.* 2018; Lundin *et al.* 1999; B. D. Ripley and Ripley 2001; R. M. Ripley, Harris, and Tarassenko 1998; Huseyin Seker *et al.* 2002), which is often not made clear until mid-way through the paper. Reviews and surveys have also conflated these different tasks, for example a very recent review concluded superior performance of ANNs over Cox models, when in fact this is only in classification (Huang et al. 2020a) (RM2) {sec:car_reduxstrats_mistakes}. To clarify, this form of classification task does fall into the general *field* of survival analysis, but not the survival *task* ((**box-task-surv?**)). Therefore this is not a comment on the classification task but a reason for omitting these models from this survey.

Using ANNs for feature selection (often in gene expression data) and computer vision is also very common in survival analysis, and indeed it is in this area that most success has been seen (Bello *et al.* 2019; Y.-C. Chen, Ke, and Chiu 2014; Cui *et al.* 2020; Lao *et al.* 2017; McKinney *et al.* 2020; Rietschel, Yoon, and Schaar 2018; H. Seker *et al.* 2002; Yucheng Zhang *et al.* 2020; X. Zhu, Yao, and Huang 2016), but these are again beyond the scope of this survey.

The key difference between neural networks is in their output layer, required data transformations, the model prediction, and the loss function used to fit the model. Therefore the following are discussed for each of the surveyed models: the loss function for training, L , the model prediction type, \hat{g} , and any required data transformation. Notation is continued from the previous surveys with the addition of θ denoting model weights (which will be different for each model).

14.0.2.1 Probabilistic Survival Models

Unlike other classes of machine learning models, the focus in ANNs has been on probabilistic models. The vast majority make these predictions via reduction to binary classification ???. Whilst almost all of these networks implicitly reduce the problem to classification, most are not transparent in exactly how they do so and none provide clear or detailed interface

¹Schwarzer conflates the prognosis and survival task, therefore it is not clear if all 10 of these are for time-to-event data (at least five definitely are).

²Created in order to run the experiments in [@Sonabend2021b].

points in implementation allowing for control over this reduction. Most importantly, the majority of these models do not detail how valid survival predictions are derived from the binary setting,³ which is not just a theoretical problem as some implementations, such as the Logistic-Hazard model in **pcox** (Kvamme 2018), have been observed to make survival predictions outside the range [0, 1]. This is not a statement about the performance of models in this section but a remark about the lack of transparency across all probabilistic ANNs.

Many of these algorithms use an approach that formulate the Cox PH as a non-linear model and minimise the partial likelihood. These are referred to as ‘neural-Cox’ models and the earliest appears to have been developed by Faraggi and Simon (Faraggi and Simon 1995). All these models are technically composites that first predict a ranking, however they assume a PH form and in implementation they all appear to return a probabilistic prediction.

ANN-COX {#mod-anncox}\ Faraggi and Simon (Faraggi and Simon 1995) proposed a non-linear PH model

$$h(\tau|X_i, \theta) = h_0(\tau) \exp(\phi(X_i\beta)) \quad (14.4)$$

where ϕ is the sigmoid function and $\theta = \{\beta\}$ are model weights. This model, ‘ANN-COX’, estimates the prediction functional, $\hat{g}(X^*) = \phi(X^*\hat{\beta})$. The model is trained with the partial-likelihood function

$$L(\hat{g}, \theta|\mathcal{D}_{train}) = \prod_{i=1}^n \frac{\exp(\sum_{m=1}^M \alpha_m \hat{g}_m(X^*))}{\sum_{j \in \mathcal{R}_{t_i}} \exp(\sum_{m=1}^M \alpha_m \hat{g}_m(X^*))}$$

where \mathcal{R}_{t_i} is the risk group alive at t_i ; M is the number of hidden units; $\hat{g}_m(X^*) = (1 + \exp(-X^*\hat{\beta}_m))^{-1}$; and $\theta = \{\beta, \alpha\}$ are model weights.

The authors proposed a single hidden layer network, trained using back-propagation and weight optimisation with Newton-Raphson. This architecture did not outperform a Cox PH (Faraggi and Simon 1995). Further adjustments including (now standard) pre-processing and hyper-parameter tuning did not improve the model performance (Mariani et al. 1997). Further independent studies demonstrated worse performance than the Cox model (Faraggi and Simon 1995; Xiang et al. 2000).

COX-NNET {#mod-coxnet}\ COX-NNET (Ching, Zhu, and Garmire 2018) updates the ANN-COX by instead maximising the regularized partial log-likelihood

$$L(\hat{g}, \theta|\mathcal{D}_{train}, \lambda) = \sum_{i=1}^n \Delta_i \left[\hat{g}(X_i) - \log \left(\sum_{j \in \mathcal{R}_{t_i}} \exp(\hat{g}(X_j)) \right) \right] + \lambda(\|\beta\|_2 + \|w\|_2)$$

with weights $\theta = (\beta, w)$ and where $\hat{g}(X_i) = \sigma(wX_i + b)^T\beta$ for bias term b , and activation function σ ; σ is chosen to be the tanh function ((14.1)). In addition to weight decay, dropout (Srivastava et al. 2014) is employed to prevent overfitting. Dropout can be thought of as a similar concept to the variable selection in random forests, as each node is randomly deactivated with probability p , where p is a hyper-parameter to be tuned.

Independent simulation studies suggest that COX-NNET does not outperform the Cox PH (Michael F. Gensheimer and Narasimhan 2019).

DeepSurv {#mod-deepsurv}\ DeepSurv (J. L. Katzman et al. 2018) extends these models to deep learning with multiple hidden layers. The chosen error function is the average

³One could assume they use procedures such as those described in Tutz and Schmid (2016) [@Tutz2016] but there is rarely transparent writing to confirm this.

negative log-partial-likelihood with weight decay

$$L(\hat{g}, \theta | \mathcal{D}_{train}, \lambda) = -\frac{1}{n^*} \sum_{i=1}^n \Delta_i \left[\left(\hat{g}(X_i) - \log \sum_{j \in \mathcal{R}_{t_i}} \exp(\hat{g}(X_j)) \right) \right] + \lambda \|\theta\|_2^2$$

where $n^* := \sum_{i=1}^n \mathbb{I}(\Delta_i = 1)$ is the number of uncensored observations and $\hat{g}(X_i) = \phi(X_i | \theta)$ is the same prediction object as the ANN-COX. State-of-the-art methods are used for data pre-processing and model training. The model architecture uses a combination of fully-connected and dropout layers. Benchmark experiments by the authors indicate that DeepSurv can outperform the Cox PH in ranking tasks (J. Katzman et al. 2016; J. L. Katzman et al. 2018) although independent experiments do not confirm this (Zhao and Feng 2020).

Cox-Time {#mod-coxtime}\ Kvamme *et al.* (Kvamme, Borgan, and Scheel 2019) build on these models by allowing time-varying effects. The loss function to minimise, with regularization, is given by

$$L(\hat{g}, \theta | \mathcal{D}_{train}, \lambda) = \frac{1}{n} \sum_{i: \Delta_i=1} \log \left(\sum_{j \in \mathcal{R}_{t_i}} \exp[\hat{g}(X_j, T_i) - \hat{g}(X_i, T_i)] \right) + \lambda \sum_{i: \Delta_i=1} \sum_{j \in \mathcal{R}_{t_i}} |\hat{g}(X_j, T_i)|$$

where $\hat{g} = \hat{g}_1, \dots, \hat{g}_n$ is the same non-linear predictor but with a time interaction and λ is the regularization parameter. The model is trained with stochastic gradient descent and the risk set, \mathcal{R}_{t_i} , in the equation above is instead reduced to batches, as opposed to the complete dataset. ReLU activations (Nair and Hinton 2010) and dropout are employed in training. Benchmark experiments indicate good performance of Cox-Time, though no formal statistical comparisons are provided and hence no comment about general performance can be made.

ANN-CDP {#mod-anncdp}\ One of the earliest ANNs that was noted by Schwarzer *et al.* (Schwarzer, Vach, and Schumacher 2000) was developed by Liestøl *et al.* (Liestøl, Andersen, and Andersen 1994) and predicts conditional death probabilities (hence ‘ANN-CDP’). The model first partitions the continuous survival times into disjoint intervals \mathcal{I}_k , $k = 1, \dots, m$ such that \mathcal{I}_k is the interval $(t_{k-1}, t_k]$. The model then studies the logistic Cox model (proportional odds) (Cox 1972) given by

$$\frac{p_k(\mathbf{x})}{q_k(\mathbf{x})} = \exp(\eta + \theta_k)$$

where $p_k = 1 - q_k$, $\theta_k = \log(p_k(0)/q_k(0))$ for some baseline probability of survival, $q_k(0)$, to be estimated; η is the usual linear predictor, and $q_k = P(T \geq T_k | T \geq T_{k-1})$ is the conditional survival probability at time T_k given survival at time T_{k-1} for $k = 1, \dots, K$ total time intervals. A logistic activation function is used to predict $\hat{g}(X^*) = \phi(\eta + \theta_k)$, which provides an estimate for \hat{p}_k .

The model is trained on discrete censoring indicators D_{ki} such that $D_{ki} = 1$ if individual i dies in interval \mathcal{I}_k and 0 otherwise. Then with K output nodes and maximum likelihood estimation to find the model parameters, $\hat{\eta}$, the final prediction provides an estimate for the conditional death probabilities \hat{p}_k . The negative log-likelihood to optimise is given by

$$L(\hat{g}, \theta | \mathcal{D}_{train}) = \sum_{i=1}^n \sum_{k=1}^{m_i} [D_{ki} \log(\hat{p}_k(X_i)) + (1 - D_{ki}) \log(\hat{q}_k(X_i))]$$

where m_i is the number of intervals in which observation i is not censored.

Liestøl *et al.*{} discuss different weighting options and how they correspond to the PH assumption. In the most generalised case, a weight-decay type regularization is applied to the model weights given by

$$\alpha \sum_l \sum_k (w_{kl} - w_{k-1,l})^2$$

where w are weights, and α is a hyper-parameter to be tuned, which can be used alongside standard weight decay. This corresponds to penalizing deviations from proportionality thus creating a model with approximate proportionality. The authors also suggest the possibility of fixing the weights to be equal in some nodes and different in others; equal weights strictly enforces the proportionality assumption. Their simulations found that removing the proportionality assumption completely, or strictly enforcing it, gave inferior results. Comparing their model to a standard Cox PH resulted in a ‘better’ negative log-likelihood, however this is not a precise evaluation metric and an independent simulation would be

preferred. Finally Listøl *et al.* included a warning “The flexibility is, however, obtained at unquestionable costs: many parameters, difficult interpretation of the parameters and a slow numerical procedure” (Liestøl, Andersen, and Andersen 1994).

PLANN {#mod-plann}\ Biganzoli *et al.* (1998) (E. Biganzoli et al. 1998) studied the same proportional-odds model as the ANN-CDP (Liestøl, Andersen, and Andersen 1994). Their model utilises partial logistic regression (Efron 1988) with added hidden nodes, hence ‘PLANN’. Unlike ANN-CDP, PLANN predicts a smoothed hazard function by using smoothing splines. The continuous time outcome is again discretised into disjoint intervals $t_m, m = 1, \dots, M$. At each time-interval, t_m , the number of events, d_m , and number of subjects at risk, n_m , can be used to calculate the discrete hazard function,⁴

$$\hat{h}_m = \frac{d_m}{n_m}, m = 1, \dots, M \quad (14.5)$$

This quantity is used as the target to train the neural network. The survival function is then estimated by the Kaplan-Meier type estimator,

$$\hat{S}(\tau) = \prod_{m:t_m \leq \tau} (1 - \hat{h}_m) \quad (14.6)$$

The model is fit by employing one of the more ‘usual’ survival reduction strategies in which an observation’s survival time is treated as a covariate in the model (Tutz and Schmid 2016). As this model uses discrete time, the survival time is discretised into one of the M intervals. This approach removes the proportional odds constraint as interaction effects between time and covariates can be modelled (as time-updated covariates). Again the model makes predictions at a given time m , $\phi(\theta_m + \eta)$, where η is the usual linear predictor, θ is the baseline proportional odds hazard $\theta_m = \log(h_m(0)/(1 - h_m(0)))$. The logistic activation provides estimates for the discrete hazard,

$$h_m(X_i) = \frac{\exp(\theta_m + \hat{\eta})}{1 + \exp(\theta_m + \hat{\eta})}$$

which is smoothed with cubic splines (Efron 1988) that require tuning.

A cross-entropy error function is used for training

$$L(\hat{h}, \theta | \mathcal{D}_{train}, a) = - \sum_{m=1}^M \left[\hat{h}_m \log \left(\frac{h_l(X_i, a_l)}{\hat{h}_m} \right) + (1 - \hat{h}_m) \log \left(\frac{1 - h_l(X_i, a_l)}{1 - \hat{h}_m} \right) \right] n_m$$

where $h_l(X_i, a_l)$ is the discrete hazard h_l with smoothing at mid-points a_l . Weight decay can be applied and the authors suggest $\lambda \approx 0.01 - 0.1$ (E. Biganzoli et al. 1998), though they make use of an AIC type criterion instead of cross-validation.

This model makes smoothed hazard predictions at a given time-point, τ , by including τ in the input covariates X_i . Therefore the model first requires transformation of the input data by replicating all observations and replacing the single survival indicator Δ_i , with a time-dependent indicator D_{ik} , the same approach as in ANN-CDP. Further developments have extended the PLANN to Bayesian modelling, and for competing risks (E. M. Biganzoli, Ambrogi, and Boracchi 2009).

No formal comparison is made to simpler model classes. The authors recommend ANNs primarily for exploration, feature selection, and understanding underlying patterns in the data (E. M. Biganzoli, Ambrogi, and Boracchi 2009).

⁴Derivation of this as a ‘hazard’ estimator follows trivially by comparison to the Nelson-Aalen estimator.

Nnet-survival {#mod-nnetsurvival}\ Aspects of the PLANN algorithm have been generalised into discrete-time survival algorithms in several papers (Michael F. Gensheimer and Narasimhan 2019; **Kvamme2019?**; Mani et al. 1999; Street 1998). Various estimates have been derived for transforming the input data to a discrete hazard or survival function. Though only one is considered here as it is the most modern and has a natural interpretation as the ‘usual’ Kaplan-Meier estimator for the survival function. Others by Street (1998) (Street 1998) and Mani (1999) (Mani et al. 1999) are acknowledged. The discrete hazard estimator (14.5), \hat{h} , is estimated and these values are used as the targets for the ANN. For the error function, the mean negative log-likelihood for discrete time (**Kvamme2019?**) is minimised to estimate \hat{h} ,

$$L(\hat{h}, \theta | \mathcal{D}_{train}) = -\frac{1}{n} \sum_{i=1}^n \sum_{j=1}^{k(T_i)} (\mathbb{I}(T_i = \tau_j, \Delta_i = 1) \log[\hat{h}_i(\tau_j)] + (1 - \mathbb{I}(T_i = \tau_j, \Delta_i = 1)) \log(1 - \hat{h}_i(\tau_j)))$$

where $k(T_i)$ is the time-interval index in which observation i dies/is censored, τ_j is the j th discrete time-interval, and the prediction of \hat{h} is obtained via

$$\hat{h}(\tau_j | \mathcal{D}_{train}) = [1 + \exp(-\hat{g}_j(\mathcal{D}_{train}))]^{-1}$$

where \hat{g}_j is the j th output for $j = 1, \dots, m$ discrete time intervals. The number of units in the output layer for these models corresponds to the number of discrete-time intervals. Deciding the width of the time-intervals is an additional hyper-parameter to consider.

Gensheimer and Narasimhan’s ‘Nnet-survival’ (Michael F. Gensheimer and Narasimhan 2019) has two different implementations. The first assumes a PH form and predicts the linear predictor in the final layer, which can then be composed to a distribution. Their second ‘flexible’ approach instead predicts the log-odds of survival in each node, which are then converted to a conditional probability of survival, $1 - h_j$, in a given interval using the sigmoid activation function. The full survival function can be derived with (14.6). The model has been demonstrated not to outperform the Cox PH with respect to Harrell’s C or the Graf (Brier) score (Michael F. Gensheimer and Narasimhan 2019).

PC-Hazard {#mod-pchazard}\ Kvamme and Borgan deviate from nnet-survival in their ‘PC-Hazard’ (**Kvamme2019?**) by first considering a discrete-time approach with a softmax activation function influenced by multi-class classification. They expand upon this by studying a piecewise constant hazard function in continuous time and defining the mean negative log-likelihood as

$$L(\hat{g}, \theta | \mathcal{D}_{train}) = -\frac{1}{n} \sum_{i=1}^n \left(\Delta_i X_i \log \tilde{\eta}_{k(T_i)} - X_i \tilde{\eta}_{k(T_i)} \rho(T_i) - \sum_{j=1}^{k(T_i)-1} \tilde{\eta}_j X_i \right)$$

where $k(T_i)$ and τ_i is the same as defined above, $\rho(t) = \frac{t - \tau_{k(t)-1}}{\Delta \tau_{k(t)}}$, $\Delta \tau_j = \tau_j - \tau_{j-1}$, and $\tilde{\eta}_j := \log(1 + \exp(\hat{g}_j(X_i)))$ where again \hat{g}_j is the j th output for $j = 1, \dots, m$ discrete time intervals. Once the weights have been estimated, the predicted survival function is given by

$$\hat{S}(\tau, X^* | \mathcal{D}_{train}) = \exp(-X^* \tilde{\eta}_{k(\tau)} \rho(\tau)) \prod_{j=1}^{k(\tau)-1} \exp(-\tilde{\eta}_j(X^*))$$

Benchmark experiments indicate similar performance to nnet-survival (**Kvamme2019?**), an unsurprising result given their implementations are identical with the exception of the

loss function (**Kvamme2019?**), which is also similar for both models. A key result found that varying values for interval width lead to significant differences and therefore should be carefully tuned.

DNNSurv {#mod-dnnsurv}\ A very recent (pre-print) approach (Zhao and Feng 2020) instead first computes ‘pseudo-survival probabilities’ and uses these to train a regression ANN with sigmoid activation and squared error loss. These pseudo-probabilities are computed using a jackknife-style estimator given by

$$\tilde{S}_{ij}(T_{j+1}, \mathcal{R}_{t_j}) = n_j \hat{S}(T_{j+1} | \mathcal{R}_{t_j}) - (n_j - 1) \hat{S}^{-i}(T_{j+1} | \mathcal{R}_{t_j})$$

where \hat{S} is the IPCW weighted Kaplan-Meier estimator (defined below) for risk set \mathcal{R}_{t_j} , \hat{S}^{-i} is the Kaplan-Meier estimator for all observations in \mathcal{R}_{t_j} excluding observation i , and $n_j := |\mathcal{R}_{t_j}|$. The IPCW weighted Kaplan-Meier estimate is found via the IPCW Nelson-Aalen estimator,

$$\hat{H}(\tau | \mathcal{D}_{train}) = \sum_{i=1}^n \int_0^\tau \frac{\mathbb{I}(T_i \leq u, \Delta_i = 1) \hat{W}_i(u)}{\sum_{j=1}^n \mathbb{I}(T_j \geq u) \hat{W}_j(u)} du$$

where \hat{W}_i, \hat{W}_j are subject specific IPC weights.

In their simulation studies, they found no improvement over other proposed neural networks. Arguably the most interesting outcome of their paper are comparisons of multiple survival ANNs at specific time-points, evaluated with C-index and Brier score. Their results indicate identical performance from all models. They also provide further evidence of neural networks not outperforming a Cox PH when the PH assumption is valid. However, in their non-PH dataset, DNNSurv appears to outperform the Cox model (no formal tests are provided). Data is replicated similarly to previous models except that no special indicator separates censoring and death, this is assumed to be handled by the IPCW pseudo probabilities.

DeepHit {#mod-deephit}\ DeepHit (C. Lee et al. 2018) was originally built to accommodate competing risks, but only the non-competing case is discussed here (Kvamme, Borgan, and Scheel 2019). The model builds on previous approaches by discretising the continuous time outcome, and makes use of a composite loss. It has the advantage of making no parametric assumptions and directly predicts the probability of failure in each time-interval (which again correspond to different terminal nodes), i.e. $\hat{g}(\tau_k | \mathcal{D}_{test}) = \hat{P}(T^* = \tau_k | X^*)$ where again $\tau_k, k = 1, \dots, K$ are the distinct time intervals. The estimated survival function is found with $\hat{S}(\tau_K | X^*) = 1 - \sum_{k=1}^K \hat{g}_i(\tau_k | X^*)$. ReLU activations were used in all fully connected layers and a softmax activation in the final layer. The losses in the composite error function are given by

$$L_1(\hat{g}, \theta | \mathcal{D}_{train}) = - \sum_{i=1}^N [\Delta_i \log(\hat{g}_i(T_i)) + (1 - \Delta_i) \log(\hat{S}_i(T_i))]$$

and

$$L_2(\hat{g}, \theta | \mathcal{D}_{train}, \sigma) = \sum_{i \neq j} \Delta_i \mathbb{I}(T_i < T_j) \sigma(\hat{S}_i(T_i), \hat{S}_j(T_i))$$

for some convex loss function σ and where $\hat{g}_i(t) = \hat{g}(t | X_i)$. Again these can be seen to be a cross-entropy loss and a ranking loss. Benchmark experiments demonstrate the model outperforming the Cox PH and RSFs (C. Lee et al. 2018) with respect to separation, and an independent experiment supports these findings (Kvamme, Borgan, and Scheel 2019). However, the same independent study demonstrated worse performance than a Cox PH with respect to the integrated Brier score (Graf et al. 1999).

14.0.2.2 Deterministic Survival Models

Whilst the vast majority of survival ANNs have focused on probabilistic predictions (often via ranking), a few have also tackled the deterministic or ‘hybrid’ problem.

RankDeepSurv {#mod-rankdeepsurv}\ Jing *et al.* (Jing et al. 2019) observed the past two decades of research in survival ANNs and then published a completely novel solution, RankDeepSurv, which makes predictions for the survival time $\hat{T} = (\hat{T}_1, \dots, \hat{T}_n)$. They proposed a composite loss function

$$L(\hat{T}, \theta | \mathcal{D}_{train}, \alpha, \gamma, \lambda) = \alpha L_1(\hat{T}, T, \Delta) + \gamma L_2(\hat{T}, T, \Delta) + \lambda \|\theta\|_2^2$$

where θ are the model weights, $\alpha, \gamma \in \mathbb{R}_{>0}$, λ is the shrinkage parameter, by a slight abuse of notation $T = (T_1, \dots, T_n)$ and $\Delta = (\Delta_1, \dots, \Delta_n)$, and

$$L_1(\hat{T}, \theta | \mathcal{D}_{train}) = \frac{1}{n} \sum_{\{i: I(i)=1\}} (\hat{T}_i - T_i)^2; \quad I(i) = \begin{cases} 1, & \Delta_i = 1 \cup (\Delta_i = 0 \cap \hat{T}_i \leq T_i) \\ 0, & \text{otherwise} \end{cases}$$

$$L_2(\hat{T}, \theta | \mathcal{D}_{train}) = \frac{1}{n} \sum_{\{i,j: I(i,j)=1\}} [(T_j - T_i) - (\hat{T}_j - \hat{T}_i)]^2; \quad I(i,j) = \begin{cases} 1, & T_j - T_i > \hat{T}_j - \hat{T}_i \\ 0, & \text{otherwise} \end{cases}$$

where \hat{T}_i is the predicted survival time for observation i . A clear contrast can be made between these loss functions and the constraints used in SSVM-Hybrid (Van Belle et al. 2011) (Section 12.2). L_1 is the squared second constraint in 12.2.3 and L_2 is the squared first constraint in 12.2.3. However L_1 in RankDeepSurv discards the squared error difference for all censored observations when the prediction is lower than the observed survival time; which is problematic as if someone is censored at time T_i then it is guaranteed that their true survival time is greater than T_i (this constraint may be more sensible if the inequality were reversed). An advantage to this loss is, like the SSVM-Hybrid, it enables a survival time interpretation for a ranking optimised model; however these ‘survival times’ should be interpreted with care.

The authors propose a model architecture with several fully connected layers with the ELU (Clevert, Unterthiner, and Hochreiter 2015) activation function and a single dropout layer. Determining the success of this model is not straightforward. The authors claim superiority of RankDeepSurv over Cox PH, DeepSurv, and RSFs however this is an unclear comparison (RM2) {sec:car_reduxstrats_mistakes} that requires independent study.

14.0.3 Conclusions

There have been many advances in neural networks for survival analysis. It is not possible to review all proposed survival neural networks without diverting too far from the book scope. This survey of ANNs should demonstrate two points: firstly that the vast majority (if not all) of survival ANNs are reduction models that either find a way around censoring via imputation or discretisation of time-intervals, or by focusing on partial likelihoods only; secondly that no survival ANN is fully accessible or transparent.

Despite ANNs being highly performant in other areas of supervised learning, there is strong evidence that the survival ANNs above are inferior to a Cox PH when the data follows the PH assumption or when variables are linearly related (Michael F. Gensheimer and Narasimhan 2018; Luxhoj and Shyur 1997; Ohno-Machado 1997; Puddu and Menotti 2012; Xiang et al. 2000; Yang 2010; Yasodhara, Bhat, and Goldenberg 2018; Zhao and Feng 2020). There are not enough experiments to make conclusions in the case when the data is non-PH.

Experiments in (R. E. B. Sonabend 2021) support the finding that survival ANNs are not performant.

There is evidence that many papers introducing neural networks do not utilise proper methods of comparison or evaluation (Király, Mateen, and Sonabend 2018) and in conducting this survey, these findings are further supported. Many papers made claims of being ‘superior’ to the Cox model based on unfair comparisons (RM2){sec:car_reduxstrats_mistakes} or miscommunicating (or misinterpreting) results (e.g. (Fotso 2018)). At this stage, it does not seem possible to make any conclusions about the effectiveness of neural networks in survival analysis. Moreover, even the authors of these models have pointed out problems with transparency (E. M. Biganzoli, Ambrogi, and Boracchi 2009; Liestol, Andersen, and Andersen 1994), which was further highlighted by Schwarzer *et al.* (Schwarzer, Vach, and Schumacher 2000).

Finally, accessibility of neural networks is also problematic. Many papers do not release their code and instead just state their networks architecture and available packages. In theory, this is enough to build the models however this does not guarantee the reproducibility that is usually expected. For users with a technical background and good coding ability, many of the models above could be implemented in one of the neural network packages in R, such as **nnet** (N. Venables and D. Ripley 2002) and **neuralnet** (Fritsch, Guenther, and N. Wright 2019); though in practice the only package that does contain these models, **survivalmodels**, does not directly implement the models in R (which is much slower than Python) but provides a method for interfacing the Python implementations in **pcox** (Kvamme 2018).

Further reading

- Schwarzer, Vach, and Schumacher (2000) provided an early survey of neural networks, focusing on ways in which neural networks have been ‘misused’ in the context of survival analysis. Whilst neural networks have moved on substantially since, their early observations remain valid today.

Part IV

Reduction Techniques

15

Reduction Techniques for Survival Analysis

TODO (150-200 WORDS)

 Minor changes expected!

This page is a work in progress and minor changes will be made over time.

In this part of the book we will introduce and formalize the concept of *reduction techniques* for survival analysis. A reduction is defined as “a complex problem decomposed into simpler subproblems so that a solution to the subproblems gives a solution to the complex problem” (Beygelzimer et al. 2016). Reduction techniques discussed here may introduce additional overhead, for example the need to perform a specific type of data pre-processing. However, they are still viewed as reductions as they reduce survival predictive problems to one or more regression and classification problems. Reduction techniques can therefore simplify the application of machine learning methods to survival analysis, particularly in situations where

- the interface of a machine learning method of choice is not designed to handle complex survival data (for example it expects a one dimensional vector as target variable, whereas survival outcomes are defined as tuples of two or more elements).
- novel machine learning methods are often developed for classification or regression but without adaptations to survival analysis
- a particular extension of a machine learning method to survival analysis is restricted to a subset of relevant survival problems, often the single event, right-censored data setting.

It should be emphasized that the reductions discussed in this part of the book go beyond the simplistic and often erroneous reductions that can unfortunately be seen in some literature; for example, treating the event indicator as a target for a classification task or directly using the observed event time as a target for a regression task whilst ignoring the censoring status (Schwarzer, Vach, and Schumacher 2000). Instead, the reductions introduced here are valid methods for survival analysis that appropriately deal with censoring and/or truncation. The reductions introduced in this part of the book

- do not make (strong) assumptions about the underlying distribution of event times, and thus have the same advantages as non-parametric (Section 10.1) and semi-parametric methods (Section 10.2),
- are applicable to many survival tasks, including competing risks and multi-state settings (Chapter 4),

- can predict different quantities of interest, including (discrete) hazards, survival probabilities and cumulative incidence functions conditional on features,
- can use any off-the-shelf implementation of machine learning or deep learning methods for regression or classification (depending on the reduction technique),
- can (explicitly) model time-varying effects and thus deal with non-proportional hazards.

The general concept of reduction techniques is depicted in Figure 15.1 .

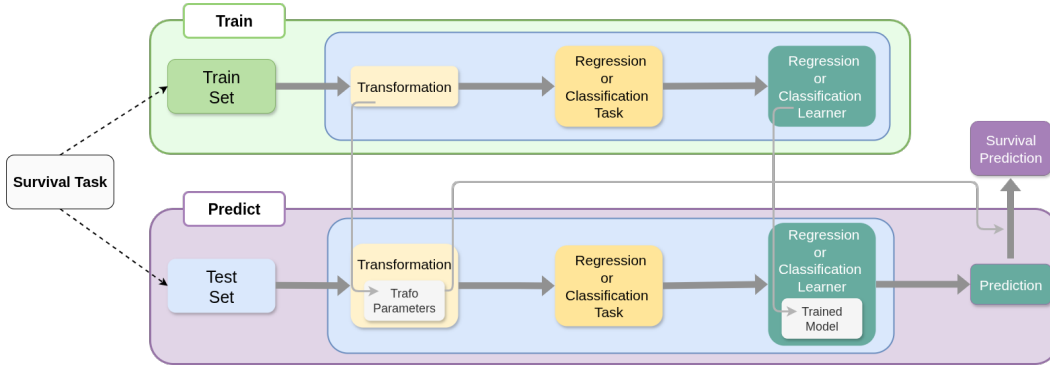


Figure 15.1: A general pipeline for reduction techniques in the context of survival analysis (close adaptation of Piller et al. (2025)).

In the training phase, the data is transformed into a different format. The specifics of the transformation will depend on the reduction technique and the survival task at hand. Once the data is transformed, the target variable becomes a one-dimensional vector of a regression or classification task (again depending on the reduction technique). At this stage, a standard machine learning model for regression or classification can be applied to the transformed data without any additional changes to the model or its implementation.

In the prediction phase, if necessary, the test data is transformed into the same format as the training data (using the pre-specified or trained parameters of the data transformation during the training phase). This yields a data set which can be passed to the previously learned regression or classification model to generate predictions. Depending on the reduction technique and the quantity of interest, the predictions may need additional post-processing to obtain the desired survival quantity of interest.

In the following chapters we introduce specific reduction techniques. We differentiate between reductions that primarily aim to estimate a specific quantity of interest (like the survival probability) at one or few time points of the follow up, in particular IPC-weighted classification (Chapter 16) and pseudo-value based regression (Chapter 17), and partition-based reductions (Chapter 18) that aim to estimate the entire event time distribution, specifically the discrete-time approach (Section 18.2), survival stacking (Section 18.3) and the piecewise exponential models (Section 18.4). Finally, Chapter 19 introduces general concepts in order to apply machine learning methods to competing risks and multi-state tasks based on simpler single event learners.

16

IPC weighted classification

TODO (150-200 WORDS)

The inverse probability of censoring weights (IPCW; Section 3.6.2) based reduction transforms a survival task to a weighted classification task (Vock et al. (2016)). Conceptually, it is one of the simplest reductions, but currently also the least general, as it only applies to single-event, right-censored data. The method is useful when one is not interested in the estimation of the entire event time distribution, but only in the probability that an event occurs before a given time point τ (sometimes referred to as τ -year prediction in survival analysis).

Consider a right-censored data set $\mathcal{D} = \{(\mathbf{x}_i, t_i, \delta_i)\}_{i=1}^n$ with $\mathbf{x}_i \in \mathbb{R}^p$ as introduced in Section 3.2. The probability of an event occurring by time τ is given by the complement of the survival probability at time τ :

$$P(Y \leq \tau | \mathbf{x}_i) = F(\tau | \mathbf{x}_i) = 1 - S(\tau | \mathbf{x}_i).$$

It might be tempting to estimate this probability by defining a binary target variable

$$e_i(\tau) := \mathbb{I}(t_i \leq \tau \wedge \delta_i = 1) \tag{16.1}$$

where all observations with event before time τ are considered ones (events) and all other observations zeros (non-events). Then the quantity of interest could be estimated using any binary classification method that outputs (calibrated) probabilities as

$$P(Y \leq \tau | \mathbf{x}_i) = P(e_i(\tau) = 1 | \mathbf{x}_i) := \pi(\mathbf{x}_i; \tau) \tag{16.2}$$

This approach could work if there was no censoring before τ in the data. However, in the presence of censoring, (16.1) does not define a valid target variable, as observations censored before time τ ($t_i < \tau \wedge \delta_i = 0$) are neither events nor non-events at time τ (as the event possibly occurred between t_i and τ). Treating those observations as non-events or removing them from the data without further modification would introduce bias.

Vock et al. (2016) suggest to adapt the estimation procedure to obtain unbiased estimates of (16.2) by first calculating weights for each observation as

$$\tilde{w}_i(\tau) = \begin{cases} 0 & \text{if } y_i < \tau \wedge \delta_i = 0, \\ \hat{w}_i(\min(y_i, \tau)) = \frac{1}{\hat{G}_{KM}(\min(y_i, \tau))} & \text{else} \end{cases} \tag{16.3}$$

where \hat{G}_{KM} is the Kaplan-Meier estimate of the censoring distribution (Section 3.6.1) and $\hat{w}_i(\min(y_i, \tau))$ are the IPC weights (3.21) introduced in Section 3.6.2. These weights then

need to be integrated into the estimation procedure, particularly by optimizing a weighted objective function. In words, censored observations are removed (the weight is zero) and uncensored observations are upweighted in order to compensate for the information loss. The higher the probability of an observation to be censored at τ , the higher its weight will be. These weights need to be integrated into the estimation procedure by optimizing a weighted objective function.

Incorporating this weighting scheme allows the binary target variable in (16.1) to be used as a valid object of prediction. Let $\ell(e_i(\tau), \pi(\mathbf{x}_i; \tau))$ be the point wise loss, then the learner needs to optimize the weighted objective function

$$\hat{\ell}(\pi, \tau) = \sum_{i=1}^n \hat{w}_i(\tau) \ell(e_i(\tau), \pi(\mathbf{x}_i; \tau)) \quad (16.4)$$

Thus, (16.4) can be optimized by any classification learner that can handle weights (which is the case for most popular machine learning methods). The exact form of (16.4) will depend on the choice of learner and objective function. For example, using the log loss (binary cross-entropy) $\ell(e_i, \pi(\mathbf{x}_i)) = e_i \log(\pi(\mathbf{x}_i)) + (1 - e_i) \log(1 - \pi(\mathbf{x}_i))$ as loss function, 16.4 becomes

$$\hat{\ell}(\pi, \tau) = \sum_{i=1}^n \hat{w}_i(\tau) (e_i(\tau) \log(\pi(\mathbf{x}_i; \tau)) + (1 - e_i(\tau)) \log(1 - \pi(\mathbf{x}_i; \tau))). \quad (16.5)$$

This simple reduction allows practitioners to estimate τ -year survival probabilities for right-censored data using classification learners. However, when using this reduction, there are some important aspects to consider:

- While the weighting in (16.4) takes into account censoring, the success of the prediction still depends on the choice of model and loss function. For example, the estimates might not be well calibrated if the chosen loss function does not yield well calibrated probabilities (for example, the hinge loss used by support vector machines).
- When evaluating predictions $\hat{\pi}(\mathbf{x}; \tau)$ on unseen test data, one cannot use standard evaluation metrics for binary classification, because the test data contains zeros (non-events), ones (events), but also censored observations. However, we can use survival metrics for evaluation, particularly rank based metrics like concordance indices (Chapter 6) and some scoring rules (Chapter 8). Use of standard classification metrics based on only uncensored data during evaluation would require IPC weighting similar to the training phase.
- Equation (16.3) implies that contributions of observations censored before time τ are multiplied with zero in (16.4) while uncensored observations are upweighted. Algorithmically, it would be more efficient to remove censored observations from the data set before training in order to avoid unnecessary computations of the loss. However, this might interfere with the usual training and evaluation procedures, for example when used in combination with cross-validation.

16.1 Conclusion

Key takeaways

- The IPCW reduction transforms a survival task to a weighted classification task.
- It can greatly simplify the estimation of survival probabilities at a specific time point of interest.
- Many learners for binary classification can be used out-of-the-box without further modifications.
- Learners that support gradient based optimization such as gradient boosting and deep learning are particularly well suited for this task, as they support specification of (custom) loss functions and support integration of weights.

Limitations

- Currently, the IPCW approach has only been described for right-censored data. Extensions to other settings might be possible, but have not been explored yet.
- Extensions to event-history analysis is also not well explored at the moment of writing, although an extension to competing risks has been proposed recently (see further reading).

Further reading

- Vock et al. (2016) provide the main reference where they explicitly show how different learners (logistic regression, bayesian networks, decision trees and k-nearest neighbors) can be adapted to obtain unbiased estimates of the event probability in the presence of censoring based on adapted IPC weights. They also discuss suitable evaluation metrics.
- Gonzalez Ginestet et al. (2021) extend the approach to the competing risks setting

17

Pseudo-value regression

TODO (150-200 WORDS)

 Minor changes expected!

This page is a work in progress and minor changes will be made over time.

Pseudo-value based approaches have been introduced in the survival analysis community quite recently (see Andersen and Pohar Perme (2010) for an overview), but have gained popularity ever since due to their flexibility and ease of application. Similar to the IPCW based reduction (Chapter 16). After data transformation, they allow the application of arbitrary regression learners for uncensored data in order to estimate a quantity of interest (like the survival probability, restricted mean survival time, cumulative incidence function, etc.) conditional on features. It's a two step approach where

- a jackknife (leave-one-out) procedure based on univariate (featureless) estimators for the quantity of interest is used to calculate pseudo-values, which are defined for all subjects in the data, regardless of their censoring status.
- the calculated pseudo-values are used as outcome in a regression task (Section 2.2.1) to learn a function that maps the features to the pseudo-values. Predictions from the model are conditional predictions of the quantity of interest.

Formally, let $\psi(\tau|\mathbf{x})$ denote some quantity of interest, for example the survival probability $S(\tau|\mathbf{x})$ or the restricted mean survival time, RMST($\tau|\mathbf{x}$). Let $\psi(\tau)$ be an univariate (featureless), unbiased estimator of the quantity of interest based on all observations and $\psi^{-i}(\tau)$ be an unbiased estimator of the same quantity obtained by omitting the i -th observation from the data set (for example $S_{KM}(\tau)$ and $S_{KM}^{-i}(\tau)$ for the survival probability). Let n the size of the data set. Pseudo-values are defined by

$$\theta_i(\tau) = n\psi(\tau) - (n - 1)\psi^{-i}(\tau). \quad (17.1)$$

Thus, the calculation of the pseudo-values requires $n + 1$ estimates of the univariate estimator $\psi(\tau)$ per time point τ (n estimates omitting each observation in the data set plus one for the overall estimate). This may seem prohibitive, but calculation of univariate estimators is usually fast and methods that use efficient approximations have been proposed in the literature (Parner, Andersen, and Overgaard (2023), Bouaziz (2023)). Also, pseudo-value analysis is usually used when the interest lies in estimation at one or few time points τ rather than the entire event time distribution.

An important property of pseudo-values is that their expectation conditional on features \mathbf{x}_i

is equal to the quantity of interest, that is

$$E(\theta_i(\tau|\mathbf{x}_i)) = \psi(\tau|\mathbf{x}_i). \quad (17.2)$$

In order to learn the relationship of features with the quantities in (17.2), the pseudo-values are regressed on the features \mathbf{x}_i by specifying

$$E(\theta_i(\tau|\mathbf{x}_i)) = h(f_\tau(\mathbf{x}_i)), \quad (17.3)$$

where $f_\tau(\mathbf{x}_i)$ is a function of the features \mathbf{x}_i (for example $f_\tau(\mathbf{x}) = \mathbf{x}^\top \boldsymbol{\beta}_\tau$) that is learned by the model and $h(\cdot)$ is a known response function (similar to the response function in a generalised linear model) that maps the predictor to the target space (for example identity or sigmoid function). From Equations (17.2) and (17.3) it follows that the predictions from the regression models give the conditional prediction of the quantity of interest. Subscript τ indicates that the function is time-dependent and will be different for each time point τ . If the response function h is the identity function, $h(f_\tau(\mathbf{x}_i)) = f_\tau(\mathbf{x}_i)$, the feature effects can be interpreted directly as effects on the quantity of interest (rather than being expressed in terms of hazard ratios or other relative measures).

The algorithm for pseudo-value based prediction is given by

1. Define the quantity of interest $\psi(\tau|\mathbf{x}_i)$, choose a suitable univariate estimator $\psi(\tau)$ and set τ (one or few time points are typically of interest).
2. Calculate the pseudo-values

$$\tilde{\theta}_i(\tau) = n\hat{\psi}(\tau) - (n-1)\hat{\psi}^{-i}(\tau)$$

by plugging in the estimates of $\psi(\tau)$ into (17.1).

3. Regress $\tilde{\theta}_i(\tau), i = 1, \dots, n$ on the features \mathbf{x}_i to obtain an estimate of $\hat{f}_\tau(\cdot)$.
4. Specify the response function $h(\cdot)$.
5. Generate predictions of the quantity of interest as

$$\hat{\theta}(\tau|\mathbf{x}) = \hat{\psi}(\tau|\mathbf{x}) = h(\hat{f}_\tau(\mathbf{x})). \quad (17.4)$$

Steps 3 and 4 can be combined in one step, for example in the specification of the mean link (and variance) function when estimating the model using generalized estimating equations (GEEs; Hardin and Hilbe (2012)). When using machine learning methods on the other hand it will often be easier to first estimate (and evaluate) the model and then apply the response function to the raw predictions.

In the following sections we provide step-by-step examples of pseudo-value based prediction for the survival probability (Section 17.1) as well as the restricted mean survival time (Section 17.2). Section 17.3 gives details on the extension to competing risks and multi-state models.

17.1 Pseudo-values for Survival Probability

This section details the use of pseudo-values for the estimation of the survival probability conditional on features. For illustration, we consider the tumor data set (introduced in Section 3.2, Table Table 3.1), that contains right-censored data on time-until-death after

operation (in days) and features age as well as complications, which indicates whether complications occurred during tumor removal at baseline. To keep it simple and intuitive, we will use a linear model for the regression step, but recall that any suitable learner for regression could be used.

We are interested in the conditional survival probability of tumor patients at different time points $\tau \in \{1000, 2000, 3000\}$ days. Therefore, we set $\psi(\tau|\mathbf{x}_i) = S(\tau|\mathbf{x}_i)$ and $\hat{\psi}(\tau) = \hat{S}_{KM}(\tau)$. Pseudo-values are then calculated as

$$\tilde{\theta}_i(\tau) = n\hat{S}_{KM}(\tau) - (n-1)\hat{S}_{KM}^{-i}(\tau). \quad (17.5)$$

The resulting estimates and calculated pseudo-values are shown for the first 4 subjects of the data in Table 17.1 for $\tau = 1000$ days. The Kaplan-Meier estimate using the entire data is given as $\hat{S}_{KM}(1000) = 0.6175$ and the leave-one-out estimates $\hat{S}_{KM}^{-i}(1000)$ are 0.6172, 0.6169, 0.6184 and 0.6183, respectively. Note that the differences are small, but for the calculation of the pseudo-values, the estimates are multiplied by n and $n-1$, respectively.

Table 17.1: Illustration of pseudo-value calculation for the first 4 subjects from the tumor data set at time point $\tau = 1000$ days. The table shows the overall Kaplan-Meier estimate $\hat{S}_{KM}(\tau)$, the leave-one-out Kaplan-Meier estimate $\hat{S}_{KM}^{-i}(\tau)$ (obtained by omitting subject i), and the calculated pseudo-value $\tilde{\theta}_i(\tau)$. The features age and complications have not been used for the calculation of the pseudo-values but can be included in the regression step.

i	t_i	δ_i	$\hat{S}_{KM}(\tau)$	$\hat{S}_{KM}^{-i}(\tau)$	$\tilde{\theta}_i(\tau)$	age	complications
1	579	0	0.6175	0.6172	0.8597	58	no
2	1192	0	0.6175	0.6169	1.0600	52	yes
3	308	1	0.6175	0.6184	-0.0442	74	no
4	33	1	0.6175	0.6183	-0.0119	57	yes

In the third step, a linear model is fitted to the pseudo-values such that

$$\hat{\theta}_i(\tau) = \hat{S}(\tau|\mathbf{x}_i) = \mathbf{x}_i^\top \hat{\beta}_\tau. \quad (17.6)$$

First, consider a linear model without features, that is $\hat{S}(\tau|\mathbf{x}_i) = \hat{\beta}_{\tau,0}$. By construction of the pseudo-values, at time point $\tau = 1000$ days we have $\hat{\theta}(1000) = \hat{\beta}_{1000,0} = \frac{1}{n} \sum_{i=1}^n \tilde{\theta}_i(1000) = 0.6175 = \hat{S}_{KM}(1000)$. Of course it doesn't really make sense to estimate $n+1$ Kaplan-Meier curves just to obtain the overall Kaplan-Meier estimate at one time-point, but this example illustrates that pseudo-value based regression provides consistent estimators of the survival probability.

In a next step, we include complications as a predictor and specify

$$\hat{S}(\tau|\mathbf{x}_i) = \hat{\beta}_{\tau,0} + \hat{\beta}_{\tau,1} x_{i,1}, \quad x_{i,1} = \mathbb{I}(\text{complications}_i = \text{"yes"}). \quad (17.7)$$

We also repeat the analysis for each time-point $\tau \in \{1000, 2000, 3000\}$ days separately. The results are shown in Figure 17.1, where the black dots indicate the survival probability predictions from the pseudo-value based approach and the solid lines are Kaplan-Meier estimates of the survival probability for comparison. Notably, the Kaplan-Meier estimates in the graphic have been obtained separately for each group (that is stratified by the complication variable) and the results indicate that the proportional hazards assumption does not hold for this example, as the shape of the survival function differs between the

two groups (intuitively, patients with complications have a higher hazard in the first days after operation and therefore lower survival probability). The Kaplan-Meier estimates used for the calculation of the pseudo-values on the other hand were obtained by applying a univariate Kaplan-Meier estimator. Despite not stratifying the estimator when calculating the pseudo-values, the pseudo-value based approach still obtains correct estimates of the survival probabilities at the selected time points for both groups. This works even when the proportional hazards assumption is violated as the linear model is fit to each time-point separately and thus is able to learn different values of $\hat{\beta}_{\tau,0}$ and $\hat{\beta}_{\tau,1}$ for each τ .

Because we use the identity response function in the linear model, $\hat{\beta}_{\tau,1}$ can be interpreted directly as the effect of complications on the survival probability at time τ . Here, $\hat{\beta}_{1000,1} \approx -0.23$ and so the expected survival probability at time $\tau = 1000$ for patients with complications is reduced by around 23 percentage points compared to patients without complications. In contrast, in a Cox model (Section 10.2) with linear predictor $\eta_i = \beta_0 + \beta_1 x_{i,1}$, β_1 can only be directly interpreted in terms of (log-)hazard ratios rather than survival probabilities (and under the proportional hazards assumption). Also note that the above results only hold for $\tau = 1000$. At $\tau = 2000$ days, $\hat{\beta}_{2000,1} \approx -0.18$, and at $\tau = 3000$ days, $\hat{\beta}_{3000,1} \approx -0.13$, thus the average effect of complications depends on τ and decreases over time (complications have a time-varying effect).

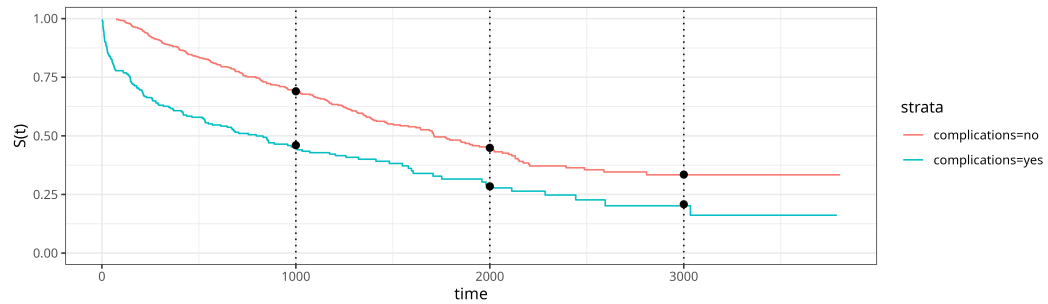


Figure 17.1: Comparison of estimates of the survival probability estimates using the Kaplan-Meier estimator and estimates of a linear model based on pseudo-values.

Besides the direct (time-varying) interpretation of the feature effects this might still feel overly complex given that similar results can be extracted from the stratified Kaplan-Meier analysis. However, once we add continuous features like age, Kaplan-Meier estimators are no longer applicable. Other models like Cox models assume proportional hazards and the estimated effects are expressed in terms of hazard ratios rather than survival probabilities.

Thus, in a final illustration, we add age to the model, such that

$$\hat{S}(\tau | \mathbf{x}_i) = \hat{\beta}_{\tau,0} + \hat{\beta}_{\tau,1} x_{i,1} + \hat{\beta}_{\tau,2} x_{i,2}, \quad x_{i,1} = \mathbb{I}(\text{complications}_i = \text{"yes"}), x_{i,2} = \text{age}_i$$

The resulting estimates are given in Table 17.2, where the effects of age and complications are given for each time-point $\tau \in \{1000, 2000, 3000\}$ days separately.

Table 17.2: Estimates of the effects of age and complications on the survival probability at different time points $\tau \in \{1000, 2000, 3000\}$ days.

τ	$\hat{\beta}_{\tau,1}$	$\hat{\beta}_{\tau,2}$
1000	-0.2205	-0.0032
2000	-0.1428	-0.0070
3000	-0.1050	-0.0071

Conditional on τ , the interpretation is equivalent to a standard multiple linear regression model. For example, at $\tau = 1000$ days, the effect of age is $\hat{\beta}_{1000,2} \approx -0.0032$, which means that, given everything else being equal, the expected survival probability is reduced by ca 0.32 percentage points per additional year of age. Considering the change of the coefficients over time, one can conclude that the effect of complications decreases over time while the effect of age increases between 1000 and 2000 days and then appears to remain stable at around 0.7 percentage points per additional year.

17.2 Pseudo-values for RMST

An unbiased, univariate estimator for the restricted mean survival time (RMST; Equation ([?@eq-rmst](#))) can be obtained via

$$\text{RMST}(\tau) = \int_0^\tau S_{KM}(u)du,$$

such that the calculated pseudo-values are given by

$$\tilde{\theta}_i(\tau) = n\widehat{\text{RMST}}(\tau) - (n-1)\widehat{\text{RMST}}^{-i}(\tau), \quad (17.8)$$

where $\tilde{\theta}_i(\tau)$ is now the pseudo-value of the restricted mean survival time at time τ for observation i .

Continuing the tumor data example from Section 17.1, we are now interested in the RMST and how it depends on covariates. The general idea is illustrated in Figure [Figure 17.2](#), which displays survival curves for each group (complications vs. no complications) with the RMST shown as the area under the curve up to $\tau = 1000$ days. If one is interested in the difference between patients with and without complications, then the difference in RMSTs between the two groups can be calculated, which around 246 days in this example. Thus, within the first 1000 days after operation, patients with complications are expected to live 246 days less than patients without complications.

For a pseudo-value based analysis, we once again fit a linear model

$$\hat{\theta}_i(\tau) = \widehat{\text{RMST}}(\tau|\mathbf{x}_i) = \hat{\beta}_{\tau,0} + \hat{\beta}_{\tau,1}x_{i,1}$$

For time point $\tau = 1000$ days, we obtain an estimate of $\hat{\beta}_1 \approx -239$. Thus, the expected RMST for patients with complications is reduced by around 239 days, which is similar to the result obtained from the Kaplan-Meier analysis in Figure [Figure 17.2](#). However, using

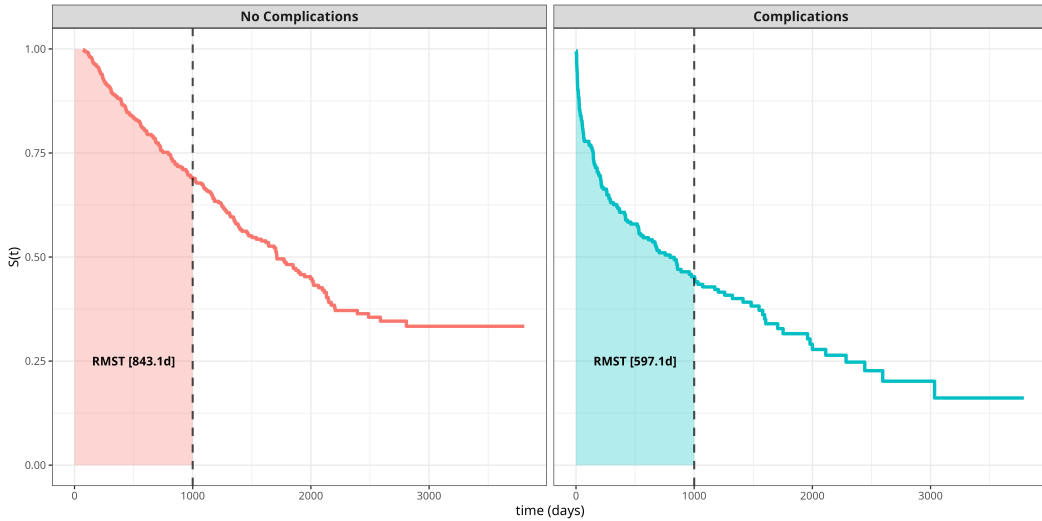


Figure 17.2: Survival curves with RMST visualization at $\tau = 1000$ days, stratified by complications status. The shaded area under each curve represents the RMST, with the numerical value displayed as text.

pseudo-values from (17.8), we can directly extend the predictor, for example by including age:

$$\hat{\theta}_i(\tau) = \hat{\beta}_{\tau,0} + \hat{\beta}_{\tau,1}x_{i,1} + \hat{\beta}_{\tau,2}x_{i,2}$$

where $x_{i,1}$ as before and $x_{i,2}$ is the age of subject i . The respective estimates are $\hat{\beta}_1 \approx -230$ and $\hat{\beta}_2 \approx -3$, such that, given everything else being equal, the expected RMST is reduced by circa 3 days per year of age. The effect of complications, $\hat{\beta}_1$, is slightly reduced when age is included and can be interpreted as the effect of complications on RMST adjusted for age.

17.3 Pseudo-values in Event-History Analysis

The pseudo-value approach can be extended to more complex event-history settings, including competing risks and multi-state models (Andersen and Pohar Perme (2010); Parner, Andersen, and Overgaard (2023); Andersen, Klein, and Rosthøj (2003)). The key idea remains the same: use univariate, non-parametric estimators of the quantity of interest to calculate pseudo-values, which can then be used as target variables in regression models.

17.3.1 Pseudo-values for Competing Risks

In the competing risks setting (Section 4.2), a quantity of particular interest is the cumulative incidence function (CIF) $F_e(\tau)$ (4.9), which represents the probability of experiencing event-type e before time τ . A suitable, univariate, unbiased estimator for the CIF is the Aalen-Johansen estimator. Pseudo-values for the CIF are thus given by

$$\theta_{i,e}(\tau) = nF_{AJ,e}(\tau) - (n-1)F_{AJ,e}^{-i}(\tau), \quad (17.9)$$

where $F_{AJ,e}^{-i}(\tau)$ is the Aalen-Johansen estimator of the CIF for event type e obtained by omitting the i -th observation from the data set.

Once calculated, these pseudo-values can once again be used as target variables in regression models to estimate the conditional CIF $F_e(\tau|\mathbf{x}_i)$ via 17.3. This allows for direct interpretation of covariate effects on the cumulative incidence of a specific event type.

17.3.2 Pseudo-values for Multi-State Models

In multi-state settings (Section 4.3), pseudo-values are often used in order to estimate state occupation probabilities conditional on features. These represent the probability of being in state e at time τ . Non-parametric estimators for state occupation probabilities can be obtained via the Aalen-Johansen estimator for multi-state models (Section 4.3.4). The pseudo-values for state occupation probabilities are then defined as

$$\tilde{\theta}_{i,e}(\tau) = nP_{AJ,e}(\tau) - (n-1)P_{AJ,e}^{-i}(\tau), \quad (17.10)$$

where $P_{AJ,e}(\tau)$ is the Aalen-Johansen estimator of the state occupation probability for event type e at time τ , and $P_{AJ,e}^{-i}(\tau)$ is the same estimator obtained by omitting the i -th observation.

These pseudo-values can be used to model conditional state occupation probabilities $P_e(\tau|\mathbf{x}_i)$ using standard regression techniques. This approach is particularly flexible as it allows for modeling state occupation probabilities directly, without the need to specify and estimate all transition hazards (Andersen, Klein, and Rosthøj (2003)).

17.4 Advantages and Limitations

Although the examples given in (Section 17.1) and (Section 17.2) are relatively simple, they illustrate the main advantages and limitations of the pseudo-value approach for machine learning based survival analysis:

On the plus side one can,

- estimate/predict various quantities of interest at selected time points τ , conditional on covariates, as long as an univariate, unbiased estimator of the quantity of interest is available,
- learn function $f(\mathbf{x})$ in 17.3 using any regression machine or deep learning method for uncensored data without any additional modifications by using the pseudo-values as target variables,
- interpret the effects of features directly as effects on the quantity of interest $\psi(\tau|\mathbf{x})$ (at least when the response function h in 17.3 is the identity function).
- when used in usual machine learning workflows, pseudo-values are calculated for the entire data set before splitting the data into training and test sets
- no survival specific metrics are needed for training and validation as pseudo-values can be considered uncensored data. However, since predictions (after application of the response function) reflect the quantity of interest, evaluation can also be performed using survival metrics in combination with the untransformed (censored data), for example when comparing the predictions with predictions from survival learners.

However, there are also some limitations:

- Pseudo-values can take on positive and negative values, therefore it is not guaranteed that the model predictions are within the range of the target. For example, survival probabilities should be within $[0, 1]$, which can only be insured if the response function h is chosen suitably. In context of statistical modeling, generalized estimating equations (Hardin and Hilbe (2012)) with suitable link functions can be used to ensure that the predictions are within the range of the target (standard GLMs are not suitable as the pseudo-values are not necessarily in the range of the target space). In machine learning, similar approaches can be used, for example by clipping the predictions to the range of the target or using suitable transformations/activation functions. However, even without transformation, predictions will often be within the desired range, especially if τ is not at the edge of the follow-up period (where the survival probability is close to 0 or 1) and if \mathbf{x} is not an outlier in the feature space.
- Pseudo-values are technically not independent (all observations are used to calculate $\hat{\psi}(\tau)$ and most to calculate $\hat{\psi}^{-i}(\tau)$); this does not affect the estimation of $f(\mathbf{x})$ too much, but robust variance estimation is preferred in context of statistical inference, for example using generalized estimating equations with robust (sandwich) variance estimation.
- Interpretation of feature effects is hindered to some extent by being time dependent; this can however also be viewed as an advantage, as the approach does not make strict assumptions like proportional hazards or accelerated failure time assumptions, which can be violated in practice.
- Calculating pseudo-values can be computationally expensive if predictions are needed at many time points τ and for many observations i , as the univariate estimator $\psi(\tau)$ has to be calculated $n + 1$ times per time point. However, for specific use cases efficient implementations based on infinitesimal jack-knife and other methods have been suggested in the literature and implemented in standard software packages (Parner, Andersen, and Overgaard (2023), Bouaziz (2023)).

17.5 Conclusion

Key takeaways

- The pseudo-value based approach allows estimation of arbitrary quantities of interest conditional on covariates, as long as an univariate, unbiased estimator of the quantity of interest is available.
- It avoids strong assumptions like the proportional hazards assumption or the accelerated failure time assumption, which can be violated in practice.
- In context of machine learning, this approach can greatly simplify analysis of time-to-event data, as standard implementations can be used out-of-the-box without any additional modifications.
- In contrast to many survival specific machine learning methods currently available, this method can be applied in complex settings, including competing risks and multi-state models.
- Feature effects can be interpreted directly as effects on the quantity of interest, rather than being expressed in terms of hazard ratios or other relative measures.

Limitations

- Pseudo-values can take positive and negative values, which may require appropriate response functions to ensure predictions are within the target range.
- Calculation of pseudo-values requires $n + 1$ estimates of the univariate estimator per time point, which can be computationally expensive for many time points. However, efficient approximations are available.

Further reading

- Andersen and Pohar Perme (2010) provides a comprehensive overview of pseudo-value methods in survival analysis.

18

Partition based reductions

TODO (150-200 WORDS)

! Major changes expected!

This page is a work in progress and major changes will be made over time.

In contrast to the previously introduced reductions that focus on the estimation of a specific quantity of interest at one or few time points, partition-based reduction aim to estimate the entire distribution of the event times (similar to Cox models and other survival learners). The general idea is to partition the time axis into J intervals $(a_0, a_1], \dots, (a_{J-1}, a_J]$ and estimate a discrete or continuous hazard rate for each interval.

For illustration, consider the partitioning of the follow up in Figure Figure 18.1. Note that the intervals do not necessarily have to be equidistant. The j th interval is given by $I_j := (a_{j-1}, a_j]$. Let further J_i the index of the interval in which observed time t_i of subject i falls, that is $t_i \in I_{J_i} = (a_{J_i-1}, a_{J_i}]$.

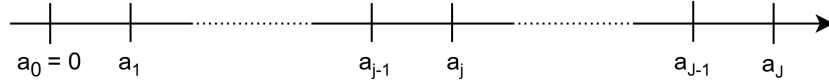


Figure 18.1: Partitioning of the follow-up time into J discrete intervals $(a_0, a_1], \dots, (a_{J-1}, a_J]$. This partitioning forms the basis for both reduction techniques discussed in this chapter.

Formally, define the partitioning of the follow-up via the set of interval boundary points a_j for $j = 0, \dots, J$ as

$$\mathcal{A} = \{a_0, \dots, a_J\}, \quad a_0 < a_1 < \dots < a_J \quad (18.1)$$

This partitioning is used to create a transformed data set. Using this transformed data, standard regression or classification methods can be used in order to estimate (discrete) hazards in each interval. Section 18.1 introduces the required data transformation formally. Section 18.2, Section 18.3 and Section 18.4 introduce specific reductions based on this data transformation, provide theoretical justification why models applied to such transformed data are valid approaches for estimation in time-to-event analysis and provide illustrative examples for such models. Section 18.5 discusses computational aspects and modeling choices (related to the choice of interval boundaries a_j).

18.1 Data Transformation

In order to apply the reduction techniques introduced in the upcoming sections, standard time-to-event data needs to be transformed into a specific format. The transformation is based on the partitioning of the follow-up as illustrated in Figure Figure 18.1 and boundaries as defined in 18.1. The new data set contains J_i rows for each subject i , that is one row for each interval in which subject i was at risk of experiencing an event.

For each subject i , we record the the subject's interval-specific event indicator

$$\delta_{ij} = \begin{cases} 1, & t_i \in (a_{j-1}, a_j] \text{ and } \delta_i = 1 \\ 0, & \text{else} \end{cases}, \quad j = 1, \dots, J_i, \quad (18.2)$$

the time at risk in interval j

$$t_{ij} = \begin{cases} a_j - a_{j-1}, & \text{if } t_i > a_j \\ t_i - a_{j-1}, & \text{if } t_i \in (a_{J_i-1}, a_{J_i}] \end{cases}, \quad j = 1, \dots, J_i, \quad (18.3)$$

as well as some representation of the time in interval j , for example the interval midpoint or endpoint

$$t_j = a_j \quad (18.4)$$

and the subject's (potentially time-dependent)features

$$\mathbf{x}_{ij} \quad (18.5)$$

with $\mathbf{x}_{ij} = \mathbf{x}_i$ for all j , if the features are constant over time.

Thus, given the partition \mathcal{A} , the standard time-to-event data $\mathcal{D} = \{(t_i, \delta_i, \mathbf{x}_i)\}_{i=1, \dots, n}$ is transformed to data

$$\mathcal{D}_{\mathcal{A}} = \{(i, j, \delta_{ij}, t_{ij}, t_j, \mathbf{x}_{ij})\}_{i=1, \dots, n; j=1, \dots, J_i}, \quad (18.6)$$

where i and j indices are usually only used for “book-keeping” purposes but are not used in modeling later on.

The data transformation procedure described above is illustrated in Figure Figure 18.2 for hypothetical data. The left hand side of Figure Figure 18.2 shows data in standard time-to-event format with one row per subject $i = 1, \dots, 3$ and $\mathcal{D} = \{(1.3, 0, 31), (0.5, 1, 57), (2.7, 1, 42)\}$. For the transformation, we choose (arbitrary) interval boundaries $\mathcal{A} = \{1, 1.5, 3\}$, which gives intervals $(0, 1], (1, 1.5], (1.5, 3]$. The right-hand side of Figure Figure 18.2 shows the transformed data $\mathcal{D}_{\mathcal{A}}$, where the first three columns keep track of subject and interval information and the other columns are the interval-specific event indicator, time at risk in the respective interval,representation of time and (time-dependent) features as defined in Equations 18.2, 18.3, 18.4 and 18.5, respectively.

Note that $\delta_{ij} = 0$ for all intervals except the last of subject i , where $\delta_{iJ_i} = \delta_i$, so either 0 or 1. Thus the total number of events is the same in both the original and transformed data. In general, both data sets contain the same time-to-event information as the original data since, given the interval boundaries \mathcal{A} , the variables δ_{ij} and t_{ij} are deterministic functions of the original data.

The figure shows two tables illustrating data transformation. On the left, a standard time-to-event format is shown with columns i , t_i , δ_i , and x_i . The data consists of three rows for subjects 1, 2, and 3. Subject 1 has $t_i = 1.3$, $\delta_i = 0$, and $x_i = 31$. Subject 2 has $t_i = 0.5$, $\delta_i = 1$, and $x_i = 57$. Subject 3 has $t_i = 2.7$, $\delta_i = 1$, and $x_i = 42$. An arrow points from this table to a larger table on the right. The right table has columns i , j , $(a_{j-1}, a_j]$, δ_{ij} , t_{ij} , t_j , and x_i . It contains 7 rows corresponding to the intervals defined by the set $A = \{1, 1.5, 3\}$. The first row covers the interval $(0, 1]$ for subject 1, with $\delta_{11} = 0$, $t_{11} = 1$, and $t_1 = 1$. The second row covers $(1, 1.5]$ for subject 1, with $\delta_{12} = 0$, $t_{12} = 0.5$, and $t_1 = 1.5$. The third row covers $(0, 1]$ for subject 2, with $\delta_{21} = 1$, $t_{21} = 0.5$, and $t_2 = 1$. The fourth row covers $(0, 1]$ for subject 3, with $\delta_{31} = 0$, $t_{31} = 1$, and $t_3 = 1$. The fifth row covers $(1, 1.5]$ for subject 3, with $\delta_{32} = 0$, $t_{32} = 0.5$, and $t_3 = 1.5$. The sixth row covers $(1.5, 3]$ for subject 3, with $\delta_{33} = 1$, $t_{33} = 1.2$, and $t_3 = 3$.

Figure 18.2: Illustration of the data transformation needed for partition based reductions. Left: Data in standard time-to-event format. Right: Transformed data using interval boundaries $\mathcal{A} = \{1, 1.5, 3\}$.

18.2 Discrete Time Survival Analysis

Consider the partitioning of the follow-up 18.1 and assume we are only interested in whether the event occurred within an interval rather than the exact event time. Using the notation from Section 3.1.2, the likelihood contribution of the i th observation is given by $P(Y_i \in (a_{J_i-1}, a_{J_i}]) = P(\bar{Y}_i = J_i)$ for subjects who experienced an event ($\delta_i = 1$) and $P(Y_i > a_{J_i}) = P(\bar{Y}_i > J_i)$ for subjects who were censored ($\delta_i = 0$).

Thus, using definitions 3.7 and 3.8, the likelihood contribution of subject i is given by

$$\begin{aligned} L_i &= P(Y_i \in (a_{J_i-1}, a_{J_i}])^{\delta_i} P(Y_i > a_{J_i})^{1-\delta_i} \\ &= [S^d(J_i - 1) h^d(J_i)]^{\delta_i} [S^d(J_i)]^{1-\delta_i} \\ &= \left[\left(\prod_{j=1}^{J_i-1} (1 - h^d(j)) \right) h^d(J_i) \right]^{\delta_i} \left[\prod_{j=1}^{J_i} (1 - h^d(j)) \right]^{1-\delta_i}, \end{aligned} \quad (18.7)$$

Now recall from Equation 18.2 the definition of the interval-specific event indicators δ_{ij} , which always take value 0, except for the last interval, where $\delta_{iJ_i} = \delta_i$. Thus, the first part of 18.7 can be written as $\prod_{j=1}^{J_i} (1 - h^d(j))^{1-\delta_{ij}} h^d(j)^{\delta_{ij}}$ and the second part as $\prod_{j=1}^{J_i} (1 - h^d(j))^{1-\delta_{ij}}$. It follows that the likelihood 18.7 can be written as

$$\begin{aligned} L_i &= \left[\prod_{j=1}^{J_i} (1 - h^d(j))^{1-\delta_{ij}} h^d(j)^{\delta_{ij}} \right]^{\delta_i} \left[\prod_{j=1}^{J_i} (1 - h^d(j))^{1-\delta_{ij}} \right]^{1-\delta_i} \\ &= \prod_{j=1}^{J_i} (1 - h^d(j))^{1-\delta_{ij}} h^d(j)^{\delta_{ij}}, \end{aligned} \quad (18.8)$$

where the last equality follows from $\delta_{ij} = 0 \ \forall j = 1, \dots, J_i$, if $\delta_i = 0$ and thus $\prod (1 - h^d(j))^{1-\delta_{ij}} h^d(j)^{\delta_{ij}} = \prod (1 - h^d(j))^{1-\delta_{ij}}$.

The importance of this result may not be immediately apparent, but recall that if $Z \sim Bernoulli(\pi)$, where $\pi = P(Z = 1)$, then likelihood contribution of Z is given by $P(Z = z) = \pi^z(1 - \pi)^{1-z}$. We therefore recognize that the likelihood contribution 18.8 can also be obtained by assuming that the interval-specific event indicators δ_{ij} are realizations of random variables $\Delta_{ij} \stackrel{iid}{\sim} Bernoulli(\pi_j = h^d(j))$. Thus

$$\begin{aligned}\pi_j &= P(\Delta_{ij} = 1 | t_j) \\ &= P(Y_i \in (a_{j-1}, a_j] | Y_i > a_{j-1}) = h^d(j)\end{aligned}\tag{18.9}$$

Note that in 18.9, $\Delta_{ij} = 1$ is equivalent to $Y_i \in (a_{j-1}, a_j]$, while the conditioning on $Y_i > a_{j-1}$ is implicit in the definition of δ_{ij} in 18.2.

This implies that we can estimate the discrete time hazards $h^d(j)$ for each interval j by fitting any binary classification model to the transformed data set

$$\mathcal{D}_A = \{(\delta_{ij}, t_j)\}_{i=1, \dots, n; j=1, \dots, J_i},\tag{18.10}$$

where δ_{ij} are the targets and t_j , some representation of time in interval j (for example $t_j = j$ or $t_j = a_j$), enters the estimation as a feature and is needed in order to estimate different hazards/probabilities in different intervals.

In the presence of features \mathbf{x}_i we assume $\Delta_{ij} | \mathbf{x}_i, t_j \stackrel{iid}{\sim} Ber(\pi_{ij})$, where $\pi_{ij} = P(\Delta_{ij} = 1 | \mathbf{x}_i, t_j) = h^d(j | \mathbf{x}_i)$ is the discrete hazard rate for interval j given features \mathbf{x}_i and is estimated by applying binary classifiers to

$$\mathcal{D}_A = \{(\delta_{ij}, \mathbf{x}_i, t_j)\}_{i=1, \dots, n; j=1, \dots, J_i}.$$

18.2.1 Example: Logistic Regression

To illustrate the discrete time reduction approach, once again consider the tumor data set introduced in Table Table 3.1. The follow-up time is partitioned into $J = 100$ equidistant intervals and the data is transformed according to the procedure described in Section 18.1. Define $x_{i1} = \mathbb{I}(\text{complications}_i = \text{"yes"})$. We then fit a logistic regression model

$$\text{logit}(\pi_{ij}) = \beta_{0j} + \beta_1 x_{i1}\tag{18.11}$$

to the transformed data set, where j denotes the interval index, β_{0j} are the interval-specific intercepts (technically we include the interval index j as a reference coded categorical feature in the model) and β_1 is the common effect of complications on the discrete hazard rate (across all intervals).

The estimated survival probabilities are obtained by calculating $\hat{S}^d(j | x_{i1}) = \prod_{k=1}^j (1 - \hat{h}^d(k | x_{i1}))$ for each interval j and complication group, where $\hat{h}^d(k | x_{i1})$ are the predicted discrete hazards from the logistic regression model.

Figure Figure 18.3 shows the estimated survival probabilities from the discrete time model (dashed lines) together with the Kaplan-Meier estimates (solid lines) for comparison. The model specified in Equation 18.11 is a proportional odds model, where the baseline hazard is the same for both complication groups, thus the shape of the hazard and therefore the survival probability curve is the same for both complication groups, shifted by the common effect of complications. This does not describe the data too well as the hazards are different in the two groups (as already established in XXX)

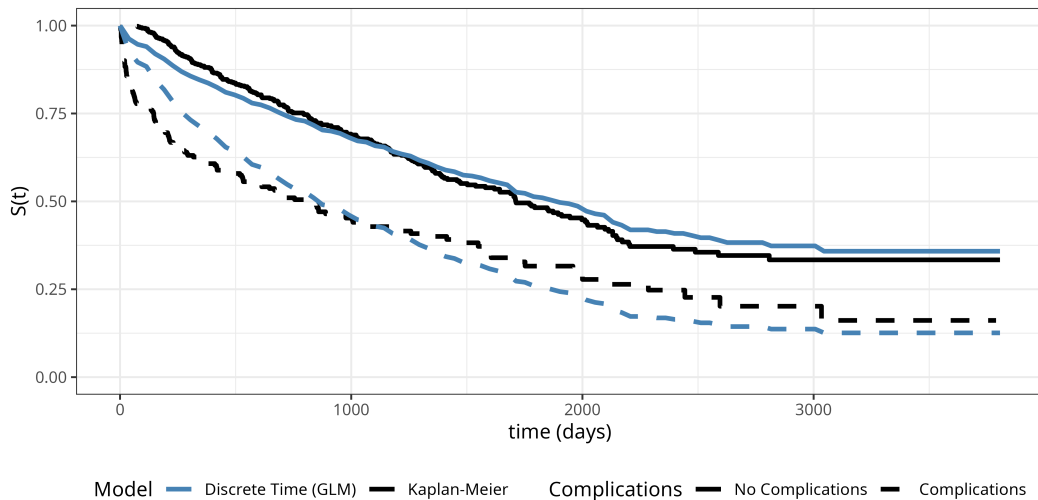


Figure 18.3: Comparison of survival probability estimates using the discrete time model (logistic regression) and the Kaplan-Meier estimator, for patients with and without complications.

In order to estimate separate discrete baseline hazards for each group, we can introduce an interaction term between the interval and complications variables.

$$\text{logit}(\pi_{ij}) = \beta_{0j} + \beta_{1j}x_{i1} \quad (18.12)$$

where β_{0j} are the interval-specific intercepts for the reference group (no complications), β_{1j} are the deviations from the reference group for the complications group (technically this is fit as an interaction model using reference coded categorical features for interval and complications). This specification allows the shape of the hazard and therefore the survival probability curve to be different for the two groups.

Figure Figure 18.4 shows the estimated survival probabilities from the interaction model (dashed lines) together with the Kaplan-Meier estimates (solid lines) for comparison. The interaction model provides a much better fit to the data compared to the proportional odds model, as it allows for separate baseline hazards for each complications group. The difference to the Kaplan-Meier estimates is barely detectable.

While this is a simple example with only one feature, it shows that the discrete time reduction approach can be used to estimate the distribution of event times well when the number of intervals is large enough, despite the fact that we ignore the information about the exact event time. Importantly, the estimated survival probabilities are discrete, representing survival probabilities at the interval endpoints. However, a simple solution to generate continuous survival function predictions is to linearly interpolate between the interval endpoints.

The example also raises the question about the choice of the number of intervals J and the placement of interval boundaries \mathcal{A} . These questions will be discussed in more detail in Section 18.5, which is relevant for both, the discrete time reduction approach and the piecewise constant hazards approach discussed in Section 18.4.

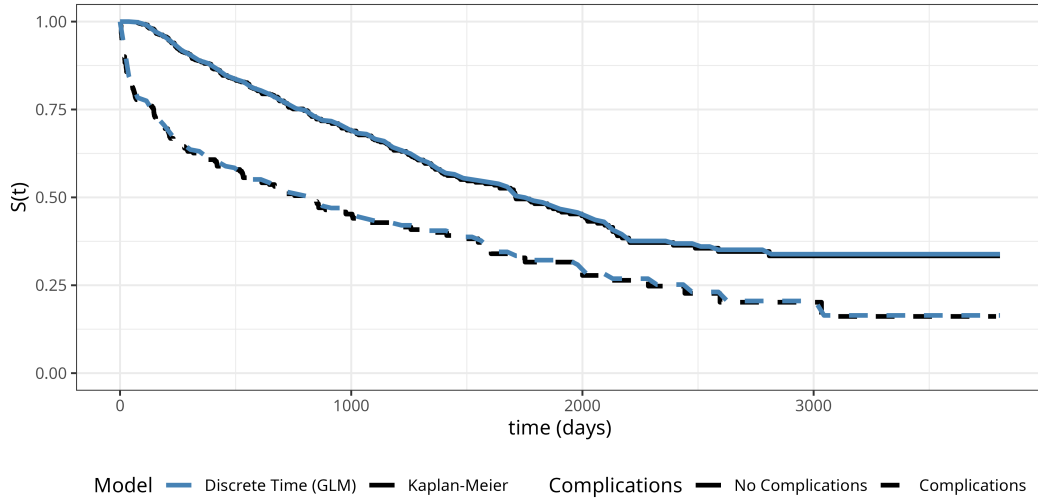


Figure 18.4: Comparison of survival probability estimates using the discrete time model with interaction (logistic regression) and the Kaplan-Meier estimator, for patients with and without complications.

18.3 Survival Stacking

Survival stacking (Craig, Zhong, and Tibshirani (2025)) casts survival tasks to classification tasks similarly to the discrete time method described in Section 18.2. However, there is a small but important difference in the creation of event indicators δ_{ij} . Rather than constructing intervals based on partitioning of the follow-up along boundary points \mathcal{A} , survival stacking uses the unique, observed, ordered event times $t_{(1)}, < \dots < t_{(m)}$ (3.9) and defines

$$\delta_{ij} = \begin{cases} 1, & t_i = t_{(j)} \text{ and } \delta_i = 1 \\ 0, & \text{else} \end{cases}, \quad j \in \{1, \dots, m : i \in R_{t_{(j)}}\} \quad (18.13)$$

where $R_{t_{(j)}}$ is the risk set (3.10) at time $t_{(j)}$.

Definition 18.13 implies that the event indicators δ_{ij} are only defined for timepoints $t_{(j)}$ at which subject i is still at risk for the event. Therefore, this method can be easily applied to left-truncated data by using the more general definition of the risk set (3.17).

For illustration, consider once again, the example from Figure 18.2. The adapted data-transformation for survival stacking is shown in Figure 18.5 (dropping columns that are not meaningful here). At the first event time $t_{(1)} = 0.5$, all subjects are still at risk for the event. At time $t_{(2)} = 2.7$, however, only subject 3 is still at risk for the event.

Note that in contrast to Figure 18.2, here subject 1 has only one row and subject 3 has two rather than three rows. This could suggest that the data transformation for survival stacking creates smaller data sets, however, we need to create a data set for each observed event time $t_{(j)}, j = 1, \dots, m$, whereas for the discrete time approach in Section 18.2 one can freely choose the number and placement of interval boundaries \mathcal{A} , such that $|\mathcal{A}| < m$ in most cases.

The figure shows two tables illustrating data transformation for survival analysis. The left table is in standard time-to-event format, with columns i , t_i , δ_i , and x_i . The right table is transformed data using unique, observed event times, with columns i , j , δ_{ij} , t_j , and x_i .

i	t_i	δ_i	x_i
1	1.3	0	31
2	0.5	1	57
3	2.7	1	42

i	j	δ_{ij}	t_j	x_i
1	1	0	0.5	31
2	1	1	0.5	57
3	1	0	0.5	42
3	2	1	2.7	42

Figure 18.5: Illustration of the data transformation needed for survival stacking. Left: Data in standard time-to-event format. Right: Transformed data using unique, observed event times $t_{(1)}, < \dots < t_{(m)}$.

Data transformation 18.13 yields data

$$\mathcal{D}_A = \{(\delta_{ij}, t_j, \mathbf{x}_{ij})\}_{i=1, \dots, n; j=1, \dots, m: i \in R_{t(j)}}, \quad (18.14)$$

where the δ_{ij} can be used as targets for binary classification and as before, any algorithm that returns class probabilities can be used for estimation.

18.4 Piecewise Constant Hazards

The general idea of the piecewise constant hazards approach is conceptually simple:

1. Partition the follow-up into many intervals
2. Estimate a constant hazard rate for each interval

Intuitively, any underlying continuous hazard function of the data generating process can be approximated arbitrarily well given enough intervals (and events). This model class is known as the piecewise exponential model (PEM) because assuming event times to be exponentially distributed, implies constant hazards within each interval.

Consider the partitioning of the follow-up as defined in 18.1 and assume that within each interval $I_j = (a_{j-1}, a_j]$, the hazard function is constant, that is

$$h(\tau) = h_j, \forall \tau \in I_j \quad (18.15)$$

First we derive the likelihood contribution of subject i under assumption 18.15, starting

with the general likelihood for right-censored data (3.12):

$$\begin{aligned}
\mathcal{L}_i &= h(t_i)^{\delta_i} S(t_i) \\
&= h(t_i)^{\delta_i} \exp \left(- \int_0^{t_i} h(u) \, du \right) \\
&= h_{J_i}^{\delta_i} \exp \left(- \left[\sum_{j=1}^{J_i-1} (a_j - a_{j-1}) h_j + (t_i - a_{J_i-1}) h_{J_i} \right] \right) \\
&= h_{J_i}^{\delta_i} \exp \left(- \sum_{j=1}^{J_i} h_j t_{ij} \right) = h_{J_i}^{\delta_i} \prod_{i=1}^{J_i} \exp(-h_j t_{ij}) \\
&= \prod_{j=1}^{J_i} h_j^{\delta_{ij}} \exp(-h_j t_{ij}),
\end{aligned} \tag{18.16}$$

where the first equality follows from 3.4, the third and fourth equalities follow from assumption 18.15 and definition 18.3, and the last equality follows from 18.2 such that $h_{J_i}^{\delta_i} = \prod_{j=1}^{J_i} h_j^{\delta_{ij}}$ (when $\delta_i = 0$, all $\delta_{ij} = 0$, when $\delta_i = 1$, only $\delta_{iJ_i} = 1$).

Now assume that the interval-specific event indicators δ_{ij} are realizations of random variables $\Delta_{ij} \stackrel{iid}{\sim} \text{Poisson}(\mu_{ij} := h_j t_{ij})$ and recall that $Z \sim \text{Poisson}(\mu)$ implies $P(Z = z) = \frac{\mu^z \exp(-\mu)}{z!}$. Thus, the likelihood contribution of subject i can be written as

$$\begin{aligned}
\mathcal{L}_{\text{Poisson},i} &= \prod_{j=1}^{J_i} P(\Delta_{ij} = \delta_{ij}) = \prod_{j=1}^{J_i} \frac{(h_j t_{ij})^{\delta_{ij}} \exp(-h_j t_{ij})}{\delta_{ij}!} \\
&= \prod_{j=1}^{J_i} h_j^{\delta_{ij}} t_{ij}^{\delta_{ij}} \exp(-h_j t_{ij}),
\end{aligned} \tag{18.17}$$

where the last equality follows from $\delta_{ij} \in \{0, 1\}$ and $0! = 1! = 1$.

Note that $\mathcal{L}_{i,\text{Poisson}} \propto \mathcal{L}_i$ from equation 18.16, since t_{ij} is a constant and does not depend on the parameters of interest (here h_j). This implies that we can estimate a model with piecewise constant hazards by optimizing the Poisson likelihood 18.17. The t_{ij} term enters as an offset term $\log(t_{ij})$ in the Poisson regression model.

More generally, in the presence of features \mathbf{x}_i , assume $\delta_{ij} | \mathbf{x}_i \stackrel{iid}{\sim} \text{Poisson}(\mu_{ij})$, where $\mu_{ij} = h_{ij} t_{ij}$ is the expected number of events in interval j given features \mathbf{x}_i and $h_{ij} = g(t_j, \mathbf{x}_i)$ is the hazard rate in interval j given features \mathbf{x}_i . This can be estimated by fitting a Poisson regression model with log-link to the transformed data set

$$\mathcal{D}_{\mathcal{A}} = \{(\delta_{ij}, t_{ij}, t_j, \mathbf{x}_{ij})\}_{i=1, \dots, n; j=1, \dots, J_i}, \tag{18.18}$$

where the model specification is

$$\log(\mathbb{E}[\Delta_{ij}]) = \log(h_{ij}) + \log(t_{ij}), \tag{18.19}$$

where $\log(h_{ij}) = g(\mathbf{x}_i, t_j)$ is the interval and feature specific hazard rate, g is a function learned by the model of choice and $\log(t_{ij})$ is included as an offset term in the Poisson likelihood/Loss function.

Importantly, in contrast to the discrete time reductions in Section 18.2, the piecewise exponential model likelihood has no information loss regarding the exact time-to-event by including the t_{ij} terms (18.3) and estimates continuous time hazards rather than discrete time hazards.

18.4.1 Example: Poisson Regression

To illustrate the piecewise constant hazards approach, we once again consider the tumor data set. We partition the follow-up time into $J = 100$ equidistant intervals. We then fit a Poisson regression model with interaction between interval and complications to allow for separate baseline hazards for each complications group:

$$\log(\mu_{ij}) = \log(\mathbb{E}[\Delta_{ij}]) = \underbrace{\beta_{0j} + \beta_{1j}x_{i1}}_{\log(h_{ij})} + \log(t_{ij}), \quad (18.20)$$

where $x_{i1} = \mathbb{I}(\text{complications}_i = \text{"yes"})$, β_{0j} are the interval-specific intercepts for the reference group (no complications), β_{1j} are the deviations from the reference group for the complications group (as in 18.12, this is estimated as an interaction model using reference coded categorical features for interval and complications), and $\log(t_{ij})$ enters as offset term.

Figure 18.6 shows the estimated survival probabilities from the piecewise exponential model (dashed lines) together with the Kaplan-Meier estimates (solid lines) for comparison. The piecewise exponential model provides an excellent fit to the data, closely approximating the Kaplan-Meier estimates. This demonstrates that the piecewise constant hazards approach can effectively estimate the survival distribution when using a sufficient number of intervals.

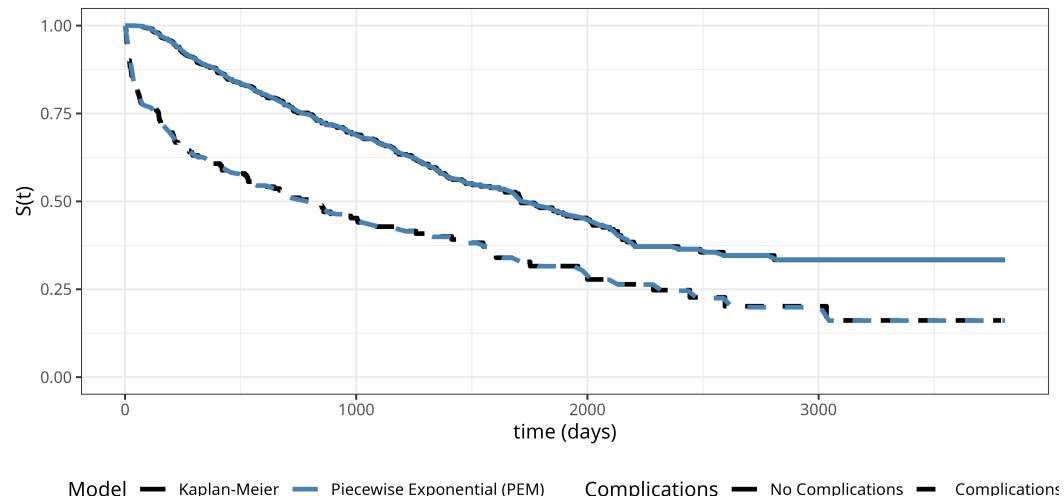


Figure 18.6: Comparison of survival probability estimates using the piecewise exponential model (Poisson regression) and the Kaplan-Meier estimator, for patients with and without complications.

18.5 Choice of Interval Boundaries

19

Reductions for Event-History Analysis

TODO (150-200 WORDS)

! Page coming soon!

We are working on this page and it will be available soon!

20

FAQs and Outlook

! Page coming soon!

We are working on this page and it will be available soon!

20.1 Common problems in survival analysis

20.1.1 Data cleaning

Events at $t=0$

Throughout this book we have defined survival times taking values in the non-negative Reals (zero inclusive) $\mathbb{R}_{\geq 0}$. In practice, model implementations assume time is over the positive Reals (zero exclusive). One must therefore consider how to deal with subjects that experience the outcome at 0. There is no established best practice for dealing with this case as the answer may be data-dependent. Possible choices include:

1. Deleting all data where the outcome occurs at $t = 0$, this may be appropriate if it only happens in a small number of observations and therefore deletion is unlikely to bias predictions;
2. Update the survival time to the next smallest observed survival time. For example, if the first observation to experience the event after $t = 0$ happens at $t = 0.1$, then set 0.1 as the survival time for any observation experiencing the event at $t = 0$. Note this method will not be appropriate when data is over a long period, for example if measuring time over years, then there could be a substantial difference between $t = 0$ and $t = 1$;
3. Update the survival time to a very small value ϵ that makes sense given the context of the data, e.g., $\epsilon = 0.0001$.

Continuous v Discrete Time

We defined survival tasks throughout this book assuming continuous time predictions in $\mathbb{R}_{\geq 0}$. In practice, many outcomes in survival analysis are recorded on a discrete scale, such as in medical statistics where outcomes are observed on a yearly, daily, monthly, hourly, etc. basis. Whilst discrete-time survival analysis exists for this purpose ([?@sec-discrete](#)), software implementations overwhelming use theory from the 'continuous-time setting'. There has not been a lot of research into whether discrete-time methods outperform continuous-time methods when correctly applied to discrete data, however available experiments do not indicate that discrete methods outperform their continuous counterparts (Suresh, Severn,

and Ghosh 2022). Therefore it is recommended to use available software implementations, even when data is recorded on a discrete scale.

20.1.2 Evaluation and prediction

- Which time points to make predictions for?
-

20.1.3 Choosing models and measures

Choosing models

In contrast to measure selection, selecting models is more straightforward and the same heuristics from regression and classification largely apply to survival analysis. Firstly, for low-dimensional data, many experiments have demonstrated that machine learning may not improve upon more standard statistical methods (Christodoulou et al. 2019) and the same holds for survival analysis (**Burk2024?**). Therefore the cost that comes with using machine learning – lower interpretability, longer training time – is unlikely to provide any performance benefits when a dataset has relatively few covariates. In settings where machine learning is more useful, then the choice largely falls into the four model classes discussed in this book: random forests, support vector machines, boosting, and neural networks (deep learning). If you have access to sufficient computational resources, then it is always worthwhile including at least one model from each class in a benchmark experiment, as models perform differently depending on the data type. However, without significant resources, the rules-of-thumb below can provide a starting point for smaller experiments.

Random survival forests and boosting methods are both good all-purpose methods that can handle different censoring types and competing risks settings. In single-event settings both have been shown to perform well on high-dimensional data, outperforming other model classes (Spooner et al. 2020). Forests require less tuning than boosting methods and the choice of hyperparameters is often more intuitive. Therefore, we generally recommend forests as the first choice for high-dimensional data. Given more resources, boosting methods such as *xgboost* are powerful to improve the predictive performance of traditional survival models. Survival support vector machines do not appear to work well in practice and to-date we have not seen any real-world use of SSVMs, therefore we generally do not recommend use of SVMs without robust training and testing first.

Neural networks are incredibly data-dependent. Moreover, given a huge increase in research into this area (Wiegerebe et al. 2024), there are no clear heuristics for recommending when to use neural networks and then which particular algorithms to use. With enough fine-tuning we have found that neural networks can work well but still without outperforming other methods. Where neural networks may shine is going beyond tabular data to incorporate other modalities, but again this area of research for survival analysis is still nascent.

Choosing measures

There are many survival measures to choose from and selecting the right one for the task might seem daunting. We have put together a few heuristics to support decision making. Evaluation should always be according to the goals of analysis, which means using discrimination measures to evaluate rankings, calibration measures to evaluate average performance, and scoring rules to evaluate overall performance and distribution predictions.

For discrimination measures, we recommend Harrell's and Uno's C. Whilst others can assess

time-dependent trends, these are also captured in scoring rules. In practice the choice of measure matters less than ensuring your reporting is transparent and honest (Therneau and Atkinson 2024; R. Sonabend et al. 2021).

To assess a single model’s calibration, graphical comparisons to the Kaplan-Meier provide a useful and interpretable method to quickly see if a model is a good fit to the data (Section 7.2.1). When choosing between models, we recommend D-calibration, which can be meaningful optimized and thus used for comparison.

When picking scoring rules, we recommend using both the ISBS and RCLL. If a model outperforms another with respect to both measures then that can be a strong indicator of performance. When reporting scoring rules, we recommend the ERV representation which provides a meaningful interpretation as ‘performance increase over baseline’.

Given the lack of research, if you are interested in survival time predictions then treat evaluation with caution and check for new developments in the literature.

For automated model optimization, we recommend tuning with a scoring rule, which should capture discrimination and calibration simultaneously [Rindt et al. (2022); Yanagisawa (2023); FIXME ECML]. Though if you are only ever using a model for ranking, then we recommend tuning with Uno’s C. Whilst it does have higher variance compared to other concordance measures (Rahman et al. 2017; Schmid and Potapov 2012), it performs better than Harrell’s C as censoring increases (Rahman et al. 2017).

Interpreting survival models

Interpreting models is increasingly important as we rely on more complex ‘black-box’ models (Molnar 2019). Classic methods that test if a model is fit well to data, such as the AIC and BIC, have been extended to survival models however are limited in application to the traditional survival models discussed in Chapter 10. As a more flexible alternative, any of the calibration measures in Chapter 7 can be used to evaluate a model’s fit to data. To assess algorithmic fairness, the majority of measures discussed in Part II can be used to detect bias in a survival context (R. Sonabend et al. 2022). Gold-standard interpretability methods such as SHAP and LIME (Molnar 2019) can be extended to survival analysis off-shelf (Langbein et al. 2024), and time-dependent extensions also exist to observe the impact of variables on the survival probability over time (Krzysiński et al. 2023; Langbein et al. 2024).

20.1.4 Competing risks

20.1.4.1 How should competing risks be handled?

There are at least three different approaches to handle competing risks: modelling, data processing, reductions. The introduction (Section 1.3) described an analysis from start to finish based on Dennis et al. (2020). This analysis looked at mortality from COVID-19 with discharge from hospital being a competing risk. In this analysis the authors considered two approaches to handle discharge from hospital.

Firstly, they consider the Fine and Gray model (Chapter 10) which is a modelling approach to handle competing risks data via subdistribution modelling. This book has also presented machine learning subdistribution models, such as CoxBoost (Chapter 13), as well as cause-specific approaches such as with random survival forests (Chapter 11).

Dennis et al. (2020) also considered a data processing approach. Instead of censoring patients at discharge (with discharge as a competing risk), they instead treated them as if they had been administratively censored at the end of the 30-day observation window. This approach

has the potential to yield similar estimates to traditional modelling strategies, but only if it is safe to assume that discharged patients are not re-admitted and that discharge means recovery from illness (Dennis et al. 2020; Docherty et al. 2020).

A third approach would be to use a reduction ([?@sec-car](#)) and model each cause independently using any of the models presented throughout this book.

Which approach you use largely depends on the data and question of interest. The data approach worked for Dennis et al. (2020) because their research question was restrictive (death within 30 days) and it was reasonable to assume discharged patients should survive at least 30 days. However, it is rare to have assumptions that work out this neatly. The modelling approach removes these restrictive assumptions however it is limited to a relatively small subset of models and metrics - so whether this can be used depends on the research question and whether the available models are suitable for the task. Finally, the reduction approach can be flexibly used with any models and measures, though may lead to models that are more difficult to interpret.

20.2 What's next for machine learning survival analysis?

References

- Aalen, Odd. 1978. “Nonparametric Inference for a Family of Counting Processes.” *The Annals of Statistics* 6 (4): 701–26.
- Aalen, Odd O., and Søren Johansen. 1978. “An Empirical Transition Matrix for Non-Homogeneous Markov Chains Based on Censored Observations.” *Scandinavian Journal of Statistics* 5 (3): 141–50. <https://www.jstor.org/stable/4615704>.
- Aalen, Odd, Ornulf Borgan, and Hakon Gjessing. 2008. *Survival and Event History Analysis: A Process Point of View*. 2008th ed. New York, NY: Springer.
- Akritas, Michael G. 1994. “Nearest Neighbor Estimation of a Bivariate Distribution Under Random Censoring.” *Ann. Statist.* 22 (3): 1299–1327. <https://doi.org/10.1214/aos/1176325630>.
- Akritas, Michael G., and Michael P. LaValley. 2005. “A Generalized Product-Limit Estimator for Truncated Data.” *Nonparametric Statistics*, September. <https://doi.org/10.1080/10485250500038637>.
- Alberge, Julie, Vincent Maladière, Olivier Grisel, Judith Abécassis, and Gaël Varoquaux. 2024. “Survival Models: Proper Scoring Rule and Stochastic Optimization with Competing Risks.” <https://arxiv.org/abs/2410.16765>.
- . 2025. “P52 - Survival Models: Proper Scoring Rule and Stochastic Optimization with Competing Risks.” *Journal of Epidemiology and Population Health* 73: 203083. <https://doi.org/https://doi.org/10.1016/j.jeph.2025.203083>.
- Allignol, Arthur, Jan Beyersmann, and Martin Schumacher. 2008. “Mvna an r Package for the Nelson-Aalen Estimator in Multistate Models.” *R News* 8 (2): 48–50.
- Andersen, Per Kragh, Mette Gerster Hansen, and John P. Klein. 2004. “Regression Analysis of Restricted Mean Survival Time Based on Pseudo-Observations.” *Lifetime Data Analysis* 10 (4): 335–50. <https://doi.org/10.1007/s10985-004-4771-0>.
- Andersen, Per Kragh, John P. Klein, and Susanne Rosthøj. 2003. “Generalised Linear Models for Correlated Pseudo-Observations, with Applications to Multi-State Models.” *Biometrika* 90 (1): 15–27. <https://www.jstor.org/stable/30042016>.
- Andersen, Per Kragh, and Maja Pohar Perme. 2010. “Pseudo-Observations in Survival Analysis.” *Statistical Methods in Medical Research* 19 (1): 71–99. <https://doi.org/10.1177/0962280209105020>.
- Andres, Axel, Aldo Montano-Loza, Russell Greiner, Max Uhlich, Ping Jin, Bret Hoehn, David Bigam, James Andrew Mark Shapiro, and Norman Mark Kneteman. 2018. “A novel learning algorithm to predict individual survival after liver transplantation for primary sclerosing cholangitis.” *PLOS ONE* 13 (3): e0193523. <https://doi.org/10.1371/journal.pone.0193523>.
- Angus, John E. 1994. “The Probability Integral Transform and Related Results.” *SIAM Review* 36 (4): 652–54. <http://www.jstor.org/stable/2132726>.
- Antolini, Laura, Patrizia Boracchi, and Elia Biganzoli. 2005. “A time-dependent discrimination index for survival data.” *Statistics in Medicine* 24 (24): 3927–44. <https://doi.org/10.1002/sim.2427>.
- Austin, Peter C., and Jason P. Fine. 2017. “Practical Recommendations for Reporting Fine-Gray Model Analyses for Competing Risk Data.” *Statistics in Medicine* 36 (27):

- 4391–4400. <https://doi.org/https://doi.org/10.1002/sim.7501>.
- Austin, Peter C., Frank E. Harrell Jr, and David van Klaveren. 2020. “Graphical Calibration Curves and the Integrated Calibration Index (ICI) for Survival Models.” *Statistics in Medicine* 39 (21): 2714–42. <https://doi.org/https://doi.org/10.1002/sim.8570>.
- Austin, Peter C., Douglas S. Lee, and Jason P. Fine. 2016. “Introduction to the Analysis of Survival Data in the Presence of Competing Risks.” *Circulation* 133 (6): 601–9. <https://doi.org/10.1161/CIRCULATIONAHA.115.017719>.
- Austin, Peter C., Hein Putter, Douglas S. Lee, and Ewout W. Steyerberg. 2022. “Estimation of the Absolute Risk of Cardiovascular Disease and Other Events: Issues with the Use of Multiple Fine-Gray Subdistribution Hazard Models.” *Circulation: Cardiovascular Quality and Outcomes* 15 (2): e008368. <https://doi.org/10.1161/CIRCOUTCOMES.121.008368>.
- Avati, Anand, Tony Duan, Sharon Zhou, Kenneth Jung, Nigam H. Shah, and Andrew Ng. 2020. “Countdown Regression: Sharp and Calibrated Survival Predictions.” In *Proceedings of Machine Learning Research*, 145–55. <https://proceedings.mlr.press/v115/avati20a.html> <http://arxiv.org/abs/1806.08324>.
- Beaulac, Cédric, Jeffrey S. Rosenthal, Qinglin Pei, Debra Friedman, Suzanne Wolden, and David Hodgson. 2020. “An Evaluation of Machine Learning Techniques to Predict the Outcome of Children Treated for Hodgkin-Lymphoma on the AHOD0031 Trial.” *Applied Artificial Intelligence* 34 (14): 1100–1114. <https://doi.org/10.1080/08839514.2020.1815151>.
- Becker, Marc, Lennart Schneider, and Sebastian Fischer. 2024. “Hyperparameter Optimization.” In *Applied Machine Learning Using mlr3 in R*, edited by Bernd Bischl, Raphael Sonabend, Lars Kotthoff, and Michel Lang. CRC Press. https://mlr3book.mlr-org.com/hyperparameter_optimization.html.
- Bello, Ghalib A, Timothy J W Dawes, Jimming Duan, Carlo Biffi, Antonio de Marvao, Luke S G E Howard, J Simon R Gibbs, et al. 2019. “Deep-learning cardiac motion analysis for human survival prediction.” *Nature Machine Intelligence* 1 (2): 95–104. <https://doi.org/10.1038/s42256-019-0019-2>.
- Benavoli, Alessio, Giorgio Corani, Janez Demšar, and Marco Zaffalon. 2017. “Time for a Change: A Tutorial for Comparing Multiple Classifiers Through Bayesian Analysis.” *Journal of Machine Learning Research* 18 (77): 1–36. <http://jmlr.org/papers/v18/16-305.html>.
- Bender, Andreas, David Rügamer, Fabian Scheipl, and Bernd Bischl. 2021. “A General Machine Learning Framework for Survival Analysis.” In *Machine Learning and Knowledge Discovery in Databases*, edited by Frank Hutter, Kristian Kersting, Jefrey Lijffjt, and Isabel Valera, 158–73. Lecture Notes in Computer Science. Cham: Springer International Publishing. https://doi.org/10.1007/978-3-030-67664-3_10.
- Bender, Andreas, and Fabian Scheipl. 2018. “pammtools: Piece-wise exponential Additive Mixed Modeling tools.” *arXiv:1806.01042 [Stat]*. <http://arxiv.org/abs/1806.01042>.
- Bennett, Steve. 1983. “Analysis of survival data by the proportional odds model.” *Statistics in Medicine* 2 (2): 273–77. <https://doi.org/https://doi.org/10.1002/sim.4780020223>.
- Beyersmann, Jan, Arthur Allignol, and Martin Schumacher. 2012. *Competing Risks and Multistate Models with R*. Use R! New York: Springer.
- Beygelzimer, Alina, Hal Daumé, John Langford, and Paul Mineiro. 2016. “Learning Reductions That Really Work.” *Proceedings of the IEEE* 104 (1): 136–47. <https://doi.org/10.1109/JPROC.2015.2494118>.
- Biganzoli, E M, F Ambrogi, and P Boracchi. 2009. “Partial logistic artificial neural networks (PLANN) for flexible modeling of censored survival data.” In *2009 International Joint Conference on Neural Networks*, 340–46. <https://doi.org/10.1109/IJCNN.2009.5178824>.
- Biganzoli, Elia, Patrizia Boracchi, Luigi Mariani, and Ettore Marubini. 1998. “Feed forward neural networks for the analysis of censored survival data: a partial logistic regression

- approach.” *Statistics in Medicine* 17 (10): 1169–86. [https://doi.org/10.1002/\(SICI\)1097-0258\(19980530\)17:10%3C1169::AID-SIM796%3E3.0.CO;2-D](https://doi.org/10.1002/(SICI)1097-0258(19980530)17:10%3C1169::AID-SIM796%3E3.0.CO;2-D).
- Binder, Harald. 2013. “CoxBoost: Cox models by likelihood based boosting for a single survival endpoint or competing risks.” CRAN.
- Binder, Harald, and Martin Schumacher. 2008. “Allowing for mandatory covariates in boosting estimation of sparse high-dimensional survival models.” *BMC Bioinformatics* 9 (1): 14. <https://doi.org/10.1186/1471-2105-9-14>.
- Bischl, Bernd, O. Mersmann, H. Trautmann, and C. Weihs. 2012. “Resampling Methods for Meta-Model Validation with Recommendations for Evolutionary Computation.” *Evolutionary Computation* 20 (2): 249–75. https://doi.org/10.1162/EVCO_a_00069.
- Bischl, Bernd, Raphael Sonabend, Lars Kotthoff, and Michel Lang, eds. 2024. *Applied Machine Learning Using mlr3 in R*. CRC Press. <https://mlr3book.mlr-org.com>.
- Bishop, Christopher M. 2006. *Pattern recognition and machine learning*. Springer.
- Blanche, Paul, Jean-François Dartigues, and Hélène Jacqmin-Gadda. 2013. “Review and comparison of ROC curve estimators for a time-dependent outcome with marker-dependent censoring.” *Biometrical Journal* 55 (5): 687–704. <https://doi.org/10.1002/bimj.201200045>.
- Blanche, Paul, Aurélien Latouche, and Vivian Viallon. 2012. “Time-dependent AUC with right-censored data: a survey study,” October. https://doi.org/10.1007/978-1-4614-8981-8_11.
- Bland, J Martin, and Douglas G. Altman. 2004. “The logrank test.” *BMJ (Clinical Research Ed.)* 328 (7447): 1073. <https://doi.org/10.1136/bmj.328.7447.1073>.
- Bommert, Andrea, Thomas Welchowski, Matthias Schmid, and Jörg Rahnenführer. 2021. “Benchmark of Filter Methods for Feature Selection in High-Dimensional Gene Expression Survival Data.” *Briefings in Bioinformatics* 23 (1): bbab354. <https://doi.org/10.1093/bib/bbab354>.
- Bonneville, Edouard F, Liesbeth C de Wreede, and Hein Putter. 2024. “Why You Should Avoid Using Multiple Fine–Gray Models: Insights from (Attempts at) Simulating Proportional Subdistribution Hazards Data.” *Journal of the Royal Statistical Society Series A: Statistics in Society* 187 (3): 580–93. <https://doi.org/10.1093/rsssa/qnae056>.
- Bouaziz, Olivier. 2023. “Fast Approximations of Pseudo-Observations in the Context of Right Censoring and Interval Censoring.” *Biometrical Journal* 65 (4): 2200071. <https://doi.org/10.1002/bimj.202200071>.
- Bou-Hamad, Imad, Denis Larocque, and Hatem Ben-Ameur. 2011. “A review of survival trees.” *Statist. Surv.* 5: 44–71. <https://doi.org/10.1214/09-SS047>.
- Bower, Hannah, Michael J Crowther, Mark J Rutherford, Therese M.-L. Andersson, Mark Clements, Xing-Rong Liu, Paul W Dickman, and Paul C Lambert. 2019. “Capturing simple and complex time-dependent effects using flexible parametric survival models: A simulation study.” *Communications in Statistics - Simulation and Computation*, July, 1–17. <https://doi.org/10.1080/03610918.2019.1634201>.
- Breiman, Leo. 1996. “Bagging Predictors.” *Machine Learning* 24 (2): 123–40. <https://doi.org/10.1023/A:1018054314350>.
- Breiman, Leo, and Philip Spector. 1992. “Submodel Selection and Evaluation in Regression. The X-Random Case.” *International Statistical Review / Revue Internationale de Statistique* 60 (3): 291–319. <https://doi.org/10.2307/1403680>.
- Breiman, L, J Friedman, C J Stone, and R A Olshen. 1984. *Classification and Regression Trees*. The Wadsworth and Brooks-Cole Statistics-Probability Series. Taylor & Francis. <https://books.google.co.uk/books?id=JwQx-WOmSyQC>.
- Breslow, N. 1972. “Discussion following ‘Regression models and life tables’ by D. R. Cox.” *Journal of the Royal Statistical Society: Series B (Statistical Methodology)* 34 (2): 187–220.
- . 1974. “Covariance Analysis of Censored Survival Data.” *Biometrics* 30 (1): 89–99. <https://doi.org/10.2307/2529620>.

- Brier, Glenn. 1950. "Verification of forecasts expressed in terms of probability." *Monthly Weather Review* 78 (1): 1–3.
- Broström, Göran. 1987. "The Influence of Mother's Death on Infant Mortality: A Case Study in Matched Data Survival Analysis." *Scandinavian Journal of Statistics* 14 (2): 113–23. <https://www.jstor.org/stable/4616055>.
- . 2024. *Eha: Event History Analysis*. <https://cran.r-project.org/package=eha>.
- Buckley, Jonathan, and Ian James. 1979. "Linear Regression with Censored Data." *Biometrika* 66 (3): 429–36. <https://doi.org/10.2307/2335161>.
- Buhlmann, Peter. 2006. "Boosting for high-dimensional linear models." *Ann. Statist.* 34 (2): 559–83. <https://doi.org/10.1214/009053606000000092>.
- Buhlmann, Peter, and Torsten Hothorn. 2007. "Boosting Algorithms: Regularization, Prediction and Model Fitting." *Statist. Sci.* 22 (4): 477–505. <https://doi.org/10.1214/07-STS242>.
- Bühlmann, Peter, and Bin Yu. 2003. "Boosting With the L2 Loss." *Journal of the American Statistical Association* 98 (462): 324–39. <https://doi.org/10.1198/016214503000125>.
- Burk, Lukas, John Zobolas, Bernd Bischl, Andreas Bender, Marvin N. Wright, and Raphael Sonabend. 2024. "A Large-Scale Neutral Comparison Study of Survival Models on Low-Dimensional Data," June. <http://arxiv.org/abs/2406.04098>.
- Candido dos Reis, Francisco J, Gordon C Wishart, Ed M Dicks, David Greenberg, Jem Rashbass, Marjanka K Schmidt, Alexandra J van den Broek, et al. 2017. "An updated PREDICT breast cancer prognostication and treatment benefit prediction model with independent validation." *Breast Cancer Research* 19 (1): 58. <https://doi.org/10.1186/s13058-017-0852-3>.
- Casalicchio, Giuseppe, and Lukas Burk. 2024. "Evaluation and Benchmarking." In *Applied Machine Learning Using mlr3 in R*, edited by Bernd Bischl, Raphael Sonabend, Lars Kotthoff, and Michel Lang. CRC Press. https://mlr3book.mlr-org.com/chapters/chapter3_evaluation_and_benchmarking.html.
- Chambless, Lloyd E, and Guoqing Diao. 2006. "Estimation of time-dependent area under the ROC curve for long-term risk prediction." *Statistics in Medicine* 25 (20): 3474–86. <https://doi.org/10.1002/sim.2299>.
- Chandrashekhar, Girish, and Ferat Sahin. 2014. "A Survey on Feature Selection Methods." *Computers & Electrical Engineering* 40 (1): 16–28. <https://doi.org/10.1016/j.compeleceng.2013.11.024>.
- Chen, Tianqi, Tong He, Michael Benesty, Vadim Khotilovich, Yuan Tang, Hyunsu Cho, Kailong Chen, et al. 2020. "xgboost: Extreme Gradient Boosting." CRAN. <https://cran.r-project.org/package=xgboost>.
- Chen, Yen-Chen, Wan-Chi Ke, and Hung-Wen Chiu. 2014. "Risk classification of cancer survival using ANN with gene expression data from multiple laboratories." *Computers in Biology and Medicine* 48: 1–7. <https://doi.org/10.1016/j.combiomed.2014.02.006>.
- Chen, Yifei, Zhenyu Jia, Dan Mercola, and Xiaohui Xie. 2013. "A Gradient Boosting Algorithm for Survival Analysis via Direct Optimization of Concordance Index." Edited by Lev Klebanov. *Computational and Mathematical Methods in Medicine* 2013: 873595. <https://doi.org/10.1155/2013/873595>.
- Ching, Travers, Xun Zhu, and Lana X Garmire. 2018. "Cox-nnet: An artificial neural network method for prognosis prediction of high-throughput omics data." *PLOS Computational Biology* 14 (4): e1006076. <https://doi.org/10.1371/journal.pcbi.1006076>.
- Choodari-Oskooei, Babak, Patrick Royston, and Mahesh K. B. Parmar. 2012a. "A simulation study of predictive ability measures in a survival model I: Explained variation measures." *Statistics in Medicine* 31 (23): 2627–43. <https://doi.org/10.1002/sim.4242>.
- . 2012b. "A simulation study of predictive ability measures in a survival model II: explained randomness and predictive accuracy." *Statistics in Medicine* 31 (23): 2644–59.

- <https://doi.org/10.1002/sim.4242>.
- Christodoulou, Evangelia, Jie Ma, Gary S Collins, Ewout W Steyerberg, Jan Y Verbakel, and Ben Van Calster. 2019. “A systematic review shows no performance benefit of machine learning over logistic regression for clinical prediction models.” *Journal of Clinical Epidemiology* 110 (June): 12–22. <https://doi.org/10.1016/j.jclinepi.2019.02.004>.
- Ciampi, Antonio, Sheilah A Hogg, Steve McKinney, and Johanne Thiffault. 1988. “RECPAM: a computer program for recursive partition and amalgamation for censored survival data and other situations frequently occurring in biostatistics. I. Methods and program features.” *Computer Methods and Programs in Biomedicine* 26 (3): 239–56. [https://doi.org/10.1016/0169-2607\(88\)90004-1](https://doi.org/10.1016/0169-2607(88)90004-1).
- Ciampi, Antonio, Johanne Thiffault, Jean Pierre Nakache, and Bernard Asselain. 1986. “Stratification by stepwise regression, correspondence analysis and recursive partition: a comparison of three methods of analysis for survival data with covariates.” *Computational Statistics and Data Analysis* 4 (3): 185–204. [https://doi.org/10.1016/0167-9473\(86\)90033-2](https://doi.org/10.1016/0167-9473(86)90033-2).
- Clevert, Djork-Arné, Thomas Unterthiner, and Sepp Hochreiter. 2015. “Fast and accurate deep network learning by exponential linear units (elus).” *arXiv Preprint arXiv:1511.07289*.
- Collett, David. 2014. *Modelling Survival Data in Medical Research*. 3rd ed. CRC.
- Cook, Richard J., and Jerald F. Lawless. 2007. *The Statistical Analysis of Recurrent Events*. Statistics for Biology and Health. New York, NY: Springer. <https://doi.org/10.1007/978-0-387-69810-6>.
- Cortes, Corinna, and Vladimir Vapnik. 1995. “Support-Vector Networks.” *Machine Learning* 20: 273–97. <https://doi.org/10.1007/BF00994018>.
- Cox, D. R. 1972. “Regression Models and Life-Tables.” *Journal of the Royal Statistical Society: Series B (Statistical Methodology)* 34 (2): 187–220.
- . 1975. “Partial Likelihood.” *Biometrika* 62 (2): 269–76. <https://doi.org/10.1080/03610910701884021>.
- Craig, Erin, Chenyang Zhong, and Robert Tibshirani. 2025. “A Review of Survival Stacking: A Method to Cast Survival Regression Analysis as a Classification Problem.” *The International Journal of Biostatistics* 21 (1): 37–51. <https://doi.org/10.1515/ijb-2022-0055>.
- Cui, Lei, Hansheng Li, Wenli Hui, Sitong Chen, Lin Yang, Yuxin Kang, Qirong Bo, and Jun Feng. 2020. “A deep learning-based framework for lung cancer survival analysis with biomarker interpretation.” *BMC Bioinformatics* 21 (1): 112. <https://doi.org/10.1186/s12859-020-3431-z>.
- Dawid, A P. 1984. “Present Position and Potential Developments: Some Personal Views: Statistical Theory: The Prequential Approach.” *Journal of the Royal Statistical Society. Series A (General)* 147 (2): 278–92. <https://doi.org/10.2307/2981683>.
- Dawid, A Philip. 1986. “Probability Forecasting.” *Encyclopedia of Statistical Sciences* 7: 210–18.
- Dawid, A Philip, and Monica Musio. 2014. “Theory and Applications of Proper Scoring Rules.” *Metron* 72 (2): 169–83. <https://arxiv.org/abs/arXiv:1401.0398v1>.
- de Wreede, Liesbeth C., Marta Fiocco, and Hein Putter. 2011. “mstate: An R Package for the Analysis of Competing Risks and Multi-State Models.” *Journal of Statistical Software* 38 (7): 1–30. <https://doi.org/10.18637/jss.v038.i07>.
- Demler, Olga V, Nina P Paynter, and Nancy R Cook. 2015. “Tests of calibration and goodness-of-fit in the survival setting.” *Statistics in Medicine* 34 (10): 1659–80. <https://doi.org/10.1002/sim.6428>.
- Demšar, Janez. 2006. “Statistical comparisons of classifiers over multiple data sets.” *Journal of Machine Learning Research* 7 (1): 1–30.

- Dennis, John M, Bilal A Mateen, Raphael Sonabend, Nicholas J Thomas, Kashyap A Patel, Andrew T Hattersley, Spiros Denaxas, Andrew P McGovern, and Sebastian J Vollmer. 2020. “Type 2 Diabetes and COVID-19-Related Mortality in the Critical Care Setting: A National Cohort Study in England, March–July 2020.” *Diabetes Care*, October, dc201444. <https://doi.org/10.2337/dc20-1444>.
- Dietterich, Thomas G. 1998. “Approximate Statistical Tests for Comparing Supervised Classification Learning Algorithms.” *Neural Computation* 10 (7): 1895–1923. <https://doi.org/10.1162/089976698300017197>.
- Docherty, Annemarie B, Ewen M Harrison, Christopher A Green, Hayley E Hardwick, Riinu Pius, Lisa Norman, Karl A Holden, et al. 2020. “Features of 20 133 UK Patients in Hospital with Covid-19 Using the ISARIC WHO Clinical Characterisation Protocol: Prospective Observational Cohort Study.” *BMJ* 369. <https://doi.org/10.1136/bmj.m1985>.
- Efron, Bradley. 1977. “The Efficiency of Cox’s Likelihood Function for Censored Data.” *Journal of the American Statistical Association* 72 (359): 557–65. <https://doi.org/10.1080/01621459.1977.10480613>.
- . 1988. “Logistic Regression, Survival Analysis, and the Kaplan-Meier Curve.” *Journal of the American Statistical Association* 83 (402): 414–25. <https://doi.org/10.2307/2288857>.
- Efron, Bradley, and Robert Tibshirani. 1997. “Improvements on Cross-Validation: The .632+ Bootstrap Method.” *Journal of the American Statistical Association* 92 (438): 548–60. <http://www.jstor.org/stable/2965703>.
- Evers, Ludger, and Claudia-Martina Messow. 2008. “Sparse kernel methods for high-dimensional survival data.” *Bioinformatics* 24 (14): 1632–38.
- Faraggi, David, and Richard Simon. 1995. “A neural network model for survival data.” *Statistics in Medicine* 14 (1): 73–82. <https://doi.org/10.1002/sim.4780140108>.
- Fine, Jason P., and Robert J. Gray. 1999. “A Proportional Hazards Model for the Subdistribution of a Competing Risk.” *Journal of the American Statistical Association* 94 (446): 496–509. <http://www.jstor.org/stable/2670170>.
- Fleming, Thomas R, Judith R O’Fallon, Peter C O’Brien, and David P Harrington. 1980. “Modified Kolmogorov-Smirnov Test Procedures with Application to Arbitrarily Right-Censored Data.” *Biometrics* 36 (4): 607–25. <https://doi.org/10.2307/2556114>.
- Foss, Natalie, and Lars Kotthoff. 2024. “Data and Basic Modeling.” In *Applied Machine Learning Using mlr3 in R*, edited by Bernd Bischl, Raphael Sonabend, Lars Kotthoff, and Michel Lang. CRC Press. https://mlr3book.mlr-org.com/data_and_basic_modeling.html.
- Fotso, Stephane. 2018. “Deep Neural Networks for Survival Analysis Based on a Multi-Task Framework.” *arXiv Preprint arXiv:1801.05512*, January. <http://arxiv.org/abs/1801.05512>.
- Fouodo, Cesaire J K, I Konig, C Weihs, A Ziegler, and M Wright. 2018. “Support vector machines for survival analysis with R.” *The R Journal* 10 (July): 412–23.
- Freund, Yoav, and Robert E Schapire. 1996. “Experiments with a new boosting algorithm.” In. Citeseer.
- Friedman, Jerome. 1999. “Stochastic Gradient Boosting.” *Computational Statistics & Data Analysis* 38 (March): 367–78. [https://doi.org/10.1016/S0167-9473\(01\)00065-2](https://doi.org/10.1016/S0167-9473(01)00065-2).
- Friedman, Jerome H. 2001. “Greedy Function Approximation: A Gradient Boosting Machine.” *The Annals of Statistics* 29 (5): 1189–1232. <http://www.jstor.org/stable/2699986>.
- Fritsch, Stefan, Frauke Guenther, and Marvin N. Wright. 2019. “neuralnet: Training of Neural Networks.” CRAN. <https://cran.r-project.org/package=neuralnet>.
- Gefeller, Olaf, and Holger Dette. 1992. “Nearest Neighbour Kernel Estimation of the Hazard Function from Censored Data.” *Journal of Statistical Computation and Simulation* 43 (1-2): 93–101. <https://doi.org/10.1080/00949659208811430>.
- Geloven, Nan van, Daniele Giardiello, Edouard F Bonneville, Lucy Teece, Chava L Ramspeck,

- Maarten van Smeden, Kym I E Snell, et al. 2022. "Validation of Prediction Models in the Presence of Competing Risks: A Guide Through Modern Methods." *BMJ* 377. <https://doi.org/10.1136/bmj-2021-069249>.
- Gensheimer, Michael F., and Balasubramanian Narasimhan. 2018. "A Simple Discrete-Time Survival Model for Neural Networks," 1–17. <https://doi.org/arXiv:1805.00917v3>.
- Gensheimer, Michael F., and Balasubramanian Narasimhan. 2019. "A scalable discrete-time survival model for neural networks." *PeerJ* 7: e6257.
- Gerds, Thomas A., and Martin Schumacher. 2006. "Consistent Estimation of the Expected Brier Score in General Survival Models with Right-Censored Event Times." *Biometrical Journal* 48 (6): 1029–40. <https://doi.org/10.1002/bimj.200610301>.
- Géron, Aurélien. 2019. *Hands-on Machine Learning with Scikit-Learn, Keras, and TensorFlow, 2nd Edition*. O'Reilly. <https://www.oreilly.com/library/view/hands-on-machine-learning/9781492032632/>.
- Giolo, Suely. 2004. "Turnbull's Nonparametric Estimator for Interval-Censored Data," January.
- Giunchiglia, Eleonora, Anton Nemchenko, and Mihaela van der Schaar. 2018. "Rnn-surv: A deep recurrent model for survival analysis." In *International Conference on Artificial Neural Networks*, 23–32. Springer.
- Gneiting, Tilmann, and Adrian E Raftery. 2007. "Strictly Proper Scoring Rules, Prediction, and Estimation." *Journal of the American Statistical Association* 102 (477): 359–78. <https://doi.org/10.1198/016214506000001437>.
- Goli, Shahrbanoo, Hossein Mahjub, Javad Faradmal, Hoda Mashayekhi, and Ali-Reza Soltanian. 2016. "Survival Prediction and Feature Selection in Patients with Breast Cancer Using Support Vector Regression." Edited by Francesco Pappalardo. *Computational and Mathematical Methods in Medicine* 2016: 2157984. <https://doi.org/10.1155/2016/2157984>.
- Goli, Shahrbanoo, Hossein Mahjub, Javad Faradmal, and Ali-Reza Soltanian. 2016. "Performance Evaluation of Support Vector Regression Models for Survival Analysis: A Simulation Study." *International Journal of Advanced Computer Science and Applications* 7 (June). <https://doi.org/10.14569/IJACSA.2016.070650>.
- Gompertz, Benjamin. 1825. "On the Nature of the Function Expressive of the Law of Human Mortality, and on a New Mode of Determining the Value of Life Contingencies." *Philosophical Transactions of the Royal Society of London* 115: 513–83.
- Gonzalez Ginestet, Pablo, Ales Kotalik, David M. Vock, Julian Wolfson, and Erin E. Gabriel. 2021. "Stacked Inverse Probability of Censoring Weighted Bagging: A Case Study In the InfCareHIV Register." *Journal of the Royal Statistical Society Series C: Applied Statistics* 70 (1): 51–65. <https://doi.org/10.1111/rssc.12448>.
- Good, I. J. 1952. "Rational Decisions." *Journal of the Royal Statistical Society. Series B (Methodological)* 14 (1): 107–14. <http://www.jstor.org/stable/2984087>.
- Gordon, Louis, and Richard A Olshen. 1985. "Tree-structured survival analysis." *Cancer Treatment Reports* 69 (10): 1065–69.
- Graf, Erika, Claudia Schmoor, Willi Sauerbrei, and Martin Schumacher. 1999. "Assessment and comparison of prognostic classification schemes for survival data." *Statistics in Medicine* 18 (17-18): 2529–45. [https://doi.org/10.1002/\(SICI\)1097-0258\(19990915/30\)18:17/18%3C2529::AID-SIM274%3E3.0.CO;2-5](https://doi.org/10.1002/(SICI)1097-0258(19990915/30)18:17/18%3C2529::AID-SIM274%3E3.0.CO;2-5).
- Graf, Erika, and Martin Schumacher. 1995. "An Investigation on Measures of Explained Variation in Survival Analysis." *Journal of the Royal Statistical Society. Series D (The Statistician)* 44 (4): 497–507. <https://doi.org/10.2307/2348898>.
- Gray, Robert J. 1988. "A Class of K-Sample Tests for Comparing the Cumulative Incidence of a Competing Risk." *The Annals of Statistics* 16 (3): 1141–54. <https://doi.org/10.1214/aos/1176350951>.
- Gressmann, Frithjof, Franz J. Király, Bilal Mateen, and Harald Oberhauser. 2018. "Proba-

- bilistic supervised learning.” <https://doi.org/10.1002/iub.552>.
- Guyon, Isabelle, and André Elisseeff. 2003. “An Introduction to Variable and Feature Selection.” *The Journal of Machine Learning Research* 3 (March): 1157–82.
- Habibi, Danial, Mohammad Rafiei, Ali Chehrei, Zahra Shayan, and Soheil Tafaqodi. 2018. “Comparison of Survival Models for Analyzing Prognostic Factors in Gastric Cancer Patients.” *Asian Pacific Journal of Cancer Prevention : APJCP* 19 (3): 749–53. <https://doi.org/10.22034/APJCP.2018.19.3.749>.
- Haider, Humza, Bret Hoehn, Sarah Davis, and Russell Greiner. 2020. “Effective ways to build and evaluate individual survival distributions.” *Journal of Machine Learning Research* 21 (85): 1–63.
- Han, Ilkyu, June Hyuk Kim, Heeseol Park, Han-Soo Kim, and Sung Wook Seo. 2018. “Deep learning approach for survival prediction for patients with synovial sarcoma.” *Tumor Biology* 40 (9): 1010428318799264. <https://doi.org/10.1177/1010428318799264>.
- Han, Kyunghwa, and Inkyung Jung. 2022. “Restricted Mean Survival Time for Survival Analysis: A Quick Guide for Clinical Researchers.” *Korean Journal of Radiology* 23 (5): 495–99. <https://doi.org/10.3348/kjr.2022.0061>.
- Hardin, James W., and Joseph M. Hilbe. 2012. *Generalized Estimating Equations*. 2nd ed. New York: Chapman and Hall/CRC. <https://doi.org/10.1201/b13880>.
- Harrell, F E Jr, K L Lee, R M Califf, D B Pryor, and R A Rosati. 1984. “Regression modelling strategies for improved prognostic prediction.” *Statistics in Medicine* 3 (2): 143–52. <https://doi.org/10.1002/sim.4780030207>.
- Harrell, Frank E., Robert M. Califf, and David B. Pryor. 1982. “Evaluating the yield of medical tests.” *JAMA* 247 (18): 2543–46. <http://dx.doi.org/10.1001/jama.1982.03320430047030>.
- Hartman, Nicholas, Sehee Kim, Kevin He, and John D. Kalbfleisch. 2022. “Concordance Indices with Left-Truncated and Right-Censored Data.” *Biometrics* 79 (3): 1624–34. <https://doi.org/10.1111/biom.13714>.
- Hastie, Trevor, Robert Tibshirani, and Jerome Friedman. 2001. *The Elements of Statistical Learning*. Springer New York Inc.
- Heagerty, Patrick J., Thomas Lumley, and Margaret S. Pepe. 2000. “Time-Dependent ROC Curves for Censored Survival Data and a Diagnostic Marker.” *Biometrics* 56 (2): 337–44. <https://doi.org/10.1111/j.0006-341X.2000.00337.x>.
- Heagerty, Patrick J., and Yingye Zheng. 2005. “Survival Model Predictive Accuracy and ROC Curves.” *Biometrics* 61 (1): 92–105. <https://doi.org/10.1111/j.0006-341X.2005.030814.x>.
- Henderson, and Velleman. 1981. “Building multiple regression models interactively.” *Biometrics* 37: 391–411.
- Herrmann, Moritz, Philipp Probst, Roman Hornung, Vindi Jurinovic, and Anne-Laure Boulesteix. 2021. “Large-scale benchmark study of survival prediction methods using multi-omics data.” *Briefings in Bioinformatics* 22 (3). <https://doi.org/10.1093/bib/bbaa167>.
- Hielscher, Thomas, Manuela Zucknick, Wiebke Werft, and Axel Benner. 2010. “On the Prognostic Value of Gene Expression Signatures for Censored Data BT - Advances in Data Analysis, Data Handling and Business Intelligence.” In, edited by Andreas Fink, Berthold Lausen, Wilfried Seidel, and Alfred Ultsch, 663–73. Berlin, Heidelberg: Springer Berlin Heidelberg.
- Hinchliffe, Sally R., and Paul C Lambert. 2013. “Flexible Parametric Modelling of Cause-Specific Hazards to Estimate Cumulative Incidence Functions.” *BMC Medical Research Methodology* 13: 13. <https://doi.org/10.1186/1471-2288-13-13>.
- Hornung, Roman, Malte Nalenz, Lennart Schneider, Andreas Bender, Ludwig Bothmann, Bernd Bischl, Thomas Augustin, and Anne-Laure Boulesteix. 2023. “Evaluating Machine Learning Models in Non-Standard Settings: An Overview and New Findings.” <https://arxiv.org/abs/2310.15108>.

- Hosmer, David W, and Stanley Lemeshow. 1980. “Goodness of fit tests for the multiple logistic regression model.” *Communications in Statistics-Theory and Methods* 9 (10): 1043–69.
- Hosmer Jr, David W, Stanley Lemeshow, and Susanne May. 2011. *Applied survival analysis: regression modeling of time-to-event data*. Vol. 618. John Wiley & Sons.
- Hothorn, Torsten, Peter Bühlmann, Thomas Kneib, Matthias Schmid, and Benjamin Hofner. 2020. “mboost: Model-Based Boosting.” CRAN. <https://cran.r-project.org/package=mboost>.
- Hothorn, Torsten, Peter Bühlmann, Sandrine Dudoit, Annette Molinaro, and Mark J Van Der Laan. 2005. “Survival ensembles.” *Biostatistics* 7 (3): 355–73. <https://doi.org/10.1093/biostatistics/kxj011>.
- Hothorn, Torsten, and Berthold Lausen. 2003. “On the exact distribution of maximally selected rank statistics.” *Computational Statistics & Data Analysis* 43 (2): 121–37. [https://doi.org/10.1016/S0167-9473\(02\)00225-6](https://doi.org/10.1016/S0167-9473(02)00225-6).
- Hothorn, Torsten, Berthold Lausen, Axel Benner, and Martin Radespiel-Tröger. 2004. “Bagging survival trees.” *Statistics in Medicine* 23 (1): 77–91. <https://doi.org/10.1002/sim.1593>.
- Huang, Shigao, Jie Yang, Simon Fong, and Qi Zhao. 2020a. “Artificial intelligence in cancer diagnosis and prognosis: Opportunities and challenges.” *Cancer Letters* 471: 61–71. <https://doi.org/https://doi.org/10.1016/j.canlet.2019.12.007>.
- . 2020b. “Artificial intelligence in cancer diagnosis and prognosis: Opportunities and challenges.” *Cancer Letters* 471: 61–71. <https://doi.org/https://doi.org/10.1016/j.canlet.2019.12.007>.
- Hung, Hung, and Chin-Tsang Chiang. 2010. “Estimation methods for time-dependent AUC models with survival data.” *The Canadian Journal of Statistics / La Revue Canadienne de Statistique* 38 (1): 8–26. <http://www.jstor.org/stable/27805213>.
- Hurvich, Clifford M, and Chih-Ling Tsai. 1989. “Regression and time series model selection in small samples.” *Biometrika* 76 (2): 297–307. <https://doi.org/10.1093/biomet/76.2.297>.
- Ibe, Oliver C. 2013. *Markov Processes for Stochastic Modeling*. 2nd ed. Academic Press. <https://www.sciencedirect.com/book/9780124077959/markov-processes-for-stochastic-modeling>.
- Ishwaran, By Hemant, Udaya B Kogalur, Eugene H Blackstone, and Michael S Lauer. 2008. “Random survival forests.” *The Annals of Statistics* 2 (3): 841–60. <https://doi.org/10.1214/08-AOAS169>.
- Ishwaran, Hemant, Eugene H Blackstone, Claire E Pothier, and Michael S Lauer. 2004. “Relative Risk Forests for Exercise Heart Rate Recovery as a Predictor of Mortality.” *Journal of the American Statistical Association* 99 (467): 591–600. <https://doi.org/10.1198/016214504000000638>.
- Ishwaran, Hemant, and Udaya B Kogalur. 2018. “randomForestSRC.” <https://cran.r-project.org/package=randomForestSRC>.
- Ishwaran, Hemant, Udaya B. Kogalur, Xi Chen, and Andy J. Minn. 2011. “Random Survival Forests for High-Dimensional Data.” *Statistical Analysis and Data Mining: The ASA Data Science Journal* 4 (1): 115–32. <https://doi.org/https://doi.org/10.1002/sam.10103>.
- Jacqmin-Gadda, Hélène, Paul Blanche, Emilie Chary, Célia Touraine, and Jean-François Dartigues. 2016. “Receiver Operating Characteristic Curve Estimation for Time to Event with Semicompeting Risks and Interval Censoring.” *Statistical Methods in Medical Research* 25 (6): 2750–66. <https://doi.org/10.1177/0962280214531691>.
- Jager, Kitty J, Paul C van Dijk, Carmine Zoccali, and Friedo W Dekker. 2008. “The analysis of survival data: the Kaplan–Meier method.” *Kidney International* 74 (5): 560–65. <https://doi.org/https://doi.org/10.1038/ki.2008.217>.
- James, Gareth, Daniela Witten, Trevor Hastie, and Robert Tibshirani. 2013. *An introduction*

- to statistical learning.* Vol. 112. New York: Springer.
- Jing, Bingzhong, Tao Zhang, Zixian Wang, Ying Jin, Kuiyuan Liu, Wenze Qiu, Liangru Ke, et al. 2019. “A deep survival analysis method based on ranking.” *Artificial Intelligence in Medicine* 98: 1–9. [https://doi.org/https://doi.org/10.1016/j.artmed.2019.06.001](https://doi.org/10.1016/j.artmed.2019.06.001).
- Johnson, Brent A, and Qi Long. 2011. “Survival ensembles by the sum of pairwise differences with application to lung cancer microarray studies.” *Ann. Appl. Stat.* 5 (2A): 1081–101. <https://doi.org/10.1214/10-AOAS426>.
- Kalbfleisch, J. D., and R. L. Prentice. 1973. “Marginal likelihoods based on Cox’s regression and life model.” *Biometrika* 60 (2): 267–78. <https://doi.org/10.1093/biomet/60.2.267>.
- Kalbfleisch, John D, and Ross L Prentice. 1980. *The statistical analysis of failure time data*. John Wiley & Sons.
- Kamarudin, Adina Najwa, Trevor Cox, and Ruwanthi Kolamunnage-Dona. 2017. “Time-dependent ROC curve analysis in medical research: Current methods and applications.” *BMC Medical Research Methodology* 17 (1): 1–19. <https://doi.org/10.1186/s12874-017-0332-6>.
- Kaplan, E. L., and Paul Meier. 1958. “Nonparametric Estimation from Incomplete Observations.” *Journal of the American Statistical Association* 53 (282): 457–81. <https://doi.org/10.2307/2281868>.
- Katzman, Jared L, Uri Shaham, Alexander Cloninger, Jonathan Bates, Tingting Jiang, and Yuval Kluger. 2018. “DeepSurv: personalized treatment recommender system using a Cox proportional hazards deep neural network.” *BMC Medical Research Methodology* 18 (1): 24. <https://doi.org/10.1186/s12874-018-0482-1>.
- Katzman, Jared, Uri Shaham, Alexander Cloninger, Jonathan Bates, Tingting Jiang, and Yuval Kluger. 2016. “Deep Survival: A Deep Cox Proportional Hazards Network,” June.
- Khan, Faisal M., and Valentina Bayer Zubek. 2008. “Support vector regression for censored data (SVRc): A novel tool for survival analysis.” *Proceedings - IEEE International Conference on Data Mining, ICDM*, 863–68. <https://doi.org/10.1109/ICDM.2008.50>.
- Király, Franz J, Bilal Mateen, and Raphael Sonabend. 2018. “NIPS - Not Even Wrong? A Systematic Review of Empirically Complete Demonstrations of Algorithmic Effectiveness in the Machine Learning and Artificial Intelligence Literature.” *arXiv*, December. <http://arxiv.org/abs/1812.07519>.
- Kirmani, S N U A, and Ramesh C Gupta. 2001. “On the Proportional Odds Model in Survival Analysis.” *Annals of the Institute of Statistical Mathematics* 53 (2): 203–16. <https://doi.org/10.1023/A:1012458303498>.
- Klein, John P, and Melvin L Moeschberger. 2003. *Survival analysis: techniques for censored and truncated data*. 2nd ed. Springer Science & Business Media.
- Kleinbaum, David G, and Mitchel Klein. 1996. *Survival Analysis a Self-Learning Text*. Springer.
- Kohavi, Ron. 1995. “A study of cross-validation and bootstrap for accuracy estimation and model selection.” *Ijcai* 14 (2): 1137–45.
- Korn, Edward L., and Richard Simon. 1990. “Measures of explained variation for survival data.” *Statistics in Medicine* 9 (5): 487–503. <https://doi.org/10.1002/sim.4780090503>.
- Korn, Edward L, and Richard Simon. 1991. “Explained Residual Variation, Explained Risk, and Goodness of Fit.” *The American Statistician* 45 (3): 201–6. <https://doi.org/10.2307/2684290>.
- Krzyżysiński, Mateusz, Mikołaj Spytek, Hubert Baniecki, and Przemysław Biecek. 2023. “SurvSHAP(t): Time-Dependent Explanations of Machine Learning Survival Models.” *Knowledge-Based Systems* 262: 110234. <https://doi.org/https://doi.org/10.1016/j.knosys.2022.110234>.
- Kuhn, Max, and Julia Silge. 2023. *Tidy Modeling with R*. <https://www.tnwr.org/>.
- Kvamme, Håvard. 2018. “Pycox.” <https://pypi.org/project/pycox/>.

- Kvamme, Håvard, and Ørnulf Borgan. 2023. “The Brier Score Under Administrative Censoring: Problems and a Solution.” *Journal of Machine Learning Research* 24 (2): 1–26. <http://jmlr.org/papers/v24/19-1030.html>.
- Kvamme, Håvard, Ørnulf Borgan, and Ida Scheel. 2019. “Time-to-event prediction with neural networks and Cox regression.” *Journal of Machine Learning Research* 20 (129): 1–30.
- Land, Walker H, Xingye Qiao, Dan Margolis, and Ron Gottlieb. 2011. “A new tool for survival analysis: evolutionary programming/evolutionary strategies (EP/ES) support vector regression hybrid using both censored / non-censored (event) data.” *Procedia Computer Science* 6: 267–72. <https://doi.org/https://doi.org/10.1016/j.procs.2011.08.050>.
- Langbein, Sophie Hanna, Mateusz Krzyżniński, Mikołaj Spytek, Hubert Baniecki, Przemysław Biecek, and Marvin N. Wright. 2024. “Interpretable Machine Learning for Survival Analysis.” <https://arxiv.org/abs/2403.10250>.
- Lao, Jiangwei, Yinsheng Chen, Zhi-Cheng Li, Qihua Li, Ji Zhang, Jing Liu, and Guangtao Zhai. 2017. “A Deep Learning-Based Radiomics Model for Prediction of Survival in Glioblastoma Multiforme.” *Scientific Reports* 7 (1): 10353. <https://doi.org/10.1038/s41598-017-10649-8>.
- LeBlanc, Michael, and John Crowley. 1992. “Relative Risk Trees for Censored Survival Data.” *Biometrics* 48 (2): 411–25. <https://doi.org/10.2307/2532300>.
- . 1993. “Survival Trees by Goodness of Split.” *Journal of the American Statistical Association* 88 (422): 457–67. <https://doi.org/10.2307/2290325>.
- Lee, Changhee, William Zame, Jinsung Yoon, and Mihaela Van der Schaar. 2018. “DeepHit: A Deep Learning Approach to Survival Analysis With Competing Risks.” *Proceedings of the AAAI Conference on Artificial Intelligence* 32 (1). <https://doi.org/10.1609/aaai.v32i1.11842>.
- Lee, Donald K K, Ningyuan Chen, and Hemant Ishwaran. 2019. “Boosted nonparametric hazards with time-dependent covariates.” <https://arxiv.org/abs/arXiv:1701.07926v6>.
- Li, Jialiang, and Shuangge Ma. 2011. “Time-Dependent ROC Analysis Under Diverse Censoring Patterns.” *Statistics in Medicine* 30 (11): 1266–77. <https://doi.org/https://doi.org/10.1002/sim.4178>.
- Li, Liang, Tom Greene, and Bo Hu. 2018. “A simple method to estimate the time-dependent receiver operating characteristic curve and the area under the curve with right censored data.” *Statistical Methods in Medical Research* 27 (8): 2264–78. <https://doi.org/10.1177/0962280216680239>.
- Liang, Hua, and Guohua Zou. 2008. “Improved AIC Selection Strategy for Survival Analysis.” *Computational Statistics & Data Analysis* 52 (5): 2538–48. <https://doi.org/10.1016/j.csda.2007.09.003>.
- Liestol, Knut, Per Kragh Andersen, and Ulrich Andersen. 1994. “Survival analysis and neural nets.” *Statistics in Medicine* 13 (12): 1189–1200. <https://doi.org/10.1002/sim.4780131202>.
- Lin, D. Y. 2007. “On the Breslow Estimator.” *Lifetime Data Analysis* 13 (4): 471–80. <https://doi.org/10.1007/s10985-007-9048-y>.
- Loh, De Rong, Elliot D Hill, Nan Liu, Geraldine Dawson, and Matthew M Engelhard. 2025. “Limitations of Binary Classification for Long-Horizon Diagnosis Prediction and Advantages of a Discrete-Time Time-to-Event Approach: Empirical Analysis.” *JMIR AI* 4 (March): e62985. <https://doi.org/10.2196/62985>.
- Lundberg, Scott M, and Su-In Lee. 2017. “A Unified Approach to Interpreting Model Predictions.” *Advances in Neural Information Processing Systems* 30.
- Lundin, M, J Lundin, H B Burke, S Toikkanen, L Pylkkänen, and H Joensuu. 1999. “Artificial Neural Networks Applied to Survival Prediction in Breast Cancer.” *Oncology* 57 (4): 281–86. <https://doi.org/10.1159/000012061>.
- Luxhoj, James T., and Huan Jyh Shyur. 1997. “Comparison of proportional hazards models

- and neural networks for reliability estimation.” *Journal of Intelligent Manufacturing* 8 (3): 227–34. <https://doi.org/10.1023/A:1018525308809>.
- Ma, Shuangge, and Jian Huang. 2006. “Regularized ROC method for disease classification and biomarker selection with microarray data.” *Bioinformatics (Oxford, England)* 21 (January): 4356–62. <https://doi.org/10.1093/bioinformatics/bti724>.
- Mani, D R, James Drew, Andrew Betz, and Piew Datta. 1999. “Statistics and data mining techniques for lifetime value modeling.” In *Proceedings of the Fifth ACM SIGKDD International Conference on Knowledge Discovery and Data Mining*, 94–103.
- Mantel, N., N. R. Bohidar, and J. L. Ciminera. 1977. “Mantel-Haenszel analyses of litter-matched time to response data, with modifications for recovery of interlitter information.” *Cancer Research* 37: 3863–68.
- Mariani, L, D Coradini, E Biganzoli, P Boracchi, E Marubini, S Pilotti, B Salvadori, et al. 1997. “Prognostic factors for metachronous contralateral breast cancer: A comparison of the linear Cox regression model and its artificial neural network extension.” *Breast Cancer Research and Treatment* 44 (2): 167–78. <https://doi.org/10.1023/A:1005765403093>.
- Mayr, Andreas, Benjamin Hofner, and Matthias Schmid. 2016. “Boosting the discriminatory power of sparse survival models via optimization of the concordance index and stability selection.” *BMC Bioinformatics* 17 (1): 288. <https://doi.org/10.1186/s12859-016-1149-8>.
- Mayr, Andreas, and Matthias Schmid. 2014. “Boosting the concordance index for survival data—a unified framework to derive and evaluate biomarker combinations.” *PloS One* 9 (1): e84483–83. <https://doi.org/10.1371/journal.pone.0084483>.
- McGough, Sarah F., Devin Incerti, Svetlana Lyalina, Ryan Copping, Balasubramanian Narasimhan, and Robert Tibshirani. 2021. “Penalized Regression for Left-Truncated and Right-Censored Survival Data.” *Statistics in Medicine* 40 (25): 5487–5500. <https://doi.org/https://doi.org/10.1002/sim.9136>.
- McKinney, Scott Mayer, Marcin Sieniek, Varun Godbole, Jonathan Godwin, Natasha Antropova, Hutan Ashrafiyan, Trevor Back, et al. 2020. “International evaluation of an AI system for breast cancer screening.” *Nature* 577 (7788): 89–94. <https://doi.org/10.1038/s41586-019-1799-6>.
- Meinshausen, Nicolai, and Peter Bühlmann. 2010. “Stability selection.” *Journal of the Royal Statistical Society: Series B (Statistical Methodology)* 72 (4): 417–73. <https://doi.org/10.1111/j.1467-9868.2010.00740.x>.
- Moghimi-dehkordi, Bijan, Azadeh Safaei, Mohamad Amin Pourhoseingholi, Reza Fatemi, Ziaoddin Tabeie, and Mohammad Reza Zali. 2008. “Statistical Comparison of Survival Models for Analysis of Cancer Data.” *Asian Pacific Journal of Cancer Prevention* 9: 417–20.
- Molnar, Christoph. 2019. *Interpretable Machine Learning*. <https://christophm.github.io/interpretable-ml-book/>.
- Monterrubio-Gómez, Karla, Nathan Constantine-Cooke, and Catalina A. Vallejos. 2024. “A Review on Statistical and Machine Learning Competing Risks Methods.” *Biometrical Journal* 66 (2): 2300060. <https://doi.org/https://doi.org/10.1002/bimj.202300060>.
- Morales-Hernández, Alejandro, Inneke Van Nieuwenhuyse, and Sebastian Rojas Gonzalez. 2023. “A survey on multi-objective hyperparameter optimization algorithms for machine learning.” *Artificial Intelligence Review* 56 (8): 8043–93. <https://doi.org/10.1007/s10462-022-10359-2>.
- Muldowney, Pat, Krzysztof Ostaszewski, and Wojciech Wojdowski. 2012. “The Darth Vader Rule.” *Tatra Mountains Mathematical Publications* 52 (1): 53–63. <https://doi.org/10.2478/v10127-012-0025-9>.
- Müller, Hans-Georg, and Jane-Ling Wang. 1994. “Hazard Rate Estimation Under Random Censoring with Varying Kernels and Bandwidths.” *Biometrics* 50 (1): 61–76. <http://www.jstor.org/stable/2533197>.

- Murphy, Allan H. 1973. "A New Vector Partition of the Probability Score." *Journal of Applied Meteorology and Climatology* 12 (4): 595–600. [https://doi.org/10.1175/1520-0450\(1973\)012%3C0595:ANVPOT%3E2.0.CO;2](https://doi.org/10.1175/1520-0450(1973)012%3C0595:ANVPOT%3E2.0.CO;2).
- N. Venables, W., and B D. Ripley. 2002. *Modern Applied Statistics with S*. Springer. <http://www.stats.ox.ac.uk/pub/MASS4>.
- Nadeau, Claude, and Yoshua Bengio. 2003. "Inference for the Generalization Error." *Machine Learning* 52 (3): 239–81. <https://doi.org/10.1023/A:1024068626366>.
- Nair, Vinod, and Geoffrey E Hinton. 2010. "Rectified linear units improve restricted boltzmann machines." In *Proceedings of the 27th International Conference on Machine Learning (ICML-10)*, 807–14.
- Nelson, Wayne. 1972. "Theory and Applications of Hazard Plotting for Censored Failure Data." *Technometrics* 14 (4): 945–66.
- Ng, Ryan, Kathy Kornas, Rinku Sutradhar, Walter P. Wodchis, and Laura C. Rosella. 2018. "The current application of the Royston-Parmar model for prognostic modeling in health research: a scoping review." *Diagnostic and Prognostic Research* 2 (1): 4. <https://doi.org/10.1186/s41512-018-0026-5>.
- Oh, Sung Eun, Sung Wook Seo, Min-Gew Choi, Tae Sung Sohn, Jae Moon Bae, and Sung Kim. 2018. "Prediction of Overall Survival and Novel Classification of Patients with Gastric Cancer Using the Survival Recurrent Network." *Annals of Surgical Oncology* 25 (5): 1153–59. <https://doi.org/10.1245/s10434-018-6343-7>.
- Ohno-Machado, Lucila. 1996. "Medical applications of artificial neural networks: connectionist models of survival." Stanford University Stanford, Calif.
- . 1997. "A COMPARISON OF COX PROPORTIONAL HAZARDS AND ARTIFICIAL NEURAL NETWORK MODELS FOR MEDICAL PROGNOSIS The theoretical advantages and disadvantages of using different methods for predicting survival have seldom been tested in real data sets [1 , 2]. Althou." *Comput. Biol. Med* 27 (1): 55–65.
- Parner, Erik T., Per K. Andersen, and Morten Overgaard. 2023. "Regression Models for Censored Time-to-Event Data Using Infinitesimal Jack-Knife Pseudo-Observations, with Applications to Left-Truncation." *Lifetime Data Analysis* 29 (3): 654–71. <https://doi.org/10.1007/s10985-023-09597-5>.
- Patel, Katie, Richard Kay, and Lucy Rowell. 2006. "Comparing proportional hazards and accelerated failure time models: An application in influenza." *Pharmaceutical Statistics* 5 (3): 213–24. <https://doi.org/10.1002/pst.213>.
- Piller, Johannes, Léa Orsini, Simon Wiegrebé, John Zobolas, Lukas Burk, Sophie Hanna Langbein, Philip Studener, Markus Goeswein, and Andreas Bender. 2025. "Reduction Techniques for Survival Analysis." arXiv. <https://doi.org/10.48550/arXiv.2508.05715>.
- Pölsterl, Sebastian. 2020. "scikit-survival: A Library for Time-to-Event Analysis Built on Top of scikit-learn." *Journal of Machine Learning Research* 21 (212): 1–6. <http://jmlr.org/papers/v21/20-729.html>.
- Probst, Philipp, Anne-Laure Boulesteix, and Bernd Bischl. 2019. "Tunability: Importance of Hyperparameters of Machine Learning Algorithms." *Journal of Machine Learning Research* 20 (53): 1–32. <http://jmlr.org/papers/v20/18-444.html>.
- Puddu, Paolo Emilio, and Alessandro Menotti. 2012. "Artificial neural networks versus proportional hazards Cox models to predict 45-year all-cause mortality in the Italian Rural Areas of the Seven Countries Study." *BMC Medical Research Methodology* 12 (1): 100. <https://doi.org/10.1186/1471-2288-12-100>.
- Qi, Jiezhī. 2009. "Comparison of Proportional Hazards and Accelerated Failure Time Models." PhD thesis.
- Qi, Shi-Ang, Neeraj Kumar, Mahtab Farrokh, Weijie Sun, Li-Hao Kuan, Rajesh Ranganath, Ricardo Henao, and Russell Greiner. 2023. "An Effective Meaningful Way to Evaluate Survival Models." In *Proceedings of the 40th International Conference on Machine Learn-*

- ing, edited by Andreas Krause, Emma Brunskill, Kyunghyun Cho, Barbara Engelhardt, Sivan Sabato, and Jonathan Scarlett, 202:28244–76. Proceedings of Machine Learning Research. PMLR. <https://proceedings.mlr.press/v202/qi23b.html>.
- R., Cox, and Snell J. 1968. “A General Definition of Residuals.” *Journal of the Royal Statistical Society: Series B (Statistical Methodology)* 30 (2): 248–75.
- Rahman, M. Shafiqur, Gareth Ambler, Babak Choodari-Oskooei, and Rumana Z. Omar. 2017. “Review and evaluation of performance measures for survival prediction models in external validation settings.” *BMC Medical Research Methodology* 17 (1): 1–15. <https://doi.org/10.1186/s12874-017-0336-2>.
- Reid, Nancy. 1994. “A Conversation with Sir David Cox.” *Statistical Science* 9 (3): 439–55. <https://doi.org/10.1214/ss/1177010394>.
- Ridgeway, Greg. 1999. “The state of boosting.” *Computing Science and Statistics* 31: 172–81.
- Rietschel, Carl, Jinsung Yoon, and Mihaela van der Schaar. 2018. “Feature Selection for Survival Analysis with Competing Risks using Deep Learning.” *arXiv Preprint arXiv:1811.09317*.
- Rindt, David, Robert Hu, David Steinsaltz, and Dino Sejdinovic. 2022. “Survival Regression with Proper Scoring Rules and Monotonic Neural Networks,” March. <http://arxiv.org/abs/2103.14755>.
- Ripley, Brian D, and Ruth M Ripley. 2001. “Neural networks as statistical methods in survival analysis.” In *Clinical Applications of Artificial Neural Networks*, edited by Richard Dybowski and Vanya Gant, 237–55. Cambridge: Cambridge University Press. <https://doi.org/DOI: 10.1017/CBO9780511543494.011>.
- Ripley, R M, A L Harris, and L Tarassenko. 1998. “Neural network models for breast cancer prognosis.” *Neural Computing & Applications* 7 (4): 367–75. <https://doi.org/10.1007/BF01428127>.
- Royston, Patrick, and Douglas G. Altman. 2013. “External validation of a Cox prognostic model: Principles and methods.” *BMC Medical Research Methodology* 13 (1). <https://doi.org/10.1186/1471-2288-13-33>.
- Royston, Patrick, and Mahesh K. B. Parmar. 2002. “Flexible parametric proportional-hazards and proportional-odds models for censored survival data, with application to prognostic modelling and estimation of treatment effects.” *Statistics in Medicine* 21 (15): 2175–97. <https://doi.org/10.1002/sim.1203>.
- . 2011. “The Use of Restricted Mean Survival Time to Estimate the Treatment Effect in Randomized Clinical Trials When the Proportional Hazards Assumption Is in Doubt.” *Statistics in Medicine* 30 (19): 2409–21. <https://doi.org/10.1002/sim.4274>.
- Royston, Patrick, and Willi Sauerbrei. 2004. “A new measure of prognostic separation in survival data.” *Statistics in Medicine* 23 (5): 723–48. <https://doi.org/10.1002/sim.1621>.
- Sasheygi, Andreas, and David Ferry. 2017. “On the Interpretation of the Hazard Ratio and Communication of Survival Benefit.” *The Oncologist* 22 (4): 484–86. <https://doi.org/10.1634/theoncologist.2016-0198>.
- Schemper, Michael, and Robin Henderson. 2000. “Predictive Accuracy and Explained Variation in Cox Regression.” *Biometrics* 56: 249–55. <https://doi.org/10.1002/sim.1486>.
- Schemper, Michael, Samo Wakounig, and Georg Heinze. 2009. “The estimation of average hazard ratios by weighted Cox regression.” *Statistics in Medicine* 28 (19): 2473–89. <https://doi.org/10.1002/sim.3623>.
- Schmid, Matthias, Thomas Hielscher, Thomas Augustin, and Olaf Gefeller. 2011. “A Robust Alternative to the Schemper-Henderson Estimator of Prediction Error.” *Biometrics* 67 (2): 524–35. <https://doi.org/10.1111/j.1541-0420.2010.01459.x>.
- Schmid, Matthias, and Torsten Hothorn. 2008a. “Boosting additive models using component-wise P-splines.” *Computational Statistics & Data Analysis* 53 (2): 298–311.

- . 2008b. “Flexible boosting of accelerated failure time models.” *BMC Bioinformatics* 9 (February): 269. <https://doi.org/10.1186/1471-2105-9-269>.
- Schmid, Matthias, and Sergej Potapov. 2012. “A comparison of estimators to evaluate the discriminatory power of time-to-event models.” *Statistics in Medicine* 31 (23): 2588–2609. <https://doi.org/10.1002/sim.5464>.
- Schmid, Matthias, Marvin Wright, and Andreas Ziegler. 2016. “On the Use of Harrell’s c for Clinical Risk Prediction via Random Survival Forests.” *Expert Systems with Applications* 63 (July). <https://doi.org/10.1016/j.eswa.2016.07.018>.
- Schoop, Rotraud, Martin Schumacher, and Erika Graf. 2011. “Measures of prediction error for survival data with longitudinal covariates.” *Biometrical Journal* 53 (2): 275–93. <https://doi.org/10.1002/bimj.201000145>.
- Schwarzer, Guido, Werner Vach, and Martin Schumacher. 2000. “On the misuses of artificial neural networks for prognostic and diagnostic classification in oncology.” *Statistics in Medicine* 19 (4): 541–61. [https://doi.org/10.1002/\(SICI\)1097-0258\(20000229\)19:4%3C541::AID-SIM355%3E3.0.CO;2-V](https://doi.org/10.1002/(SICI)1097-0258(20000229)19:4%3C541::AID-SIM355%3E3.0.CO;2-V).
- Segal, Mark Robert. 1988. “Regression Trees for Censored Data.” *Biometrics* 44 (1): 35–47.
- Seker, H., M. O. Odetayo, D. Petrovic, R. N. G. Naguib, C. Bartoli, L. Alasio, M. S. Lakshmi, G. V. Sherbet, and O. R. Hinton. 2002. “An Artificial Neural Network Based Feature Evaluation Index for the Assessment of Clinical Factors in Breast Cancer Survival Analysis.” In *IEEE CCECE2002. Canadian Conference on Electrical and Computer Engineering. Conference Proceedings (Cat. No.02CH37373)*, 2:1211–1215 vol.2. <https://doi.org/10.1109/CCECE.2002.1013121>.
- Seker, Huseyin, Michael O Odetayo, Dobrila Petrovic, Raouf N G Naguib, C Bartoli, L Alasio, M S Lakshmi, and G V Sherbet. 2002. “Assessment of nodal involvement and survival analysis in breast cancer patients using image cytometric data: statistical, neural network and fuzzy approaches.” *Anticancer Research* 22 (1A): 433–38. <http://europepmc.org/abstract/MED/12017328>.
- Shivaswamy, Pannagadatta K., Wei Chu, and Martin Jansche. 2007. “A support vector approach to censored targets.” In *Proceedings - IEEE International Conference on Data Mining, ICDM*, 655–60. <https://doi.org/10.1109/ICDM.2007.93>.
- Simon, Noah, Jerome H. Friedman, Trevor Hastie, and Rob Tibshirani. 2011. “Regularization Paths for Cox’s Proportional Hazards Model via Coordinate Descent.” *Journal of Statistical Software* 39 (5): 1–13. <https://doi.org/10.18637/jss.v039.i05>.
- Simon, Richard. 2007. “Resampling Strategies for Model Assessment and Selection.” In *Fundamentals of Data Mining in Genomics and Proteomics*, edited by Werner Dubitzky, Martin Granzow, and Daniel Berrar, 173–86. Boston, MA: Springer US. https://doi.org/10.1007/978-0-387-47509-7_8.
- Sonabend, Raphael. 2020. “survivalmodels: Models for Survival Analysis.” CRAN. <https://raphael.s1.r-universe.dev/ui#package:survivalmodels>.
- Sonabend, Raphael Edward Benjamin. 2021. “A Theoretical and Methodological Framework for Machine Learning in Survival Analysis: Enabling Transparent and Accessible Predictive Modelling on Right-Censored Time-to-Event Data.” PhD, University College London (UCL). <https://discovery.ucl.ac.uk/id/eprint/10129352/>.
- Sonabend, Raphael, Andreas Bender, and Sebastian Vollmer. 2022. “Avoiding C-hacking when evaluating survival distribution predictions with discrimination measures.” Edited by Zhiyong Lu. *Bioinformatics* 38 (17): 4178–84. <https://doi.org/10.1093/bioinformatics/btac451>.
- Sonabend, Raphael, Florian Pfisterer, Alan Mishler, Moritz Schauer, Lukas Burk, Sumantrak Mukherjee, and Sebastian Vollmer. 2022. “Flexible Group Fairness Metrics for Survival Analysis.” In *DSHealth 2022 Workshop on Applied Data Science for Healthcare at KDD2022*. <http://arxiv.org/abs/2206.03256>.

- Sonabend, Raphael, Lilith K Whittles, Natsuko Imai, Pablo N Perez-Guzman, Edward S Knock, Thomas Rawson, Katy A M Gaythorpe, et al. 2021. “Non-pharmaceutical interventions, vaccination, and the SARS-CoV-2 delta variant in England: a mathematical modelling study.” *The Lancet*. [https://doi.org/https://doi.org/10.1016/S0140-6736\(21\)02276-5](https://doi.org/10.1016/S0140-6736(21)02276-5).
- Sonabend, Raphael, John Zobolas, Riccardo Be Bin, Philipp Kopper, Lukas Burk, and Andreas Bender. 2025. “Examining Marginal Properness in the External Validation of Survival Models with Squared and Logarithmic Losses.” <https://arxiv.org/abs/2212.05260>.
- Song, Xiao, and Xiao-Hua Zhou. 2008. “A semiparametric approach for the covariate specific ROC curve with survival outcome.” *Statistica Sinica* 18 (July): 947–65.
- Spooner, Annette, Emily Chen, Arcot Sowmya, Perminder Sachdev, Nicole A Kochan, Julian Trollor, and Henry Brodaty. 2020. “A comparison of machine learning methods for survival analysis of high-dimensional clinical data for dementia prediction.” *Scientific Reports* 10 (1): 20410. <https://doi.org/10.1038/s41598-020-77220-w>.
- Spruance, Spotswood L, Julia E Reid, Michael Grace, and Matthew Samore. 2004. “Hazard ratio in clinical trials.” *Antimicrobial Agents and Chemotherapy* 48 (8): 2787–92. <https://doi.org/10.1128/AAC.48.8.2787-2792.2004>.
- Srivastava, Nitish, Geoffrey Hinton, Alex Krizhevsky, Ilya Sutskever, and Ruslan Salakhutdinov. 2014. “Dropout: a simple way to prevent neural networks from overfitting.” *The Journal of Machine Learning Research* 15 (1): 1929–58.
- Stasinopoulos, Mikis, Bob Rigby, Vlasios Voudouris, and Daniil Kiose. 2020. “gamlss.add: Extra Additive Terms for Generalized Additive Models for Location Scale and Shape.” CRAN. <https://cran.r-project.org/package=gamlss.add>.
- Street, W Nick. 1998. “A Neural Network Model for Prognostic Prediction.” In *Proceedings of the Fifteenth International Conference on Machine Learning*. San Francisco.
- Suresh, Krithika, Cameron Severn, and Debashis Ghosh. 2022. “Survival prediction models: an introduction to discrete-time modeling.” *BMC Medical Research Methodology* 22 (1): 207. <https://doi.org/10.1186/s12874-022-01679-6>.
- Therneau, Terry M. 2015. “A Package for Survival Analysis in S.” <https://cran.r-project.org/package=survival>.
- Therneau, Terry M., and Elizabeth Atkinson. 2024. “Concordance.” <https://cran.r-project.org/web/packages/survival/vignettes/concordance.pdf>.
- Therneau, Terry M., and Patricia M. Grambsch. 2001. *Modeling Survival Data: Extending the Cox Model*. 1st ed. 2000. Corr. 2nd printing 2001. New York: Springer.
- Therneau, Terry M., Patricia M. Grambsch, and Thomas R. Fleming. 1990. “Martingale-based residuals for survival models.” *Biometrika* 77 (1): 147–60. <https://doi.org/10.1093/biomet/77.1.147>.
- Tibshirani, Robert. 1997. “The Lasso Method for Variable Selection in the Cox Model.” *Statistics in Medicine* 16 (4): 385–95. [https://doi.org/https://doi.org/10.1002/\(SICI\)1097-0258\(19970228\)16:4%3C385::AID-SIM380%3E3.0.CO;2-3](https://doi.org/10.1002/(SICI)1097-0258(19970228)16:4%3C385::AID-SIM380%3E3.0.CO;2-3).
- Tsouprou, Sofia. 2015. “Measures of Discrimination and Predictive Accuracy for Interval Censored Survival Data.” Master's thesis.
- Turnbull, Bruce W. 1974. “Nonparametric Estimation of a Survivorship Function with Doubly Censored Data.” *Journal of the American Statistical Association* 69 (345): 169–73. <https://doi.org/10.1080/01621459.1974.10480146>.
- Tutz, Gerhard, and Harald Binder. 2007. “Boosting Ridge Regression.” *Computational Statistics & Data Analysis* 51 (February): 6044–59. <https://doi.org/10.1016/j.csda.2006.11.041>.
- Tutz, Gerhard, and Matthias Schmid. 2016. *Modeling Discrete Time-to-Event Data*. Springer Series in Statistics. Cham: Springer International Publishing. <https://doi.org/10.1007/>

- [978-3-319-28158-2](#).
- Uno, Hajime, Tianxi Cai, Michael J. Pencina, Ralph B. D'Agostino, and L J Wei. 2011. "On the C-statistics for Evaluating Overall Adequacy of Risk Prediction Procedures with Censored Survival Data." *Statistics in Medicine* 30 (10): 1105–17. <https://doi.org/10.1002/sim.4154>.
- Uno, Hajime, Tianxi Cai, Lu Tian, and L J Wei. 2007. "Evaluating Prediction Rules for t-Year Survivors with Censored Regression Models." *Journal of the American Statistical Association* 102 (478): 527–37. <http://www.jstor.org/stable/27639883>.
- Uno, Hajime, Brian Claggett, Lu Tian, Eisuke Inoue, Paul Gallo, Toshio Miyata, Deborah Schrag, et al. 2014. "Moving Beyond the Hazard Ratio in Quantifying the Between-Group Difference in Survival Analysis." *Journal of Clinical Oncology* 32 (22): 2380–85. <https://doi.org/10.1200/JCO.2014.55.2208>.
- Ushey, Kevin, J J Allaire, and Yuan Tang. 2020. "reticulate: Interface to 'Python'." CRAN. <https://cran.r-project.org/package=reticulate>.
- Vakulenko-Lagun, Bella, Micha Mandel, and Rebecca A. Betensky. 2020. "Inverse Probability Weighting Methods for Cox Regression with Right-Truncated Data." *Biometrics* 76 (2): 484–95. <https://doi.org/10.1111/biom.13162>.
- Van Belle, Vanya, Kristiaan Pelckmans, Johan A K Suykens, and Sabine Van Huffel. 2008. "Survival SVM: a practical scalable algorithm." In *Proceedings of the 16th European Symposium on Artificial Neural Networks (ESANN)*, 89–94.
- Van Belle, Vanya, Kristiaan Pelckmans, Johan A. K. Suykens, and Sabine Van Huffel. 2007. "Support Vector Machines for Survival Analysis." In *In Proceedings of the Third International Conference on Computational Intelligence in Medicine and Healthcare*. 1.
- Van Belle, Vanya, Kristiaan Pelckmans, Sabine Van Huffel, and Johan A. K. Suykens. 2011. "Support vector methods for survival analysis: A comparison between ranking and regression approaches." *Artificial Intelligence in Medicine* 53 (2): 107–18. <https://doi.org/10.1016/j.artmed.2011.06.006>.
- Van Houwelingen, Hans C. 2000. "Validation, calibration, revision and combination of prognostic survival models." *Statistics in Medicine* 19 (24): 3401–15. [https://doi.org/10.1002/1097-0258\(20001230\)19:24%3C3401::AID-SIM554%3E3.0.CO;2-2](https://doi.org/10.1002/1097-0258(20001230)19:24%3C3401::AID-SIM554%3E3.0.CO;2-2).
- . 2007. "Dynamic prediction by landmarking in event history analysis." *Scandinavian Journal of Statistics* 34 (1): 70–85. <https://doi.org/10.1111/j.1467-9469.2006.00529.x>.
- Vock, David M, Julian Wolfson, Sunayan Bandyopadhyay, Gediminas Adomavicius, Paul E Johnson, Gabriela Vazquez-Benitez, and Patrick J O'Connor. 2016. "Adapting machine learning techniques to censored time-to-event health record data: A general-purpose approach using inverse probability of censoring weighting." *Journal of Biomedical Informatics* 61: 119–31. <https://doi.org/https://doi.org/10.1016/j.jbi.2016.03.009>.
- Volinsky, Chris T, and Adrian E Raftery. 2000. "Bayesian Information Criterion for Censored Survival Models." *International Biometric Society* 56 (1): 256–62.
- Wang, Ping, Yan Li, and Chandan K. Reddy. 2019. "Machine Learning for Survival Analysis." *ACM Computing Surveys* 51 (6): 1–36. <https://doi.org/10.1145/3214306>.
- Wang, Zhu, and C Y Wang. 2010. "Buckley-James Boosting for Survival Analysis with High-Dimensional Biomarker Data." *Statistical Applications in Genetics and Molecular Biology* 9 (1). <https://doi.org/https://doi.org/10.2202/1544-6115.1550>.
- Wei, L J. 1992. "The Accelerated Failure Time Model: A Useful Alternative to the Cox Regression Model in Survival Analysis." *Statistics in Medicine* 11: 1871–79.
- Wiegerebe, Simon, Philipp Kopper, Raphael Sonabend, Bernd Bischl, and Andreas Bender. 2024. "Deep learning for survival analysis: a review." *Artificial Intelligence Review* 57 (3): 65. <https://doi.org/10.1007/s10462-023-10681-3>.
- Wilks, Daniel S. 1990. "On the Combination of Forecast Probabilities for Consecutive Precipitation Periods." *Weather and Forecasting* 5 (4): 640–50. <https://doi.org/10.1175/>

- 1520-0434(1990)005%3C0640:OTCOFP%3E2.0.CO;2.
- Willemse, SJW, A Schat, MS van Noorden, and M Fiocco. 2018. "Correcting for Dependent Censoring in Routine Outcome Monitoring Data by Applying the Inverse Probability Censoring Weighted Estimator." *Statistical Methods in Medical Research* 27 (2): 323–35. <https://doi.org/10.1177/0962280216628900>.
- Wright, Marvin N., and Andreas Ziegler. 2017. "ranger: A Fast Implementation of Random Forests for High Dimensional Data in C++ and R." *Journal of Statistical Software* 77 (1): 1–17.
- Wu, Ying, and Richard J Cook. 2020. "Assessing the Accuracy of Predictive Models with Interval-Censored Data." *Biostatistics* 23 (1): 18–33. <https://doi.org/10.1093/biostatistics/kxaa011>.
- Wu, Yuan, Xiaofei Wang, Jiaxing Lin, Beilin Jia, and Kouros Owzar. 2020. "Predictive Accuracy of Markers or Risk Scores for Interval Censored Survival Data." *Statistics in Medicine* 39 (18): 2437–46. [https://doi.org/https://doi.org/10.1002/sim.8547](https://doi.org/10.1002/sim.8547).
- Xiang, Anny, Pablo Lapuerta, Alex Ryutov, Jonathan Buckley, and Stanley Azen. 2000. "Comparison of the performance of neural network methods and Cox regression for censored survival data." *Computational Statistics & Data Analysis* 34 (2): 243–57. [https://doi.org/https://doi.org/10.1016/S0167-9473\(99\)00098-5](https://doi.org/https://doi.org/10.1016/S0167-9473(99)00098-5).
- Yanagisawa, Hiroki. 2023. "Proper Scoring Rules for Survival Analysis." In *Proceedings of the 40th International Conference on Machine Learning*, edited by Andreas Krause, Emma Brunskill, Kyunghyun Cho, Barbara Engelhardt, Sivan Sabato, and Jonathan Scarlett, 202:39165–82. Proceedings of Machine Learning Research. PMLR. <https://proceedings.mlr.press/v202/yanagisawa23a.html>.
- Yang, Yanying. 2010. "Neural Network Survival Analysis." PhD thesis, Universiteit Gent.
- Yasodhara, Angeline, Mamatha Bhat, and Anna Goldenberg. 2018. *Prediction of New Onset Diabetes after Liver Transplant*.
- Zare, Ali, Mostafa Hosseini, Mahmood Mahmoodi, Kazem Mohammad, Hojjat Zeraati, and Kourosh Holakouie Naieni. 2015. "A Comparison between Accelerated Failure-time and Cox Proportional Hazard Models in Analyzing the Survival of Gastric Cancer Patients." *Iranian Journal of Public Health* 44 (8): 1095–1102. <https://doi.org/10.1007/s00606-006-0435-8>.
- Zhang, Yucheng, Edrise M Lobo-Mueller, Paul Karanicolas, Steven Gallinger, Masoom A Haider, and Farzad Khalvati. 2020. "CNN-based survival model for pancreatic ductal adenocarcinoma in medical imaging." *BMC Medical Imaging* 20 (1): 11. <https://doi.org/10.1186/s12880-020-0418-1>.
- Zhang, Yunwei, Germaine Wong, Graham Mann, Samuel Muller, and Jean Y H Yang. 2021. "SurvBenchmark: comprehensive benchmarking study of survival analysis methods using both omics data and clinical data." *bioRxiv*, January, 2021.07.11.451967. <https://doi.org/10.1101/2021.07.11.451967>.
- Zhang, Zhigang, and Jianguo Sun. 2010. "Interval Censoring." *Statistical Methods in Medical Research* 19 (1): 53–70. <https://doi.org/10.1177/0962280209105023>.
- Zhao, Lili, and Dai Feng. 2020. "Deep Neural Networks for Survival Analysis Using Pseudo Values." *IEEE Journal of Biomedical and Health Informatics* 24 (11): 3308–14. <https://doi.org/10.1109/JBHI.2020.2980204>.
- Zhu, Wan, Longxiang Xie, Jianye Han, and Xiangqian Guo. 2020. "The Application of Deep Learning in Cancer Prognosis Prediction." *Cancers* 12 (3): 603. <https://doi.org/10.3390/cancers12030603>.
- Zhu, X, J Yao, and J Huang. 2016. "Deep convolutional neural network for survival analysis with pathological images." In *2016 IEEE International Conference on Bioinformatics and Biomedicine (BIBM)*, 544–47. <https://doi.org/10.1109/BIBM.2016.7822579>.
- Zou, Hui, and Trevor Hastie. 2005. "Regularization and Variable Selection via the Elastic

Net." *Journal of the Royal Statistical Society Series B: Statistical Methodology* 67 (2): 301–20. <https://doi.org/10.1111/j.1467-9868.2005.00503.x>.